

VOL. 646 NO. 2 SEPTEMBER 3, 1993

THIS ISSUE COMPLETES VOL. 646

JOURNAL OF

CHROMATOGRAPHY

INCLUDING ELECTROPHORESIS AND OTHER SEPARATION METHODS

EDITORS

U.A.Th. Brinkman (Amsterdam)

R.W. Giese (Boston, MA)

J.K. Haken (Kensington, N.S.W.)

K. Macek (Prague)

L.R. Snyder (Orinda, CA)

EDITORS, SYMPOSIUM VOLUMES,

E. Heftmann (Orinda, CA), Z. Deyl (Prague)

EDITORIAL BOARD

D.W. Armstrong (Rolla, MO)

W.A. Aue (Halifax)

P. Boček (Brno)

A.A. Boulton (Saskatoon)

P.W. Carr (Minneapolis, MN)

N.H.C. Cooke (San Ramon, CA)

V.A. Davankov (Moscow)

Z. Deyl (Prague)

S. Dilli (Kensington, N.S.W.)

H. Engelhardt (Saarbrücken)

F. Erni (Basle)

M.B. Evans (Hatfield)

J.L. Glajch (N. Billerica, MA)

G.A. Guiochon (Knoxville, TN)

P.R. Haddad (Hobart, Tasmania)

I.M. Hais (Hradec Králové)

W.S. Hancock (San Francisco, CA)

S. Hjertén (Uppsala)

S. Honda (Higashi-Osaka)

Cs. Horváth (New Haven, CT)

J.F.K. Huber (Vienna)

K.-P. Hupe (Waldbronn)

T.W. Hutchens (Houston, TX)

J. Janák (Brno)

P. Jandera (Pardubice)

B.L. Karger (Boston, MA)

J.J. Kirkland (Newport, DE)

E. sz. Kováts (Lausanne)

A.J.P. Martin (Cambridge)

L.W. McLaughlin (Chestnut Hill, MA)

E.D. Morgan (Keele)

J.D. Pearson (Kalamazoo, MI)

H. Poppe (Amsterdam)

F.E. Regnier (West Lafayette, IN)

P.G. Righetti (Milan)

P. Schoenmakers (Eindhoven)

R. Schwarzenbach (Dübendorf)

R.E. Shoup (West Lafayette, IN)

R.P. Singhal (Wichita, KS)

A.M. Siouffi (Marseille)

D.J. Strydom (Boston, MA)

N. Tanaka (Kyoto)

S. Terabe (Hyogo)

K.K. Unger (Mainz)

R. Verpoorte (Leiden)

Gy. Vigh (College Station, TX)

J.T. Watson (East Lansing, MI)

B.D. Westerlund (Uppsala)

EDITORS, BIBLIOGRAPHY SECTION

Z. Deyl (Prague), J. Janák (Brno), V. Schwartz (Prague)

ELSEVIER

JOURNAL OF CHROMATOGRAPHY

INCLUDING ELECTROPHORESIS AND OTHER SEPARATION METHODS

Scope. The *Journal of Chromatography* publishes papers on all aspects of **chromatography, electrophoresis** and related methods. Contributions consist mainly of research papers dealing with chromatographic theory, instrumental developments and their applications. The section *Biomedical Applications*, which is under separate editorship, deals with the following aspects: developments in and applications of chromatographic and electrophoretic techniques related to clinical diagnosis or alterations during medical treatment; screening and profiling of body fluids or tissues related to the analysis of active substances and to metabolic disorders; drug level monitoring and pharmacokinetic studies; clinical toxicology; forensic medicine; veterinary medicine; occupational medicine; results from basic medical research with direct consequences in clinical practice. In *Symposium volumes*, which are under separate editorship, proceedings of symposia on chromatography, electrophoresis and related methods are published.

Submission of Papers. The preferred medium of submission is on disk with accompanying manuscript (see *Electronic manuscripts* in the Instructions to Authors, which can be obtained from the publisher, Elsevier Science Publishers B.V., P.O. Box 330, 1000 AH Amsterdam, Netherlands). Manuscripts (in English; four copies are required) should be submitted to: Editorial Office of *Journal of Chromatography*, P.O. Box 681, 1000 AR Amsterdam, Netherlands, Telefax (+31-20) 5862 304, or to: The Editor of *Journal of Chromatography, Biomedical Applications*, P.O. Box 681, 1000 AR Amsterdam, Netherlands. Review articles are invited or proposed in writing to the Editors who welcome suggestions for subjects. An outline of the proposed review should first be forwarded to the Editors for preliminary discussion prior to preparation. Submission of an article is understood to imply that the article is original and unpublished and is not being considered for publication elsewhere. For copyright regulations, see below.

Publication. The *Journal of Chromatography* (incl. *Biomedical Applications*) has 40 volumes in 1993. The subscription prices for 1993 are:

J. Chromatogr. (incl. *Cum. Indexes, Vols. 601–650*) + *Biomed. Appl.* (Vols. 612–651):

Dfl. 8520.00 plus Dfl. 1320.00 (p.p.h.) (total ca. US\$ 5466.75)

J. Chromatogr. (incl. *Cum Indexes, Vols. 601–650*) only (Vols. 623–651):

Dfl. 7047.00 plus Dfl. 957.00 (p.p.h.) (total ca. US\$ 4446.75)

Biomed. Appl. only (Vols. 612–622):

Dfl. 2783.00 plus Dfl. 363.00 (p.p.h.) (total ca. US\$ 1747.75).

Subscription Orders. The Dutch guilder price is definitive. The US\$ price is subject to exchange-rate fluctuations and is given as a guide. Subscriptions are accepted on a prepaid basis only, unless different terms have been previously agreed upon. Subscriptions orders can be entered only by calendar year (Jan.–Dec.) and should be sent to Elsevier Science Publishers, Journal Department, P.O. Box 211, 1000 AE Amsterdam, Netherlands, Tel. (+31-20) 5803 642, Telefax (+31-20) 5803 598, or to your usual subscription agent. Postage and handling charges include surface delivery except to the following countries where air delivery via SAL (Surface Air Lift) mail is ensured: Argentina, Australia, Brazil, Canada, China, Hong Kong, India, Israel, Japan*, Malaysia, Mexico, New Zealand, Pakistan, Singapore, South Africa, South Korea, Taiwan, Thailand, USA. *For Japan air delivery (SAL) requires 25% additional charge of the normal postage and handling charge. For all other countries airmail rates are available upon request. Claims for missing issues must be made within six months of our publication (mailing) date, otherwise such claims cannot be honoured free of charge. Back volumes of the *Journal of Chromatography* (Vols. 1–611) are available at Dfl. 230.00 (plus postage). Customers in the USA and Canada wishing information on this and other Elsevier journals, please contact Journal Information Center, Elsevier Science Publishing Co. Inc., 655 Avenue of the Americas, New York, NY 10010, USA, Tel. (+1-212) 633 3750, Telefax (+1-212) 633 3764.

Abstracts/Contents Lists published in Analytical Abstracts, Biochemical Abstracts, Biological Abstracts, Chemical Abstracts, Chemical Titles, Chromatography Abstracts, Current Awareness in Biological Sciences (CABS), Current Contents/Life Sciences, Current Contents/Physical, Chemical & Earth Sciences, Deep-Sea Research/Part B: Oceanographic Literature Review, Excerpta Medica, Index Medicus, Mass Spectrometry Bulletin, PASCAL-CNRS, Referativnyi Zhurnal, Research Alert and Science Citation Index.

US Mailing Notice. *Journal of Chromatography* (ISSN 0021-9673) is published weekly (total 52 issues) by Elsevier Science Publishers (Sara Burgerhartstraat 25, P.O. Box 211, 1000 AE Amsterdam, Netherlands). Annual subscription price in the USA US\$ 4446.75 (subject to change), including air speed delivery. Second class postage paid at Jamaica, NY 11431. **USA POSTMASTERS:** Send address changes to *Journal of Chromatography*, Publications Expediting, Inc., 200 Meacham Avenue, Elmont, NY 11003. Airfreight and mailing in the USA by Publications Expediting.

See inside back cover for Publication Schedule, Information for Authors and information on Advertisements.

© 1993 ELSEVIER SCIENCE PUBLISHERS B.V. All rights reserved.

0021-9673/93/\$06.00

No part of this publication may be reproduced, stored in a retrieval system or transmitted in any form or by any means, electronic, mechanical, photocopying, recording or otherwise, without the prior written permission of the publisher, Elsevier Science Publishers B.V., Copyright and Permissions Department, P.O. Box 521, 1000 AM Amsterdam, Netherlands.

Upon acceptance of an article by the journal, the author(s) will be asked to transfer copyright of the article to the publisher. The transfer will ensure the widest possible dissemination of information.

Special regulations for readers in the USA. This journal has been registered with the Copyright Clearance Center, Inc. Consent is given for copying of articles for personal or internal use, or for the personal use of specific clients. This consent is given on the condition that the copier pays through the Center the per-copy fee stated in the code on the first page of each article for copying beyond that permitted by Sections 107 or 108 of the US Copyright Law. The appropriate fee should be forwarded with a copy of the first page of the article to the Copyright Clearance Center, Inc., 27 Congress Street, Salem, MA 01970, USA. If no code appears in an article, the author has not given broad consent to copy and permission to copy must be obtained directly from the author. All articles published prior to 1980 may be copied for a per-copy fee of US\$ 2.25, also payable through the Center. This consent does not extend to other kinds of copying, such as for general distribution, resale, advertising and promotion purposes, or for creating new collective works. Special written permission must be obtained from the publisher for such copying.

No responsibility is assumed by the Publisher for any injury and/or damage to persons or property as a matter of products liability, negligence or otherwise, or from any use or operation of any methods, products, instructions or ideas contained in the materials herein. Because of rapid advances in the medical sciences, the Publisher recommends that independent verification of diagnoses and drug dosages should be made.

Although all advertising material is expected to conform to ethical (medical) standards, inclusion in this publication does not constitute a guarantee or endorsement of the quality or value of such product or of the claims made of it by its manufacturer.

This issue is printed on acid-free paper.

CONTENTS

(Abstracts/Contents Lists published in Analytical Abstracts, Biochemical Abstracts, Biological Abstracts, Chemical Abstracts, Chemical Titles, Chromatography Abstracts, Current Awareness in Biological Sciences (CABS), Current Contents/Life Sciences, Current Contents/Physical, Chemical & Earth Sciences, Deep-Sea Research/Part B: Oceanographic Literature Review, Excerpta Medica, Index Medicus, Mass Spectrometry Bulletin, PASCAL-CNRS, Referativnyi Zhurnal, Research Alert and Science Citation Index)

REVIEW

- Quantitative aspects of the application of capillary electrophoresis to the analysis of pharmaceuticals and drug related impurities
by K.D. Altria (Herts., UK) (Received May 12th, 1993) 245

REGULAR PAPERS

Column Liquid Chromatography

- High-performance chiral displacement chromatographic separations in the normal-phase mode. Separation of the enantiomers of 1,2-O-dihexadecyl-*rac*-glycerol-3-O-(3,5-dinitrophenyl)carbamate using the Pirkle-type naphthylalanine silica stationary phase
by P.L. Camacho-Torralba, M.D. Beeson and Gy. Vigh (College Station, TX, USA) and D.H. Thompson (Beaverton, OR, USA) (Received May 11th, 1993) 259
- Nitroxide radicals in studies of the fine bonded layer structure of modified silicas
by P.G. Mingalyov, A.Yu. Fadeev, S.M. Staroverov, G.V. Lisichkin and E.V. Lunina (Moscow, Russian Federation) (Received February 22nd, 1993) 267
- High-performance membrane chromatography: highly efficient separation method for proteins in ion-exchange, hydrophobic interaction and reversed-phase modes
by T.B. Tennikova and F. Svec (Prague, Czech Republic) (Received May 5th, 1993) 279
- Enzyme-based high-performance liquid chromatography stationary phases as metabolic reactors. Immobilization of non-solubilized rat liver microsomes on an immobilized artificial membrane high-performance liquid chromatography support
by T. Alebić-Kolbah and I.W. Wainer (Montreal, Canada) (Received May 26th, 1993) 289
- Optimization of the separation selectivity of a group of benzene and naphthalene derivatives in micellar high-performance liquid chromatography using a C₁₈ column and alcohols as modifiers in the mobile phase
by M.A. García, S. Vera, M. Bombín and M.L. Marina (Madrid, Spain) (Received April 26th, 1993) 297
- Retention behaviour of volatile compounds in normal-phase high-performance liquid chromatography on a diol column
by M. Lübke, J.-L. Le Quééré and D. Barron (La Tronche, France) (Received April 27th, 1993) 307
- Use of a porous graphitised carbon column for the high-performance liquid chromatography of oligosaccharides, alditols and glycopeptides with subsequent mass spectrometry analysis
by M.J. Davies, K.D. Smith, R.A. Carruthers, W. Chai, A.M. Lawson and E.F. Hounsell (Harrow, UK) (Received June 15th, 1993) 317
- Study of lectin-ganglioside interactions by high-performance liquid affinity chromatography
by M. Caron and R. Joubert-Caron (Bobigny, France), J.R. Cartier (Marcy l'Etoile, France) and A. Chadli and D. Bladier (Bobigny, France) (Received May 14th, 1993) 327
- Analysis and configuration assignments of the amino acids in a pyoverdine-type siderophore by reversed-phase high-performance liquid chromatography
by D.K. Hancock and D.J. Reeder (Gaithersburg, MD, USA) (Received June 2nd, 1993) 335
- Characterisation of the photochemotherapeutic agent disulphonated aluminium phthalocyanine and its high-performance liquid chromatographic separated components
by S.M. Bishop, B.J. Khoo, A.J. MacRobert, M.S.C. Simpson and D. Phillips (London, UK) and A. Beeby (Durham, UK) (Received June 7th, 1993) 45

Contents (continued)

Gas Chromatography

- Hydrogen bonding. XXVIII. Comparison of the solvation theories of Abraham and Poole, using a new acidic gas-liquid chromatography stationary phase
by M.H. Abraham and J. Andonian-Haftvan (London, UK), I. Hamerton (Surrey, UK) and C.F. Poole and T.O. Kollie (Detroit, MI, USA) (Received May 21st, 1993) 351
- Evaluation of the polarity of packed and capillary columns by different classification methods
by G. Castello, G. D'Amato and S. Vezzani (Genova, Italy) (Received April 15th, 1993). 361
- Development of a high-temperature gas chromatography-inductively coupled plasma mass spectrometry interface for the determination of metalloporphyrins
by W.G. Pretorius, L. Ebdon and S.J. Rowland (Plymouth, UK) (Received May 18th, 1993). 369

Electrophoresis

- Electrophoretic behavior of aromatic-containing organic acids and the determination of selected compounds in water and soil by capillary electrophoresis
by W.C. Brumley and C.M. Brownrigg (Las Vegas, NV, USA) (Received May 25th, 1993) 377
- The analysis of multiple phosphoserine-containing casein peptides using capillary zone electrophoresis
by N. Adamson, P.F. Riley and E.C. Reynolds (Melbourne, Australia) (Received June 1st, 1993) 391
- Micellar electrokinetic capillary chromatography of haematoporphyrin, protoporphyrin and their copper and zinc complexes
by C. Kiyohara, K. Saitoh and N. Suzuki (Miyagi, Japan) (Received May 14th, 1993). 397
- Investigation of vanadate as a pH sensitive analyte anion using capillary zone electrophoresis
by T. Groh and K. Bächmann (Darmstadt, Germany) (Received May 18th, 1993). 405

SHORT COMMUNICATIONS

Column Liquid Chromatography

- Behaviour of polyhydroxyethyl methacrylate sorbent with dextran-filled macropores in dye-affinity chromatography of proteins
by D. Mislovičová, M. Petro and D. Berek (Bratislava, Slovak Republic) (Received May 27th, 1993) 411
- Identification of lichen substances by a standardized high-performance liquid chromatographic method
by G.B. Feige and H.T. Lumsch (Essen, Germany), S. Huneck (Halle, Germany) and J.A. Elix (Canberra, Australia) (Received May 24th, 1993). 417
- High-performance liquid chromatographic method for the monitoring of the synthesis of the precursor for tetramisole
by J.S. Wagh, A.A. Mokashi and A. Datta (Maharashtra, India) (Received April 27th, 1993) 428

Planar Chromatography

- Analysis of plant extracts by multiple development thin-layer chromatography
by W. Markowski and G. Matysik (Lublin, Poland) (Received May 12th, 1993) 434

DISCUSSION

- Discussion on "Alternatives to methanol-water elution of solid-phase extraction columns for the fractionation of high log K_{ow} organic compounds in aqueous environmental samples" by Durhan *et al.*, *J. Chromatogr.*, 629 (1993) 67-74
by S.-L. Lau and M.K. Stenstrom (Los Angeles, CA, USA) (Received June 16th, 1993) 439

BOOK REVIEW

- Detectors for capillary chromatography (by H.H. Hill and D.G. McMinn), reviewed by M. Dressler (Brno, Czech Republic) 442

- AUTHOR INDEX 443

Review

Quantitative aspects of the application of capillary electrophoresis to the analysis of pharmaceuticals and drug related impurities

K.D. Altria

Pharmaceutical Analysis, Glaxo Group Research, Park Road, Ware, Herts. (UK)

(First received March 9th, 1993; revised manuscript received May 12th, 1993)

ABSTRACT

Capillary electrophoresis (CE) is a collection of associated electrokinetic techniques, the principal ones being free solution capillary electrophoresis (FSCE) and micellar electrokinetic capillary chromatography (MECC). Both FSCE and MECC have been utilised for the separation of drug species. Several reports have demonstrated that CE is an attractive complement or alternative to HPLC which is widely used for pharmaceutical analyses. CE methods have been validated and are now in routine use within a number of pharmaceutical companies. This review details both applications taken from within a working pharmaceutical analysis laboratory and also provides selected literature examples. Applications include the quantitative analysis of drug related impurities, determinations of drug content in formulations, chiral analysis, stoichiometric determinations, and micro-preparative CE.

CONTENTS

1. Introduction	246
2. Instrument performance data	247
3. Application areas	247
3.1. Procedures for performing quantitative analysis	247
3.2. Determination of drug related impurities	249
3.3. Main drug determinations	251
3.4. Chiral analysis	252
3.4.1. Performance of chiral CE	253
3.4.2. Applications of chiral CE	254
3.5. Micro-preparative CE	255
3.6. Identity confirmation	255
3.7. Stoichiometric determinations	255
4. Features of CE methods	255
5. Future developments	256
6. Conclusions	256
References	256

1. INTRODUCTION

Great demands are placed on the analytical methods that are used for the determination and assay of both the active ingredient and impurities in pharmaceuticals. Impurities may be present from either synthetic or degradative sources and these therefore may have widely differing structures and/or polarities. Impurity levels may be of the order of 0.05–1% area/area of the main component which necessitates a detection system with a suitable linear range. During the development of a drug candidate, and the subsequent quality control of the marketed pharmaceutical product a considerable number of samples will be analysed. This volume of samples therefore requires that the analytical method employed be relatively inexpensive, simple, quick and robust. Currently the majority of these analyses are conducted by HPLC which can offer all the above required features. Similarly CE is capable of meeting these requirements and is now being recognised as an important option within pharmaceutical analysis.

The work of Jorgenson and Lukacs [1] popularised the technique of CE and encouraged academic and industrial investigators to enter this area of research. Terabe *et al.* [2] developed micellar electrokinetic capillary chromatography (MECC). Both free solution capillary electrophoresis (FSCE) and MECC offer different selectivity principles compared to each other and to chromatographic techniques such as HPLC. CE based methods are being increasingly applied to supplement and complement chromatographic generated data, in a wide and diverse number of application areas.

FSCE separates solutes by virtue of their different electrophoretic mobilities. A more mobile species travels along the capillary faster than a less mobile analyte. Under a given set of operating conditions the electrophoretic mobility has a fixed electrochemical value and the migration time is characteristic of the test solute. High peak efficiencies can be obtained using CE which can allow discrimination of closely related species. For example CE has been used for the separation of benzoic acids containing isotopically substituted oxygen atoms [3] and also positional isomers [4].

MECC is the most popular of the variants of electrokinetic chromatography, others being electro-osmotically driven chromatography [5] and solvophobic association electrophoresis [6]. In MECC a micellar solution of surfactant is used as the electrolyte. This combination permits resolution on both an electrophoretic and chromatographic basis enabling the resolution of neutral compounds which cannot be achieved by FSCE.

Highly automated PC-controlled CE instrumentation is now commercially available from a number of suppliers. These systems incorporate [7] sample introduction devices, UV absorbance detectors, a high-voltage supply, and an auto-sampler. CE detectors may be an order of magnitude less sensitive as compared to those available for HPLC. This can in part be compensated for by the high peak efficiencies obtained (with resulting ease of integration and improved resolution) and the use of low UV detection wavelengths (down to 185 nm) where many solutes have enhanced UV activity.

Precision of injection, as measured in peak area reproducibility is generally poorer in CE than in HPLC, typical values being 1–2% and 0.5–1% R.S.D., respectively. This failing is due to the technical difficulties involved in forcing a tiny sample volume into a narrow bore capillary.

There are a number of FSCE parameters than can be varied to achieve a required separation. These include the use of various pH conditions, electrolyte strength and nature, additives such as cyclodextrins, urea, ion-pair reagents and organic modifiers. Nielen [8] has reported the effect of varying such parameters upon the separation of aminobenzoic acid positional isomers. A similar number of variations can be used for optimisation of an MECC method. However, in addition the surfactant type and concentration may also be varied to alter selectivity.

Kuhr and Monnig [9] have provided an excellent general survey of recent CE developments. CE has been employed for the analysis of a wide and diverse range of compounds. These include biomolecules [10,11] such as amino acids, peptides, proteins and nucleotides where traditional forms of electrophoresis are extensively currently employed. In these areas CE is being widely used as previously developed methodologies can

be transferred to the capillary format. However, conventional electrophoresis has had only limited application to the analysis of pharmaceuticals where the emphasis and experience has been concentrated on the use of chromatographic techniques.

The possibilities of applying MECC to the analysis of pharmaceuticals was earlier reviewed by Nishi and Terabe [12]. There have been a large number of pharmaceutical related reports subsequent to this paper. The application of FSCE to the analysis of drugs has not been comprehensively summarized to-date. Therefore it is useful to review the quantitative applications and capabilities of CE in the area of pharmaceutical analysis.

2. INSTRUMENT PERFORMANCE DATA

Commercial instrumentation became available in 1988 and equipment is now available from a number of suppliers either as complete systems or in modular form. The instrumentation employed has been described many times and comprises a high-voltage supply, detector, a length of capillary tubing and a means of introducing sample into the capillary. Good performance is required in terms of reproducible peak areas and migration times to allow both qualitative and quantitative analysis.

The following levels can typically be obtained on the commercial automated instruments currently employed within our laboratory. Detection limits in the low mg/l levels in solution may be obtained for typical pharmaceuticals. Related impurity levels can be routinely monitored at *ca.* 0.1% area/area of the main component. These detection levels may be improved to *ca.* 0.02% (w/w) of main component using external calibrations when the main peak is off-scale. The precision of migration time precision is *ca.* 1% R.S.D. which allows qualitative identification of components within a mixture. Peak area precision is in the order of 1–2% R.S.D. This figure can be improved by employing internal standards. Analysis times are similar to those used in HPLC (*i.e.* 1–30 min). The range of detection wavelengths (185–760 nm) is also similar to those available for HPLC detectors. Typical operating temperatures are in the order of 20–50°C.

3. APPLICATION AREAS

It is intended that reported application areas will be covered in detail, few aspects concerning background theory or method development options will be mentioned. Papers on these subjects have recently been published by McLaughlin *et al.* [13] and Swartz [14].

The viability of employing CE for the analysis of pharmaceuticals was demonstrated in 1987 using homemade equipment [15,16]. Since then reliable commercial equipment has become available and the number of investigators has dramatically increased. Examples from most of the major drug classes have been resolved by CE. A survey of the therapeutic areas covered and the nature of the sample is given in Table I.

The application areas described to-date fall into the following categories: (i) determination of related impurities, (ii) main peak assay, (iii) chiral analysis, (iv) micropreparative CE, (v) identity confirmation, (vi) stoichiometric determinations.

3.1. Procedures for performing quantitative analysis

The procedures for conducting quantitative analysis are similar to those employed in HPLC. Main drug determinations are performed by obtaining response factors from calibration solutions [13,14,38,40]. Drug contents are then calculated applying these response factors to the results obtained for the sample solutions. As in HPLC, internal standards can be incorporated to improve precision as this eliminates injection based errors.

Peak areas are generally employed in quantitative analysis as peak height increases are non-linear at high sample concentrations. It is recommended to employ relatively high sample loadings to obtain good peak area precision.

Levels of impurities may be calculated using procedures similar to those employed in HPLC. Levels of individual impurities may be calculated [42] using response factors obtained from calibration solutions of the impurities. Alternatively [14,60] impurity levels may be quoted as %area/area of the electropherogram. This second approach is the most widely employed method as

TABLE I

SUMMARY TABLE OF THE DRUG CLASSES THAT THE DIFFERENT MODES OF CAPILLARY ELECTROPHORESIS HAVE BEEN APPLIED TO

Class	Electrolyte ^a	Sample composition	Ref.	Class	Electrolyte ^a	Sample composition	Ref.
<i>Antibiotics</i>				<i>Steroids</i>			
Penicillins	MECC, SDS	Test mixtures	14	Corticosteroids	MECC, SDS	Test mixtures	33
Sulphonamides	FSCE, CD	Test mixtures	17	Corticosteroids	MECC, SDC	Test mixture	43
Benzylpenicillin	High pH FSCE	Formulations	18	Various	MECC, SDS + CDs	Test mixtures	44
Various	MECC, SDS and LMT	Test mixture	19	Various	MECC, SDC	Test mixtures	45
Cephalosporins	MECC, SDS + TAA	Test mixtures	20	Testosterone esters	MECC, SDS	Test mixtures	46
Cefuroxime axetil	MECC, SDS	Formulations	21	<i>Antihistamines</i>			
Aspoxicillin	MECC, SDS	Plasma	22	Various	MECC, SDS	Formulations	47
Sulphonamides	FSCE, pH 3–7	Pork meat extracts	23	<i>Anti-cancer</i>			
Cefixime	FSCE, pH 7	Test mixtures	24	Methotrexate and metabolites	FSCE, pH 7	Serum	48
(and metabolites)	+methanol			<i>Analgesics</i>			
Cefpiramide	MECC, SDS	Plasma	25	Various	FSCE and MECC, SDS	Formulations	7
Amoxicillin and impurities	MECC, SDS	Drug substance	26	Various	FSCE and MECC, SDS	Test mixtures	14
Neomycin	FSCE, various	Eardrops	27	Paracetamol	MECC, SDS	Plasma	49
Quinolone and impurities	FSCE, pH 2	Drug substance	28	Various	MECC	Test mixtures	13
<i>Antimalarial agents</i>				Various	MECC, SDS	Formulations	50
Quinine	FSCE, pH 7	Test mixture	29	<i>Mucolytic agents</i>			
<i>Antidepressants</i>				<i>S</i> -carboxymethyl-L-cysteine	FSCE, pH 9	Urine	51
Various tricyclics	MECC	Test mixtures	30	<i>Drugs of abuse</i>			
Fluparoxan	MECC	Drug substance	31	Various	MECC, SDS	Plasma	52
Benzodiazepines	MECC	Urine	32	Barbiturates	MECC, SDS	Test mixtures	53
Diltiazem and impurities	MECC, SDC	Tablets	33	Various	MECC, SDS	Urine	54
Various	MECC	Test mixtures	34	<i>Non-steroidal anti-inflammatories</i>			
Various	MECC	Test mixtures	35	Various	MECC, SDS	Test mixtures	20
<i>Anti-ulcer</i>				Various	MECC, SDS	Test mixtures	45
Ranitidine	FSCE, low pH	Syrup formulation	21	Various	MECC, SDS	Test mixtures	55
Cimetidine	MECC	Plasma	36	Various	MECC, SDS	Test mixtures	56
Ranitidine and impurities	FSCE, low pH	Syrup formulation	37	<i>Anti-migraine</i>			
Cimetidine	FSCE, pH 7	Formulations	38	Sumatriptan	FSCE, pH 2	Urine	57
<i>Bronchodilators</i>				Sumatriptan	FSCE, pH 2	Formulations	58
Inolin (and others)	FSCE, low pH	Test solution	39	<i>Radiolabelled pharmaceuticals</i>			
Salbutamol	FSCE, pH 5	Formulations	40	⁹⁹ Tc ^m complexes	FSCE, various	Test mixtures	59
Theopylline	MECC, SDS	Body fluids	41				
Salbutamol and impurities	FSCE, pH 2	Drug substance	42				

^a CD = cyclodextrin; TAA = tetra-alkylammonium salts (ion-pairing reagent); SDS = sodium dodecyl sulphate (surfactant); LMT = sodium N-lauroyl-N-methyl taurate (surfactant); SDC = sodium deoxycholate (surfactant); SC = sodium cholate (surfactant).

standards of all impurities may not be readily available.

Normalisation of peak areas with migration times in CE is essential prior to reporting impurity level results as %area/area. This requirement arises due to differential residence times of peaks within the detector. Unless area normalisation is

adopted it makes the cross correlation of %area/area impurity results between CE and others separative methods such as HPLC impossible to perform accurately [61]. If unnormalised peak areas are employed for calculation purposes peaks migrating before the main component will be underestimated whilst those migrating later

will be overestimated [61]. This normalisation is relatively simple to perform and involves the division of the peak area of each peak of the electropherogram by its corresponding migration time.

Determination of drug counter-ion levels are performed by external standardisation. Calibration solutions are prepared from appropriate AnalaR grade ionic materials such as NaCl and MgSO₄ depending upon the analyte of concern.

3.2. Determination of drug related impurities

This area is currently considered to be the primary role for CE within pharmaceutical analysis as FSCE and MECC offer alternative separation selectivities to the widely used technique of HPLC. CE is therefore a useful option to confirm purity results as obtained by HPLC.

Typical limits of detection (LODs) for impurities may be set at 0.1%area/area with reference to the main component. This LOD is approaching the linear dynamic range of commercial CE detectors. Swartz [14] reported a LOD of 0.1%area/area for salicylamide related impurities by MECC with a precision of ~5% R.S.D. for low level impurities. Bile salt based MECC [33] has been used to determine levels of diltiazem impurities in tablets with a reported LOD of 0.1%area/area for related impurities.

FSCE, TLC and HPLC were simultaneously employed [60] for the determination of domperidone related impurities in drug substance samples (Table II). Impurity levels for individual impurities agreed well between the techniques, however CE resolved an additional impurity

which apparently co-eluted with another impurity on both HPLC and TLC.

To improve detection limits to below 0.1%area/area CE can be obtained by employing variable sample loadings [62]. An initial analysis is performed to obtain a main component just within the operating range of the detector. The sample loading is then increased to a higher level by a preset factor (*i.e.* 10 fold increase). The analysis of the higher sample loading will result in a off-scale peak for the main component but will allow detection of trace impurities. These impurities are then quoted as a % of total peak area. The peak area of the main peak in the off-scale separation is calculated by multiplying the peak area obtained in the on-scale separation by the factor relating to the sample loading increase.

The determination of the impurities of ranitidine is used [62] to illustrate the performance gains when employing high-low sample loading. HPLC and TLC methods [63] are employed for the analysis of ranitidine, several impurities are present at low (<0.1%) levels which cannot be directly quantified by CE. Fig. 1a shows a 2-s injection of a solution of a degraded ranitidine sample with the main peak on-scale, an LOD of 0.1%area/area was obtained. Fig. 1b shows a 20-s injection of the same solution with the main peak off-scale the LOD is calculated as 0.02%area/area. Both 2- and 10-s injections of the sample were repeated to assess the precision and increase in detection levels (Table III). There are also clear improvements in the precision of determining low level impurities using this procedure.

TABLE II

DOMPERIDONE RELATED IMPURITIES IN DRUG SUBSTANCE BATCHES (%AREA/AREA)

From ref. 60.

Impurity	Batch 1			Batch 2			Batch 3		
	CE	LC	TLC	CE	LC	TLC	CE	LC	TLC
R45571	0.24	0.26	0.19	0.22	0.23	0.15	0.26	0.27	0.23
R48557	0.15	0.35	0.34	0.15	0.34	0.36	0.15	0.30	0.27
Unknown	0.17	–	–	0.24	–	–	0.18	–	–

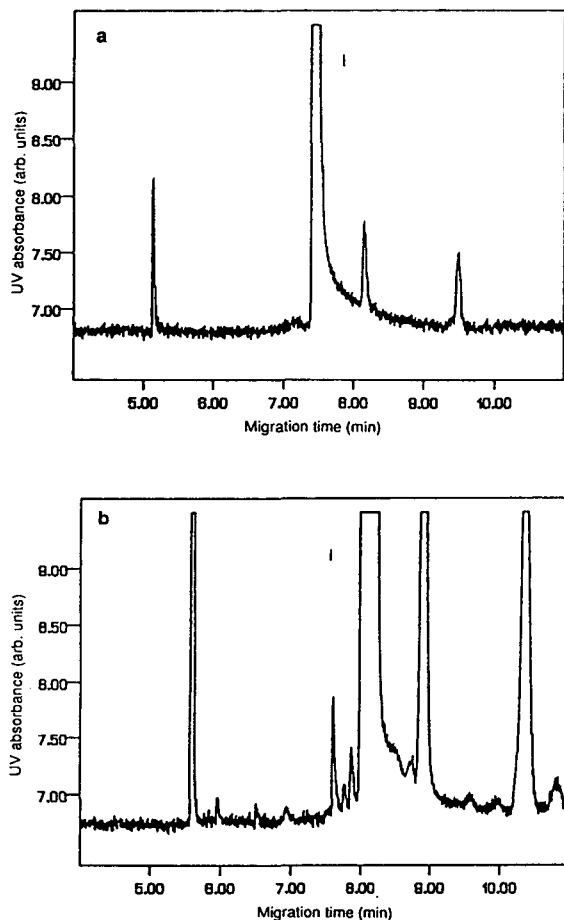


Fig. 1. (a) 2-s loading of degraded ranitidine solution; (b) 10-s loading. I = ranitidine. Reproduced with permission from ref. 62.

An alternative approach to improving detection limits is to employ high sample concentrations and to quantify impurities against external standards. FSCE has been employed [42] for the quantitative determination of 2 dimeric impurities (“dimer” and “bis ether”) present in experimental salbutamol sulphate drug substance. To achieve the low detection level required a relatively high sample concentration (1 mg/ml) and a detection wavelength of 200 nm were employed. The salbutamol peak was off-scale and the impurities were quantified against external standards of the impurities. Linearity of response over the required impurity content range, and a detection limit of 0.02% (w/w) were obtained. A linear detector response (peak

TABLE III

RANITIDINE RELATED IMPURITY DATA (%AREA/AREA) ($n = 5$)

O/S = Peak off-scale; RMT = relative migration time with reference to ranitidine; N/D = not detected. From ref. 62.

	2 s	10 s
Ranitidine peak area (R.S.D.)	399586 (0.8%)	O/S
Total impurity level (R.S.D.)	4.5 (2.9%)	4.4 (1.2%)
Number of impurities	4	8
Peak at RMT 0.69 (R.S.D.)	1.90 (4.0%)	1.68 (1.5%)
Peak at RMT 0.94	N/D	0.13
Peak at RMT 0.96	N/D	0.03
Peak at RMT 0.97	N/D	0.08
Peak at RMT 1.08 (R.S.D.)	0.13 (21%)	0.12 (2.2%)
Peak at RMT 1.10 (R.S.D.)	1.30 (9.3%)	1.25 (1.6%)
Peak at RMT 1.28 (R.S.D.)	1.17 (5.0%)	1.16 (1.5%)
Peak at RMT 1.34	N/D	0.07

area) with bis ether content was obtained with a correlation coefficient of 0.999 and intercept of less than 1% of typical values. Precision data of <5% R.S.D. was obtained for response factors, which given the low levels being determined, were considered acceptable. Quantitative impurity results for salbutamol drug substance batches obtained by CE compared well [42] to those obtained by HPLC and TLC.

Typical analysis times reported in CE are similar to those encountered in HPLC, *i.e.* 10–40 min. However, the use of high voltages applied across short capillaries can greatly reduce the required times with only a marginal loss of separation efficiency [37]. A fluparoxan drug substance batch, prior to purification, containing high levels of related impurities was analysed by CE using both a standard length and a short capillary (Fig. 2a and b). This sample was analysed 5 times using both techniques to give the data in Table IV. The impurity profiles and levels are similar in both instances. The precision of main peak areas are 0.7 and 1.1% R.S.D. for conventional CE and high-speed CE, respective-

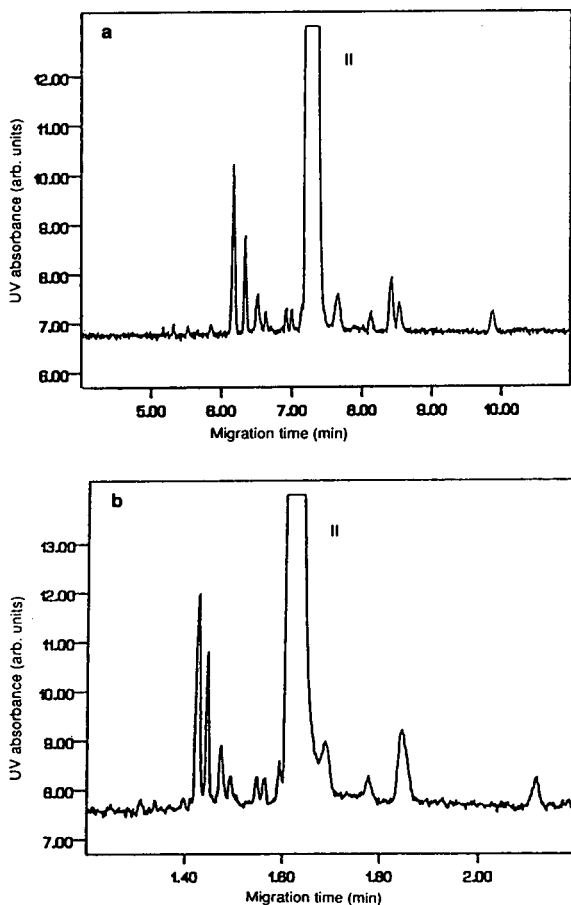


Fig. 2. (a) Normal-speed CE separation of fluparoxan related impurities; (b) High-speed CE separation of fluparoxan related impurities. II = fluparoxan. Reproduced with permission from ref. 37.

TABLE IV
COMPARISON OF CE AND HIGH-SPEED CE
FLUPAROXAN IMPURITY DATA

No. of injections = 5. From ref. 37.

	CE	HSCE
Fluparoxan area	613792	750578
Fluparoxan area R.S.D.	0.7%	1.1%
Total no. impurities	15	14
Total %area/area (%a/a)	11.04	11.95
Total %area/area R.S.D.	1.8%	2.2%
Impurity RMT 0.85 %a/a	3.4	3.4
Impurity RMT 0.85 %a/a R.S.D.	1.6%	1.8%
Impurity RMT 0.87 %a/a	1.6	1.8
Impurity RMT 0.87 %a/a R.S.D.	4.0%	4.9%

ly, which indicates that high-speed quantitative determinations could also be considered.

Clearly CE has the ability to provide quantitative impurity data with an acceptable level of performance.

3.3. Main drug determinations

Increasing attention is being paid to the quantitative aspect of CE. Typical peak area R.S.D.s reported are in the region of 1–2% [7,13]. However, the use of internal standards permits improved quantitative precision to be obtained [64], as this compensates for any variability in injection volume.

CE has been applied to a number of drugs in a variety of formulations. Hoyt and Sepaniak reported [18] the first quantitative analysis by using CE to determine the penicillin G content of tablets employing phenol as an internal standard. The cimetidine content of several formulation presentations were determined by FSCE [38] and fair agreement was obtained with the label claim. Weinberger and Albin [56] employed SDS-based MECC to determine non-steroidal anti-inflammatories in tablets and obtained data equivalent to the label claim with good precision.

The techniques of CE and HPLC were simultaneously used [40] to obtain drug content results in bronchodilator formulations. Good correlation between the three techniques and label claim was achieved (Table V). Correlation coefficients of greater than 0.999 for CE detector linearity were obtained. Precision data for CE assay results were in the order of 1–2% R.S.D.

Exploiting indirect UV detection Ackermans *et al.* [27] were able to quantify the levels of selected aminoglycosides in eardrops with both good precision and linearity. FSCE has also been employed [47] to quantify levels of antihistamines in tablets.

Nishi *et al.* [50] employed MECC to determine the levels of analgesics in formulations, the results were concordant with the label claim. Plyum *et al.* [60] determined the domperidone content in three formulation types by both CE and HPLC. The results showed reasonable agreement in terms of assay and precision, an

TABLE V

QUANTITATIVE ANALYSIS OF FORMULATIONS BY CE AND HPLC (mg/dose)

From ref. 40.

Sample	HPLC	CE
<i>Salbutamol</i>		
Tablets (4 mg/tablet)	4.05, 4.00	3.94, 3.72
Infusions (1 mg/ml)	1.04, 1.02	0.99, 1.00
Syrups (0.4 mg/ml)	0.40, 0.40	0.41, 0.39
<i>Terbutaline</i>		
Tablets (5 mg/tablet)	4.92, 4.89	4.68, 4.67
Ampoules (0.5 mg/ml)	0.51, 0.51	0.52, 0.50
Syrups (0.3 mg/ml)	0.31, 0.30	0.30, 0.30
<i>Fenoterol</i>		
Tablets (2 mg/tablet)	1.84, 1.86	1.88, 1.97
Respirator (5 mg/ml)	4.98, 4.92	4.89, 4.91

internal standard was employed in both analytical methods.

A particular feature of CE is that the capillaries are sufficiently rugged to enable direct injection of particularly "dirty" samples which would require extensive sample pretreatment prior to HPLC analysis. Drug levels have been determined from direct injection of plasma [22,32,49], urine [21,55] and syrup formulations [21].

Demonstrations of quantitative CE assays have largely originated from academic laboratories. A working pharmaceutical analysis report has been described in which a migraine treatment, sumatriptan, was quantified by CE [58] in solutions for injection. An internal standard was used for quantitation and external sumatriptan standards were used to obtain response factors. The CE method gave good performance in terms of precision (<1% R.S.D. for peak area precision), linearity and inter-day repeatability of both injection and analysis. Fig. 3 shows two replicate analyses of a sumatriptan sample solution. Results were simultaneously generated by both CE and HPLC [58] for four on-going stability batches of (12 mg/ml) injection solutions and compared well (Table VI). The excellent cross-correlation of HPLC and CE results for sumatriptan content suggests that CE could

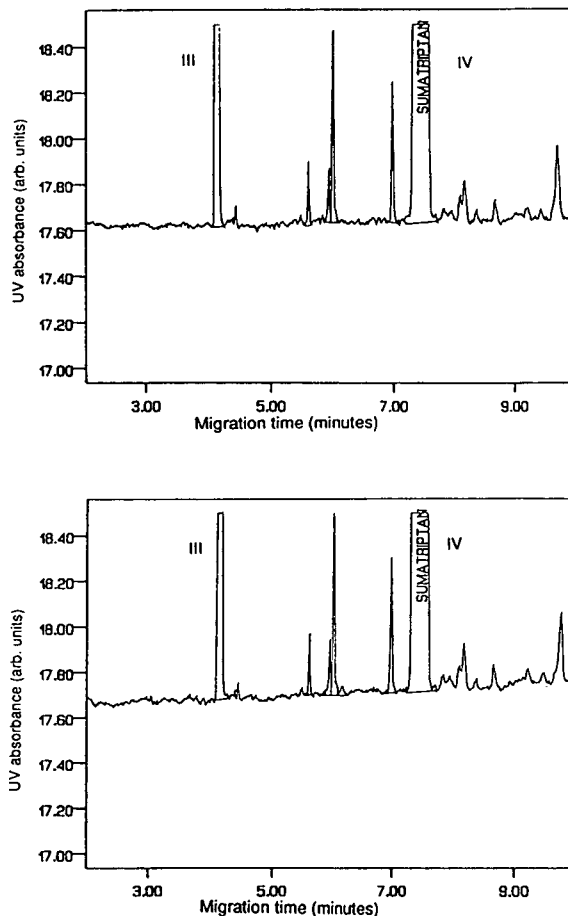


Fig. 3. Replicate CE separations of a sumatriptan sample solution. III = internal standard; IV = sumatriptan. Reproduced with permission from ref. 58.

be successfully employed for this and other quantitative main peak assays. In addition the good agreement between the results obtained by the two independent methods increases the validity of the results and could be considered as part of method validation for either method.

3.4. Chiral analysis

CE has been successful in enantioselectively separating several racemic pharmaceuticals. Several separation options have been reported and are given in Table VII.

A number of compounds have been separated including ephedrine, norephedrine [71], epinephrine [72], isoproterenol [71], terbutaline [73],

TABLE VI

DETERMINATION OF SUMATRIPTAN CONTENT BY CE AND HPLC FOR DIFFERENT FORMULATION BATCHES UNDER VARIOUS STORAGE CONDITIONS

From ref. 58.

Sample	Sumatriptan content (mg/ml)	
	CE	HPLC
<i>Batch 2</i>		
Condition 1 (aliquot 1)	11.5	11.6
Condition 1 (aliquot 2)	11.6	11.6
Condition 2 (aliquot 1)	11.6	11.7
Condition 2 (aliquot 2)	11.6	11.7
<i>Batch 3</i>		
Condition 1 (aliquot 1)	11.7	11.8
Condition 1 (aliquot 2)	11.8	11.8
Condition 2 (aliquot 1)	11.6	11.7
Condition 2 (aliquot 2)	11.6	11.7
<i>Batch 4</i>		
Condition 1 (aliquot 1)	11.7	11.8
Condition 1 (aliquot 2)	11.8	11.8
Condition 2 (aliquot 1)	11.7	11.7
Condition 2 (aliquot 2)	11.6	11.7

propranolol [66,67], trimequinol [70], dopa [69], and clenbuterol [68]. Similar levels of chiral recognition are often obtained in both HPLC and CE, however the superior peak efficiencies achieved in CE enables improved baseline separations to be obtained.

Peak area normalisation (section 3.1.) is required in chiral analysis as the later migrating enantiomer migrates more slowly through the detector giving an overestimation of peak area [61].

TABLE VII

MODES OF CHIRAL SEPARATION

Mode	References
FSCE with cyclodextrins (CDs)	65–68
FSCE with crown ethers	69
MECC with SDS and CDs	34
MECC with bile salts	70

3.4.1. Performance of chiral CE

The enantiomers of the bronchodilator clenbuterol have been resolved by CE [68]. A clenbuterol sample was injected 10 times and produced the performance data given in Table VIII.

The use of short capillaries for chiral high-speed CE separations is possible. The chiral FSCE separation of the racemate, of which picumeterol is the active enantiomer, has been reported [68]. A typical separation is given in Fig. 4a. This analysis was conducted utilising dimethyl- β -cyclodextrin as the chiral selector and applying 20 kV across a 57-cm (50 cm to detector) capillary. Fig. 4b shows the HSCE separation [74] of the racemate within a reduced analysis time of 3 min applying 13 kV across a 27-cm (20 cm to detector) capillary. Some resolution is sacrificed but this represents a reasonable and useful reduction in analysis time and could be applied to the monitoring of enantioselective synthesis or the enantiomeric purity of chiral drugs present in pharmaceutical formulations undergoing stability trials.

Nishi *et al.* [33] chirally resolved trimetoquinol using sodium taurodeoxycholate based MECC, an LOD of 1% of the inactive enantiomer was obtained. An LOD of 0.5% has been reported for 2'-deoxy-3'-thiacytidine (BCH189) [75].

TABLE VIII

PERFORMANCE OF CHIRAL SEPARATION OF CLENBUTEROL ($n = 10$)

The peak area data confirms the 1:1 ratio of the two enantiomers. From ref. 76.

	Precision (R.S.D.)
Migration time of enantiomer 1	1.3%
Migration time of enantiomer 1 relative to enantiomer	0.8%
Peak area for enantiomer 1	1.2%
Normalised peak area for enantiomer 1	0.8%
Peak area ratio of enantiomer 1 cf enantiomer 2	0.4%
Peak area ratio of enantiomer 1 and enantiomer 2	49:50

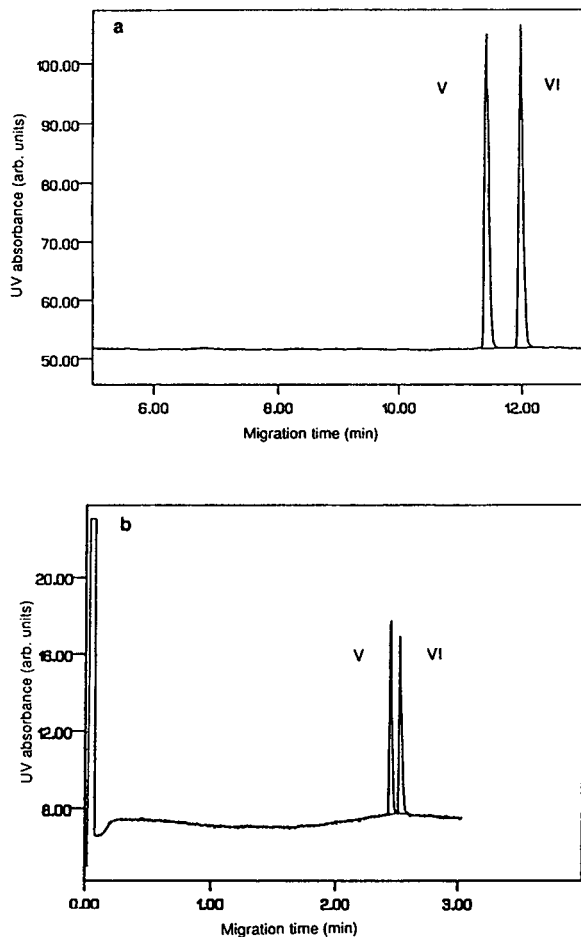


Fig. 4. (a) Chiral CE separation of picumeterol; (b) High-speed CE separation of picumeterol. V = (*R*)-picumeterol; VI = (*S*)-picumeterol. Unpublished data. Separation conditions: 50 mM borax with 30 mM dimethyl-beta-cyclodextrin (pH 2.2 with conc. H_3PO_4), sample concentration 0.5 mg/ml in water, 214 nm, 10-s pressure injection. Fig. 4a applying 20 kV across a 57-cm (50 cm to detector) 50- μ m capillary. Fig. 4b as Fig. 4a except 13 kV applied across a 27-cm (20 cm to detector) 50- μ m capillary.

3.4.2. Applications of chiral CE

FSCE has been reported [69] for the in-process control testing of the chiral purity of a precursor to a Sandoz drug with a limit of detection of 0.2% for the inactive enantiomer. Nishi *et al.* [33] employed MECC with sodium deoxytaurocholate micelles at pH 7.0 to determine the optical purity of five batches of trimetoquinol down to 1% of the *R* enantiomer in the presence of the *S*. Peterson and Trowbridge [72] performed quantitative chiral analysis of *l*-

epinephrine in a pharmaceutical formulation using pseudoephedrine as an internal standard.

Rogan *et al.* [75] have also used CDs for the chiral separation of the anti-HIV drug BCH 189. The required (+) enantiomer is produced by an enzymatic biotransformation. The progress of biotransformation was monitored by chiral CE over a 51-h period. These CE data were used to calculate the reaction rate, order, and half-life.

Good agreement between the enantiomeric excess ratios for three batches of the single enantiomer compound picumeterol, as determined by both CE and HPLC has been obtained [76]. The HPLC method employed [68] for this analysis failed to give effective baseline resolution of the two enantiomers whilst the CE method enabled clear monitoring of the trace enantiomer (Fig. 5). An LOD of 0.1% area/area was obtained for the undesired enantiomer.

A CE method has been validated [77] for the enantiomeric purity determination of the enantiomers of fluparoxan. The method allowed determination of 1% of either enantiomer in the presence of its stereoisomer. Method validation showed adequate detector linearity over the required range. The method also gave good performance in terms of sensitivity for trace levels of the undesired enantiomers, injection precision and recovery.

An inter-company cross-validation exercise

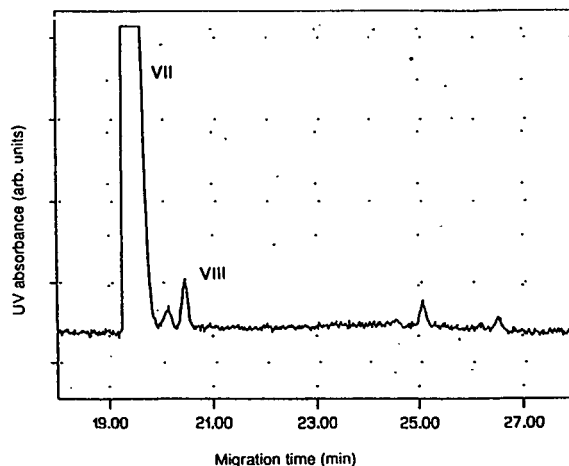


Fig. 5. CE separation of a single enantiomeric form of picumeterol from its stereoisomer. VII = (*R*)-picumeterol; VIII = (*S*)-picumeterol. Reproduced with permission from ref. 76.

has been conducted between seven pharmaceutical companies for a chiral CE method. Using a standard set of conditions each company was able to achieve baseline resolution, or greater, of the enantiomers of clenbuterol. Validation was simultaneously performed and acceptable levels of precision, accuracy, and linearity were achieved [78].

3.5. Micro-preparative CE

The micro-preparative use of CE has been reported to collect fractions, principally for protein and nucleotide separations [79–83]. The amounts collected are tiny, however sufficient material has been collected to enable protein sequencing.

Micro-preparative CE has been used [84] in pharmaceutical analysis to confirm peak homogeneity of a drug related impurity. An unrefined batch of fluparoxan drug substance was analysed by FSCE (Fig. 2b) and HPLC. Fractions containing a specific impurity were obtained by HPLC and CE. The fractions were then analysed by the alternative technique and peak identities confirmed by retention or migration time. Each fraction was shown to consist of a single peak at the position corresponding to the impurity of interest. CE and HPLC were used to quantify total impurity levels and levels of the selected impurity in three batches of fluparoxan drug substance and good agreement was obtained between the two techniques.

Due to the low amounts collected CE is not routinely considered for micro-preparative analysis. However, the advent of instrumentation in which numerous capillaries are employed in an array configuration [85] and the use of wider bore capillaries [86] may increase activity in this area.

3.6. Identity confirmation

Chemical identity confirmation is required following production of a batch of drug substance, or formulation. Typically, this is performed using a spectroscopic method and a separative method. Combinations of HPLC with NMR or IR are commonly applied testing regimes. The features of CE (section 4) make it an

attractive alternative [87] to chromatographic methods for identity confirmation purposes. Use of a coinjection procedure can be employed [87] in a standard addition type operation to perform quantitative identity confirmation.

3.7. Stoichiometric determinations

Many drugs are converted to salts to produce the required solubility and physical properties. The extent of this conversion is typically determined by microanalysis or titrimetry. Capillary electrophoresis methods, exploiting indirect UV detection, have been developed [88] to determine inorganic anions and cations. Applying similar methodology it is possible [89] to determine levels of drug counter-ions such as chloride and sulphate with good precision, linearity and repeatability. Results obtained by CE are in accord with those generated by microanalytical techniques and ion exchange chromatography.

4. FEATURES OF CE METHODS

The relative merits of CE, HPLC and SFC have previously been considered [90] in depth. The main drawbacks and advantages of CE based analysis are discussed below.

The principal disadvantages of CE are instrument based and mainly relate to the precision and detection levels achieved. Typically the precision of injection is 1–2% R.S.D. for the main component. This is compared to HPLC where R.S.D.s of <1% can be obtained. To obtain improved precision levels in CE it may be necessary to incorporate internal standards. In addition the detection limits obtained in CE may be up to an order of magnitude less sensitive when directly compared to HPLC at a common UV wavelength. However, in CE it is possible to employ wavelengths as low as 185 nm where significant enhancements in UV absorbance activity are often possible. The preparative options available in CE are limited by the tiny volumes involved.

Some of the favourable features of CE compared to HPLC are that high separation efficiencies can be obtained which may enable resolu-

tion of closely related species. There are minimal sample volume requirements in CE. Multiple injections from as little as 10 μl can be achieved as typical injection volumes are in the order of 10 nl. Solvent and reagent consumption are reduced as daily reagent consumption is typically 20 ml of electrolyte. This represents considerable savings in terms of solvent purchasing and disposal. Sample pretreatment requirements may also be minimised as sample solutions can often be directly injected. The cost of capillaries is low compared to the expense of HPLC columns.

Overall CE should be viewed as a complementary and alternative technique to HPLC and should be employed for applications when appropriate.

5. FUTURE DEVELOPMENTS

As discussed in section 4 the current principal limitations of CE are instrumentation based. It is anticipated that the next generation of CE instrumentation will address the identified weakness areas. Emerging technologies will include the increased use of electrochromatography [91]. This technique involves the use of an electric field to drive solvent through a capillary packed with reversed-phase material [5]. Due to the nature of this electrically driven flow, high separation efficiencies can be obtained. It is anticipated that the commercialisation of capillary array instruments will be of great importance where high sample throughput is of concern.

6. CONCLUSIONS

Without doubt CE is an established analytical alternative and complement to HPLC in the area of quantitative drug analysis. CE is capable of generating high quality data with acceptable levels of precision, accuracy and linearity. Methods are capable of undergoing validation and are in routine use within pharmaceutical companies and CE data has been submitted to, and accepted by, regulatory authorities. There are several features of CE compared to other separative techniques and the choice of technique should greatly depend upon the nature and requirements of the application.

REFERENCES

- 1 J.W. Jorgenson and K.D. Lukacs, *Science*, 222 (1983) 266.
- 2 S. Terabe, K. Otsuka, A. Ichikawa, A. Tsuchiya and T. Ando, *Anal. Chem.*, 56 (1984) 111.
- 3 S. Terabe, T. Yashima, N. Tanaka and M. Araki, *Anal. Chem.*, 59 (1987) 487.
- 4 S. Fujiwara and S. Honda, *Anal. Chem.*, 59 (1987) 2773.
- 5 J.H. Knox and I.H. Grant, *Chromatographia*, 24 (1987) 135.
- 6 Y. Walbroehl and J.W. Jorgenson, *Anal. Chem.*, 58 (1986) 479.
- 7 S.E. Moring, J.C. Colburn, P.D. Grossman and H.H. Lauer, *LC-GC Int.*, 3 (1990) 46.
- 8 M.W.F. Nielsen, *J. Chromatogr.*, 542 (1991) 173.
- 9 W. Kuhr and C.A. Monning, *Anal. Chem.*, 64 (1992) 389R.
- 10 B.L. Karger, A.S. Cohen and A. Guttman, *J. Chromatogr.*, 492 (1989) 585.
- 11 M.J. Gordon, X. Huang, S.I. Pentoney and R.N. Zare, *Science*, 242 (1988) 224.
- 12 H. Nishi and S. Terabe, *Electrophoresis*, 11 (1990) 691.
- 13 G.M. McLaughlin, J.A. Nolan, J.L. Lindahl, J.A. Morrison and T.J. Bronzert, *J. Liq. Chromatogr.*, 15 (1992) 961.
- 14 M. Swartz, *J. Liq. Chromatogr.*, 14 (1991) 923.
- 15 S. Fujiwara and S. Honda, *Anal. Chem.*, 59 (1987) 2773.
- 16 K.D. Altria and C.F. Simpson, presented at 1st International Symposium on Pharmaceutical and Biomedical Analysis, Barcelona, September 1987.
- 17 C.L. Ng, H.K. Lee and S.F.Y. Li, *J. Chromatogr.*, 598 (1992) 133.
- 18 A.M. Hoyt and M.J. Sepaniak, *Anal. Lett.*, (1989) 861.
- 19 H. Nishi, N. Tsumagari, T. Kakimoto and S. Terabe, *J. Chromatogr.*, 477 (1989) 259.
- 20 H. Nishi, N. Tsumagari and S. Terabe, *Anal. Chem.*, 61 (1989) 2434.
- 21 K.D. Altria and M.M. Rogan, *J. Pharm. Biomed. Anal.*, 8 (1990) 1005.
- 22 H. Nishi, T. Fukuyama and M. Matsuo, *J. Chromatogr.*, 515 (1990) 245.
- 23 M.T. Ackermans, J.L. Beckers, F.M. Everaerts, H. Hoogland and M.J.H. Tomassen, *J. Chromatogr.*, 596 (1992) 101.
- 24 S. Honda, A. Taga, K. Kakehi, S. Koda and Y. Okamoto, *J. Chromatogr.*, 590 (1992) 364.
- 25 T. Nagawaka, Y. Oda, A. Shibukawa, H. Fukuda and H. Tanaka, *Chem. Pharm. Bull.*, 37 (1989) 707.
- 26 G.N. Okafo and P. Camilleri, *Analyst*, 117 (1992) 1421.
- 27 M.T. Ackermans, F.M. Everaerts and J.L. Beckers, *J. Chromatogr.*, 606 (1992) 229.
- 28 K.D. Altria and Y.L. Chanter, *J. Chromatogr.*, 652 (1993) in press.
- 29 K.D. Altria and C.F. Simpson, *J. Pharm. Biomed. Anal.*, 6 (1988) 801.
- 30 K. Salomon, D.S. Burgi and J.C. Helmer, *J. Chromatogr.*, 588 (1991) 335.
- 31 K.D. Altria and N.W. Smith, *J. Chromatogr.*, 538 (1991) 506.

- 32 M. Johannson, R. Pavelka and J.D. Henion, *J. Chromatogr.*, 559 (1991) 515.
- 33 H. Nishi, T. Fukuyama, M. Matsuo and S. Terabe, *J. Chromatogr.*, 513 (1990) 279.
- 34 H. Nishi, T. Fukuyama, M. Matsuo and S. Terabe, *J. Chromatogr.*, 515 (1990) 233.
- 35 Z. Chmela and Z. Stransky, *Cs. Farm.*, 39 (1990) 172.
- 36 H. Soini, T. Tsuda and M.V. Novotny, *J. Chromatogr.*, 559 (1991) 547.
- 37 K.D. Altria, *J. Chromatogr.*, 636 (1993) 125.
- 38 S. Arrowood and A.M. Hoyt Jr., *J. Chromatogr.*, 586 (1991) 177.
- 39 H. Nishi, T. Fukuyama, M. Matsuo and S. Terabe, *Anal. Chim. Acta*, 236 (1990) 281.
- 40 M.T. Ackermans, J.L. Beckers, F.M. Everaerts and I.G.J.A. Seelen, *J. Chromatogr.*, 590 (1992) 341.
- 41 W. Thormann, A. Minger, S. Molteni, J. Caslavská and P. Gebauer, *J. Chromatogr.*, 593 (1992) 275.
- 42 K.D. Altria, *J. Chromatogr.*, 634 (1993) 323.
- 43 Y. Miyashita, S. Terabe and H. Nishi, *Chromatogram*, 11 (1990) 7.
- 44 N. Nishi and M. Matsuo, *J. Liq. Chromatogr.*, 14 (1991) 973.
- 45 H. Nishi, T. Fukuyama, M. Matsuo and S. Terabe, *J. Chromatogr.*, 498 (1990) 313.
- 46 J. Vindevogel and P. Sandra, *Anal. Chem.*, 63 (1991) 1530.
- 47 C.P. Ong, C.L. Ng, H.K. Lee and S.F.Y. Li, *J. Chromatogr.*, 588 (1991) 335.
- 48 M.C. Roach, P. Gozel and R.N. Zare, *J. Chromatogr.*, 428 (1988) 129.
- 49 D. Perrett and G. Ross, *Trends Anal. Chem.*, 11 (1992) 156.
- 50 H. Nishi, T. Fukuyama, M. Matsuo and S. Terabe, *J. Pharm. Sci.*, 79 (1990) 519.
- 51 Y. Tanaka and W. Thormann, *Electrophoresis*, 11 (1990) 760.
- 52 P. Wernly and W. Thormann, *Anal. Chem.*, 63 (1992) 2878.
- 53 W. Thormann, P. Meier, C. Marcolli and F. Binder, *J. Chromatogr.*, 545 (1991) 445.
- 54 P. Wernly and W. Thormann, *Anal. Chem.*, 64 (1992) 2155.
- 55 A. Wainwright, *J. Microcol. Sep.*, 2 (1990) 166.
- 56 R. Weinberger and M. Albin, *J. Liq. Chromatogr.*, 14 (1991) 953.
- 57 K.D. Altria, M.M. Rogan and G. Finlay, *Chromatogr. Anal.*, Aug. (1990) 9.
- 58 K.D. Altria and S.D. Filbey, *J. Liq. Chromatogr.*, 16 (1993) 2281.
- 59 K.D. Altria, C.F. Simpson, A.K. Bharij and A.E. Theobald, *Electrophoresis*, 11 (1990) 732.
- 60 A. Pluym, W. van Ael and M. de Smet, *Trends Anal. Chem.*, 11 (1992) 27.
- 61 K.D. Altria, *Chromatographia*, 35 (1993) 177.
- 62 K.D. Altria, *Chromatographia*, 35 (1993) 493.
- 63 M.B. Evans, P.A. Haywood, D. Johnson, M. Martin-Smith, G. Munro and J.C. Wahlich, *J. Pharm. Biomed. Anal.*, 7 (1989) 1.
- 64 E.V. Dose and G.A. Guiochon, *Anal. Chem.*, 63 (1991) 1154.
- 65 M.J. Sepaniak, R.O. Cole and B.K. Clark, *J. Liq. Chromatogr.*, 15 (1992) 1023.
- 66 S. Fanali and P. Bocek, *Electrophoresis*, 11 (1990) 757.
- 67 S. Wren and R. Rowe, *J. Chromatogr.*, 603 (1992) 235.
- 68 K.D. Altria, D.M. Goodall and M.M. Rogan, *Chromatographia*, 34 (1992) 19.
- 69 R. Kuhn, F. Stoecklin and F. Erni, *Chromatographia*, 33 (1992) 32.
- 70 H. Nishi, T. Fukuyama, M. Matsuo and S. Terabe, *J. Microcolumn Sep.*, 1 (1989) 234.
- 71 S. Fanali, *J. Chromatogr.*, 474 (1989) 441.
- 72 T.E. Peterson and D. Trowbridge, *J. Chromatogr.*, 603 (1992) 298.
- 73 S. Fanali, *J. Chromatogr.*, 545 (1991) 437.
- 74 K.D. Altria, unpublished results.
- 75 M.M. Rogan, C. Drake, D.M. Goodall and K.D. Altria, *Anal. Biochem.*, 208 (1993) 343.
- 76 M.M. Rogan and K.D. Altria, presented at the 5th International Symposium on Chiral Discrimination, Rome, May 1991.
- 77 K.D. Altria, A.R. Walsh and N.W. Smith, *J. Chromatogr.*, in press.
- 78 K.D. Altria, R.C. Harden, P.A. Hailey, M. Hart, J. Hevizi, J. Makwana and M. Portsmouth, *J. Chromatogr.*, in press.
- 79 A. Guttman, A.S. Cohen, D.N. Heiger and B.L. Karger, *Anal. Chem.*, 62 (1990) 137.
- 80 A.S. Cohen, D.R. Najarian, A. Paulus, A. Guttman, J.A. Smith and B.L. Karger, *Proc. Natl. Acad. Sci.*, 85 (1988) 9660.
- 81 D.J. Rose and J.W. Jorgenson, *J. Chromatogr.*, 438 (1988) 23.
- 82 P. Camilleri, G.N. Okafo, C. Southan and R. Brown, *Anal. Biochem.*, 198 (1991) 36.
- 83 N.A. Guzman, L. Hernandez and B.G. Hoebel, *Biopharm.*, 2 (1989) 22.
- 84 K.D. Altria and Y.K. Dave, *J. Chromatogr.*, 633 (1993) 221.
- 85 X.C. Huang, M.A. Quesada and R.A. Mathies, *Anal. Chem.*, 64 (1992) 2149.
- 86 K.D. Altria, *LC-GC Int.*, 6 (March) 1993, 164.
- 87 K.D. Altria and D.C.M. Luscombe, *J. Pharm. Biomed. Anal.*, 11 (1993) 415.
- 88 W.R. Jones and P. Jandik, *J. Chromatogr.*, 546 (1991) 445.
- 89 M.M. Rogan, K.D. Altria and M. Parker, presented at *Ionex '93, Wrexham, March 1993, Chromatographia*, submitted for publication.
- 90 W. Steuer, I. Grant and F. Erni, *J. Chromatogr.*, 507 (1990) 125.
- 91 H. Yamamoto, J. Bauman and F. Erni, *J. Chromatogr.*, 593 (1992) 313.

High-performance chiral displacement chromatographic separations in the normal-phase mode

II. Separation of the enantiomers of 1,2-O-dihexadecyl-*rac*-glycerol-3-O-(3,5-dinitrophenyl)carbamate using the Pirkle-type naphthylalanine silica stationary phase

Pearle L. Camacho-Torralba^{*}, Michelle D. Beeson and Gy. Vigh^{*}

Chemistry Department, Texas A&M University, College Station, TX 77843 (USA)

David H. Thompson

Oregon Graduate Institute of Science & Technology, Beaverton, OR 97006 (USA)

(First received April 2nd, 1993; revised manuscript received May 11th, 1993)

ABSTRACT

A normal-phase displacement chromatographic method has been developed for the preparative-scale separation of the enantiomers of 1,2-O-dihexadecyl-*rac*-glycerol-3-O-(3,5-dinitrophenyl)carbamate using the Pirkle-type covalently bonded naphthylalanine silica chiral stationary phase. The separation selectivity of the system has been maximized by varying the tetrahydrofuran concentration and the temperature of the tetrahydrofuran–hexane eluent within the range constrained by the solubility of the sample and the displacer. The 3,5-dinitrobenzoyl ester of *n*-heptanol, which is more retained under the selected separation conditions than any of the enantiomers of the glycerol ether derivative, was selected and used as displacer in a preparative displacement chromatographic separation of a 20-mg sample of the glycerol ether derivative. For comparison purposes, an analogous overloaded elution mode separation was also completed under identical separation conditions. A large number of product fractions were collected during both the displacement chromatographic run and the corresponding overloaded elution mode run; these were analyzed for enantiomeric purity such that the percent recoveries and the production rates for both separation methods could be calculated.

INTRODUCTION

Earlier, we published an HPLC method [1] for the analytical-scale separation of the enantio-

mers of platelet-aggregating factor analogues and 1,2-O-dihexadecyl-*rac*-glycerol ether derivatives. N-(2)-naphthyl-alaninate silica, a π -electron donor chiral stationary phase developed by Pirkle *et al.* [3–6] for resolution of the enantiomers of solutes which contain a π -acid functional group (most often a 3,5-dinitrobenzoyl or 3,5-dinitrophenylcarbamoyl group) and an H-donor or H-acceptor group, was used for the separation.

^{*} Corresponding author.

^{*} Present address: Lyphomed, Division of Fujisawa USA, Inc., Melrose Park, IL 60160, USA.

Since pure, individual glycerol ether enantiomers are needed for the determination of their respective physico-chemical and pharmacological properties, an attempt was made to develop a preparative displacement chromatographic HPLC method for the production, in 50–500-mg quantities, of these individual enantiomers. Both the chiral displacement chromatographic separations and the displacers used for them have recently been described in detail [7–11]. This paper describes the use of the retention and chiral selectivity data pertaining to the glycerol ether derivatives [1], and 3,5-dinitrobenzoyl ester displacer adsorption data [7] to develop an overloaded elution mode and a displacement mode preparative chiral separation.

EXPERIMENTAL

Materials

Three 250 mm × 4.6 mm I.D. Rexchrom columns, packed with a 5- μ m D-naphthylalanine silica (DNAS) were obtained from Regis (Morton Grove, IL, USA). One column was used for the selectivity optimization studies and analysis of the fractions collected during the preparative chromatographic separations. Two columns, connected in series, were used for the preparative displacement chromatographic separations and the overloaded elution mode separations. All columns were equipped with water jackets and thermostatted by a UF-3 type recirculating water bath (Science/Electronics, Dayton, OH, USA). The temperature was maintained at 5, 10, 15, 20, 30 and 35°C, respectively, as indicated in the legends. Fractions were collected with a Cygnet fraction collector (ISCO, Lincoln, NE, USA).

The eluents, carrier solutions and displacer solutions were prepared by using HPLC-grade *n*-hexane (Baxter, Muskegon, MI, USA) and tetrahydrofuran (THF) (Fisher Scientific, Fair Lawn, NJ, USA). The displacers were synthesized using reagent-grade 3,5-dinitrobenzoyl chloride (DNB) and *n*-pentanol and *n*-heptanol, respectively (Aldrich, Milwaukee, WI, USA). The other chemicals used were obtained from Aldrich, Fluka, Eastman-Kodak (Rochester, NY, USA), Fisher Scientific, or Wiley Organic

(Cochocton, OH, USA), and used without further purification.

Synthetic procedures

The details of displacer synthesis are described elsewhere [7,11]. Briefly, ester-type displacers were synthesized according to the general Schotten-Baumann reaction scheme and purified by repeated crystallization. Some of the displacers designed for chiral separations in the normal-phase mode are now commercially available from ASTEC (Whippany, NJ, USA).

The 1,2-O-dihexadecyl glycerol ether-3-O-(3,5-dinitrophenyl)carbamate derivative (HGC) was synthesized as described in detail in refs. 1 and 12. Briefly, triflic acid-catalyzed opening of the epoxy ring of glycidol 3-nitrobenzenesulfonate ester in the presence of excess *n*-hexadecanol was followed by alkylation with excess *n*-hexadecyl triflate in the presence of equimolar 1,8-bis(dimethylamino)naphthalene, deprotection with tetrabutylammonium hydroxide, isolation of the diether derivative and finally, reaction of the remaining hydroxyl group with 3,5-dinitrophenylisocyanate, generated *in situ* by thermal decomposition of the corresponding azide [6].

Apparatus

A liquid chromatograph consisting of a Type 2020 pump, a Type 2050 variable wavelength UV detector (all from Varian, Walnut Creek, CA, USA), a pneumatically activated, computer-controlled Type 7125 injection valve (Rheodyne, Cotati, CA, USA) equipped with 10 and 50- μ l sample loops, and a Maxima 820 Chromatographic Work Station (Millipore, Bedford, MA, USA) was used for the selectivity optimization and the fraction analysis work. All preparative separations were carried out with a custom-built displacement chromatograph consisting of two Type 2020 pumps, a Type 2050 variable-wavelength UV detector (set at 390 nm) and a Type RI-3 differential refractive index (RI) detector (all from Varian) [8]. The samples were injected by a pneumatically activated, computer-controlled Type 7125 injection valve (Rheodyne) equipped with 100- μ l to 5-ml sample loops, and a Type 7010 switching valve (Rheodyne). The

dead volume of each individual column was determined at the respective separation temperature by injecting an *n*-heptane:THF sample into the *n*-hexane:THF eluent and recording the signal of the differential refractive index detector. At 15°C, the dead volume of the preparative separation column was 5.91 ± 0.02 ml. A Type 4270 integrator (Varian), connected to a NEC Powermate I AT computer (Computer Access, College Station, TX, USA) and running the Chromplot-1 program developed in our laboratory [8], was used for system control, data collection and analysis.

Displacement chromatographic separations

The operational sequence described in ref. 8 was followed here. Briefly, at first, the columns were equilibrated with the carrier solvent, while the displacer solution was pumped into a dummy column to precompress it to the operating pressure. Next, the sample, dissolved in the carrier solvent and loaded into the sample loop, was injected by activating the Rheodyne 7125 valve. After an experimentally determined period of time, the Rheodyne 7125 injection valve was turned back to the load position, and the Rheodyne 7010 switching valve was activated to introduce the displacer solution into the analytical column and re-route the carrier solvent into the dummy column. This injection sequence prevented the displacer from passing through the loop behind the sample and losing some of the sharpness of its rear boundary. Both the UV detector signals and the RI detector signals were recorded simultaneously. As soon as the first enantiomer began to emerge from the column, 32.5- μ l sample fractions were collected with the Cygnet fraction collector. The data collection and the fraction collection processes were terminated when the RI detector signal reached its plateau corresponding to the feed concentration of the displacer.

Column regeneration

Following the displacement chromatographic runs, the displacer was removed from the columns by pumping THF through them at flow-rates as high as permitted by the pressure limit of the system. After the absorbance of the effluent

decreased back to that of the THF wash, the carrier solvent pump was turned on to re-equilibrate the column for the next run.

Overloaded elution mode separations

For a simple, direct comparison, overloaded elution mode separations were completed under the same (non-optimized) conditions as the displacement mode separations, except that no displacer was used and no column regeneration step was necessary.

Fraction analysis

Once the preparative separation was completed, the solvent was evaporated from each collected fraction. The residues were redissolved in identical volumes of the eluent that contained an achiral internal standard as well, and analyzed for chiral purity. The analysis conditions were optimized to achieve complete separation of both enantiomers and the displacer in the shortest period of time. Peak areas were converted to concentrations using individual calibration curves. The reconstructed displacement chromatograms and the reconstructed overloaded elution mode chromatograms were derived from these concentrations and from the fraction volume data.

RESULTS AND DISCUSSION

Retention studies of the HGC enantiomers

The retention behavior of the HGC enantiomers was studied at 35°C using various THF–*n*-hexane eluents. The capacity factor values, k' , and the separation selectivity values, α , as a function of the % (v/v) THF concentration are shown in Figs. 1 and 2, respectively. Both the capacity factors and the separation selectivity increase monotonously with decreasing THF content in the eluent.

Because the column temperature effects both the retention of the solutes and the separation selectivity, the k'_2 and the α values of HGC were also determined at 5, 10, 15, 20 and 30°C using the THF–*n*-hexane (7.5:92.5, v/v) eluent. The results are shown in Figs. 3 and 4; the expected van 't Hoff-type behavior is observed. Though the chiral selectivity is the highest at

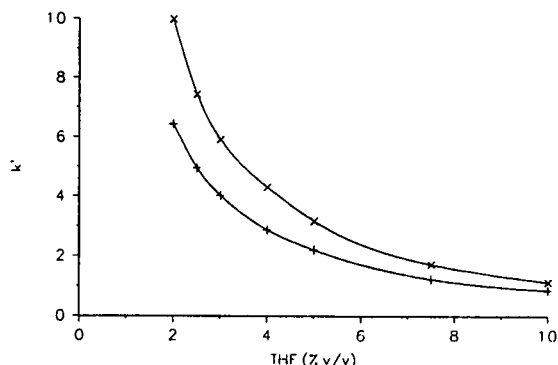


Fig. 1. k' values of the *R*- and the *S*-enantiomers of HGC as a function of the % (v/v) THF concentration in the THF-*n*-hexane eluent at 35°C. Symbols: + = *S*-HGC; × = *R*-HGC.

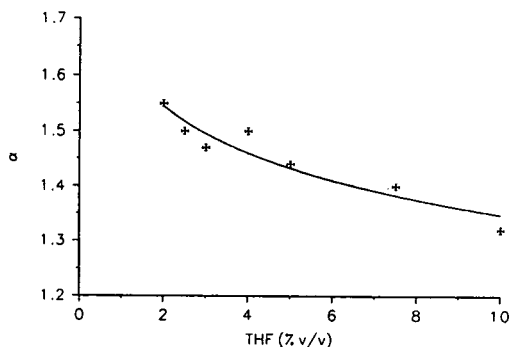


Fig. 2. α values for the separation of the *R*- and the *S*-enantiomers of HGC as a function of the % (v/v) THF concentration in the THF-*n*-hexane eluent at 35°C.

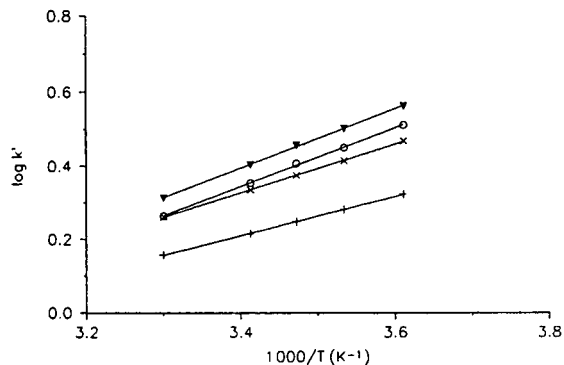


Fig. 3. $\log k'$ of the *R*- and *S*-enantiomers of HGC, and the DNB esters of *n*-pentanol and *n*-heptanol as a function of the inverse absolute column temperature. Eluent: 7.5% (v/v) THF in *n*-hexane. Symbols: + = *S*-HGC; × = *R*-HGC; ○ = C_7 DNB; ▼ = C_5 DNB.

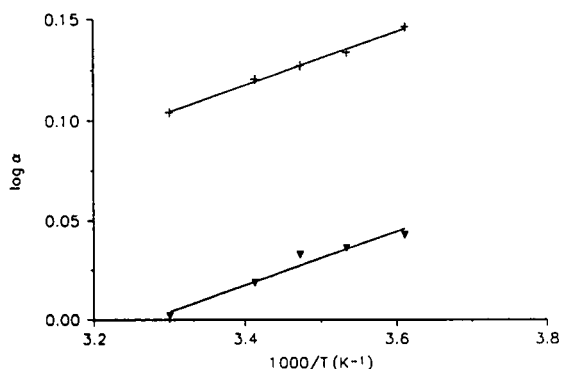


Fig. 4. α values for the separation of the enantiomers of HGC, and the *R*-enantiomer of HGC and the DNB ester of *n*-heptanol as a function of the inverse absolute column temperature. Eluent: 7.5% (v/v) THF in hexane. Symbols: + = *R*-HGC/*S*-HGC; ▼ = C_7 DNB/*R*-HGC.

5°C, a highly desirable feature for preparative work, the solubility of the HGC enantiomers is much lower there than at 15°C. Therefore, as a practical compromise, all preparative separations were completed at 15°C.

The chromatogram of a very dilute sample of the racemic mixture of HGC, obtained using THF-*n*-hexane (7.5:92.5, v/v) eluent at a 15°C and a 0.5 ml/min flow-rate, is shown in Fig. 5. This eluent represents a promising carrier solution composition for preparative displacement chromatography given the resolution characteristics observed.

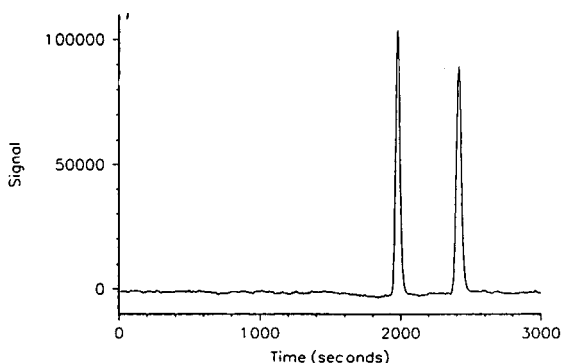


Fig. 5. Chromatogram of a very dilute sample of the racemic mixture of HGC. Eluent: 7.5% (v/v) THF in *n*-hexane at 15°C and 0.5 ml/min flow-rate. First peak: *S*-HGC, second peak: *R*-HGC.

Selection of the displacer

The success of a displacement chromatographic separation critically depends not only on the value of the selectivity factor, but also, on the availability of a suitable displacer. The displacer must meet contradictory criteria: its chromatographic characteristics should, preferably, be similar to those of the solute, have a convex adsorption isotherm, be adsorbed more strongly on the stationary phase than the more retained of the enantiomers, and be highly soluble in the carrier solvent to allow the preparation of concentrated displacer solutions. For Pirkle-type stationary phases, a successful generic displacer structure has been determined: the displacer should contain a π -acid (e.g. a 3,5-dinitrophenyl) or π -base (e.g. a naphthylamine-) anchor group, a hydrogen-donor/acceptor group (e.g. an amide group), and a hydrophobic, solubility adjusting group (e.g. a long-chain alkyl group) [7]. Preferably, these functional groups should be attachable to a common core structure using inexpensive reagents and simple preparative methods. Recently, we synthesized a homologous series of 3,5-dinitrobenzoyl esters of alcohols (DNB esters) and determined their retention and adsorption characteristics on Pirkle-type stationary phases [7]. These data indicate that at 35°C, the 3,5-dinitrobenzoyl esters of *n*-heptanol (C_7 DNB ester) and *n*-pentanol (C_5 DNB ester) are more retained than the *R*-enantiomer of HGC, and could be considered as potential displacers. k' values of the C_5 DNB esters and C_7 DNB esters, determined as a function of temperature, are shown in Fig. 3. The selectivity factor calculated for the separation of the *R*-enantiomer of HGC and the less retained displacer, the C_7 DNB ester, is shown in Fig. 4. The *n*-heptyl derivative was selected as displacer, since both the separation selectivity and the solubility of the C_7 DNB ester are sufficiently high in the carrier solution at 15°C.

The displacement chromatographic separation

The displacement chromatogram of a 20.1 mg sample of crude HGC racemate using two 250 mm \times 4.6 mm I.D. Rexchrom DNAS columns at 15°C, 7.5% (v/v) THF in *n*-hexane carrier, 150 mM *n*-heptyl DNB displacer, and a flow-rate of

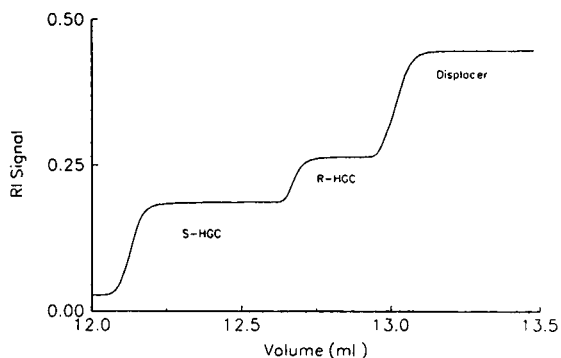


Fig. 6. Displacement chromatogram of a 20.1-mg sample of crude racemic HGC. For conditions see text.

0.5 ml/min is shown in Fig. 6. The reconstructed chromatogram (determined from the analysis of the collected fractions), is shown in Fig. 7. (An impurity, the DNB carbamate of *n*-hexadecanol, a by-product in the synthesis of the HGC sample, is more retained than the *R*-enantiomer of HGC, but less than the C_7 DNB ester displacer.) The bands of the enantiomers are clearly separated and sharp indicating that the 20 mg sample does not exhaust the loading capacity of the column.

For the sake of comparison, an overloaded elution mode separation of a 24-mg aliquot of the HGC sample was also completed using the same experimental conditions as in the displacement mode. The recorded and reconstructed chromatograms are shown in Figs. 8 and 9,

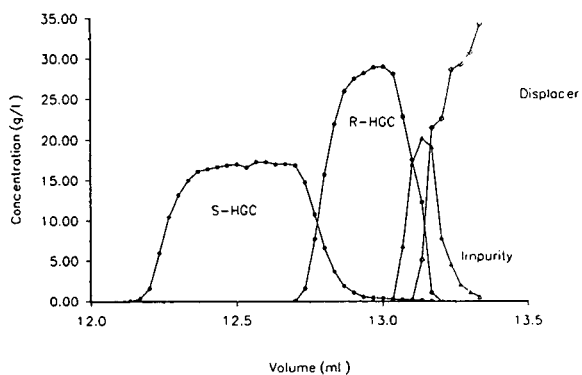


Fig. 7. Reconstructed displacement chromatogram of a 20.1-mg sample of crude racemic HGC. For conditions see text.

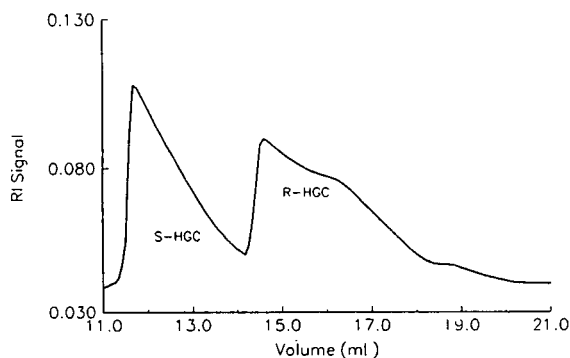


Fig. 8. Overloaded elution mode chromatogram of a 24-mg sample of crude racemic HGC. For conditions see text.

respectively. These chromatograms display a prominent tag-along effect, first described by Golshan-Shirazi and Guiochon [13], and the splitting of the *R*-HGC band into two parts by the impurity. The concentration maxima are about three-to-four times lower than in the displacement mode.

Purity calculations

Enantiomeric purity calculations. The reconstructed chromatograms can be unambiguously charted from the well defined purities of the individually collected fractions. However, the collected fractions can be pooled in a number of ways resulting in products of different enantiomeric purity. For example, in forward pooling, the pooling for the less retained enantiomer starts with the first fraction and proceeds toward

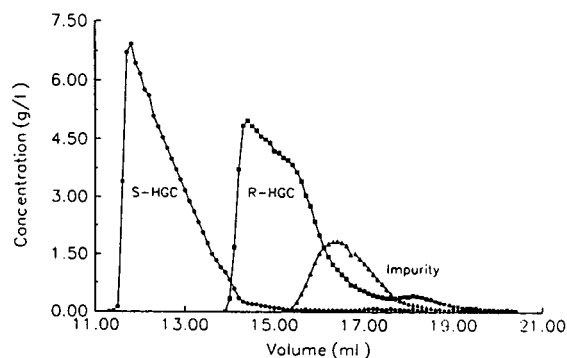


Fig. 9. Reconstructed overloaded elution mode chromatogram of a 24-mg sample of crude racemic HGC. For conditions see text.

increasing fraction numbers; the enantiomeric purity remains high, up to the point where the more retained enantiomer first appears in the individual fractions. At this point, the enantiomeric purity of the pooled material begins to decrease rapidly. Therefore, a certain target level of purity for the pooled product can be specified and the pooling process can be stopped there. To forward pool the more retained enantiomer, one can start where pooling of the less retained enantiomer was stopped and proceed towards increasing fraction numbers. In this case, the enantiomeric purity for the more retained enantiomer increases from an initial low value towards a high, but certainly less than 100%, value. Naturally, the purity level for the pooled, more retained enantiomer will be constrained by the amount of the less retained enantiomer contamination introduced in the first few fractions. Alternatively, backward pooling can be used for the more retained enantiomer; here pooling starts with the last collected fraction and proceeds towards decreasing fraction numbers. The enantiomeric purity of the pooled material then decreases from 100% (*i.e.*, no less retained enantiomer tailing into the last fractions of the more retained enantiomer), or from a high, but less than 100% value, towards a pre-specified enantiomeric purity level for the pooled (more retained) product. Pooling can be stopped once this target purity level is reached. A number of other pooling schemes are also possible. Pooling then becomes an involved optimization problem, but once optimized, it will yield the highest amount of material at a specified level of enantiomeric purity. Often, though, the latter schemes are not practical due to the amount of labor involved. Therefore, only the simple schemes were used in the subsequent calculations: forward pooling for the less retained enantiomer and backward pooling for the more retained enantiomer.

The calculated enantiomeric purity of the pooled fractions as a function of the amount of the pure enantiomer recovered is shown in Fig. 10 for the displacement mode separation, and in Fig. 11, for the overloaded elution mode separation. In the displacement mode, if one wants to recover 7.5 mg of each enantiomer, it can be

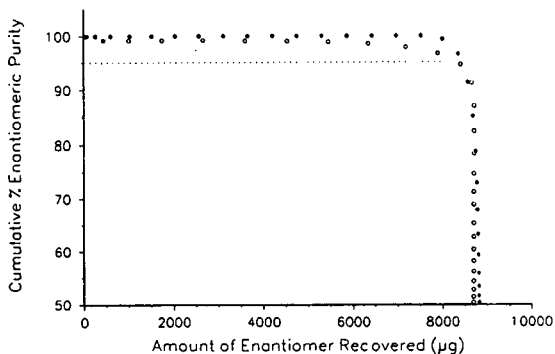


Fig. 10. Cumulative % enantiomeric purity as a function of the amount of HGC enantiomer recovered in the displacement mode separation. Symbols as in Fig. 7.

done at 100% enantiomeric purity for the less retained enantiomer (*S*-HGC) and at 97.5% enantiomeric purity for the more retained enantiomer (*R*-HGC). However, if one wants recover more of the enantiomers, the optical purity of the pooled products decreases very rapidly. In the overloaded elution mode, 10 mg of the *S*-enantiomer of HGC can be recovered at a 100% enantiomeric purity, however, due to the steady presence of the less retained enantiomer in the band of the more retained one (tag-along effect), enantiomeric purity of the *R*-enantiomer of HGC is never higher than 95%, regardless of the quantity recovered.

Component purities. In addition to the enantiomeric purities, the component purities of the pooled fractions were also calculated,

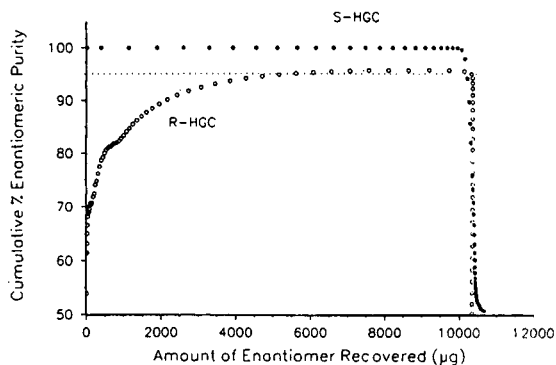


Fig. 11. Cumulative % enantiomeric purity as a function of the amount of HGC enantiomer recovered in the overloaded elution mode separation. Symbols as in Fig. 7.

because a contaminant of different chemical composition was also present in the sample. In displacement mode, the percent component purities for *S*-HGC (forward pooling) are the same as the enantiomeric purities, because the additional contaminant does not interfere with the band of *S*-HGC. However, because *R*-HGC is flanked on both sides by an interfering component (*S*-HGC at the front, and the contaminant at the rear), the amount of material that can be recovered at the 97.5% component purity level is only 5.4 mg. If the purity requirement for the pooled material is relaxed to 95%, 6.3 mg of *R*-HGC (63% of the loaded amount) can be recovered.

In overloaded elution mode for *S*-HGC, the % component purities are the same as the enantiomeric purities, because the contaminant does not interfere with the *S*-HGC band. For the more retained enantiomer the component purities are lower due to the presence of the reaction by-product; 2.8 mg of *R*-HGC can be recovered at the 97.5% component purity level (28% of the loaded material), and 5.6 mg at the 95% purity level (56% of the loaded material).

% Recoveries. When the pooled amounts of each enantiomer are divided by the total amount of the respective enantiomer loaded and plotted against the enantiomeric purity of the pooled fraction, the cumulative recovery curves for the enantiomers are obtained for the displacement (Fig. 12) and overloaded elution modes (Fig. 13). For *S*-HGC, the % recoveries are similar in

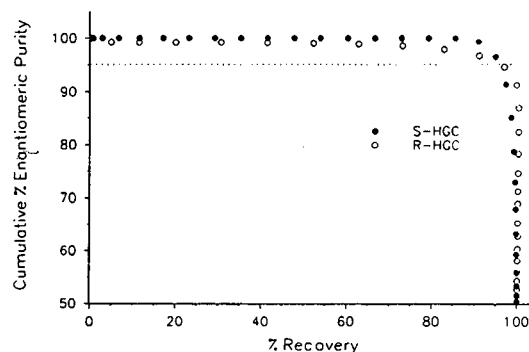


Fig. 12. Cumulative % enantiomeric purity as a function of the % recovery rate of the HGC enantiomers in the displacement mode separation. Symbols as in Fig. 7.

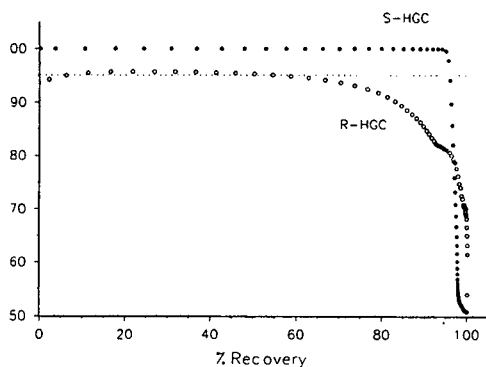


Fig. 13. Cumulative % enantiomeric purity as a function of the % recovery rate of the HGC enantiomers in the overloaded elution mode separation. Symbols as in Fig. 7.

both the displacement and the overloaded elution modes. For *R*-HGC, however, the % recoveries are slightly better in the displacement mode.

CONCLUSIONS

It has been found that the selectivity factor could be maximized by varying the THF concentration and eluent temperature over the range constrained by the solubility limits of the sample; capacity factors of the more retained glycerol ether enantiomer could be adjusted to the $2 < k' < 10$ range, as desired for the displacement chromatographic separation. Using *n*-heptyl DNB ester as displacer, 20 mg of a crude racemic HGC sample could be separated on 4.6 mm I.D. analytical columns at good enantiomeric purity and yield. By injecting 24 mg of the same crude racemic HGC sample, broadly comparable purity and yield values were observed in the complementary overloaded elution mode separation.

ACKNOWLEDGEMENTS

Partial financial support by the National Science Foundation (CH-8919151), the Texas Coordinating Board of Higher Education TATR Program (Grant Number 3376) and the Dow Chemical Company, Midland, MI, USA to Gy.V., and by the Department of Energy, Office of Basic Energy Sciences (DE-FG 06-88 ER13963) to D.H.T. is gratefully acknowledged.

REFERENCES

- 1 P.L. Camacho, E. Geiger, Gy. Vigh, R. Webster and D.H. Thompson, *J. Chromatogr.*, 506 (1990) 611.
- 2 W.H. Pirkle, J.M. Finn, J. L. Schreiner and B.C. Hamper, *J. Am. Chem. Soc.*, 103 (1981) 3964.
- 3 W.H. Pirkle and T.C. Pochapsky, *J. Org. Chem.*, 51 (1986) 102.
- 4 W.H. Pirkle and T.C. Pochapsky, *J. Am. Chem. Soc.*, 108 (1986) 352.
- 5 W.H. Pirkle and T.C. Pochapsky, *J. Am. Chem. Soc.*, 108 (1986) 5267.
- 6 W.H. Pirkle, T.C. Pochapsky, G.S. Mahler, D.E. Corey, D.S. Reno and D.M. Alessi, *J. Org. Chem.*, 51 (1986) 102.
- 7 P.L. Camacho, Gy. Vigh, and D.H. Thompson, *J. Chromatogr.*, 641 (1993) 31.
- 8 Gy. Vigh, G. Quintero and Gy. Farkas, *J. Chromatogr.*, 484 (1989) 251.
- 9 Gy. Vigh, G. Quintero and Gy. Farkas, *J. Chromatogr.*, 484 (1989) 256.
- 10 Gy. Vigh, L.H. Irgens and Gy. Farkas, *J. Chromatogr.*, 502 (1990) 11.
- 11 P.L. Camacho, *Dissertation*, Texas A&M University, College Station, TX, 1991.
- 12 D.H. Thompson, C.B. Svendsen, C. Di Meglio, V.C. Anderson, *J. Org. Chem.*, submitted for publication.
- 13 S. Golshan-Shirazi and G. Guiochon, *Anal. Chem.*, 62 (1990) 220.

CHROM. 25 223

Nitroxide radicals in studies of the fine bonded layer structure of modified silicas

Pavel G. Mingalyov, Alexander Yu. Fadeev*, Sergei M. Staroverov and Georgii V. Lisichkin

Laboratory of Petrochemical Synthesis, Chemical Department, Lomonosov State University, Len. Gory, 119899 Moscow (Russian Federation)

Elena V. Lunina

Laboratory of Adsorption, Chemical Department, Lomonosov State University, Len. Gory, 119899 Moscow (Russian Federation)

(First received April 2nd, 1992; revised manuscript received February 22nd, 1993)

ABSTRACT

Spin probe and spin label methods were applied in studies of the fine structure of both reversed-phase and functionalized modified silicas. The concept of a “rigid” structure for narrow-pore alkyl-modified silicas was experimentally supported. “Two-level” sorption of the solute in the bonded layer of end-capped alkyl-modified silicas was discovered. The stability of arch structures arising in the bonded layer of functionalized modified silicas was studied. It was shown that arch structures could be effectively destroyed in solvents with high basicity.

INTRODUCTION

Electron spin resonance (ESR) spectroscopy using paramagnetic probes and labels seems to be one of the most promising and informative techniques for the characterization of bonded layers of chemically modified silicas. The application of paramagnetic labels allows one to obtain important data on the organization of bonded molecules over the silica surface [1–6], the structure of bonded affinity ligands [7] and the dynamic behaviour of bonded molecules under various conditions [1,2,8–11].

Unfortunately, spin labelling in general leads to misrepresentation of the bonded layer structure and does not allow the study of some real

stationary phases. On the other hand, the paramagnetic probe method, unlike spin labelling, is more suitable for studying both the nature of the adsorption sites of an adsorbent and the behaviour of an adsorbate. The main advantages of the application of the spin probe method in surface science have been described in reviews [12,13].

This paper summarizes results obtained in our laboratory on the application of both spin probes and labels in the characterization of chemically modified silicas, which are widely employed as stationary phases in modern HPLC.

EXPERIMENTAL

Synthesis of reversed-phase bonded silicas

Modification of the initial silicas was carried out using trichloro- and monochlorosilanes. A

* Corresponding author.

portion of sample was end-capped with a mixture of trimethylchlorosilane and hexamethyldisilazane (1:1). Modification and end-capping were done as described elsewhere [14–16] using anhydrous toluene as a solvent and pyridine as an activator.

Adsorption of a spin probe

Adsorption of 2,2,6,6-tetramethylpiperidone-4-oxyl-1 (TEMPO) and 2,2,6,6-tetramethyl-4-aminopiperidine-1-oxyl (TEMPO-Amine) was carried out from dilute diethyl ether solutions with further evaporation of the solvent *in vacuo*. The amount of adsorbed radical (m_r) was varied from 0.007 to 0.049 mmol/g. The surface concentration of adsorbed radicals (C_r) was calculated as [17–19]

$$C_r \text{ (mmol/m}^2\text{)} = m_r/S_r \quad (1)$$

where S_r is the surface area accessible to 2,2,6,6-tetramethylpiperidone-4-oxyl-1, calculated as [17–19]

$$S_r = S_{\text{BET}}(\sigma_r/\sigma_{\text{benz}})^{(2-d)/2} \quad (2)$$

where S_{BET} is the specific surface area determined by benzene adsorption, σ_{benz} and σ_r are the adsorptional areas of benzene and radicals on silica, 0.49 [20] and 1.21 m² [21], respectively, and d is the surface fractal dimension of the silicas used: $d = 2.0$ for S-80, S-120 and Li-500, 2.3 for A-300, 2.6 for Si-100 and Si-60 and 2.8 for Si-600 [19].

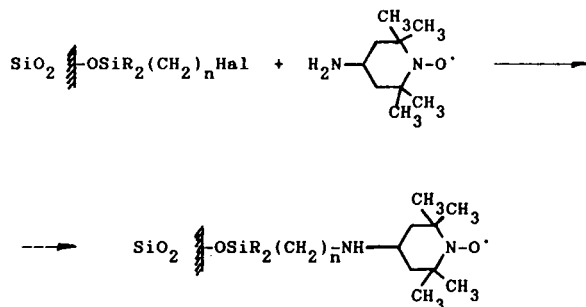
Synthesis of ω -haloalkyl-bonded silicas

Modification of the initial silicas was carried out using ω -haloalkylchlorosilanes, $\text{ClR}_2\text{Si}(\text{CH}_2)_n\text{Hal}$, as modifiers: $n = 1$ and 3, $\text{R} = \text{CH}_3$, $\text{Hal} = \text{Br}$ and $n = 11$, $\text{R} = \text{Cl}$, $\text{Hal} = \text{Cl}$. The latter sample was end-capped with trimethylchlorosilane.

The procedure for modification was as follows: 1 g of vacuum-dried silica was stirred in boiling anhydrous toluene containing 1 mmol of modifier for 10 h, then the sorbents were washed consecutively with anhydrous toluene, toluene, acetone, acetone–water (1:1) and acetone and subsequently washed in a Soxhlet apparatus with diethyl ether for 6 days.

Spin labelling

2,2,6,6-Tetramethyl-4-aminopiperidine-1-oxyl was attached to the modified silicas via the following reaction:



A 1-g amount of ω -haloalkyl-bonded silica was stirred with absolute dimethylformamide containing 1 mmol of label and 1 mmol of N,N-diisopropylethylamine for 3 h at 80–90°C. The labelled sorbents were washed consecutively with acetone, distilled water, saturated NaHCO_3 solution and distilled water and then washed in a Soxhlet apparatus with acetone–water (1:1) for 2 days.

ESR measurements

Measurements were made with an RE-1307 ESR spectrometer. Dry sample was placed in a glass tube and evacuated to a pressure of 0.01 Torr (1 Torr = 133.322 Pa). The sample covered with a solvent was placed in a glass tube, frozen with liquid nitrogen and evacuated to a pressure of 0.01 Torr. The correlation time τ_c was determined in accordance with published methods [22,23].

A_{\parallel} was determined from the ESR spectra as described [22,23]. The isotropic g -factor was obtained using diphenylpicrylhydrazyl as internal standard. The total amount of both immobilized and adsorbed radicals was determined by integrating the ESR spectra.

Determination of bonding density

Bonding densities of attached molecules were calculated from the carbon analysis data and specific surface area [24,25].

Determination of specific surface area

Specific surface area was determined by benzene adsorption [20].

RESULTS AND DISCUSSION

Modelling of behaviour of an adsorbate on the reversed-phase bonded silica surface

Effects of alkyl chain length, type of anchor group and end-capping. The radical used (2,2,6,6-tetramethylpiperidone-4-oxyl-1) seems to be suitable for probing various adsorption sites on reversed-phase bonded silicas. Indeed, this probe can interact both with bonded alkyl groups via Van der Waals's forces and specifically with residual silanol groups. As a measure of the probe mobility the correlation time τ_c was chosen. This value is the reciprocal of the radical rotation frequency [23] and can easily be obtained from ESR spectra.

The characteristics of the sorbents under study are presented in Table I. To avoid the effect of surface concavity, wide-pore silicas were used.

The synthesized sorbents may be classified into four groups on the basis of the functionality of the silane used and end-capping.

(I) The first group consists of sorbents modified with trichlorosilanes (Table I, Nos. 1–3). When adsorbed on such samples, the probe shows only a slow rotation mode in the ESR spectra (Table II). This seems to be connected with the strong specific interaction between the probe and silanol groups (Fig. 1A). The latter have been shown to exist on the surface in large amounts after hydrolysis of non-reacted Si–Cl groups [14,15,26]. It should be emphasized that “rapid” rotation of probes does not occur even at 130°C.

Thus, accessible silanol groups obviate the role of Van der Waals interactions between an adsor-

TABLE I
CHARACTERISTICS OF THE MODIFIED SILICAS STUDIED

No.	Initial silica	Modifier	Specific surface area (m ² /g)	Average pore diameter (nm)	Carbon percentage	Bonding density ^a (μmol/m ²)	End-capping	Designation
1	Silokhrom (S-80)	C ₈ H ₁₇ SiCl ₃	67	50	1.8	2.50	–	C ₈ T
2	S-80	C ₁₂ H ₂₅ SiCl ₃	67	50	4.0	3.66	–	C ₁₂ T
3	S-80	C ₁₈ H ₃₇ SiCl ₃	67	50	5.5	3.66	–	C ₁₈ T
4	S-80	(CH ₃) ₃ SiCl	67	50	1.3	3.83	–	C ₁ M
5	S-80	<i>t</i> -C ₄ H ₉ SiMe ₂ Cl	67	50	2.0	3.66	–	<i>t</i> -C ₄ M
6	LiChrosorb (Li-500)	C ₄ H ₉ SiMe ₂ Cl	90	50	2.7	3.83	–	C ₄ M
7	Li-500	C ₆ H ₁₃ SiMe ₂ Cl	90	50	3.0	3.66	–	C ₆ M
8	Armsorb A-300	C ₁₆ H ₃₃ SiMe ₂ Cl	166	25	10.3	3.33	–	C ₁₆ M
9	S-80	C ₈ H ₁₇ SiCl ₃	67	50	2.0	2.50	+	C ₈ T/s
10	S-80	C ₁₂ H ₂₅ SiCl ₃	67	50	4.1	3.66	+	C ₁₂ T/s
11	A-300	C ₁₆ H ₃₃ SiCl ₃	166	25	10.6	3.50	+	C ₁₆ T/s
12	S-80	C ₁₈ H ₃₇ SiCl ₃	67	50	5.6	3.66	+	C ₁₈ T/s
13	Li-500	C ₄ H ₉ SiMe ₂ Cl	90	50	2.7	3.83	+	C ₄ M/s
14	Li-500	C ₆ H ₁₃ SiMe ₂ Cl	90	50	3.0	3.66	+	C ₆ M/s
15	S-80	C ₁₆ H ₃₃ SiMe ₂ Cl	67	50	5.0	3.66	+	C ₁₆ M/s
16	Silasorb Si-100	C ₁₆ H ₃₃ SiMe ₂ Cl	283	11.3	15.3	3.25	–	C ₁₆ /Si-100
17	Silasorb Si-60	C ₁₆ H ₃₃ SiMe ₂ Cl	213	10.5	10.9	2.90	–	C ₁₆ /Si-60
18	Silasorb Si-600	C ₁₆ H ₃₃ SiMe ₂ Cl	476	5.4	17.6	2.24	–	C ₁₆ /Si-600

^a Determined before end-capping.

TABLE II

EFFECT OF TYPE OF MODIFIER ON STATE OF THE PROBE ADSORBED IN THE BONDED LAYER

No.	Designation ^a	Probe concentration (mmol/g)	Correlation time τ_c (s)		Activation energy of rotation (kJ/mol)	Log of dispersion of probe distribution on correlation time	
			20°C	136°C		20°C	136°C
<i>Modifier RSiCl₃, probe TEMPON</i>							
1	C ₈ T		1.5 · 10 ⁻⁸	5 · 10 ⁻⁹	9.1		
2	C ₁₂ T		2 · 10 ⁻⁸	5 · 10 ⁻⁹	12.9		
3	C ₁₈ T		2 · 10 ⁻⁸	N.d. ^b	N.d.		
<i>Modifier RSiMe₂Cl, probe TEMPON</i>							
4	C ₁ M	0.0067	5 · 10 ⁻⁹	2.5 · 10 ⁻⁹	5.1	1	1
5	<i>t</i> -C ₄ M	0.0067	2 · 10 ⁻⁸	3.9 · 10 ⁻⁹	11.2	1	1
6	C ₄ M	0.0090	2 · 10 ⁻⁸	3.2 · 10 ⁻⁹	14.4	1	1
7	C ₆ M	0.0090	1 · 10 ⁻⁸	N.d.	N.d.	1	N.d.
8	C ₁₆ M	0.0067	2 · 10 ⁻⁸	7 · 10 ⁻⁹	N.d.	1	4
8	C ₁₆ M	0.0110	1 · 10 ⁻⁸	N.d.	N.d.	2	N.d.

^a According to Table I.^b Not determined.

bate and attached chains and completely define the state of adsorbed molecules. It is noteworthy that an analogous result was obtained earlier for fluorescent probes adsorbed on alkylated silicas [19,27].

(II) Sorbents modified with monochlorosilanes belongs to the second group (Table I, Nos. 4–8). The adsorbed probe, like that on the trichlorosilane-modified silicas, shows only a slow rotation mode at room temperature. For long-chain silicas an increase in temperature leads to a substantial increase in the dispersion of the radical distribution with their correlation times. An analogous effect also takes place as the probe concentration increases (Table II).

The observed phenomena are probably connected with the weaker “adsorbate–silanol

group” interaction compared with that for silicas modified with trichlorosilanes. The weakest hydrogen bonds are evidently destroyed on increasing the temperature. On the other hand, the amount of comparatively strong hydrogen bonds is limited and an increase in probe concentration leads to an increase in weaker hydrogen bonds. We assume that these effects result in polydispersity of adsorption states.

(III) The third group contains sorbents modified with trichlorosilane and further end-capped (Table I, Nos. 9–12). End-capping is known to change considerably the bonded layer structure of modified silicas [14,15]. First, end-capping shields surface silanol groups and therefore increases markedly the hydrophobicity of the bonded layer [8,19,28–30]. Second, the chain mobility was found to decrease after end-capping. This was ascribed to association between alkyl chains and trimethylsilyl groups [31]. Spin-lattice relaxation time measurements on the ¹³C NMR signals also showed that the mobility of bonded alkyl chains decreases after end-capping [26,32].

The above features of end-capped samples must influence the behaviour of adsorbed probes. Indeed, for the samples obtained using

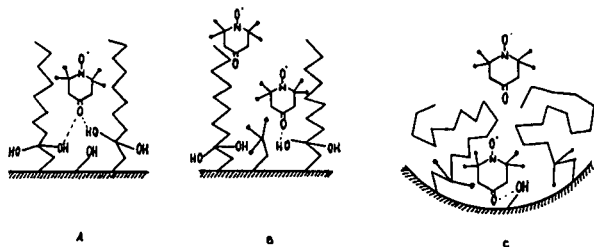


Fig. 1. Various states of probe adsorbed in the bonded layer.

long-chain trichlorosilanes and further end-capped, one can observe two different adsorption states: “rapidly” and “slowly” rotating probes (Table III). This may be connected with the “loosening” of the bonded layer due to bulky trimethylsilyl attached groups (Fig. 1B). Rapidly rotating probes are adsorbed in the upper part of the bonded layer and interact with bonded alkyl chains only by Van der Waals's forces. On the other hand, the slow type of rotation is inherent in probes which are specifically adsorbed on residual silanol groups. It was shown that the number of accessible silanol groups is limited. Hence increasing the probe loading results in an increase in the proportion of rapid rotation. Increasing the temperature also leads to an increase in the proportion of rapid rotation (Table III).

The observed results show that specific interaction of the probe with the surface is weaker

than for non-end-capped samples. Hence end-capping of silicas modified with trichlorosilanes shields residual silanol groups, although the total shielding could hardly be achieved in this way.

(IV) Greater shielding of the silica surface can be achieved using monochlorosilanes with further end-capping (Table I, Nos. 13–15). On these samples the proportion of rapid rotation is three to four times greater than that one for samples modified with trichlorosilanes at room temperature and the value even reaches 100% at 100°C (Table III). It is remarkable that such an effect of “two-level” sorption is so sharply pronounced only for long bonded chains (more than eight carbon atoms). The proportion of rapidly rotating probes decreases as the chain length is decreased and for short-chained samples the value reaches zero (Table III).

Effect of the support pore diameter. In our previous theoretical [25,33] and experimental

TABLE III

EFFECT OF END-CAPPING ON STATE OF THE PROBE ADSORBED IN THE BONDED LAYER

<i>Modifier RSiCl₃/end-capped</i>									
No.	Designation ^a	Probe	Correlation time τ_c of “slow” form (s)		Proportion of “slow” form (%)		Correlation time τ_c of “rapid” form (s)		
			20°C	92°C	20°C	92°C	20°C	92°C	
9	C ₈ T/s	TEMPO	2 · 10 ⁻⁸	5 · 10 ⁻⁹	70	70	5 · 10 ⁻⁹	1 · 10 ⁻⁹	
10	C ₁₂ T/s	TEMPO	2 · 10 ⁻⁸	1 · 10 ⁻⁸	50	50	2 · 10 ⁻⁹	1 · 10 ⁻⁹	
11	C ₁₆ T/s	TEMPO	2 · 10 ⁻⁸	1 · 10 ⁻⁸	90	70	1 · 10 ⁻¹⁰	1 · 10 ⁻¹¹	
	C ₁₆ T/s	TEMPO-Amine	2 · 10 ⁻⁸	N.d. ^b	ca. 100	N.d.	N.d.	N.d.	
12	C ₁₈ T/s	TEMPO	2 · 10 ⁻⁸	N.d.	85	N.d.	1 · 10 ⁻¹⁰	N.d.	

<i>Modifier RSiMe₂Cl/end-capped, probe TEMPO</i>									
No.	Designation ^a	Probe concentration (mmol/g)	Correlations time τ_c of “slow” form (s)		Proportion of “slow” form (%)		Correlation time τ_c of “rapid” form (s)		Activation energy of rotation (kJ/mol)
			20°C	136°C	20°C	136°C	20°C	136°C	
13	C ₄ M/s	0.009	3 · 10 ⁻⁹	1.5 · 10 ⁻⁹	100	100	–	–	10.7
14	C ₆ M/s	0.009	1 · 10 ⁻⁸	5 · 10 ⁻⁹	ca. 100	95	N.d.	1 · 10 ⁻⁹	N.d.
15	C ₁₆ M/s	0.007	1 · 10 ⁻⁸	–	60	0	1 · 10 ⁻⁹	1 · 10 ⁻⁹	15.4

^a According to Table I.

^b Not determined.

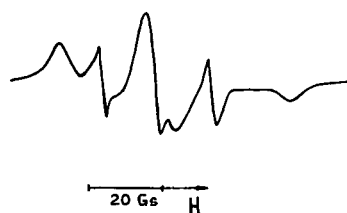


Fig. 2. ESR spectrum of TEMPON adsorbed on Si-600 hexadecyldimethylchlorosilane-modified silica. Surface concentration of TEMPON = 0.130 nm^{-2} .

[19] studies it was shown that the conformational structure of bonded layers formed with long alkyl chains depends considerably on the initial support pore diameter. A decrease in the average pore diameter reduces the bonded layer of the “rigid” structure in contrast to the “flexible” structure found in wide-pore silicas. This section considers the effect of the initial silica pore diameter on the nature of the adsorption states in the bonded layer of silicas modified with hexadecyldimethylchlorosilane. The characteristics of the samples used are presented in Table I, Nos. 16–18.

The behaviour of a probe adsorbed on narrow-pore silicas modified with hexadecyldimethylchlorosilane differs drastically from that on wide-pore sorbents. First, one can observe two-level adsorption for all the samples studied, but the

correlation time for slow radicals is 10^4 times greater than τ_c for rapid radicals (Fig. 2). This ratio is 100 times greater than for the wide-pore samples (Table IV). Second, unlike the wide-pore silicas modified with monochlorosilanes without end-capping, the proportion of rapid radicals increases as the probes loading increases. Third, increasing the temperature to 130°C does not result in an increase in the dispersion of the radical distribution on their correlation times.

The observed phenomena could be explained in the framework of the rigid structure concept [25,34]. Indeed, at low concentrations of the probe adsorption occurs on the residual silanol groups under interlaced bonded alkyl chains. Molecules of adsorbate are surrounded by bonded chains on one side and with the surface on the other. The probe is as if it were in a “molecular closet” (Fig. 1C).

Rotational activation energy values of slow radicals are given in Table IV. The values increase as the pore diameter decreases, and therefore as the proportion of rigid structure increases [34]. The observed values are greater than those of probes adsorbed both on pure silica and on modified wide-pore silicas.

Increasing the amount of the probe leads to the appearance of probes adsorbed on the

TABLE IV

EFFECT OF AVERAGE SILICA SUPPORT PORE DIAMETER ON STATE OF THE PROBE ADSORBED IN THE BONDED LAYER OF HEXADECYLDIMETHYLCHLOROSILANE-MODIFIED SILICAS

No.	Modified silica ^a	Average pore diameter (nm)	Concentration of probe ^b (nm^{-2})	τ_c of “slow” form (s)		Proportion of “slow” form (%)	τ_c of “rapid” form at 20°C (s)	Activation energy of rotation (kJ/mol)
				20°C	136°C			
16	C ₁₆ /Si-100	11.3	0.074	$1.6 \cdot 10^{-8}$	$2 \cdot 10^{-9}$	100	—	17.9
16	C ₁₆ /Si-100	11.3	0.120	$1.6 \cdot 10^{-8}$	N.d. ^c	ca. 100	N.d.	N.d.
17	C ₁₆ /Si-60	10.5	0.074	$1.7 \cdot 10^{-8}$	$2 \cdot 10^{-9}$	100	—	18.0
17	C ₁₆ /Si-60	10.5	0.120	$1.6 \cdot 10^{-8}$	N.d.	ca. 100	N.d.	N.d.
18	C ₁₆ /Si-600	5.4	0.013	$3.2 \cdot 10^{-8}$	$1.8 \cdot 10^{-9}$	100	—	24.0
18	C ₁₆ /Si-600	5.4	0.080	$3.2 \cdot 10^{-8}$	N.d.	ca. 100	N.d.	N.d.
18	C ₁₆ /Si-600	5.4	0.130	$1 \cdot 10^{-7}$	N.d.	95	$1 \cdot 10^{-11}$	N.d.
18	C ₁₆ /Si-600	5.4	0.080	$3.2 \cdot 10^{-8}$	N.d.	100	—	N.d.

^a According to Table I.

^b First seven entries, probe = TEMPON; bottom entry, probe = TEMPO-Amine.

^c Not determined.

bonded layer. These radicals are hardly dissolved in the bonded layer as they are too mobile.

It is paradoxical, but the probes adsorbed on the bonded layer at room temperature have the same mobility as those adsorbed in the “upper” part of the bonded layer of wide-pore silicas at 130°C. At the same time, the probes adsorbed “under” the bonded layer behave as if they are frozen by liquid nitrogen!

Effect of the nature of the adsorbate. This section considers the effect of the nature of the adsorbate on its behaviour. Two nitroxide radicals containing keto (TEMPO) or amino groups (TEMPO-Amine) were selected as adsorbates (see Experimental).

These radicals have different capabilities of forming hydrogen bonds with surface silanols. The presence of a primary amino group in the probe molecule increases markedly the specific interaction between the probe and the silica surface. Indeed, TEMPO-Amine, unlike TEMPO, virtually does not “sense” end-capping of the sorbents. The proportion of rapidly rotating probes for TEMPO-Amine adsorbed on the end-capped alkyl-modified silicas is almost zero, whereas for TEMPO this value is about 10% (Table III).

On the sorbents with a rigid structure of the bonded layer the rapidly rotating probes in the case of TEMPO appear at a lower loading than those for TEMPO-Amine (Table IV). Hence the effectiveness of surface shielding depends considerably on the nature of the adsorbate. We consider that the “total” shielding of the surface of the modified silicas is hardly possible, especially for adsorbates such as amines.

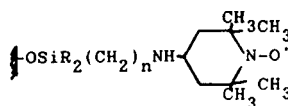
Formation–destruction of hydrogen bonds in bonded layers of functionalized silicas

Functionalized silica sorbents are as commonly used as reversed phases in modern liquid chromatography. They are various stationary phases for normal-phase, ion-exchange, ligand-exchange, affinity and other chromatographic modes [15,24,35].

Bonded functional groups are known to form cyclic structures with the silanol groups of the silica surface [15,24]. These are often referred to as “arch” structures. Various arch structures have

been studied using NMR [36–39] and IR spectrometry [37,40–43] and titrimetric [44], adsorption [45] and liquid chromatographic techniques [46]. In this work, the application of spin labels allowed us to observe directly the processes of formation and destruction of arch structures under various conditions.

Behaviour of spin labels on dry sorbents. The following spin-labelled modified silicas were used:



where $R = \text{CH}_3$, $n = 1$ and 3 or $R = \text{Cl}$, $n = 11$, designated C_1 , C_3 and C_{11} , respectively. The last sample was end-capped.

Without a solvent, immobilized radicals have a correlation time of *ca.* 10^{-8} s. Such a high value of τ_c confirms the strong interaction between the amino groups of the modifier and the silanol groups of the silica surface. Indeed, the correlation times of radicals that are immobilized on a non-specific surface can reach 10^{-10} s at the same temperature [47].

We assumed the formation of arch structures either by amino groups of the modifier or by nitroxyl groups of label (Fig. 3). Apparently both types of arch structures are present on the surface. However, the contribution of amino groups decreases as the spacer length is decreased. Indeed, A_{\parallel} increases from C_1 to C_{11} (Table V), and for C_1 samples it corresponds to that usually observed when nitroxide groups forms hydrogen bonds with surface silanols [12]. Thus, according to [23,48–50], on the basis of the absolute values of A_{\parallel} one can say that the polarity of the bonded layer decreases as the

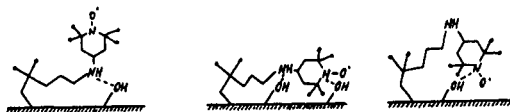


Fig. 3. Possible types of arch structures on modified silicas.

TABLE V

EFFECT OF SPACER LENGTH ON THE STATE OF THE BONDED SPIN LABEL

Spacer length (C atoms)	τ_c (s)		Proportion of "rapid" form (%)		g-Factor	A_{\parallel} (G)
	20°C	83°C	20°C	83°C		
	1	$2 \cdot 10^{-8}$	$8 \cdot 10^{-9}$	0		
3	$2 \cdot 10^{-8}$	$6 \cdot 10^{-9}$	0	0	2.0055	36.2
11	$2 \cdot 10^{-8} + 2 \cdot 10^{-9}$	$1 \cdot 10^{-8} + 5 \cdot 10^{-10}$	5	5	2.0057	35.5

spacer length increases. The increase in the g-factor from C_1 to C_{11} also confirms this tendency [51,52].

It was unexpected that arch structures could not be destroyed up to 83°C (Table V).

Effect of solvent on stability of arch structures. Series of solvents having approximately the same viscosity but different dielectric permeability (ϵ) and basicity function (B) according to Palm [54] were chosen. The characteristics of the solvents used are given in Table VI.

Effect of solvent dielectric permeability. There are two possibilities of destroying an arch structure in the presence of a solvent (Fig. 4). If arch structures were destroyed forming ion pairs (Fig. 4, top), this process would be markedly facilitated in solvents with a high dielectric permeability. However, for all the samples studied a sixfold increase in dielectric permeability from ethyl acetate to acetonitrile did not lead to an increase in the proportion of rapid radicals.

TABLE VI

CHARACTERISTICS OF THE SOLVENTS EMPLOYED

Solvent	η (mPs) [53]	ϵ [53]	B [54]
Carbon tetrachloride	9.7	2.2	0
Bromobenzene	9.9	5.4	40
Nitromethane	6.1	38.6	65
Acetonitrile	3.45	36.2	160
Ethyl acetate	4.41	6.02	181
Ethanol	9.45	12.3	229
Pyridine	10.8	24.3	472

Hence the destruction of arch structures occurs without the formation of ion pairs.

Effect of solvent basicity. The ease of destruction of arch structures without the formation of ion pairs (Fig. 4, bottom) must increase as the solvent basicity (B) [54] increases. However, this dependence is complicated (Figs. 5–7).

The observed stepped character of these diagrams is probably connected with the consequent destruction of hydrogen bonds. The weakest hydrogen bonds, corresponding to nitroxyl groups, are destroyed first. Then more stronger hydrogen bonds, formed by more basic amino groups, are destroyed. However, for the sample with the shortest spacer there is only one step on the diagram. This is evidently connected with the impossibility of hydrogen bond formation between amino and silanol groups because the spacer is too short.

The proportion of rapid radicals increases as

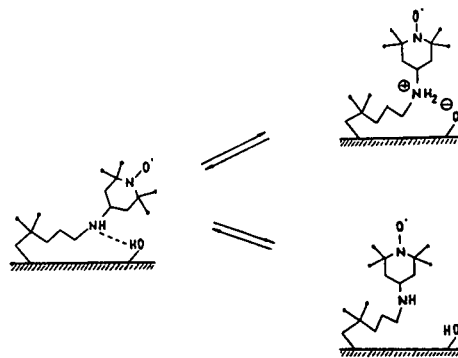


Fig. 4. Possible mechanisms of destruction of arch structure.

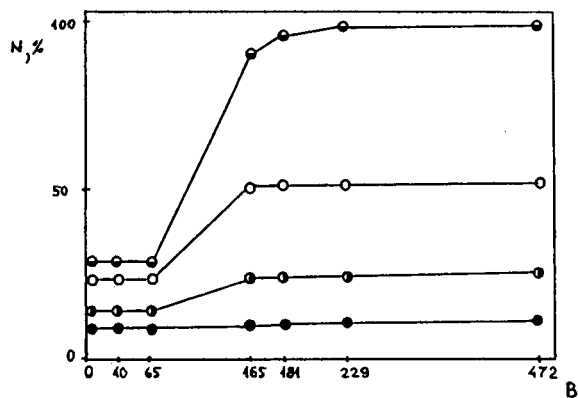


Fig. 5. Proportion of "rapid" radicals on solvent Palm basicity function for sample C_1 . ● = 28°C; ● = 53°C; ○ = 70°C; ○ = 83°C.

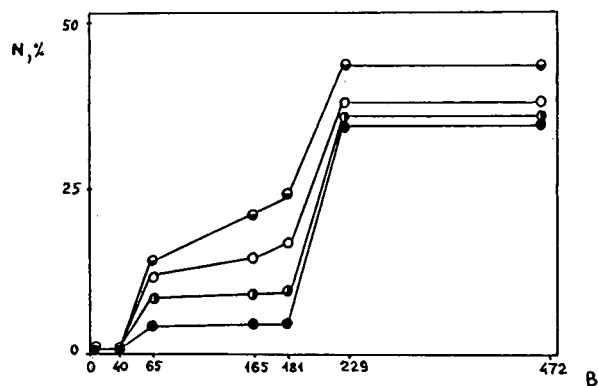


Fig. 6. Proportion of "rapid" radicals on solvent Palm basicity function for sample C_3 . ● = 28°C; ● = 53°C; ○ = 70°C; ○ = 83°C.

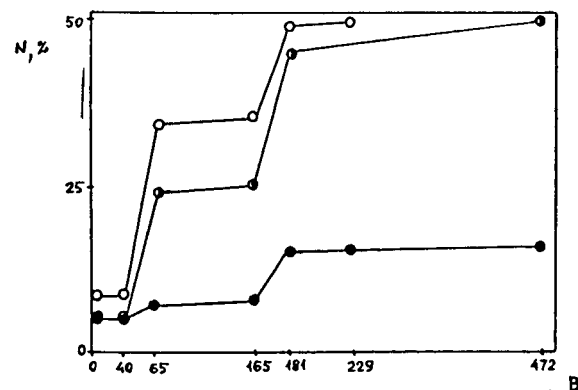
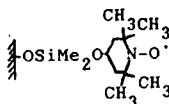


Fig. 7. Proportion of "rapid" radicals on solvent Palm basicity function for sample C_{11} . ● = 28°C; ● = 53°C; ○ = 70°C.

the temperature increases, unlike for the dry samples.

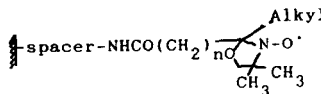
It is interesting that the strength of the arch structure formed by amino groups for C_{11} is lower than that for C_3 . Indeed, the latter is destroyed in solvents with a lower B (Figs. 6 and 7). We consider that this may be connected with the more shielded surface due to the end-capping procedure and long hydrophobic spacer.

Here we discuss our own results and literature data on the strength of the arch structure in the presence of a solvent. Gilpin *et al.* [9] studied the following nitroxide label:



Arch structures were found to be stable in non-basic solvents (aliphatic hydrocarbons; $B = 0$, and toluene, $B = 58$ [54]). However, they were destroyed in *n*-butanol, $B = 234$, 2-propanol, $B = 240$, and *tert.*-butanol, $B = 247$ [54].

Sistovaris *et al.* [2] studied nitroxide labels bonded to silica surface via various spacers:



It was shown that in the presence of methylene chloride ($B = 23$) the mobility of the bonded label had increased as much as if the label had been dissolved in a common solvent. However, it was observed only for samples that contained nitroxyl fragments located far from the amido group (ten or even fourteen methylene groups). In addition, nitroxyl fragments were shielded strongly with alkyl groups situated in an α -position with respect to the nitroxyl groups. Here one finds that, first, a hydrogen bond formed between such a nitroxyl group and the surface is less strong than that observed in our study. Second, one can hardly say anything about the arch structure formed between silanol groups and amido groups. Indeed, the amido groups are too far from the nitroxyl groups. Anyway, arch

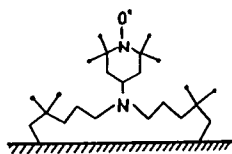


Fig. 8. Doubly alkylated label on silica surface.

structures formed by amino groups are stronger than those formed by either amido or nitroxyl groups (typical values of B for amides are 250–350 and for amines 600–700 [54]).

It should be noted that even in such basic solvents as pyridine and ethanol about 50% of the labels are in the slow form (Figs. 6 and 7). We assume that immobilization of 2,2,6,6-tetramethyl-4-aminopiperidine-1-oxyl yields both singly and doubly alkylated labels. Multi-site alkylation of immobilized ligand occurs with high concentrations of surface-bonded reactive groups and a comparatively low loading of ligand [7,55–57].

Doubly alkylated labels can hardly possess enough rotational mobility (Fig. 8). On the other hand, the double alkylation evidently is impossible for samples with a short spacer owing to steric hindrance.

REFERENCES

- 1 L.D. Hall and J.C. Waterton, *J. Amer. Chem. Soc.*, 101 (1979) 3697.
- 2 N. Sistovaris, W.O. Riede and H. Sillescu, *Ber. Bunsenges. Phys. Chem.*, 79 (1975) 882.
- 3 V.A. Semikolenov, V.A. Likhonobov and Yu.I. Ermakov, in *Katalizatory, Soderzhaschie Nanesennyye Kompleksy*, Novosibirsk, Nauka, Moscow, 1977, p. 47.
- 4 G.V. Lisichkin, S.M. Staroverov, V.B. Golubev and A.Yu. Fadeev, *Dokl. Akad. Nauk. SSSR*, 294 (1987) 1165.
- 5 S.M. Staroverov, A.Yu. Fadeev, V.B. Golubev and G.V. Lisichkin, *Khim. Fiz.*, 7 (1988) 93.
- 6 V.B. Golubev, G.V. Kudryavtsev, G.V. Lisichkin and D.V. Milchenko, *Zh. Fiz. Khim.*, 59 (1985) 2804.
- 7 A.Yu. Fadeev, P.G. Mingalyov, S.M. Staroverov, G.V. Lisichkin, E.V. Lunina, A.V. Gaida and V.A. Monastirski, *J. Chromatogr.*, 596 (1992) 114.
- 8 S.M. Staroverov, A.A. Serdan and G.V. Lisichkin, *J. Chromatogr.*, 364 (1986) 377.
- 9 R.K. Gilpin, A. Kasturi and E. Gelerinter, *Anal. Chem.*, 59 (1987) 1177.
- 10 V.B. Golubev, V.V. Matveev, S.M. Staroverov and G.V. Lisichkin, *Teor. Eksp. Khim.*, 24 (1988) 701.
- 11 H. Hommel, A.P. Legrand, H. Balard and E. Parirer, *Polymer*, 24 (1983) 959.
- 12 V.B. Golubev, E.V. Lunina and A.K. Selivanovskii, *Usp. Khim.*, 50 (1981) 792.
- 13 G. Martini, *Colloids Surf.*, 45 (1990) 83.
- 14 K.K. Unger, *Porous Silica (Journal of Chromatography Library, Vol. 16)*, Elsevier, Amsterdam, 1979.
- 15 L.C. Sander and S. Wise, *CRC Crit. Rev. Anal. Chem.*, 18 (1987) 299.
- 16 G.E. Berendsen and L. de Galan, *J. Liq. Chromatogr.*, 3 (1980) 1437.
- 17 D. Avnir, *J. Am. Chem. Soc.*, 109 (1987) 2931.
- 18 D. Farin and D. Avnir, *J. Chromatogr.*, 406 (1987) 317.
- 19 A.Yu. Fadeev, G.V. Lisichkin, V.K. Runov and S.M. Staroverov, *J. Chromatogr.*, 558 (1991) 31.
- 20 A.V. Kiselev and V.P. Dreving (Editors), *Ekspperimental'nye Metody v Adsorbtsii i Khromatografii*, MGU Press, Moscow, 1973.
- 21 I.I. Baranova, A.L. Kovarskii and A.M. Vasserman, *Vysokomol. Soedin.*, 24A (1982) 91.
- 22 A.L. Buchachenko (Editor), *Atlas Spectrov Nitroksil'nykh Radikalov*, Nauka, Moscow, 1977.
- 23 A.L. Buchachenko and A.M. Vasserman, *Stabil'nyye Radically*, Khimiya, Moscow, 1977, Ch. 11.
- 24 G.V. Lisichkin (Editor), *Modifitsirovannyye Kremnezemy v Sorbtsii, Katalize i Khromatografii*, Khimiya, Moscow, 1986.
- 25 A.Yu. Fadeev and S.M. Staroverov, *J. Chromatogr.*, 447 (1988) 103.
- 26 K. Albert and E. Bayer, *J. Chromatogr.*, 544 (1991) 345.
- 27 D. Avnir, R. Busse, M. Ottolenghi, E. Wellner and K.A. Zachariasse, *J. Phys. Chem.*, 89 (1985) 3521.
- 28 H. Engelgardt, B. Dryer and H. Schmidt, *Chromatographia*, 16 (1982) 11.
- 29 C.H. Lochmuller, M.T. Kersey and M.L. Hunnicutt, *Anal. Chim. Acta*, 175 (1985) 267.
- 30 A.V. Kiselev, G.V. Lisichkin, Yu.S. Nikitin, A.A. Serdan, S.M. Staroverov and N.K. Shonia, *Zh. Fiz. Khim.*, 57 (1983) 1829.
- 31 R.K. Gilpin and M.E. Gangoda, *J. Chromatogr. Sci.*, 21 (1983) 352.
- 32 K. Albert, B. Evers and E. Bayer, *J. Magn. Reson.*, 62 (1985) 428.
- 33 A.Yu. Fadeev and S.M. Staroverov, *J. Chromatogr.*, 465 (1989) 233.
- 34 S.M. Staroverov and A.Yu. Fadeev, *J. Chromatogr.*, 544 (1991) 77.
- 35 K.K. Unger, *Packings and Stationary Phases in Chromatographic Techniques*, Marcel Dekker, New York, 1990.
- 36 D.E. Leyden, D.S. Kendal and T.G. Waddell, *Anal. Chim. Acta*, 126 (1981) 207.
- 37 D.E. Leyden, D.S. Kendal, L.C. Burggraff, F.L. Pern and M. de Bello, *Anal. Chem.*, 54 (1982) 101.
- 38 S. Shinoda and Y. Saito, *J. Colloid Interface Sci.*, 89 (1982) 293.
- 39 S.G. Caravajal, D.E. Leyden, G.R. Quinting and G.E. Maciel, *Anal. Chem.*, 60 (1988) 1776.
- 40 B.R. Suffolk and R.K. Gilpin, *Anal. Chem.*, 57 (1985) 596.

- 41 C.-H. Chiang and J.L. Koenig, *J. Colloid Interface Sci.*, 83 (1981) 361.
- 42 C.-H. Chiang, H. Ishida and J.L. Koenig, *J. Colloid Interface Sci.*, 86 (1982) 26.
- 43 S. Kondo, T. Ishikawa, N. Jamagami, K. Yoshioka and Y. Nakahara, *Bull. Chem. Soc. Jpn.*, 60 (1987) 95.
- 44 G.V. Kudryavtsev, G.V. Lisichkin and V.M. Ivanov, *Zh. Anal. Khim.*, 38 (1983) 22.
- 45 N.K. Shonia, S.M. Staroverov, Yu.S. Nikitin and G.V. Lisichkin, *Zh. Fiz. Khim.*, 58 (1984) 702.
- 46 S.M. Staroverov, G.V. Lisichkin and E.L. Styskin, *Chromatographia*, 21 (1986) 165.
- 47 V.I. Krinichnii and N.V. Kostina, in *International Conference on Nitroxide Radicals, Novosibirsk, USSR, 1989*, Abstracts, p. 63P.
- 48 H.A. Coher and B.M. Hoffman, *Inorg. Chem.*, 13 (1974) 1484.
- 49 G.P. Lozos and B.M. Hoffman, *J. Phys. Chem.*, 78 (1974) 2110.
- 50 A.I. Kuznetsov, *Metod Spinovogo Zonda*, Nauka, Moscow, 1976, p. 23.
- 50 A.I. Kuznetsov, *Metod Spinovogo Zonda*, Nauka, Moscow, 1976, p. 23.
- 51 E.G. Rozantsev and R.I. Zhdanov (Editors), *Nitrosil'nye Radikaly. Sintez, Khimiya, Prilozhenia*, Nauka, Moscow, 1987, p. 180.
- 52 T. Kawamura, S. Matsunami, T. Gonezawa and K. Fukui, *Bull. Chem. Soc. Jpn.*, 38 (1965) 1935.
- 53 A.J. Gordon and R.A. Ford, *The Chemist's Companion. A Handbook of Practical Data, Techniques and References*, Wiley, New York, 1972.
- 54 V.A. Palm, *Osnovy Kolichestvennoy Teorii Organicheskikh Reaktsiy*, Khimiya, Leningrad, 1977, p. 332.
- 55 E.V. Patton and D.M. Wonnacott, *J. Chromatogr.*, 389 (1987) 115.
- 56 A.Yu. Fadeev, *Ph.D. Thesis*, MGU, Moscow, 1990.
- 57 M.A. Ditzler, L.H. Melendez, T.J. Onofrey and K.A. Milis, *Anal. Chim. Acta*, 228 (1990) 235.

High-performance membrane chromatography: highly efficient separation method for proteins in ion-exchange, hydrophobic interaction and reversed-phase modes

Tatiana B. Tennikova and Frantisek Svec*

Institute of Macromolecular Chemistry, Czech Academy of Sciences, 162 06 Prague (Czech Republic)

(First received August 28th, 1992; revised manuscript received May 5th, 1993)

ABSTRACT

High-performance membrane chromatography (HPMC) is a very effective chromatographic method in which all the mobile phase flows through the separation medium. The effects of process variables such as concentration of displacement agent, flow-rate and gradient slope on HPMC separations in the ion-exchange, hydrophobic interaction and reversed-phase modes were studied using model protein mixtures. The basic relationships characterizing column HPLC also apply in HPMC. Whereas the efficiency of the HPMC membrane does not depend on flow-rate, the resolution increases with increasing gradient volume. Separations obtained with a continuous linear gradient were used for the design of a stepwise gradient profile which decreases the consumption of both time and mobile phase in separations of proteins. According to calculations, the protein diffusivity enhanced by the convective flow through the membrane is about four orders of magnitude higher than the “free” diffusivity of the protein in the stagnant mobile phase located in the pores of a standard separation medium. This considerably speeds up the process and improves the efficiency of the separation.

INTRODUCTION

High-performance liquid chromatography (HPLC) revolutionized analytical chemistry by facilitating very rapid and efficient separations and the detection and determination of the components of virtually any mixture. The separation, isolation and purification of biopolymers is very important for their effective application. The analytical and preparative HPLC separations of individual biological macromolecules from their mixtures with both low- and high-

molecular mass compounds has been reviewed several times [1–6].

At present, most chromatographic separations are carried out in columns packed almost exclusively with bead-shaped particles. As the technology of bead preparation has been known for more than two decades [7,8], current research is focused on the design of new shapes [9].

Traditional membranes were introduced into affinity chromatography in 1988 [10–18]. Ion-exchange cellulose membranes stacked in a cartridge also gave good results in the separation and purification of proteins [19–23]. The recently introduced high-performance membrane chromatography (HPMC) combines the advantages of both membrane technology (simple scale-up, low pressure drop across a membrane) and

* Corresponding author. Present address: Baker Laboratory, Department of Chemistry, Cornell University, Ithaca, NY 14853-1301, USA.

column chromatography (high selectivity and efficiency of separation, high loading capacity) [24–28]. The efficiency of HPMC has been demonstrated in a number of protein separations in ion-exchange, hydrophobic interaction and affinity chromatographic modes. Quick Disc cartridges using HPMC technology are commercially available [29].

HPMC is characterized by high efficiency and rapid separation. The effects of some variables, such as membrane thickness, cartridge construction and surface chemistry, on HPMC have been reported in previous papers [24–28]. This paper gives a quantitative description of the separation process in a macroporous membrane and optimization of separation conditions for different modes of HPMC.

EXPERIMENTAL

Preparation of membranes

Macroporous membranes were prepared by free radical copolymerization of a mixture containing, a monovinyl monomer [glycidyl methacrylate (GMA), octyl methacrylate, dodecyl methacrylate or styrene (ST)], a divinyl monomer [ethylene dimethacrylate (EDMA) or divinylbenzene [DVB]], an initiator [azobisisobutyronitrile; 1% (w/w) with respect to the monomers] and porogenic diluents (cyclohexanol and dodecanol) in a heated mould [25]. The polymer sheets were consecutively washed with methanol, benzene, methanol and water.

From the resulting 2–3-mm thick flat sheet of poly(glycidyl methacrylate-co-ethylene dimethacrylate) (50:50, v/v) discs about 20 mm in diameter were cut, modified with diethylamine [30] and placed in specially designed cartridges, which were a kind gift from Säulentchnik Knauer (Berlin, Germany) [29]. Discs cut from poly(glycidyl methacrylate-co-dodecyl methacrylate-co-ethylene dimethacrylate) and poly(glycidyl methacrylate-co-octyl methacrylate-co-ethylene dimethacrylate) (both 45:15:40, v/v/v) sheets were treated with 0.1 mol/l sulphuric acid at 80°C for 5 h. The epoxide groups of the glycidyl methacrylate units yield two adjacent hydroxyls and the hydrophilicity of the original matrix increases. Poly[styrene-co-divinylben-

zene (tech.)] (50:50, v/v) membranes were cut and used without any additional treatment.

Chromatography

Mobile phase gradients were produced by an HPLC gradient pump (LKB) with a maximum flow-rate of 10 ml/min. The programmed and detected gradients were found to be almost identical. Samples were injected through a Rheodyne C7125 valve loop injector (200 μ l). The separation was monitored using a dual variable-wave length UV detector (LKB). A detailed description of the experiments has been published elsewhere [25].

Protein anion-exchange standard mixture (Bio-Rad Labs.) containing horse heart myoglobin, conalbumin, Chicken egg albumin and soybean trypsin inhibitor was used as a model mixture in ion-exchange chromatography. Chymotrypsinogen A (type II, from bovine pancreas), myoglobin and chicken egg albumin were purchased from Sigma and lysozyme (from hen egg white) and ribonuclease A (from bovine pancreas) from Boehringer Mannheim. All these proteins were used for the hydrophobic interaction chromatographic tests. Reversed-phase membranes were tested with a mixture consisting of chicken egg albumin and human serum albumin.

RESULTS AND DISCUSSION

Current knowledge of gradient elution HPLC clearly supports the fact that the column length has only a small effect on the resolution of large molecules such as proteins in any mode of retentive chromatography [31,32]. The characteristics of separation efficiency such as peak capacity (PC), resolution factor (R_s) and chromatographic band spreading expressed as band width in time or volume units (σ) or as peak height (PH) are functions of gradient time (t_G), particle size of packing (d_p), flow-rate (F) and solute diffusion coefficient (D_m). According to the theory [33]:

$$PC \approx R_s \approx t_G^{1/2} F^0 L^0 d_p^{-1} \quad (1)$$

$$1/\sigma_t \approx PH \approx t_G^{-1/2} F^{-1} L^0 d_p^{-1} \quad (2)$$

where L is the column length.

Although the column length does not affect the separation, it can alter the actual gradient shape and complicate the optimization of a chromatographic separation. Two variables are essential in elution chromatography: the capacity factor (k' or \bar{k}) and the chromatographic band spreading (σ). These are included in all basic expressions for both isocratic and gradient HPLC. More attention should be paid to σ as it not only depends on the kinetics of interactions between the solute and stationary phase but also includes contributions of both diffusion and instrumentation quality.

Comparison of column and membrane chromatography

Although the similarity of HPMC and HPLC has already been documented [24,25], there are also some substantial differences between the two techniques. For example, the chromatographic columns are typically several centimetres long. Therefore, the compositions of the mobile phase at the inlet and outlet of the column during a gradient elution are different and a gradient is formed also inside the column; the k' values for a particular compound differ along the column. An average capacity factor \bar{k} , defined as the value of k' when the band has moved half way through the column, has to be used for gradient elution [34]. The “length” of a membrane, which is actually the thickness of the membrane across which the mobile phase flows, is only a few millimetres. Therefore, a mobile phase gradient within the membrane is hardly conceivable at standard flow-rates. The column dead volume depends on the quality of the packing technique and exceeds 40% of the total column volume. In contrast to the columns packed with individual particles, the macroporous membrane is a single body and has no void volume of that kind. If part of the membrane pore volume contained in very large pores were to be taken as a “dead volume”, it still would be very small in comparison with the packed column void volume. Moreover, the membrane dead volume probably equals the extra-membrane volumes. The total pore volume of a membrane 2 mm thick, 25 mm in diameter and

of 50% porosity is 0.6 ml. A similar pore volume is present in a 120 × 4 mm I.D. column well packed with beads of 50% porosity. However, the interparticular void volume of such a column represents an additional 0.6 ml. This doubles the column dead time and increases the retention time of a non-retained compound. Owing to the differences, some equations describing gradient elution separation in a column may not completely apply in HPMC. However, we decided to operate with k' and σ determined experimentally from chromatographic data or calculated according to equations derived for HPLC anyway, as the differences seems not to be in the art but more likely in the degree.

Effect of the mobile phase gradient in HPMC

Important factors influencing the separation in gradient elution chromatography generally are the gradient volume V_G and gradient steepness B , defined by

$$B = (c_f - c_0)/V_G = \Delta c/V_G \quad (3)$$

where $\Delta c = c_f - c_0$ is the difference between the final and initial concentrations of the displacement agent in the eluent. Fig. 1 shows the effects of gradient variables on the HPMC separation of a model protein mixtures in ion-exchange (IEC, Fig. 1a), hydrophobic interaction (HIC, Fig. 1b) and reversed-phase (RPC, 1c) modes.

The retention volume V_R depends in standard column chromatography on the gradient slope and, after substitution for B from eqn. 3, on the gradient volume:

$$\log V_R = a - b \log B = a' + b \log V_G \quad (4)$$

where a , a' and b are constants characteristic of the gradient shape. The straight lines shown in Fig. 2 confirm that membrane chromatography obeys the same rules as HPLC. The gradient slope provides an effect on the band width σ particularly in the range of small B (Fig. 3), as documented by the HPMC separation of the protein pairs conalbumin–soybean trypsin inhibitor in the IEC mode (Fig. 3a) and lysozyme–chymotrypsinogen in the HIC mode (Fig. 3b). The resolution factor of the proteins, R_s , decreases with increase in gradient steepness in

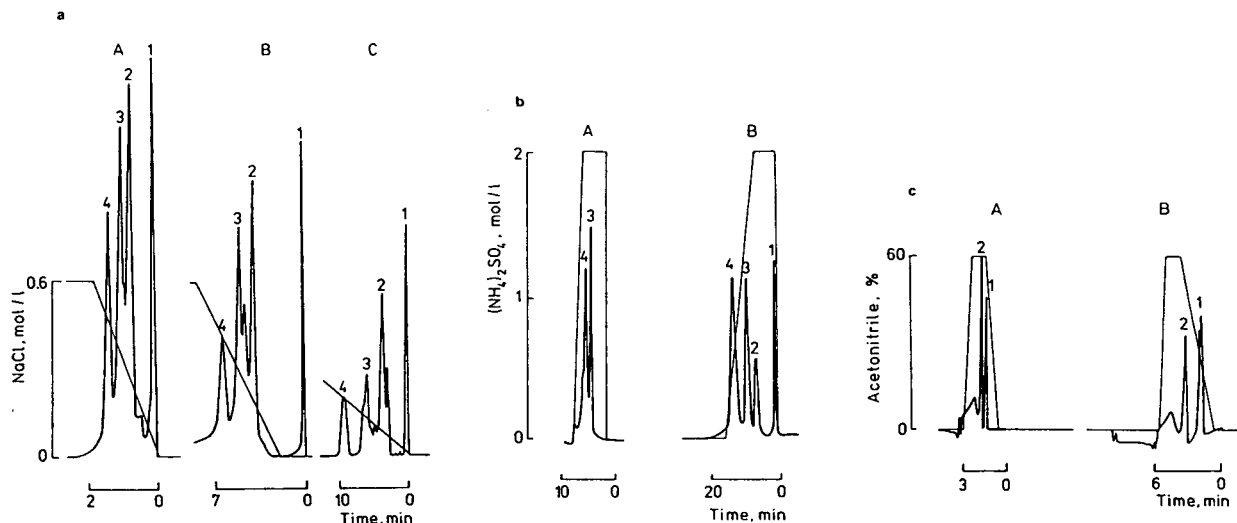


Fig. 1. Effect of various gradient volumes, V_G , on the separation of protein mixtures by (a) anion-exchange, (b) hydrophobic interaction and (c) reversed-phase high-performance membrane chromatography. (a) GMA-EDMA (50:50) modified membrane containing 1 mmol/g DEA groups, mobile phase 0.01 mol/l Tris-HCl buffer solution (pH 7.6), gradient from 0 to 0.6 mol/l NaCl in the buffer, gradient time (A) 2, (B) 6 and (C) 15 min, flow-rate 5 ml/min. Peaks: 1 = myoglobin; 2 = conalbumin; 3 = chicken egg albumin; 4 = soybean trypsin inhibitor. (b) Dodecyl methacrylate-GMA-EDMA (15:35:50) membrane, mobile phase 5 vol.% of 2-propanol in 0.02 mol/l phosphate buffer (pH 6.8), gradient from 2 to 0 mol/l $(\text{NH}_4)_2\text{SO}_4$ in the buffer, gradient time (A) 4 and (B) 10 min, flow-rate 3 ml/min. Peaks: 1 = myoglobin; 2 = ribonuclease A; 3 = lysozyme; 4 = chymotrypsinogen. (c) ST-DVB (50:50) membrane, mobile phase gradient from 0 to 60 vol.% aqueous acetonitrile, flow-rate 6 ml/min, gradient time (A) 2 and (B) 5 min. Peaks: 1 = chicken egg albumin; 2 = human serum albumin.

both IEC and HIC (Fig. 4). However, the band width of chymotrypsinogen eluted with a strong eluent in the HIC mode does not depend on the gradient slope.

An increase in the gradient volume in all the chromatographic modes tested improves the resolution up to the point beyond which even the single compound band splits into several peaks (Fig. 5). This may reflect the inhomogeneity of the solid surface of the separation medium, resulting in different interaction energies between the attached proteins and the surface or different accessibility of interacting areas.

In gradient elution chromatography, the capacity factor k' generally depends on the composition of the mobile phase. For ion-exchange chromatography,

$$\log k' = \log K - Z \log C \quad (5)$$

where K is a constant that includes the equilibrium formation constant, the phase ratio and the bound solute concentration, Z is the number of

interaction sites for a particular solute and stationary phase and C is the actual total concentration of salts in the mobile phase [31]. The Z and $\log K$ data, calculated according to eqn. 5 from a series of isocratic membrane chromatographic runs, is summarized in Table I. Both Z and $\log K$ are smaller in HPMC than those obtained in HPLC under similar conditions [32].

Effect of flow-rate, gradient time and gradient profile

Flow-rate and gradient time are independent variables in gradient elution chromatography. Fig. 6 shows the effect of flow-rate on σ_v at constant gradient time and gradient volume in IEC with changing gradient volume and time, respectively. The band width decreases dramatically as the flow-rate increases, particularly at very low flow-rates. Similar effects were also observed in HIC HPMC. This is in contrast to gradient elution HPLC, in which a decrease in flow-rate may cause either a decrease or an increase in the resolution as a result of the

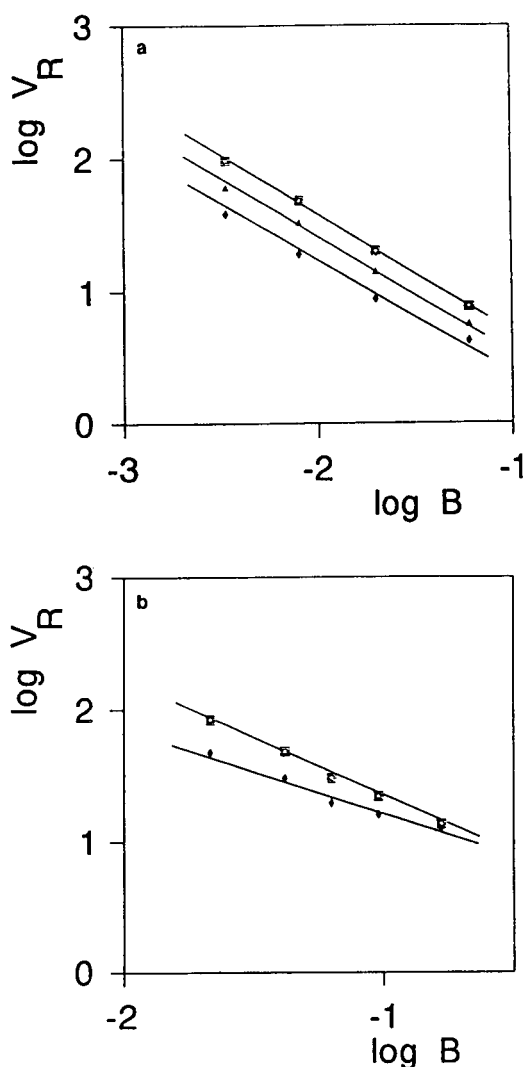


Fig. 2. Effect of the gradient slope B on the retention volume V_R for (a) anion-exchange HPMC of (◆) conalbumin, (▲) chicken egg albumin and (■) soybean trypsin inhibitor and (b) hydrophobic interaction HPMC of (◆) lysozyme and (■) chymotrypsinogen A.

trade-off between the increase in N and the decrease in k' [31].

Experiments revealed that the height equivalent to a theoretical plate as determined with myoglobin and acetone is about 0.4 mm (not taking in account the extra-column volume effects) and the efficiency does not change with flow-rate (Fig. 7). As the membrane efficiency does not depend on the linear flow velocity in range 0.04–1 cm/min, a decrease in separation

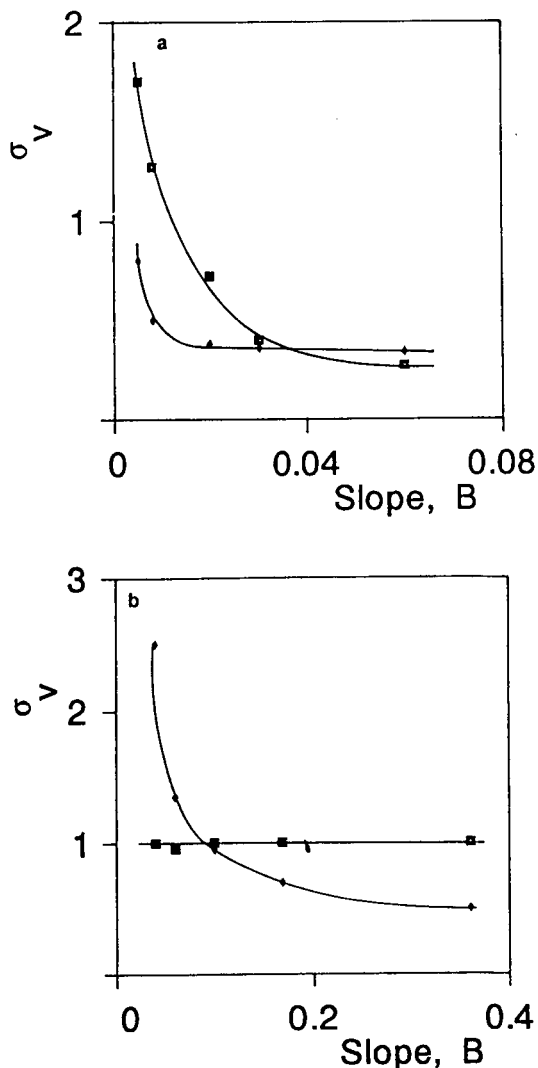


Fig. 3. Effect of the mobile phase gradient slope B on band spreading σ_v in (a) anion-exchange HPMC of (◆) conalbumin and (■) soybean trypsin inhibitor and (b) hydrophobic interaction HPMC of (◆) lysozyme and (■) chymotrypsinogen A.

quality occurs at higher flow-rates on account of the increase in k' . The calculated difference in composition of the mobile phase at the inlet and outlet of the cartridge (the mobile phase gradient within a 2 mm thick membrane) at constant gradient volume is 20% at 0.3 ml/min but only 2% at 3 ml/min. In the former instance k' may vary across the membrane whereas in the latter it remains almost the same in any part of the membrane. If the gradient time is constant, the

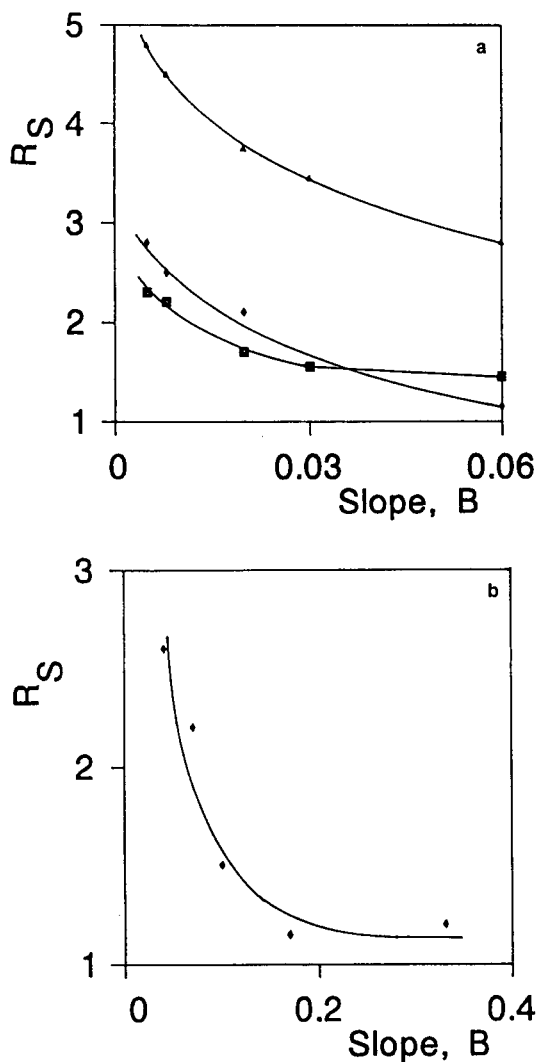


Fig. 4. Effect of the mobile phase gradient slope B on peak resolution R_s for (a) anion-exchange HPMC separation of the pairs (◆) conalbumin–chicken egg albumin, (■) chicken egg albumin–soybean trypsin inhibitor and (▲) conalbumin–soybean trypsin inhibitor and (b) hydrophobic interaction HPMC separation of (◆) lysozyme and chymotrypsinogen A.

gradient across the membrane does not change with the flow-rate and σ_v also remains constant. The effect of gradient steepness is similar to that observed in ion-exchange and reversed-phase HPLC [31,34,35].

The step-by-step optimization of the HPMC separation conditions results in a gradient the slope and lower and upper limits of which provide for good resolution at a chosen flow-

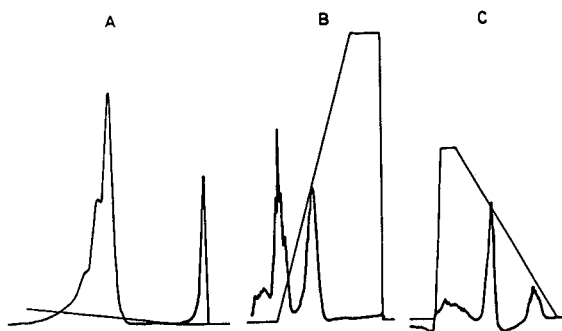


Fig. 5. Effect of increasing gradient volume on peak splitting. (a) Anion-exchange HPMC, gradient volume 150 ml; (b) hydrophobic interaction HPMC, gradient volume 90 ml; (c) reversed-phase HPMC, gradient volume 90 ml. Conditions as in Fig. 1.

TABLE I

CONSTANTS OF EQUATION 5 FOR PROTEINS IN ION-EXCHANGE HIGH-PERFORMANCE MEMBRANE CHROMATOGRAPHY

Protein	Log K^a	Z^a
Conalbumin	1.69 (4.31)	1.78 (2.39)
Chicken egg albumin	2.51 (6.39)	2.38 (6.66)
Soybean trypsin inhibitor	2.15	1.85

^a Data in parentheses are from ref. 35.

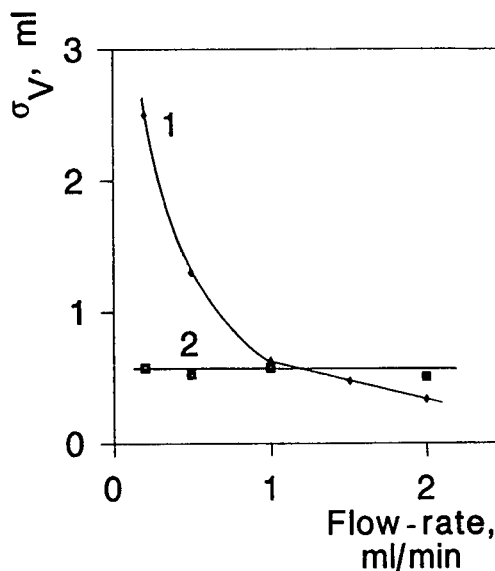


Fig. 6. Effect of the mobile phase flow-rate on band width σ_v of chicken egg albumin in anion-exchange HPMC with (1) constant gradient time and (2) constant gradient volume.

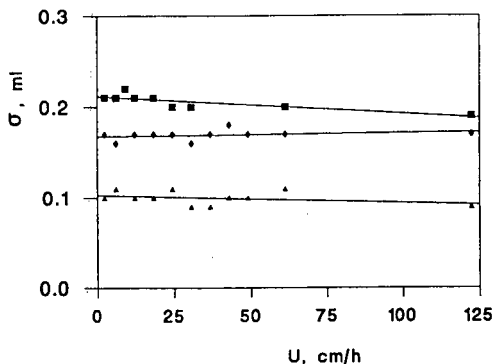


Fig. 7. Effect of flow velocity U on band width σ for various solutes. ■ = Myoglobin in 0.01 mol/l Tris-HCl buffer solution (pH 7.6); (□) acetone in water; ▲ = chicken egg albumin in 0.01 mol/l Tris-HCl buffer solution (pH 7.6) containing 0.5 mol/l NaCl.

rate. However, the continuity of a linear gradient is also an inherent disadvantage. The gradient runs continuously regardless of the difference between the retention times of adjacent peaks. The dead period between the peaks leads to a waste of both time and mobile phase, which should be avoided, particularly in large-scale preparative separations. Therefore, changes of the mobile phase composition in steps are more efficient provided that the concentration steps and the duration of each isocratic elution are set properly. To do that, an indicative shallow linear gradient separation has to be run to determine the composition of the mobile phase at the band maximum and the height and duration of each step are set according to these data. Fig. 8 shows the slow gradient HPMC separation of a model mixture from which the mobile phase composition at the elution of each peak was obtained and used in designing the gradient steps. The separation of individual components of the mixture with a stepwise gradient is better, overlapping of peaks is avoided and the separation time is still kept short. Fig. 9 shows an excellent separation of model protein mixtures by ion-exchange and hydrophobic interaction HPMC with a stepwise gradient.

Effect of flow-rate

Fig. 10 demonstrates the dependence of the resolution factor on the linear flow velocity for

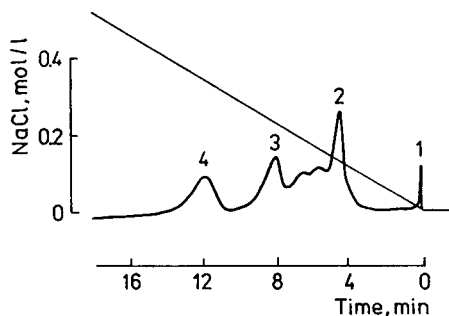


Fig. 8. HPMC separation of (1) myoglobin, (2) conalbumin, (3) chicken egg albumin and (4) soybean trypsin inhibitor using a linear mobile phase gradient. Conditions: GMA-EDMA (50:50) modified membrane containing 1 mmol/g DEA groups; mobile phase 0.01 mol/l Tris-HCl buffer solution (pH 7.6), gradient from 0 to 0.6 mol/l NaCl in the buffer, gradient time 36 min, flow-rate 5 ml/min.

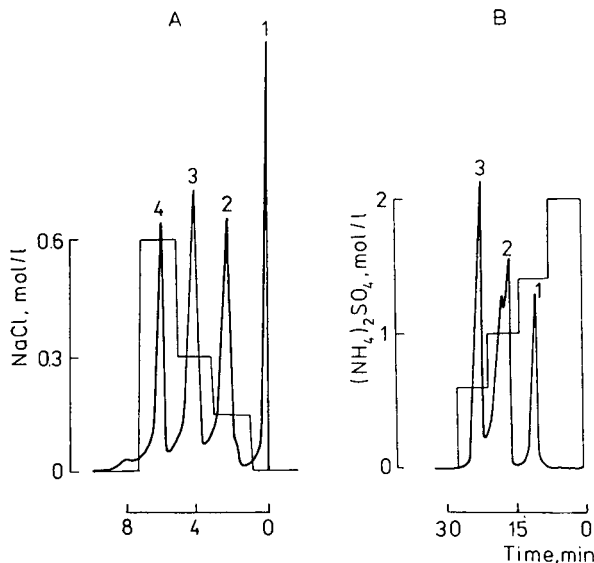


Fig. 9. HPMC separation of protein mixtures in a multiple step gradient operation. (A) GMA-EDMA (50:50) modified membrane containing 1 mmol/g DEA groups, mobile phase 0.01 mol/l Tris-HCl buffer solution (pH 7.6), gradient steps 0 (1 min), 0.15 (2 min), 0.30 (2 min) and 0.6 mol/l NaCl in the buffer (2 min), flow-rate 3 ml/min. Peaks: 1 = myoglobin; 2 = conalbumin; 3 = chicken egg albumin; 4 = soybean trypsin inhibitor. (B) Octyl methacrylate-GMA-EDMA (15:35:50) membrane, mobile phase 5 vol.% of 2-propanol in 0.02 mol/l phosphate buffer (pH 6.8), gradient steps 2, 1.4, 1.0 and 0.6 mol/l $(\text{NH}_4)_2\text{SO}_4$ in the buffer taking 6 min each, flow-rate 3 ml/min. Peaks: 1 = lysozyme; 2 = chicken egg albumin; 3 = chymotrypsinogen.

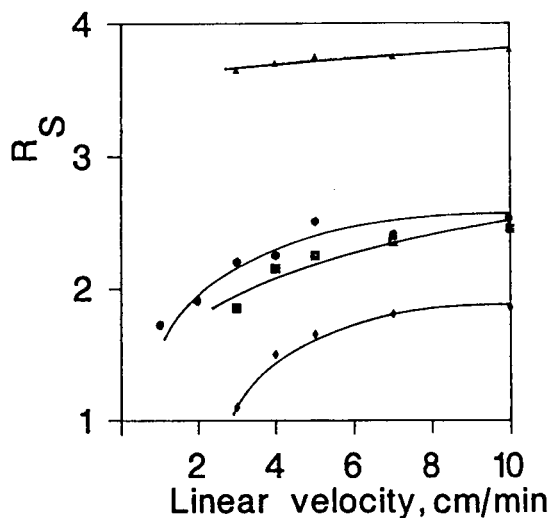


Fig. 10. Effect of the mobile phase linear velocity U on peak resolution, R_s , in HPMC. Anion-exchange separation of the pairs (■) conalbumin–chicken egg albumin, (●) chicken egg albumin–soybean trypsin inhibitor and (▲) conalbumin–soybean trypsin inhibitor and (◆) hydrophobic interaction separation of lysozyme and chymotrypsinogen A.

the pair chymotrypsinogen–lysozyme in hydrophobic interaction HPMC and for pairs formed by conalbumin, chicken egg albumin and soybean trypsin inhibitor in anion-exchange HPMC. The resolution factor increases slightly with increasing flow-rate in both modes, probably owing to narrowing of the peaks. Similar effects were also observed in the reversed-phase chromatography of tryptic digests on a column packed with poly(styrene-co-divinylbenzene) beads [36].

While the resolution changes with the linear flow velocity in all modes of HPMC, k' does so only in the ion-exchange mode and remains constant in the hydrophobic interaction mode (Fig. 11).

Enhanced diffusivity

An important characteristic of membrane chromatography is that there is almost no change in the column efficiency with increasing flow-rate (Fig. 7). Moreover, the calculated convective velocity in membrane chromatography should equal the linear flow velocity as all the mobile phase flows through the pores of the flat-body

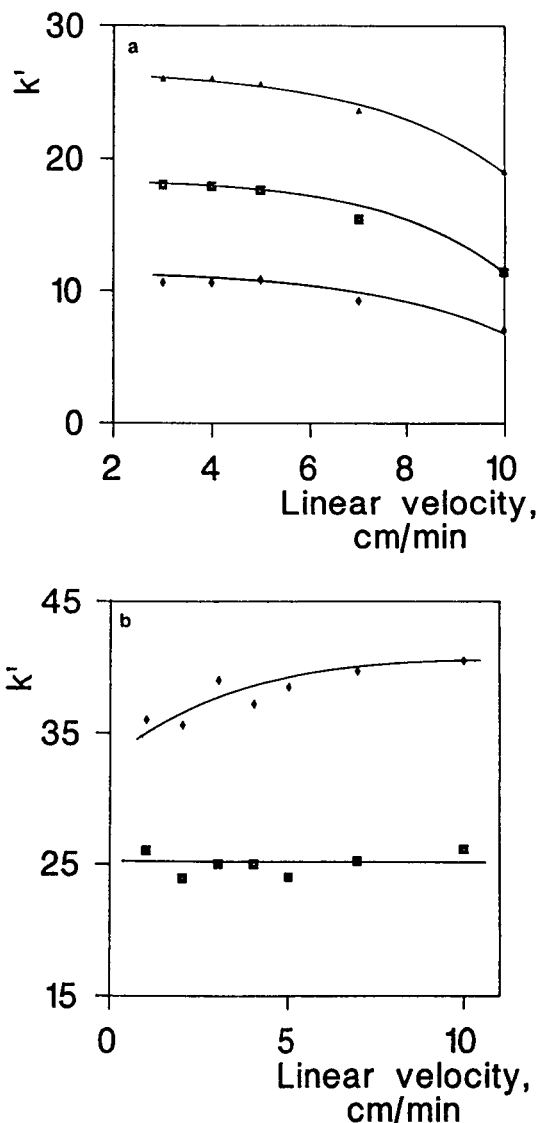


Fig. 11. Effect of the mobile phase linear velocity U on protein capacity factor k' . (a) Anion-exchange HPMC of a mixture consisting of (◆) conalbumin, (■) chicken egg albumin and (▲) soybean trypsin inhibitor; (b) hydrophobic interaction HPMC of (◆) lysozyme and (■) chymotrypsinogen A.

membrane having a slab-like geometry. The membrane permeability B_m is [37].

$$\begin{aligned}
 B_m &= \varepsilon_m^3 d_g^2 / 150(1 - \varepsilon_m)^2 \\
 &= a\varepsilon_m^2 d_{\text{pore}}^2 / 150(1 - \varepsilon_m)^2
 \end{aligned}
 \quad (6)$$

where ε_m is the membrane porosity, d_g is the diameter of the globule (microsphere) clusters within the membrane among which the transport canals are formed, d_{pore} is the pore diameter and a is defined as

$$a = d_g^2 / d_{\text{pore}}^2 \quad (7)$$

Darcy's law relates the convective velocity ν_0 to the membrane permeability B_m , fluid viscosity μ and pressure drop across the membrane of thickness $l(\Delta p/l)$:

$$\nu_0 = -(B_m \Delta p / 2\mu l) \quad (8)$$

Substitution of $d_{\text{pore}} = 400$ nm and $d_g = 450$ nm determined from scanning electron micrographs, and $\varepsilon_m = 0.5$ gives $B_m = 0.66 \cdot 10^{-11}$ cm². The intramembrane convective velocity calculated using the actual pressure drop of 5.8 MPa at a water flow-rate of 10 ml/min and a membrane thickness of 3 mm is $\nu_0 = 0.128$ cm/s. As the linear velocity calculated from the flow-rate divided by the cross-section is 0.12 cm/s, the above-expressed assumption of equivalence of the linear and intramembrane convective velocity seems to be adequate for the chromatographic membranes.

The convection of the mobile phase through a membrane also increases the diffusivity inside the pores as compared with "free" diffusion. The "apparent" or "augmented" effective diffusivity \bar{D}_e is a function of both effective diffusivity D_e and Peclet number λ ($\lambda = \nu_0 l / D_e$) [37]. The Peclet number for the membrane is $1.92 \cdot 10^5$, which is high enough to permit the use of the simplified equation for the calculation of the apparent diffusivity [37]:

$$\bar{D}_e = \nu_0 l / 3 \quad (9)$$

The calculation gives $\bar{D}_e = 6.4 \cdot 10^{-3}$. In contrast to the "free" effective diffusivity of proteins ($D_e \approx 10^{-7}$ cm²/s), the diffusivity forced by the convection is more than four order of magnitude higher and the mass transfer faster. Therefore, separation in membrane chromatography is faster than in standard column methods. The dramatic increase in diffusivity in HPMC permits the use of higher flow-rates and, accordingly, with the exact gradient slope and shape, also a

significant acceleration of the separation process. Moreover, the separation seems to proceed mostly in the large transport canals where convection plays the major role. It indicates that even the absence of small pores does not affect the separation properties in the HPMC membrane [38]. The concept of mass transfer enhancement by convection has already been used in heterogeneous catalysis [39] and in perfusion chromatography [40–42].

CONCLUSIONS

Detailed studies of individual effects of variable parameters in ion-exchange, hydrophobic interaction and reversed-phase protein separations confirmed that HPMC obeys the rules typical of column chromatography. The use of a stepwise gradient during the elution decreases the time necessary for separation and the amount of mobile phase used, thus decreasing the costs of the separation process. This is particularly advantageous in preparative separations. Owing to the unique absence of interparticular voids in the membrane, all the mobile phase flows through the pores of the separation medium. This results in an increase in diffusivity by several orders of magnitude augmented by the convective flow.

ACKNOWLEDGEMENTS

Financial support of this research by a grant from the Grant Agency of the Czech Academy of Sciences (No. 45004) and support from Säulentchnik Knauer, Berlin, Germany, are gratefully acknowledged. The authors also thank Dr. P. Jandera, Professor A. Rodrigues and Dr. G. Carta for stimulating and fruitful discussions.

REFERENCES

- 1 J. Frenz and Cs. Horváth, in Cs. Horváth (Editor), *High Performance Liquid Chromatography: Advances and Perspectives*, Vol. 5, Academic Press, New York, 1988, p. 211.
- 2 R. Epton (Editor), *Chromatography of Synthetic and Biological Polymers*, Vols. 1 and 2, Ellis Horwood, Chichester, 1988.

- 3 L.R. Snyder and M.A. Stadalius, in Cs. Horváth (Editor), *High Performance Liquid Chromatography: Advances and Perspectives*, Vol. 4, Academic Press, New York, 1986, p. 294.
- 4 P.R. Brown and R.A. Hartwick (Editors), *High Performance Liquid Chromatography*, Wiley, New York, 1989.
- 5 K.M. Gooding and F.E. Regnier (Editors), *HPLC of Biological Molecules, Methods and Applications*, Marcel Dekker, New York, 1990.
- 6 C.T. Mant and R.S. Hodges (Editors), *High-Performance Liquid Chromatography of Peptides and Proteins: Separation, Analysis and Conformation*, CRC Press, Boca Raton, FL, 1991.
- 7 J.C. Moore, *J. Polym. Sci., Part A*, 2 (1964) 835.
- 8 K.K. Unger (Editor), *Packings and Stationary Phases in Chromatographic Techniques*, Marcel Dekker, New York, 1990.
- 9 K.K. Unger, presented at the 11th International Symposium on HPLC of Proteins, Peptides and Polynucleotides, Washington, DC, October 20–23, 1991.
- 10 S. Brandt, R.A. Goffe, S.B. Kessler, J.L. O'Conner and S.E. Zale, *Bio/Technology*, 6 (1988) 779.
- 11 S.H. Huang, S. Roy, K.C. Hou and G.T. Tsao, *Biotechnol. Prog.*, 4 (1988) 159.
- 12 M. Unarska, P.A. Davis, M.P. Esnouf and B.J. Bellhouse, *J. Chromatogr.*, 519 (1990) 53.
- 13 K.C. Hou and R. Zaniewski, *J. Chromatogr.*, 525 (1990) 159.
- 14 S. Krause, K.H. Kroner and W.D. Deckwer, *Biotechnol. Tech.*, 5 (1991) 199.
- 15 B. Champluvier and M.R. Kula, *J. Chromatogr.*, 539 (1991) 315.
- 16 M. Kim, K. Saito, S. Furusaki, T. Sugo and I. Ishigaki, *J. Chromatogr.*, 585 (1991) 45.
- 17 M. Kim, K. Saito, S. Furusaki, T. Sugo and I. Ishigaki, *J. Chromatogr.*, 586 (1991) 27.
- 18 P. Langlotz and K.H. Kroner, *J. Chromatogr.*, 591 (1992) 107.
- 19 Y. Kikumoto, Y.M. Hong, T. Nishida, S. Nakai, Y. Masui and Y. Hirai, *Biochem. Biophys. Res. Commun.*, 147b (1987) 315.
- 20 A. Upshall, A.A. Kumar, M.C. Baley, M.D. Parker, M.A. Favreau, K.P. Lewinson, M.L. Joseph, J.M. Maragnora and G.L. McKnight, *Bio/Technology*, 5 (1987) 1301.
- 21 L.U.L. Tan, E.K.C. Yu, G.W. Luis-Seize and J.N. Saddler, *Biotechnol. Bioeng.* 30 (1987) 96.
- 22 A. Jungbauer, F. Unterluggauer, K. Uhl, A. Buchacher, F. Steindl, D. Pettaufer and E. Wenish, *Biotechnol. Bioeng.*, 32 (1988) 326.
- 23 J.A. Gerstner, R. Hamilton and S.M. Cramer, *J. Chromatogr.* 596 (1992) 173.
- 24 T.B. Tennikova, F. Svec and B.G. Belenkii, *J. Liq. Chromatogr.*, 13 (1990) 63.
- 25 T.B. Tennikova, M. Bleha, F. Svec, T.V. Almazova and B.G. Belenkii, *J. Chromatogr.*, 555 (1991) 97.
- 26 F. Svec and T.B. Tennikova, *J. Bioact. Compat. Polym.*, 6 (1991) 393.
- 27 H. Abou-Rebyeh, F. Korber, K. Schubert-Rehberg, J. Reusch and Dj. Josic, *J. Chromatogr.*, 566 (1991) 341.
- 28 Dj. Josic, J. Reusch, K. Loster, O. Baum and W. Reutter, *J. Chromatogr.*, 590 (1992) 59.
- 29 *Quick Disk™ Cartridge, Application Sheet*, Säulenteknik Knauer, Berlin, 1991.
- 30 F. Svec, H. Hrudkova, D. Horak and J. Kalal, *Angew. Makromol. Chem.*, 87 (1977) 23.
- 31 L.R. Snyder, in K.M. Gooding and F.E. Regnier (Editors), *HPLC of Biological Molecules, Methods and Applications*, Marcel Dekker, New York, 1990, p. 231.
- 32 F.E. Regnier and R.M. Chicz, in K.M. Gooding and F.E. Regnier (Editors), *HPLC of Biological Molecules, Methods and Applications*, Marcel Dekker, New York, 1990, p. 89.
- 33 L.R. Snyder and M.A. Stadalius, in Cs. Horváth (Editor), *High Performance Liquid Chromatography: Advances and Perspectives*, Vol. 1, Academic Press, New York, 1980, p. 207.
- 34 L.R. Snyder, M.A. Stadalius and M.A. Quarry, *Anal. Chem.*, 55 (1983) 1412A.
- 35 Y.F. Maa, F.D. Autia, Z.E. Rassia and Cs. Horváth, *J. Chromatogr.*, 452 (1988) 331.
- 36 J.S. Swadesh, *J. Chromatogr.*, 512 (1990) 315.
- 37 A.E. Rodrigues, J.C. Lopez, Z.P. Lu, J.M. Loureiro and M.M. Diaz, *J. Chromatogr.*, 590 (1992) 93.
- 38 T.B. Tennikova and F. Svec, in *Proceedings of the 9th International Symposium on Preparative and Industrial Chromatography*, Nancy, 1992, p. 353.
- 39 A. Nir and L. Pismen, *Chem. Eng. Sci.*, 32 (1977) 35.
- 40 N.B. Afeyan, N. Gordon, I. Maszaroff, I. Varady, S.P. Fulton, Y. Yang and F.E. Regnier, *J. Chromatogr.*, 519 (1990) 1.
- 41 N.B. Afeyan, S.P. Fulton and F.E. Regnier, *J. Chromatogr.*, 544 (1991) 267.
- 42 S.P. Fulton, N.B. Afeyan, N.F. Gordon and F.E. Regnier, *J. Chromatogr.*, 547 (1992) 452.

Enzyme-based high-performance liquid chromatography stationary phases as metabolic reactors

Immobilization of non-solubilized rat liver microsomes on an immobilized artificial membrane high-performance liquid chromatography support

Tanja Alebić-Kolbah[☆] and Irving W. Wainer*

McGill University, Department of Oncology, Montreal General Hospital, 1650 Cedar Avenue, Room B7113, Montreal, PQ H3G 1A4 (Canada)

(First received March 24th, 1993; revised manuscript received May 26th, 1993)

ABSTRACT

Non-solubilized rat liver microsomes have been non-covalently immobilized on an immobilized artificial membrane (IAM) HPLC stationary phase. The microsomes were immobilized on the IAM interphase of both loose IAM support and in a 1 cm × 3 mm I.D. HPLC column filled with IAM stationary phase. The activity of the immobilized microsomes was assessed by following the formation of 7-hydroxycoumarin (7-OHC) from the O-deethylation of 7-ethoxycoumarin. The 7-OHC was quantified by either HPLC analysis of an aliquot from an incubation mixture containing the loose microsome–IAM support or directly using the chromatogram from the microsome–IAM HPLC column. Both forms of the IAM-immobilized microsomes were active. The result of this study indicate that the IAM stationary phase can be used to produce immobilized microsomal reactors which can be used in HPLC systems for direct on-line determination of biosynthetic and metabolic processes.

INTRODUCTION

Immobilized enzyme reactors (IMERs) have been developed by a number of groups and applied to synthetic and pharmacological studies. IMERs are of interest because they have a number of advantages relative to soluble enzymes including: the immobilized enzymes can be reused; isolation of the products from the reaction mixture is easier; processes can be run continuously; immobilization can stabilize the enzymes.

The ability to follow biosynthetic and metabolic processes using an IMER has been demonstrated by a number of research groups. Fenselau *et al.* [1] covalently immobilized solubilized microsomal enzymes on cyanogen bromide-activated Sepharose beads and used the resulting IMER to synthesize glucuronides. Lehman *et al.* [2] used the same system in the N-demethylation of ethylmorphine and the O-demethylation of *p*-nitroanisole. The Sepharose-based IMERs were not only active, but also showed excellent stability with respect to both time and temperature [2].

Solubilized microsomes have also been immobilized by entrapment into alginate beads in

* Corresponding author.

[☆] On leave from Pliva Research Institute, Zagreb, Croatia.

the presence of polyethyleneimine [3]. The resulting IMER showed a substantial increase in UDP-glucuronyltransferase activity compared to free microsomes or microsomes immobilized by other methods. The alginate bead-entrapped microsomes were used to synthesize 3'-azido-3'-deoxythymidine (AZT), ether- and acyl(ester)-glucuronides.

Another approach to the non-covalent immobilization of enzymes involves their entrapment in the interphase of an immobilized artificial membrane (IAM) HPLC stationary phase. IAM phases are produced through the covalent immobilization of 1-myristoyl-2-[(13-carboxyl)-tridecanoyl]-*sn*-3-glycerophosphocholine on an aminopropyl silica through an ω -carboxyl group on the C-2 fatty acid chain [4]. In the resulting support, the phosphatidylcholine head-groups form the surface of the support and the hydrocarbon side chains produce hydrophobic cavities which extend from the charged head-group to the surface of the aminopropyl silica.

IAM stationary phases have been used to non-covalently immobilize the enzymes α -chymotrypsin (AHT) and trypsin [5]. The resulting IAM-IMERs retained the hydrolytic activity of the non-immobilized enzymes and their sensitivity to enzyme inhibitors, pH and temperature. When a substrate was chromatographed on the IAM-AHT, the activity of the immobilized enzyme could be determined directly from the chromatogram by calculating the substrate/product ratios. IAM-immobilized AHT and trypsin can be used as chromatographic probes for qualitative determinations of enzyme/substrate and enzyme/inhibitor interactions [5].

The IAM support has also been used to purify several P-450 isozymes in functional conformations [6]. This has led us to investigate the possibility of producing a new category of biosynthetic IMERs through the entrapment of non-solubilized microsomes on the IAM support. One of the objectives of this work is the development of a microsomal IMER which can be directly linked to an analytical HPLC column for on-line monitoring of metabolic conversions. This note reports the initial results of this project.

EXPERIMENTAL

Materials

7-Ethoxycoumarin (7-EtOC), 7-hydroxycoumarin (7-OHC; umbelliferone), 2-methyl-1,2-di-3-pyridyl-1-propanone (metyrapone) and NADPH were obtained from Sigma (St. Louis, MO, USA). IAM HPLC columns and cartridges, as well as loose IAM packing material were from Regis (Morton Grove, IL, USA).

Rat liver microsomes

Rat liver microsomes were prepared by ultracentrifugation from male rats pretreated with phenobarbital. A solution of phenobarbital in saline was administered intraperitoneally for three days in a dose of 80 mg/kg per day and the animals were decapitated 24 h after the last dose. The microsomes (36.2 mg microsomal protein/ml) were frozen as pellet at -80°C until use. The P-450 content of the microsomal pellet after thawing was 0.45 nmol P-450/mg protein.

Non-covalent immobilization of microsomes

To 25 mg of loose IAM material in a 1.5-ml Eppendorf test tube, prewashed with 3×1 ml sodium phosphate buffer (0.1 M, pH 7.47), 100 μl of microsomal pellet (equal to 3.62 mg microsomal protein) were added. The slurry was vortexed and left to equilibrate for 10 min. It was then washed with 3×1 ml of the same phosphate buffer and the washings collected for protein determination. The immobilization was performed twice using the same microsomal preparation and 3.43 (± 0.01) mg microsomal protein were bound to 25 mg IAM material.

The non-covalent immobilization of microsomes on the HPLC column was performed by injecting $5 \times 20 \mu\text{l}$ of microsomal pellet (equal to 3.62 mg of microsomal protein) onto the 1 cm \times 3.0 mm I.D. HPLC cartridge filled with IAM stationary phase. The mobile phase flow-rate was 0.1 ml/min. The cartridge was perfused with the suspension containing microsomes in reversed position in order to bypass the cartridge frit and enable non-solubilized microsomes to penetrate into the IAM interphase. The eluate (2 ml) was collected and analyzed for unretained protein; 0.44 mg were detected. The cartridge was re-

versed and the eluate collected in 2-ml fractions to check for the possible leak of microsomes. These fractions did not contain any protein and the total amount of microsomal protein retained non-covalently on the IAM interphase was 3.18 mg.

Analytical methods

Protein was determined according to the method of Lowry *et al.* [7]. P-450 content of microsomes was quantitated by the method of Omura and Sato [8] from the reduced carbon monoxide difference spectrum utilizing an extinction coefficient of $91 \text{ mM}^{-1} \text{ cm}^{-1}$ for the 490–450-nm wavelength pair.

7-Ethoxycoumarin-O-deethylase activity

7-Ethoxycoumarin-O-deethylase activity of both non-immobilized and non-covalently immobilized rat liver microsomes on loose IAM material, as well as of the microsomes non-covalently immobilized on the IAM interphase in a HPLC cartridge, was measured by the fluorimetric method of Ullrich and Weber [9] adapted for HPLC.

With non-immobilized microsomes and microsomes non-covalently immobilized on loose IAM support. A 1-ml volume of 0.1 mM 7-EtOC in sodium phosphate buffer (0.1 M, pH 7.47) was pipetted into two Eppendorf 1.5-ml test tubes (each containing 3.43 mg of non-covalently immobilized microsomal protein on 25 mg of loose IAM chromatographic support), and into two test tubes each containing 50 μl of microsomal pellet (corresponding to 1.81 mg microsomal protein). After short vortexing and equilibration for 5 min at 37°C in a water bath, the enzymatic reaction was started by addition of 5 μl of 10 mM NADPH. The test tubes were incubated unstoppered in a water bath at 37°C and vortexed every 5 min to facilitate the oxygenation of the incubation mixture. After 20 min, the test tubes were spun for 2 min at 15 000 g and a 100- μl aliquot of the supernatant removed and injected into the HPLC system. Blanks without microsomes and without NADPH were run together with the samples. Before the start of each new incubation with a fresh substrate, the

microsomes–IAM slurry was washed with 3×1 ml of sodium phosphate buffer (0.1 M, pH 7.47).

The productivity of the non-covalently immobilized microsomes, measured as nmoles of 7-OHC/mg microsomal protein, was measured using the same approach. In this experiment, aliquots of the incubation mixtures were removed for HPLC analysis of 7-OHC concentration at 0, 20, 40, 60, 80 and 100 min total incubation time. At each sampling time from 20 to 80 min, 5 μl of 10 mM NADPH were added to the incubation mixture.

With microsomes non-covalently immobilized on IAM chromatographic column. A 20- μl volume of mixture A or B were injected directly into the chromatographic system, where: A = 5 ml of 0.1 mM 7-EtOC in sodium phosphate buffer (0.1 M, pH 7.47) with 5 μl of 10 mM NADPH/ml; B = 5 ml of 1 mM 7-EtOC in sodium phosphate buffer (0.1 M, pH 7.47) with 20 μl of 10 mM NADPH/ml. Controls contained the 7-EtOC solution but no NADPH.

Inhibition of 7-ethoxycoumarin-O-deethylase activity with metyrapone

After the first 20-min incubation (carried out as described above), 10 μl of metyrapone (0.01 M) (final concentration in incubation mixture 0.1 mM) were added to one test tube with non-covalently immobilized microsomes on IAM, and 10 μl of buffer to the control. After addition of another 5 μl of 10 mM NADPH to both test tubes, the incubation at 37°C was continued for another 20 min. The 7-OHC generated was determined by direct injection of the supernatant into the HPLC system as described above.

Stability (time vs. activity profile) of non-covalently immobilized microsomes

This was studied by testing the O-deethylase activity of the immobilized microsomes.

(a) On loose IAM material, the same microsomes were kept at 37°C while incubating and at 25°C for all other manipulations during the days 1 and 2 (*ca.* 10 h/day) and days 7 and 10 (*ca.* 4 h/day). The rest of time microsomes were kept refrigerated at 4°C.

(b) On the microsomes–IAM chromatographic

column, all the experiments were done at 25°C in one day.

Chromatographic system

The chromatographic system consisted of an Spectroflow 400 pump (ABI Kratos, Ramsey, NJ, USA), 7125 Rheodyne injector (Rheodyne, Cotati, CA, USA) with a 20- μ l sample loop, 470 Waters scanning fluorescence detector (Millipore Waters, Milford, MA, USA) and a Data Jet integrator (Spectra-Physics, San Jose, CA, USA). The chromatographic columns used were an 1 cm \times 3.0 mm I.D. cartridge (used as an IMER while containing microsomes) and an 3 cm \times 4.6 mm I.D. column, in series, both filled with the IAM chromatographic support (Regis). The mobile phase used was sodium phosphate buffer (0.1 M, pH 7.47). The flow was kept at 0.5 ml/min except where otherwise stated. The excitation and emission wavelengths for fluorescence detection were set at 360 and 460 nm, respectively.

RESULTS AND DISCUSSION

The catalytic activity of the microsomal monooxygenatic system of mammalian liver is determined by interactions between the three essential components: P-450, NADPH-P-450 reductase, and phosphatidylcholine. Due to the membrane-bound character, protein-phospholipid interactions are considered of special importance for the functional activity. Although IAM.PC (acronym of the first commercially available IAM based on the most prevalent membrane lipid, phosphatidylcholine, PC) contains monolayers of amphiphilic membrane lipid molecules bonded to silica, this chromatographic support has the hydrophobicity of only a C₃ reversed-phase chromatographic surface. Therefore quite mild mobile phases, like buffers, may be used, which makes IAM.PC columns suitable for protein immobilization. Pidgeon *et al.* [6] have found that solubilized P-450 isozymes bind to IAM in the presence of 0.6% cholate. (The presence of detergent was necessary to maintain membrane proteins in solution and prevent protein aggregation.) They have also found, however, that most other microsomal proteins, including NADPH-P-450 reductase, do not bind

to IAM under the same conditions. Thus, the lack of possibility to immobilize all three essential components for microsomal monooxygenation prompted us to try to immobilize non-solubilized microsomes into the IAM.PC interphase. Consequently, we were able to perform P-450-catalysed reactions on-line in the HPLC system without undergoing the lengthy procedure of solubilization of microsomes.

The monooxygenase activity of the non-immobilized and immobilized microsomes was monitored by following the formation of 7-OHC from the O-deethylation of 7-EtOC [9]. This assay is a sensitive indicator of monooxygenase activity but the ability of this approach to detect low levels of 7-ethoxycoumarin-O-deethylase activity using a spectrofluorometer cuvette is limited by the presence in the reaction mixture of other fluorescent compounds, NADPH and 7-EtOC. Several authors have overcome this problem by extracting 7-OHC from the reaction mixture [10,11]. In this study, extractions were avoided by direct HPLC analysis of the incubation mixture. The chromatography was able to directly separate and quantify the product 7-OHC in the presence of the substrate (7-EtOC) and cofactor (NADPH). Representative chromatograms from this study are presented in Fig. 1.

The non-solubilized microsomes were initially immobilized on loose IAM chromatographic support and the monooxygenase activity assessed using Eppendorf test tubes as reaction vessels. Parallel studies were performed using aliquots of the same microsomal pellet suspension from which the immobilized microsomes were obtained. The results of this comparison indicate that the immobilized enzymes retained only 14% of the initial activity of the non-immobilized microsomes (Table I).

While the reason for the initial loss of enzymatic activity is not immediately apparent, it may be due to the positioning of the functional membrane proteins within the interstitial cavities of the IAM support. Thus, the access of the substrate to the binding site is inhibited because of the topology of the protein on the immobilized surface. A similar effect has been suggested for the observed 50% decrease in the proteolytic activity of α -chymotrypsin [5]. The positioning,

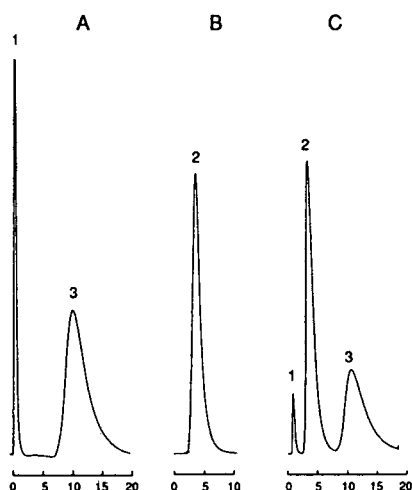


Fig. 1. Chromatograms of (A) the incubation mixture before addition of microsomes, containing only NADPH and the substrate; (B) the 7-OHC standard solution; and (C) the complete incubation mixture containing rat liver microsomal 7-ethoxycoumarin deethylase non-covalently immobilized on loose IAM. Peaks: 1 = NADPH; 2 = 7-OHC; 3 = 7-EtOC. Abscissa = time in min; ordinate = fluorescence.

or shielding, of the microsomes entrapped in the IAM chromatographic support may also explain the fact that immobilization reduced the inhibitory effect of metyrapone; 0.1 mM metyrapone produced a 23% decrease in the 7-ethoxycoumarin-O-deethylase activity of the IAM-immobilized microsomes and a 62% decrease in the same activity of the non-immobilized enzymes.

TABLE I

TIME PROFILE OF THE AVERAGE 7-ETHOXYCOUMARIN O-DEETHYLASE ACTIVITY FROM RAT LIVER MICROSOMES NON-COVALENTLY IMMOBILIZED ON LOOSE IAM CHROMATOGRAPHIC SUPPORT IN COMPARISON WITH NON-IMMOBILIZED MICROSOMES

	nmol 7-OHC per mg microsomal protein per 20 min			
	Day 1	Day 2	Day 7	Day 10
Non-immobilized microsomes	1.785	0.794	0.128	0.019
Range	1.464–2.265	0.540–1.000	0.115–0.140	0.016–0.022
<i>n</i>	4	4	2	2
Microsomes on loose IAM	0.249	0.167	0.091	0.090
Range	0.233–0.272	0.105–0.212	0.086–0.096	0.118–0.061
<i>n</i>	6	4	2	2

It should also be mentioned that the functional activity of a protein may be diminished by the lack of cofactors at the site of reaction. Taking into account that the enzymatic reaction takes place in the chromatographic column, it is of utmost importance to ensure the simultaneous presence of both substrate and cofactor(s) at the reaction site. If the cofactor(s) and the substrate do not have more or less the same k' , they will be separated after the first few mm of the HPLC column and no enzymatic reaction could be expected.

As has been previously demonstrated for microsomes covalently attached to Sepharose beads [2], immobilization enhanced the stability of the enzymes relative to the non-immobilized microsomes (Table I). Both immobilized and non-immobilized microsomes were stored under the same conditions, 4°C, and the 7-ethoxycoumarin-O-deethylase activity determined on days 2, 7 and 14 post immobilization. The non-immobilized enzymes lost 55.5% of their activity by day 2, 92.8% by day 7 and 98.9% by day 14. The IAM-immobilized microsomes lost 32.9% of their activity by day 2, 63.4% by day 7 and 63.8% by day 14. As a result, the relative difference between the activity of the immobilized:non-immobilized microsomes went from 0.13:1 on day 1 to 4.74:1 on day 14.

The productivity of the microsomal IMER as measured by the O-deethylation of 7-EtOC and the production of 7-OHC was studied by sup-

plying the same incubation mixture with fresh NADPH every 20 min after removing aliquots from the reaction mixture for HPLC determination of 7-OHC concentration. The increase in product formation was linear (Fig. 2).

When the non-solubilized microsomes were immobilized on an IAM support packed in a 1-cm HPLC column, measurable 7-ethoxycoumarin-O-deethylase activity was observed after the injection onto the IMER of 7-EtOC and NADPH by the appearance of 7-OHC in the chromatogram. The chromatographic peak corresponding to 7-OHC was not present when 7-EtOC without NADPH was injected onto the IMER indicating that the appearance of 7-OHC was due to enzymatic activity and not to interactions with the chromatographic phase. The productivity of the IMER (expressed as nmol 7-OHC/mg microsomal protein) was dependent upon the flow-rate of the mobile phase, which, in turn, was a measure of the time that 7-EtOC was in contact with the microsomes (Table II). A decrease in the flow-rate from 0.50 to 0.20 ml/min increased the productivity by 475%. However, this effect appears to be saturable as a decrease in flow-rate from 0.20 to 0.10 ml/min only increased the productivity by 14.4%.

The stability of IMER relative to its 7-ethoxycoumarin-O-deethylase activity was followed during one day (Table III). The observed de-

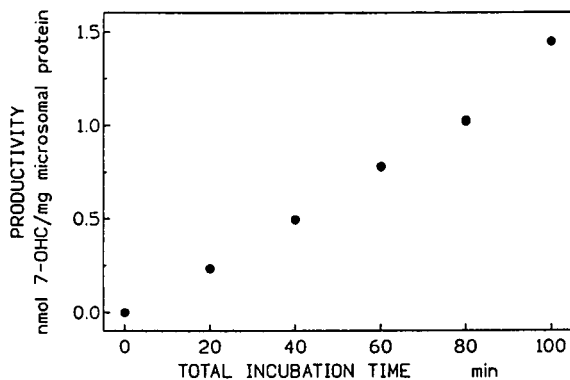


Fig. 2. Production of 7-OHC by rat liver microsomal 7-ethoxycoumarin deethylase non-covalently immobilized on loose IAM chromatographic support. The incubation mixture contained 1 ml of 0.1 mM 7-EtOC; 5 μ l of 10 mM NADPH was added at 0, 20, 40, 60 and 80 min total incubation time. The experiment was performed on day 1, $n = 2$.

TABLE II

7-ETHOXYCOUMARIN O-DEETHYLASE ACTIVITY OF RAT LIVER MICROSOMES NON-COVALENTLY IMMOBILIZED ON IAM CHROMATOGRAPHIC COLUMN IN RELATION TO THE MOBILE PHASE FLOW THROUGH THE HPLC SYSTEM

The experiments were performed within 1 h.

Mobile phase flow (ml/min)	7-EtOC-microsomes contact time (min)	Productivity (nmol 7-OHC/mg microsomal protein)
0.50	2	0.073
0.20	5	0.347
0.10	10	0.397

crease in enzymatic activity (*ca.* 85%) was greater than the 33% decrease observed for the microsomes immobilized on the loose IAM chromatographic support. This difference may have been caused by the lack of requisite molecular oxygen in the mobile phase or by the pressure exerted on the microsomes during the chromatographic process. Pidgeon *et al.* [6] have reported that with IAM-immobilized microsomes, the P-

TABLE III

TIME-YIELD PROFILE OF 7-HYDROXYCOUMARIN GENERATED FROM 7-ETHOXYCOUMARIN INJECTED INTO A HPLC CHROMATOGRAPHIC COLUMN WITH RAT LIVER MICROSOMES NON-COVALENTLY IMMOBILIZED ON IAM CHROMATOGRAPHIC SUPPORT

Elapsed time after immobilization (h)	Substrate and cofactor concentrations (nmol 7-OHC/mg microsomal protein)	
	0.1 mM 7-EtOC, 0.05 mM NADPH	1 mM 7-EtOC, 0.20 mM NADPH
1.51	0.059	
1.87	0.069	
2.22		0.384
2.65	0.073	
3.20		0.199
4.55	0.035	
4.87	0.033	
5.65	0.019	
5.97	0.024	
6.35	0.011	

450 tertiary conformation about the haeme catalytic centre appears to be pressure sensitive. This is most likely the result of shearing forces generated at the solid support–mobile phase interface and the best chromatographic results were obtained by maintaining HPLC back pressure below 800–1000 p.s.i. (1 p.s.i. = 6894.76 Pa).

The results of this study indicate that non-solubilized microsomes can be entrapped on an IAM chromatographic support with retention of their enzymatic activity. Further, they indicate that an HPLC system composed of a microsomal IMER can be developed for the direct study of metabolic processes. Additional work in the development of this system is underway in our laboratory.

REFERENCES

- 1 C. Fenselau, S. Pallante and I. Parikh, *J. Med. Chem.*, 19 (1976) 679.
- 2 J.P. Lehman, L. Ferrin, C. Fenselau and G.S. Yost, *Drug Metab. Dispos.*, 9 (1981) 15.
- 3 M. Haumont, J. Magdalou, J.-C. Ziegler, R. Bidault, J.-P. Siest and G. Siest, *Appl. Microbiol. Biotechnol.*, 35 (1991) 440.
- 4 C. Pidgeon, C. Marcus and F. Alvarez, in T.O. Baldwin and J.W. Kelly (Editors), *Applications of Enzyme Biotechnology*, Plenum Press, New York, 1992, p. 201.
- 5 W.-K. Chui, and I.W. Wainer, *Anal. Biochem.*, 201 (1992) 237.
- 6 C. Pidgeon, J. Stevens, S. Otto, C. Jefcoate and C. Marcus, *Anal. Biochem.*, 194 (1991) 163.
- 7 O.H. Lowry, N.J. Rosebrough, A.L. Farr and R.J. Randall, *J. Biol. Chem.*, 193 (1951) 265.
- 8 T. Omura and R. Sato, *J. Biol. Chem.*, 239 (1964) 2370.
- 9 V. Ullrich, and P. Weber, *Hoppe-Seyler's Z. Physiol. Chem.*, 353 (1972) 1171.
- 10 M. Jacobson, W. Levin, P.J. Poppers, A.W. Wood and A.H. Conney, *Clin. Pharmacol. Ther.*, 16 (1974) 701.
- 11 W.F. Greenlee and A. Poland, *J. Pharmacol. Exp. Ther.*, 205 (1978) 596.

Optimization of the separation selectivity of a group of benzene and naphthalene derivatives in micellar high-performance liquid chromatography using a C₁₈ column and alcohols as modifiers in the mobile phase

M.A. García, S. Vera, M. Bombín and M.L. Marina*

Departamento de Química Analítica, Facultad de Ciencias, Universidad de Alcalá de Henares, 28871 Alcalá de Henares (Madrid) (Spain)

(First received January 4th, 1993; revised manuscript received April 26th, 1993)

ABSTRACT

The separation selectivity of fifteen benzene and naphthalene derivatives in micellar high-performance liquid chromatography, using a C₁₈ column, was studied as a function of the parameters on which it depends. A multiple linear regression programme was used to find the dependence of the selectivity coefficient on the following parameters: nature of the surfactant in the mobile phase (sodium dodecyl sulphate or hexadecyltrimethylammonium bromide), surfactant concentration (0.02–0.1 M), nature of the additive in the mobile phase (methanol, *n*-propanol, *n*-butanol and sodium chloride) and percentage of the alcohol (0, 5 or 10%). Selectivity optimization corresponds to the use of sodium dodecyl sulphate at low concentrations and the addition of an alcohol of medium chain length.

INTRODUCTION

The use of surfactant solutions, at a concentration above the critical micelle concentration (c.m.c.) as mobile phases for reversed-phase liquid chromatography has received much attention. The popularity of micellar liquid chromatography (MLC) is due to its ability for the simultaneous separation of ionic and non-ionic compounds, rapid gradient elution, possibility of direct injection of physiological fluids, enhancement of fluorescence and absorption detection, etc. [1–11].

The interaction between solutes and micelles can be evaluated through the calculation of the solute–micelle binding constant using equations

that describe solute retention as a function of micelle concentration, based on a three-way partition model proposed by Armstrong and Nome [4] and Arunyanart and Cline-Love [5]. These equations have also been experimentally verified for a large number of organic solutes [12–20]. The reported values for the solute–micelle binding constant can be used to facilitate systematic optimization in MLC [14].

As in reversed-phase liquid chromatography (RPLC), selectivity in MLC is primarily controlled by the composition of the mobile phase, *i.e.*, the type and concentration of surfactant present as micellar aggregates. The solute behaviour in MLC was attributed to different factors such as the special association of solutes with micelles through a combination of electrostatic, hydrophobic and steric interactions [21,22], the heterogeneous nature of micelles

* Corresponding author.

that provides a different microenvironmental polarity for compounds in a given mobile phase, and the existence of two competing equilibria, namely solute partitioning in the stationary phase and solute partitioning in the mobile phase micelles [6,15,23,24].

A serious drawback of all MLC systems studied to date is their poor chromatographic efficiency. This deficiency is most important when viewed in the context of resolution when compared with that of commonly used aqueous organic mobile phases [25]. Poor wetting of the stationary phase [26] and restricted mass transfer [27] are the reasons for the decrease in efficiency. Several workers have investigated this aspect. Dorsey *et al.* [26] proposed the use of organic modifiers, addition of 3% of *n*-propanol to the micellar mobile phase and an elevated column temperature. Yarmchuck *et al.* [27] recommended the use of low mobile phase flow-rates, elevated operating temperatures and minimum surfactant concentrations. It was also suspected that surfactant adsorption on the stationary phase had a great impact on the MLC efficiency [28–31]. It was shown that the addition of a short- or medium-chain alcohol causes surfactant desorption from the stationary phase and improves the efficiency [32].

Surprisingly, the effect of organic modifiers on chromatographic selectivity has been ignored for a long time and only a few papers have appeared. Khaledi and co-workers [15,23] studied the effect of organic solvents on retention and methylene group selectivity in MLC, and the effect of adding organic solvents to micellar eluents on the chromatographic selectivity of polar and ionic solutes [24,33,34]. More recently, they studied the role of organic modifiers and micelles in controlling solvent strength and selectivity in MLC [35,36].

Achieving a satisfactory separation within a reasonable run time requires the selection of experimental conditions that optimize the separation factor (α), the column plate number (N) and the solute capacity factor (k') [37]. Our aim in this work was the study of MLC selectivity in terms of the separation factor. The effect of the nature and concentration of the surfactant and the type and concentration of the additive used

in the mobile phase (methanol, *n*-propanol, *n*-butanol and sodium chloride) on separation selectivity was studied. Chemometric methods were also applied to the retention data for fifteen aromatic compounds (benzene and naphthalene derivatives) to find the optimum analytical conditions.

EXPERIMENTAL

Apparatus

The chromatograph consisted of a Model 510 pump, a Model U6K injector, a Model 440 fixed-wavelength (254 nm) detector and a Model 740 data module (all from Waters). Retention data were obtained with a 15 cm \times 3.9 mm I.D. Spherisorb ODS 2 ($d_p = 5 \mu\text{m}$) column (Teknokroma) and a 15 cm \times 3.9 mm I.D. Nova-Pak C₁₈ ($d_p = 4 \mu\text{m}$) column (Waters). Final separations were achieved on a 10 cm \times 4.0 mm I.D. Hyper-sil ODS ($d_p = 3 \mu\text{m}$) column (Teknokroma). A 0.45- μm filter and filtration system (Millipore) were used. A Model 522 conductimeter (Crison) was employed.

Reagents

The surfactants sodium dodecyl sulphate (SDS) and hexadecyltrimethylammonium bromide (CTAB) (Merck), methanol (Scharlau) and *n*-propanol and *n*-butanol (Merck), were used as received.

Benzene and naphthalene derivatives of analytical-reagent grade were as follows: (1) benzene, (2) benzylic alcohol, (3) benzamide, (4) toluene, (5) benzonitrile, (6) nitrobenzene, (7) phenol, (8) 2-phenylethanol, (9) chlorobenzene, (10) phenylacetonitrile, (11) 3,5-dimethylphenol, (12) naphthalene, (13) 1-naphthol, (14) 2-naphthol and (15) 1-naphthylamine. Water purified with a Milli-Q system (Millipore) was used.

Procedure

Micellar mobile phases (with a surfactant concentration from 0.02 to 0.1 *M*) were prepared by dissolving the appropriate amount of surfactants and methanol, *n*-propanol or *n*-butanol in water in a ultrasonic bath followed by filtration. Stock solutions of test solutes were prepared in the

mobile phase itself and their concentrations were adjusted to permit their detection from the injection of a 20- μ l volume of sample.

The void volume for SDS micelles was determined from the retention time of the peak originating from the injection of the nitrate anion into the chromatographic system. For CTAB mobile phases, the first deviation of the baseline was employed.

The column and the mobile phase were water jacketed and thermostated at $25 \pm 1^\circ\text{C}$ with a circulating water bath.

Determination of the c.m.c. for SDS–10% methanol solutions was achieved by conductivity measurements at constant temperature ($25 \pm 1^\circ\text{C}$).

RESULTS AND DISCUSSION

The capacity factors of fifteen benzene and naphthalene derivatives in an MLC system in the presence of methanol and *n*-propanol were determined by using SDS and CTAB as surfactants in the mobile phase. The results obtained were compared with those obtained previously for the same compounds in the absence of modifiers [12] and in the presence of *n*-butanol and sodium chloride [13]. All these data allowed conclusions to be drawn regarding the separation selectivity, the effects of the nature and concentration of the surfactant and the effects of the nature and percentage of alcohol used in the mobile phase. The c.m.c. values for SDS and CTAB in the absence and presence of the different alcohols are given in Table I.

Variation of the capacity factor

Figs. 1 and 2 show the variation of the logarithm of the capacity factor ($\log k'$) for the fifteen benzene and naphthalene derivatives as a function of the SDS and CTAB concentration, respectively. In both instances, the mobile phase was modified with 5% of *n*-butanol. For all compounds, the retention decreases when the eluent strength increases, as expected. The rate of change in retention of the different solutes varies with the solute charge and hydrophobicity and the length of the alkyl chain, charge and concentration of the micelles [35]. Regarding

TABLE I

CRITICAL MICELLAR CONCENTRATIONS OF MICELLAR SYSTEMS USED AS MOBILE PHASES

Micellar system	C.m.c. (M)	Ref.
SDS	$8.08 \cdot 10^{-3}$	38
SDS–10% MeOH	$8.20 \cdot 10^{-3}$	This work
SDS–10% PrOH	$4.70 \cdot 10^{-3}$	39
SDS–5% BuOH	$1.34 \cdot 10^{-3}$	40
SDS–10% BuOH	$2.27 \cdot 10^{-4}$	40
SDS–0.1 M NaCl	$1.40 \cdot 10^{-3}$	41
CTAB	$9.20 \cdot 10^{-4}$	38
CTAB–5% PrOH	$2.69 \cdot 10^{-3}$	42
CTAB–10% PrOH	$1.94 \cdot 10^{-3}$	42
CTAB–5% BuOH	$8.80 \cdot 10^{-4}$	43

selectivity, in Figs. 1 and 2 and also in similar figures obtained with other mobile phases, it was observed that the separation selectivity increases when the surfactant concentration in mobile phase decreases for both surfactants (SDS and CTAB). An enhancement in selectivity as a result of decreasing micelle concentration has

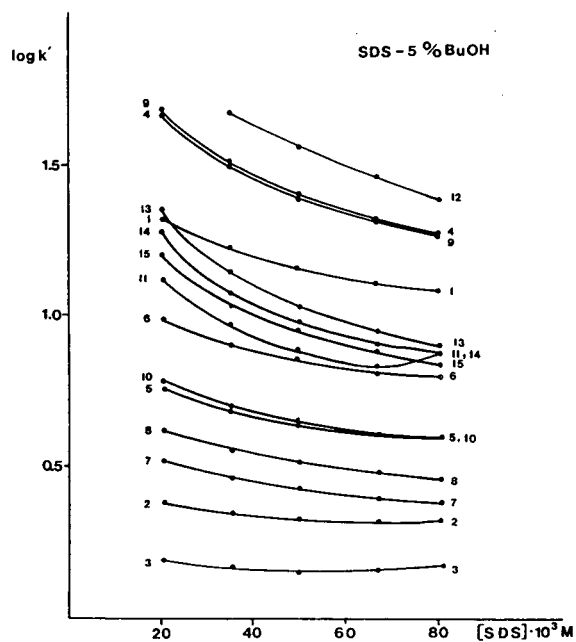


Fig. 1. Variation of $\log k'$ for the studied compounds (for numbers see *Reagents*) as a function of the concentration of SDS in a mobile phase modified with 5% butanol. Column: Nova-Pak C_{18} (15 cm \times 3.9 mm I.D.) ($d_p = 4 \mu\text{m}$). Data from ref. 13.

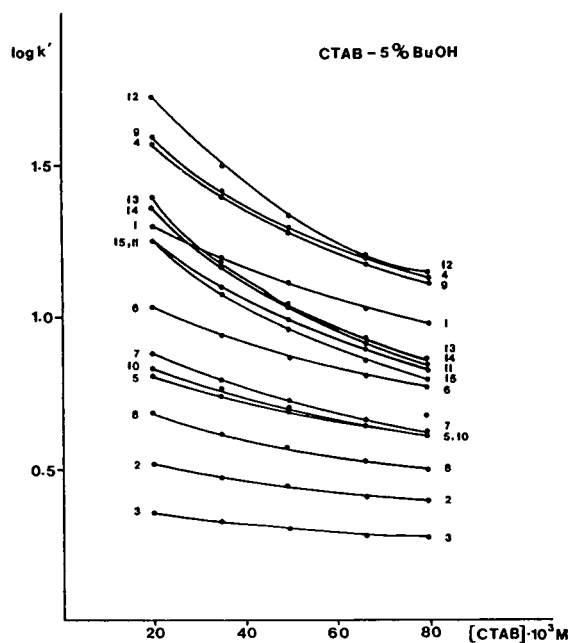


Fig. 2. Variation of $\log k'$ for the studied compounds as a function of the concentration of CTAB in a mobile phase modified with 5% butanol. Column: Nova-Pak C_{18} (15 cm \times 3.9 mm I.D.) ($d_p = 4 \mu\text{m}$). Data from ref. 13.

also been observed by other workers [35]. On the other hand, in all the mobile phases for which the comparison between SDS and CTAB was possible, the separation selectivity was, in general, better for SDS than for CTAB. Taking into account that CTAB eluents are inherently stronger for uncharged solutes owing to the longer surfactant chain length and that selectivity increases with decreasing micelle concentration, it seems that the separation selectivity decreases with increasing eluent strength (through an increase in concentration and chain length of the micelles).

In order to study the influence of the number of carbon atoms in the alcohol on the retention and selectivity for the fifteen compounds studied, the variation of $\log k'$ as a function of this parameter is plotted in Fig. 3 for a 0.035 M SDS mobile phase modified by a fixed percentage of each alcohol (10%). The results obtained in the absence of alcohol [12] are also included. Fig. 3 shows that the behaviour of all the compounds is similar. Retention, in general, decreases when

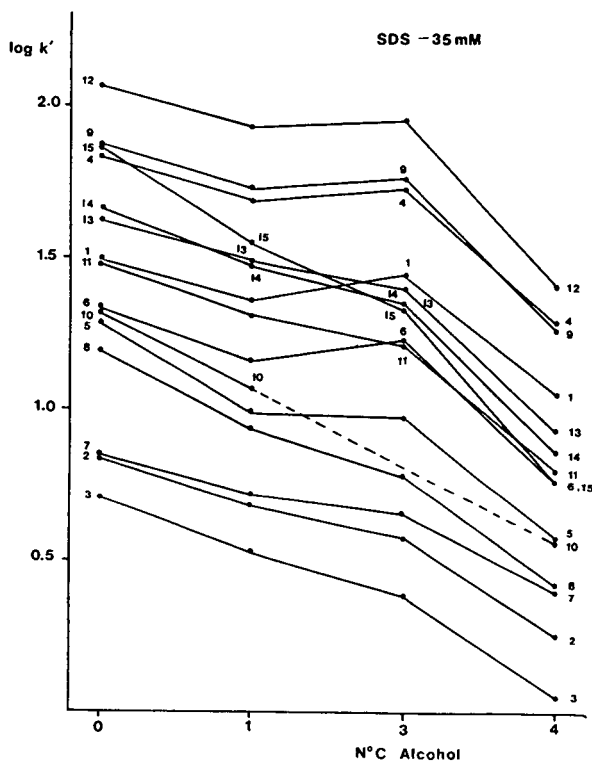


Fig. 3. Variation of $\log k'$ for the studied compounds as a function of the number of carbon atoms in the alcohol added at 10% to a mobile phase of 0.035 M SDS. Column: Nova-Pak C_{18} (15 cm \times 3.9 mm I.D.) ($d_p = 4 \mu\text{m}$), except Spherisorb ODS-2 (15 cm \times 3.9 mm I.D.) ($d_p = 5 \mu\text{m}$) for *n*-propanol. Data for aqueous mobile phases from ref. 12 and data for *n*-butanol from ref. 13.

the number of carbons in the alcohol increases. These results are in agreement with those obtained by other workers showing that butanol is the strongest and methanol the weakest solvent as in conventional aqueous–organic systems [24]. The larger solvent strength for butanol and propanol indicates that these solvents have a stronger interaction with micelles and, consequently, can solvate more effectively or can compete better with micelles for interaction with solutes. Six of the fifteen compounds (benzonitrile, nitrobenzene, benzene, toluene, chlorobenzene and naphthalene) show a retention with SDS–propanol eluent equivalent to or even larger than that with SDS–methanol. This result may be due to the fact that for *n*-propanol a different column was used, as indicated in Fig. 3.

Regarding selectivity, Fig. 3 shows that there are some pairs of compounds for which the separation selectivity is poor for any alcohol–chlorobenzene–toluene. On the other hand, the separation selectivity for some pairs decreases when the number of carbon atoms in the alcohol increases, which is the case with phenol–2-phenylethanol and 3,5-dimethylphenol–nitrobenzene. However, the separation selectivity increases for a greater number of pairs with increasing number of carbon atoms in the alcohol. It is possible, therefore, to state that even if the variation of the separation selectivity as a function of the nature of the alcohol depends on the nature of the compounds, in general terms *n*-butanol allows better selectivities than methanol or *n*-propanol to be obtained. These results indicate that separation selectivity in MLC increases with increasing solvent strength, in contrast to that obtained with conventional aqueous–organic systems where an increase in solvent strength causes a decrease in selectivity.

Fig. 4 shows the variation in $\log k'$ for the compounds studied as a function of the percentage of *n*-butanol in a 0.035 M SDS mobile phase. The eluent strength increases as the organic modifier concentration increases, resulting in a decrease in retention. In fact, it was observed that the retention for all compounds decreases in the presence of *n*-butanol, this reduction being more significant from 0% to 5% of alcohol than from 5% to 10%. The selectivity is better in the presence of *n*-butanol than in its absence, although there are some exceptions relating to the pairs which in Fig. 3 showed a decrease in selectivity with increasing number of carbons in the alcohol, *i.e.*, phenol–2-phenylethanol and 3,5-dimethylphenol–nitrobenzene. The fact that the separation selectivity is better in the presence of an alcohol agrees with the results obtained by other workers, who found in MLC a simultaneous enhancement of elution strength and selectivity [24,35]. However, Fig. 4 shows that the separation selectivity is slightly better at 5% *n*-butanol. This result can be justified by the existence of pairs of compounds for which the selectivity increases when the eluent strength decreases. A medium eluent strength can allow maximization of the separa-

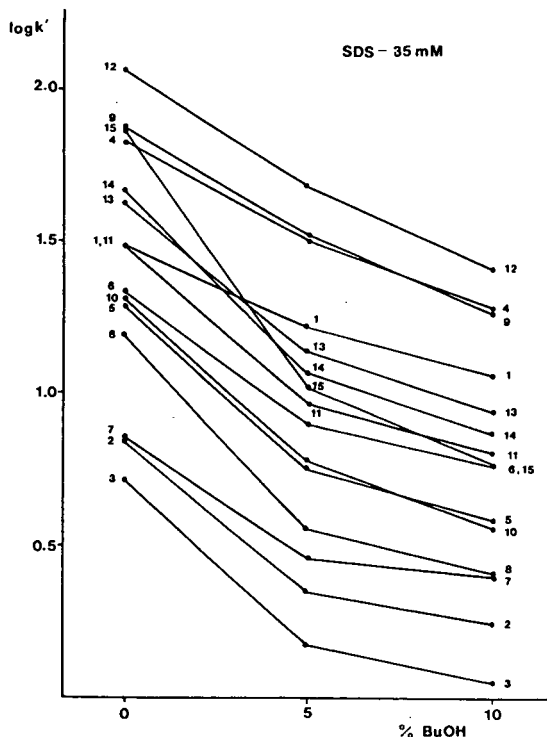


Fig. 4. Variation of $\log k'$ for the studied compounds as a function of the percentage of *n*-butanol in a mobile phase of 0.035 M SDS. Column: Nova-Pak C₁₈ (15 cm × 3.9 mm I.D.) ($d_p = 4 \mu\text{m}$). Data from refs. 12 and 13.

tion selectivity for all kinds of compounds. A model has been developed [35] explaining the dependence of the solvation ability of organic solvents in MLC (represented by the solvent strength parameter, *S*, of solutes) and the degree of solute interactions with micelles. Whenever the difference in solvent strength parameter values of two solutes in micellar eluents, dS , is positive, maximum selectivity is observed at the weakest eluent strength. When the above-mentioned difference dS is negative, there exists an inverse relationship between the retention and solvent strength parameter so that the selectivity increases with increasing volume fraction of organic modifier in micellar eluents. The pairs whose separation selectivity decreases when the organic modifier concentration increases (phenol–2-phenylethanol and 3,5-dimethylphenol–nitrobenzene) are the same pairs whose selectivity decreases with increasing number of carbons in

the alcohol, that is, their selectivity also decreases when the eluent strength is increased by changing the chain length of the alcohol.

The variation of $\log k'$ as a function of the percentage of *n*-propanol in a 0.035 M CTAB mobile phase was measured to study the influence of the percentage of other alcohols. The results are shown in Fig. 5. It is observed that the effect that *n*-propanol has on the retention of the compounds in a CTAB mobile phase is similar to the effect that *n*-butanol has on the retention of the compounds in an SDS mobile phase. Retention decreases when the percentage of *n*-propanol in the mobile phase increases, that is, when the solvent strength also increases. In this instance maximum selectivity is obtained at 3% *n*-propanol, a percentage with which a greater number of pairs can be separated with a CTAB mobile phase. Again, a medium alcohol percentage seems to give better selectivity.

The addition of 0.1 M sodium chloride to an SDS mobile phase did not allow the selectivity of the separation to be increased significantly.

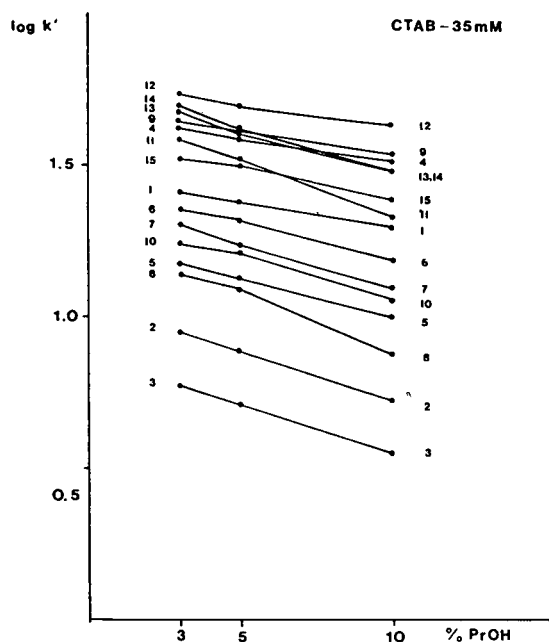


Fig. 5. Variation of $\log k'$ for the studied compounds as a function of the percentage of *n*-propanol in a mobile phase of 0.035 M CTAB. Column: Spherisorb ODS-2 (15 cm \times 3.9 mm I.D.) ($d_p = 5 \mu\text{m}$).

Multiple regression study

To optimize the separation in MLC, a statistical study of the selectivity under the different experimental conditions studied was performed. The selectivity coefficient (α), defined as the ratio between the capacity factors of two compounds, was calculated for the pairs that can be obtained from the fifteen compounds under the different experimental conditions.

To study these results by means of a multiple linear regression programme, only selectivity coefficients that vary with the experimental conditions were chosen. This implies the exclusion of the selectivity coefficients of pairs that are either never separated or that can always be separated regardless of the experimental conditions. Therefore, the number of pairs considered in the programme was equal to 25 under the different experimental conditions which involved 45 different possibilities excluding 5 concentrations of SDS modified with 0.1 M NaCl.

The average value of the selectivity coefficient for the 25 pairs studied was calculated ($\bar{\alpha}$). The absolute value of $(1 - \alpha)(|1 - \alpha|)$ is chosen as the dependent variable for using the programme. The greater is $|1 - \alpha|$, the better is the selectivity. The independent variables used in the programme and the possible values for each are given at Table II.

The best results correspond to the combina-

TABLE II
ASSIGNED VALUES FOR THE INDEPENDENT VARIABLES USED IN THE MULTIPLE REGRESSION ANALYSIS

Variable	Symbol	Assigned values
Nature of surfactant	A	1 (SDS) 2 (CTAB)
Surfactant concentration (mol/l)	B	0.020 0.035 0.050 0.067 0.080 0.100
Carbon number of the alcohol	C	0, 1, 3, 4
Alcohol percentage (v/v)	D	0, 5, 10

tion of the variables C and D , *i.e.*, assuming that the number of carbons in the alcohol and its percentage operate together.

The parameter $|\overline{1 - \alpha}|$ can be expressed by the equation

$$\begin{aligned} |\overline{1 - \alpha}| = & 1.05(\pm 6.60 \cdot 10^{-2}) - 0.22(\pm 2.97 \cdot 10^{-2})A \\ & - 3.27 \cdot 10^{-3}(\pm 6.28 \cdot 10^{-4})B \\ & + 6.51 \cdot 10^{-3}(\pm 1.16 \cdot 10^{-3})CD \end{aligned} \quad (1)$$

$$n = 25; r^2 = 0.7784; s = 0.098; F = 48.01$$

where the values in parentheses are the standard errors.

Although the signs and the magnitudes of the coefficients of a regression equation may not have any physical meaning, it is interesting to compare the information that could be obtained from these coefficients and from the experimental results. The negative coefficient obtained for the variables A and B could indicate an increase in the separation selectivity when the variables A and B decrease, *i.e.*, for the use of SDS as a surfactant and for low concentrations of surfactant in the mobile phase. This agrees with the experimental results presented here. The positive coefficient obtained on combining variables C and D implies that the selectivity increases when the variables C and D also increase, *i.e.*,

the effect of the percentage of alcohol increases when the length of the chain of the alcohol also increases. Hence it is easier to modify the selectivity by means of the percentage of the alcohol when it has the maximum number of carbons (*n*-butanol). The experimental results show maximum selectivity for *n*-butanol at a level of 5%. Eqn. 1 provides the best combination for coefficient values that result in the least error in predicting $(1 - \alpha)$.

Separation of mixtures

To test the validity of the above-mentioned conditions for the optimization of a separation, a mixture of the fifteen benzene and naphthalene derivatives was injected into an MLC system in which a C_{18} column ($d_p = 3 \mu\text{m}$) was used. The mobile phase chosen was to contain 0.035 *M* SDS. As modifiers *n*-propanol and *n*-butanol as alcohols with a greater number of carbons in the molecule and at concentrations of 5% and 10% were tested. Mobile phases containing 0.035 *M* SDS and 10% *n*-propanol or *n*-butanol allowed the separation of twelve peaks, but the pairs that could not be separated were not the same for the two mobile phases. With 10% *n*-butanol, phenol–2-phenylethanol, nitrobenzene–1-naphthylamine and toluene–chlorobenzene and with 10% *n*-propanol, benzonitrile–phenylacetone-trile, nitrobenzene–3,5-dimethylphenol and

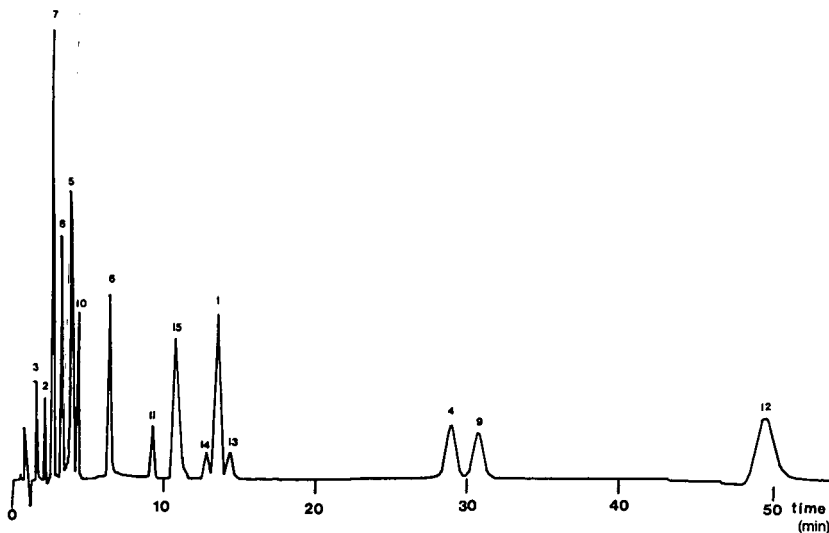


Fig. 6. Chromatogram for the separation of a mixture of fifteen benzene and naphthalene derivatives by using a 0.020 *M* SDS mobile phase modified with 5% butanol. Column: Hypersil ODS (10 cm × 4.0 mm I.D.) ($d_p = 3 \mu\text{m}$).

toluene–chlorobenzene could not be separated. It is important to emphasize that when the separation selectivity is similar for *n*-butanol and *n*-propanol, *n*-butanol provides a shorter analysis time. A concentration of 5% *n*-propanol or *n*-butanol allowed the separation of fourteen peaks from the mixture using a 0.035 M SDS mobile phase. The pair that could not be separated with 5% *n*-butanol was toluene–chlorobenzene and that with 5% *n*-propanol was benzonitrile–phenylacetonitrile. In this instance also (5% alcohol) the analysis time was shorter with *n*-butanol than *n*-propanol.

In order to separate all fifteen benzene and naphthalene derivatives, a 5% *n*-butanol–0.020 M SDS mobile phase was used to attempt the separation of toluene and chlorobenzene, which were not separated at a 0.035 M concentration of SDS. Fig. 6 shows the separation obtained under these conditions. Although the analysis time was longer because the retention of the compounds increased when the surfactant concentration decreased, a 0.020 M SDS concentration in the mobile phase allowed the separation of all the compounds in the mixture.

To study in greater depth the influence of the percentage of alcohol on selectivity, the effect of the nature and percentage of the alcohol on the efficiency obtained in MLC is currently being investigated.

CONCLUSIONS

For the benzene and naphthalene derivatives, SDS seems to give a better separation selectivity than CTAB and the separation selectivity generally increases when the surfactant concentration in mobile phase decreases. Medium-chain alcohols such as *n*-propanol and *n*-butanol positively influence the separation selectivity of the mixture studied, but *n*-butanol also shortens the analysis time. In the experimental separations, better selectivity was obtained with medium percentages of alcohol.

ACKNOWLEDGEMENTS

We gratefully acknowledge the support of this work through a research project from DGICYT

(Spain) (reference PS90-0026). We also thank Manuel Pastor for his contribution to the chemometric study.

REFERENCES

- 1 W.L. Hinze, in K.L. Mittal (Editor), *Solution Chemistry of Surfactants*, Vol. 1, Plenum Press, New York, 1979, p. 79.
- 2 L.J. Cline-Love, J.G. Habarta and J.G. Dorsey, *Anal. Chem.*, 56 (1984) 1132A.
- 3 D.W. Armstrong and S.J. Henry, *J. Liq. Chromatogr.*, 3 (1980) 657.
- 4 D.W. Armstrong and F. Nome, *Anal. Chem.*, 53 (1981) 1662.
- 5 M. Arunyanart and L.J. Cline-Love, *Anal. Chem.*, 56 (1984) 1557.
- 6 D.W. Armstrong, *Sep. Purif. Methods*, 14 (1985) 213.
- 7 J.G. Dorsey, *Adv. Chromatogr.*, 27 (1987) 167.
- 8 W.L. Hinze, *Ann. Chim. (Rome)*, 77 (1987) 167.
- 9 W.L. Hinze (Editor), *Ordered Media in Chemical Separations (ACS Symposium Series, No. 342)*, American Chemical Society, Washington, DC, 1987.
- 10 A. Berthod and J.G. Dorsey, *Analysis*, 16 (1988) 75.
- 11 M.G. Khaledi, *Trends Anal. Chem.*, 7 (1988) 293.
- 12 M.L. Marina, S. Vera and A.R. Rodriguez, *Chromatographia*, 28 (1989) 379.
- 13 M.A. García, S. Vera and M.L. Marina, *Chromatographia*, 32 (1991) 148.
- 14 J. P. Foley, *Anal. Chim. Acta*, 231 (1990) 237.
- 15 M.G. Khaledi, E. Peuler and J. Ngeh-Ngwainbi, *Anal. Chem.*, 59 (1987) 2738.
- 16 E. Pramauro, G. Saini and E. Pelizzetti, *Anal. Chim. Acta*, 166 (1984) 233.
- 17 E. Pelizzetti and E. Pramauro, *J. Phys. Chem.*, 88 (1984) 233.
- 18 M.F. Borgerding, F.H. Quina, W.L. Hinze, J. Bowermaster and H.M. McNair, *Anal. Chem.*, 60 (1988) 2520.
- 19 A. Berthod, I. Girard and C. Gonnet, *Anal. Chem.*, 58 (1986) 1362.
- 20 B.K. Lavine, A.J. White and J. Hwa Han, *J. Chromatogr.*, 542 (1991) 29.
- 21 W.L. Hinze, *Sep. Purif. Methods*, 10 (1981) 159.
- 22 D.W. Armstrong and G.Y. Stine, *Anal. Chem.*, 55 (1983) 2317.
- 23 M.G. Khaledi, *Anal. Chem.*, 60 (1988) 876.
- 24 M.G. Khaledi, J.K. Strasters, A.H. Rodgers and E.D. Breyer, *Anal. Chem.*, 62 (1990) 130.
- 25 A. Berthod, M.F. Borgerding and W.L. Hinze, *J. Chromatogr.*, 556 (1991) 263.
- 26 J.G. Dorsey, M.T. De Echegaray and J.S. Landy, *Anal. Chem.*, 55 (1983) 924.
- 27 P. Yarmchuck, R. Weinberger, R.F. Hirsch and L.J. Cline-Love, *J. Chromatogr.*, 283 (1984) 47.
- 28 M.F. Borgerding and W.L. Hinze, *Anal. Chem.*, 57 (1985) 2183.

- 29 D.W. Armstrong, T.J. Ward and A. Berthod, *Anal. Chem.*, 58 (1986) 579.
- 30 M.F. Borgerding, W.L. Hinze, L.D. Stafford, G.W. Fulp and W.C. Hamlin, *Anal. Chem.*, 61 (1989) 1353.
- 31 R. Bailey and R.M. Cassidy, *Anal. Chem.*, 64 (1992) 2277.
- 32 A. Berthod and A. Roussel, *J. Chromatogr.*, 449 (1988) 349.
- 33 J.K. Strasters, E.D. Breyer, A.H. Rodgers and M.G. Khaledi, *J. Chromatogr.*, 511 (1990) 17.
- 34 J.K. Strasters, S.T. Kim and M.G. Khaledi, *J. Chromatogr.*, 586 (1991) 221.
- 35 A.S. Kord and M.G. Khaledi, *Anal. Chem.*, 64 (1992) 1894.
- 36 A.S. Kord and M.G. Khaledi, *Anal. Chem.*, 64 (1992) 1901.
- 37 L.R. Snyder, *Analyst*, 116 (1991) 1237.
- 38 P. Mukerjee and K.J. Mysels, in *Critical Micelle Concentrations of Aqueous Surfactant Systems*, NSRDS-NBS 36, National Bureau of Standards, Washington, DC, 1971.
- 39 A.K. Jain and R.P.B. Singh, *J. Colloid Interface Sci.*, 81 (1981) 536.
- 40 K. Hayase and S. Hayano, *Bull. Chem. Soc. Jpn.*, 50 (1977) 83.
- 41 A. Berthod, I. Girard and C. Gonnet, in W.L. Hinze (Editor), *Ordered Media in Chemical Separations (ACS Symposium Series, No. 342)*, American Chemical Society, Washington DC, 1987, p. 130.
- 42 R. Zana, S. Yiv, C. Strazielle and P. Lianos, *J. Colloid Interface Sci.*, 80 (1981) 208.
- 43 M. Valiente and E. Rodenas, *An. Quim.*, 85 (1989) 192.

Retention behaviour of volatile compounds in normal-phase high-performance liquid chromatography on a diol column

Markus Lübke* and Jean-Luc Le Quéré

INRA, Laboratoire de Recherche sur les Arômes, 17 Rue Sully, 21034 Dijon Cédex (France)

Denis Barron

Université Joseph Fourier, UFR de Pharmacie, Laboratoire de Pharmacognosie, 38706 La Tronche Cédex (France)

(First received February 4th, 1993; revised manuscript received April 27th, 1993)

ABSTRACT

Retention data on a diol column for over 300 compounds of the chemical classes usually contained in aroma extracts of plants and foodstuffs are reported. A concept that largely corrects for minor fluctuations of the mobile phase composition and of the flow-rate was used to measure capacity factors. The mobile phase was composed of pentane and diethyl ether. The high volatility of these two solvents makes the method perfectly adaptable to the prefractionation of aroma extracts and the semi-preparative isolation of compounds. Non-polar compounds such as hydrocarbons are not retained on diol. Polar compounds can be readily eluted, with the exception of strong acids and bases.

INTRODUCTION

For over 30 years, the preferred tool of aroma researchers has been capillary gas chromatography (GC). This technique is well adapted to the analysis of volatile compounds. High-performance liquid chromatography (HPLC) certainly cannot compete with GC in terms of separation efficiency or, if so, not within an acceptable analysis time. However, HPLC analyses are usually carried out at ambient temperature; scaling up to semi-preparative analysis is straightforward; volatile and non-volatile compounds can be analysed in a single HPLC run; for simple separation problems, rapid analyses are possible.

Depending on the nature of compounds to be

analysed, several scenarios for applications of HPLC in aroma research are imaginable: quantification of major compounds in aroma extracts or of compounds which can be detected with high sensitivity, where, in general, the method of choice is reversed-phase HPLC owing to the convenient use of aqueous mobile phases; prefractionation of aroma extracts in order to obtain less complex fractions that can be further analysed by GC or HPLC, which can be an advantageous approach in trace analysis; purification of compounds for structural investigations or use in sensory evaluation, where the starting solution will generally be an already prefractionated aroma extract.

The concentration of HPLC fractions prior to the next step of analysis necessitates their extraction when employing aqueous or other high-boiling solvents as a mobile phase. The use of highly volatile HPLC solvents greatly facilitates

* Corresponding author.

the concentration of fractions without an important loss of aroma compounds, and also on-line coupling to capillary GC [1]. It implies, however, the normal-phase mode.

The use of polar bonded silica-based supports continues to grow. Compared with bare silica, they offer the advantage of easier handling, as the equilibration time after changing the mobile phase is much shorter (permitting gradient runs) and the mobile phase components do not have to be water saturated. In the aroma field, however, the applications of this type of column (mainly cyano) are rather scarce [2–7].

In this work, we focused on the diol support in the normal-phase mode, in view of the encouraging results obtained in our laboratory in pre-fractionating aroma extracts and in isolating some compounds of interest [8]. Some fundamental work aimed at understanding the mechanisms of retention on this support has already been done [9–12]. Capacity factors for selected compounds (essentially hydrocarbons and some phenols) have been reported.

The aim of this work was to determine the capacity factors of compounds within all important chemical classes present in aroma extracts of plants and foodstuffs, in order to obtain a database for the prediction of retention behaviour. Particular attention was paid to a highly volatile mobile phase system, with a view to facilitating the concentration of fractions or the recovery of pure compounds.

EXPERIMENTAL

Chemicals

Pentane was of spectroscopic grade (SDS, Peypin, France) or HPLC grade (Fisons, Loughborough, UK). Diethyl ether (HPLC grade) was obtained from SDS. Prior to use, all solvents were filtered through a 0.45- μ m membrane filter (Millipore, Bedford, MA, USA).

The standards were from our laboratory collection of volatile compounds, except vitispirane, which was a gift from Dr. Y. Le Fur (ENITA, Dijon, France).

Equipment

A Varian Model 9010 gradient pump and a

Varian 9050 programmable UV detector were used. Sample injection was achieved with a Gilson 232 autosampler, equipped with a Rheodyne Model 7010 injection valve. The pump head was maintained at constant temperature by a laboratory-made cooling jacket. The column was LiChrospher 100 Diol (5 μ m), 250 \times 4.0 mm I.D., from Merck (Darmstadt, Germany). Its temperature was controlled by a water-jacket. Both cooling devices were connected to a Maton TH 50 LF S2 cryocooler, adjusted to 15.0 \pm 0.1°C. The room was air conditioned at 20°C.

The solvent bottles contained 25 g of 4 Å molecular sieve for 2.5 l of solvent and were continuously sparged with a gentle stream of helium to reduce detector noise.

The pump flow-rate was set to 1.5 ml/min and controlled by a PhaseSep (Deeside, UK) digital flow meter with analogous output. Chromatographic and flow data were recorded and treated by Coconut, a PC-based four-channel acquisition and treatment software developed in our laboratory.

Procedures

The mobile phase was pentane with various amounts of diethyl ether to adjust the polarity. Five different mobile phases were employed (Table I). The amounts of diethyl ether were chosen in such a manner that a capacity factor of about 10 for one compound with a defined mobile phase composition corresponds to a capacity factor of about 2 for the same compound with a mobile phase of immediately higher polarity.

A solution of each compound, at a concentration of about 200 mg/l, was prepared in pentane. Three injections were made, choosing an eluent for which the resulting capacity factor was between *ca.* 2 and 10.

Dead time determination

The dead time was obtained by measuring the retention time of the signal observed when injecting pentane on to the column equilibrated with a diethyl ether-containing mobile phase.

There are two requirements for a suitable dead time marker [13,14]: no retention under the

TABLE I
MOBILE PHASES AND STANDARD COMPOUNDS

Mobile phase no.	Pentane (%)	Diethyl ether (%)	Standard compound	$\overline{k'_s}^a$
1	100	0	Methyl benzoate	3.22
2	99.2	0.8	Benzaldehyde	2.18
3	95	5	Anisaldehyde	4.67
4	80	20	Indole	2.20
5	50	50	Coniferaldehyde	3.32

^a $\overline{k'_s}$ is the mean capacity factor of the standard compound.

operating conditions, and the same extent of exclusion by the pores of the support as the solutes under investigation. Pentane approximately fulfils the first condition, but not necessarily the second, as exclusion depends on the molecule size. With regard to the range of molecule size of the solutes studied (from formaldehyde to molecules such as ethyl tetradecanoate) and to the necessity of using one dead time marker only to obtain comparable results, pentane seems a reasonable compromise. The error incurred is assumed to be negligible.

When measuring the dead time in this way for different mobile phase compositions, a decrease was observed with an increase in the amount of diethyl ether. An extrapolation allowed the determination of the corresponding dead time for pure pentane. A direct measurement is not possible because no signal is obtained on injecting pentane with pure pentane as the mobile

phase. The results of the regression analysis are presented in Table II.

Calculations

Preliminary determinations of capacity factors showed that the repeatability was not always satisfactory. Over a period of some days, significant variations of the k' were observed. As virtually all chromatographic parameters that could influence the retention time have been controlled, we suspected that the percentage of diethyl ether added to pentane by the pump varied to some extent.

To correct for these variations, the concept of selectivity coefficients [15] was employed. For each mobile phase composition, a standard was chosen and co-injected with the compounds of interest. Once all injections had been accomplished, a mean capacity factor ($\overline{k'_s}$) for each standard was calculated (Table I). Taking the

TABLE II
COLUMN DEAD TIME AS A FUNCTION OF MOBILE PHASE COMPOSITION

Mobile phase no.	Diethyl ether (%)	Mean t_0 (s)	n	R.S.D. (%)	t_0 from regression analysis (s) ^a
1	0	–	–	–	114.4
2	0.8	114.3	12	1.02	114.3
3	5	113.6	15	1.81	113.8
4	20	112.0	25	0.97	111.8
5	50	107.7	9	1.67	107.8

^a Regression data: Slope = -0.1326 (S.D. 0.0054); intercept = 114.4 (S.D. 0.208); standard error = 0.208; correlation coefficient = 0.998; number of observations = 4.

TABLE III
REPEATABILITY OF THE SELECTIVITY COEFFICIENTS

k'_C , k'_S and α are the capacity factors of the sample and the standard and their ratio, respectively. Measurements over a period of 3 days. Mobile phase, pentane-diethyl ether (99.5:0.5); sample, methyl propionate; standard, methyl cinnamate. For other operating conditions, see text.

Injection no.	k'_C	k'_S	α
1	1.45	3.71	0.392
2	1.47	3.74	0.394
3	1.48	3.75	0.396
4	1.54	3.86	0.398
5	1.54	3.86	0.398
6	1.53	3.86	0.398
7	1.57	4.06	0.387
8	1.56	4.06	0.385
9	1.55	4.04	0.384
Mean			0.393 ^a

^a R.S.D. = 1.41%.

mean capacity factor of the corresponding standard, the capacity factors for the compounds of interest were then calculated according to the equation

$$k' = k'_S \cdot \frac{t_C f_C - t_N f_N}{t_S f_S - t_N f_N}$$

where t_C and t_S are the retention times of the compound and of the standard, and f_C and f_S are the mean flow-rates during elution of the compound and of the standard, respectively. The flow-rate was introduced in the calculation in order to eliminate residual flow variations we observed in spite of thermostating of the pump head. Good day-to-day repeatability was obtained, as shown in Table III.

This procedure for the determination of capacity factors is assumed to give values of higher precision, as minor fluctuations of the mobile phase composition and of the flow-rate are largely corrected for.

RESULTS AND DISCUSSION

The compounds used in this work were chosen within the chemical classes commonly contained in the volatiles fraction of plants and foodstuffs,

i.e., hydrocarbons, alcohols, phenols, aldehydes, ketones, esters, sulphur- and nitrogen-containing compounds and heterocyclics.

Two classes of compounds, acids and amines, exhibited a particular elution behaviour. Even though elution of carboxylic acids with a moderately polar mobile phase [pentane-diethyl ether (80:20)] was possible, successive injections decreased their retention and the peak shape degraded markedly. Moreover, the retention times of neutral compounds were affected after injection of acids. This effect was reversible; the initial state of the column could be re-established by flushing it with diethyl ether. Aliphatic amines gave rise to the same phenomena, confirming observations of Smith and Cooper [10].

We attributed this behaviour to partial adsorption of the compounds on active sites of the support. Addition of a polar modifier in small amounts to the mobile phase would certainly eliminate this problem, but would also be detrimental to its volatility. Taking into account the objectives of this work, strongly acidic and basic compounds were not considered further.

Discussion of k' values

The k' values obtained as described above are given in Table IV and Fig. 1 shows their subdivision according to the chemical classes.

Even the most polar compounds under investigation, *e.g.*, veratryl alcohol, maltol and sinapaldehyde, which are likely to be irreversibly adsorbed on silica, can be eluted with pentane-diethyl ether (50:50). On the other hand, very non-polar compounds (hydrocarbons, thiols, thioethers, furans and thiophenes) undergo no or only slight retention, precluding the separation of individual compounds. Most classes of volatiles, however, are situated between these two extremes.

The presence or absence of a hydroxyl group (or, to a lesser extent, an aromatic methoxy group) essentially governs retention. In the absence of such a group, the retention increases in the order hydrocarbons < ethers < aldehydes < esters < ketones < nitriles for comparable molecular structures (same chain length). The corresponding retention order on bare silica [16], hydrocarbons < ethers < nitriles < esters <

TABLE IV
CAPACITY FACTORS OF AROMA COMPOUNDS ON DIOL

For compositions of mobile phases, see Table I.

Compound	Mobile phase	k'	Compound	Mobile phase	k'
<i>Hydrocarbons</i>			α -Bisabolol	3	6.84
Camphene	1	<0.5	Guaiol	3	10.21
Myrcene	1	<0.5	8(15)-Cedren-9-ol	4	2.13
Benzene	1	<0.5	Geraniol	4	3.69
Styrene	1	<0.5	Nerol	4	3.17
Naphthalene	1	<0.5	Citronellol	4	3.00
Phenanthrene	1	1.19	Linalool	3	5.38
<i>Saturated alcohols</i>			Lavandulol	3	5.18
Ethanol	4	3.40	Farnesol	4	3.05
1-Propanol	4	3.14	(Z)-Nerolidol	3	4.97
1-Butanol	4	2.96	(E)-Nerolidol	3	5.10
1-Pentanol	4	2.82	<i>Aromatic alcohols</i>		
1-Hexanol	4	2.74	Benzyl alcohol	4	3.88
1-Octanol	4	2.61	2-Phenylethanol	4	4.52
1-Dodecanol	4	2.41	Cinnamyl alcohol	4	5.42
2-Butanol	4	2.58	Anisyl alcohol	4	3.95
2-Pentanol	4	2.39	Veratryl alcohol	5	5.30
3-Octanol	3	8.34	<i>p</i> -Cymen-7-ol	4	3.61
2-Methyl-1-butanol	4	2.20	<i>p</i> -Cymen-8-ol	4	2.40
3-Methyl-1-butanol	4	2.75	Furfuryl alcohol	4	4.15
2-Methyl-2-butanol	4	2.39	<i>Phenols</i>		
3-Methyl-2-butanol	4	1.99	Phenol	4	2.01
Menthol	4	1.85	2-Methylphenol	3	7.21
Thujyl alcohol	3	2.07	3-Methylphenol	4	1.99
Fenchyl alcohol	3	4.19	4-Methylphenol	4	1.99
Isolongifolol	4	3.07	4-Ethylphenol	4	1.92
Myrtanol	4	3.33	5-Isopropyl-2-methylphenol	3	5.67
<i>Unsaturated alcohols</i>			4-Vinylphenol	4	1.58
2-Buten-1-ol	4	3.16	2-Methoxyphenol	3	4.40
(E)-2-Hexen-1-ol	4	2.89	2-Methoxy-4-vinylphenol	4	1.57
(Z)-3-Hexen-1-ol	4	2.92	2-Methoxy-4-allylphenol	3	4.43
(E)-2-Octen-1-ol	4	2.72	2-Methoxy-4-(1-propenyl)phenol	4	1.86
(Z)-3-Octen-1-ol	4	2.68	2,6-Dimethoxyphenol	5	3.33
(Z)-6-Nonen-1-ol	4	3.22	<i>Aliphatic ethers</i>		
(E,Z)-2,6-Nonadien-1-ol	4	2.99	Diethyl ether	1	1.09
1-Penten-2-ol	3	7.20	Vitispirane	1	1.15
1-Hexen-2-ol	3	6.80	<i>Aromatic ethers</i>		
1-Octen-2-ol	2	9.52	Methoxybenzene	1	0.74
α -Terpineol	4	2.38	1,4-Dimethoxybenzene	1	3.83
4-Terpineol	3	4.36	<i>Epoxides</i>		
<i>p</i> -Menth-1-en-9-ol	4	2.71	β -Caryophyllene oxide	2	3.53
Isopulegol	3	5.03	Limonene-1,2-epoxide	1	4.84
Dihydrocarveol	4	2.37	<i>Thiols</i>		
Pinocarveol	3	6.00	Butanethiol	1	<0.5
Myrtenol	4	2.37			
Carveol	4	2.25			
1,8-Menthadien-4-ol	3	5.69			

(Continued on p. 312)

TABLE IV (continued)

Compound	Mobile phase	k'	Compound	Mobile phase	k'
<i>Aliphatic saturated aldehydes</i>			<i>Aliphatic unsaturated ketones</i>		
Formaldehyde	4	1.59	5-Hexen-2-one	2	2.94
Propionaldehyde	2	1.92	6-Methyl-5-hepten-2-one	2	2.84
Butyraldehyde	1	2.22	6-Methyl-3,5-heptadien-2-one	3	3.84
Nonanal	1	1.65	2,6-Dimethyl-2,5-heptadien-4-one	2	1.96
<i>Aliphatic unsaturated aldehydes</i>			Artemisia ketone	1	2.20
Propenal	2	2.89	Carvone	2	4.43
2-Butenal	2	5.39	Dihydrocarvone	2	2.61
2-Pentenal	2	3.58	α -ionone	2	4.41
(<i>E</i>)-2-Hexenal	2	3.02	β -ionone	2	5.40
(<i>E</i>)-2-Nonenal	2	2.70	<i>cis</i> -Jasmone	3	6.53
(<i>Z</i>)-6-Nonenal	1	4.56	Nootkatone	3	7.28
(<i>E,E</i>)-2,6-Nonadienal	2	3.18	Piperitone	3	3.25
Geranial	2	5.49	Pulegone	2	4.13
Neral	2	5.16	Verbenone	3	6.77
Citronellal	1	2.61	Damascenone	2	2.99
3-Cyclocitral	1	1.80	Geranylacetone	2	3.03
Perillaldehyde	2	3.13	Isophorone	2	4.84
Myrtenal	2	2.51	<i>Aromatic ketones</i>		
Phenylacetaldehyde	3	4.99	Acetophenone	2	3.73
<i>Aromatic aldehydes</i>			Indonone	3	5.16
Benzaldehyde	2	2.18	Benzyl methyl ketone	2	6.31
4-Methylbenzaldehyde	2	2.55	<i>Heterocyclic ketones</i>		
Cinnamaldehyde	2	7.46	2-Acetylfuran	3	4.27
α -Amylcinnamaldehyde	2	2.72	2-Acetylpyridine	3	4.20
<i>Aromatic hydroxylated aldehydes</i>			2-Acetylpyrrole	4	4.80
4-Hydroxybenzaldehyde	4	9.32	2-Acetylthiazole	3	3.11
Anisaldehyde	3	4.67	<i>Aromatic hydroxylated ketones</i>		
Vanillin	4	7.03	3-Hydroxy-4-phenyl-2-butanone	2	9.49
Piperonal	3	4.66	Anisylacetone	3	5.28
Coniferaldehyde	5	3.32	Propiovanillone	4	5.11
Sinapaldehyde	5	6.72	Acetosyringone	5	4.61
<i>Heterocyclic aldehydes</i>			Acetovanillone	4	7.74
Furfural	3	4.35	<i>Aliphatic hydroxylated ketones</i>		
5-Methylfurfural	3	4.53	Acetoin	4	5.00
5-Hydroxymethylfurfural	5	4.62	3-Hydroxy-3-methyl-2-butanone	4	2.40
2-Formylpyrrole	4	4.65	4-Hydroxy-4-methyl-2-pentanone	4	5.44
<i>Aliphatic saturated ketones</i>			4-Hydroxy-2,5-dimethyl-3-hexanone	3	2.19
Acetone	3	4.68	Epoxy- β -ionone	3	3.21
2-Pentanone	2	2.82	<i>Aliphatic diketones</i>		
2-Hexanone	2	2.65	Diacetyl	2	1.69
2-Heptanone	2	2.52	Pentane-2,4-Dione	2	2.79
2-Nonanone	2	2.42	Hexane-2,5-Dione	4	4.37
2-Undecanone	2	2.37	<i>Miscellaneous cyclic enones</i>		
5-Undecanone	1	3.17	4-Hydroxy-2,5-dimethyl-3(2 <i>H</i>)-furanone	2	3.60
Camphor	2	3.43	3-Hydroxy-4,5-dimethyl-2(5 <i>H</i>)-furanone	5	3.34
Menthone	1	2.42	2-Hydroxy-3-methyl-2-cyclopenten-1-one	4	4.40
3-Thujone	2	1.95			

TABLE IV (continued)

Compound	Mobile phase	<i>k'</i>	Compound	Mobile phase	<i>k'</i>
Maltol	5	6.07	<i>Aromatic hydroxylated esters</i>		
Diosphenol	2	2.89	Methyl salicylate	1	1.66
Mesifuran	3	3.22	Methyl vanillate	4	4.99
			Methyl anthranilate	3	4.37
<i>Saturated esters</i>			<i>Heterocyclic esters</i>		
Methyl acetate	1	5.40	Methyl nicotinate	4	4.06
Methyl propionate	1	3.58	<i>Aliphatic hydroxylated esters</i>		
Methyl butyrate	1	2.71	Ethyl lactate	4	2.74
Methyl hexanoate	1	2.50	Ethyl 3-hydroxybutyrate	4	4.48
Methyl octanoate	1	2.40	Ethyl 2-hydroxyhexanoate	3	6.14
Methyl tetradecanoate	1	2.31	Diethyl tartrate	5	3.16
Ethyl formate	1	2.47	<i>Keto esters</i>		
Ethyl acetate	1	5.42	Ethyl acetoacetate	3	2.96
Ethyl propionate	1	3.00	<i>Diesters</i>		
Ethyl butyrate	1	2.68	Diethyl malonate	3	2.87
Ethyl hexanoate	1	2.51	Diethyl succinate	3	2.90
Ethyl heptanoate	1	2.30	<i>Triglycerides</i>		
Ethyl octanoate	1	2.42	Tributylin	3	5.11
Ethyl tetradecanoate	1	2.29	Tristearin	3	9.10
Propyl hexanoate	1	2.01	<i>Saturated lactones</i>		
Butyl pentanoate	1	1.91	γ -Butyrolactone	2	6.47
Pentyl butyrate	1	2.14	γ -Decalactone	2	6.42
Hexyl propionate	1	2.29	δ -Decalactone	2	6.38
Pentyl pentanoate	1	1.98	β -Methyl- γ -octalactone	2	6.43
Isopentyl pentanoate	1	1.89	<i>Unsaturated lactones</i>		
Pentyl isopentanoate	1	1.86	α -Methylene- γ -butyrolactone	2	6.46
Pentyl 2-methylbutyrate	1	1.75	β -Angelica lactone	1	4.48
Isopentyl 2-methylbutyrate	1	1.68	6-Pentyl-2-pyrone	3	9.65
Isopentyl isopentanoate	1	1.72	<i>Nitriles</i>		
Bornyl acetate	1	1.87	Acetonitrile	4	3.45
Fenchyl acetate	1	2.02	Allyl cyanide	2	2.86
Menthyl acetate	1	2.86	Benzyl cyanide	3	3.57
<i>Aliphatic unsaturated esters</i>			<i>Cyanohydrins</i>		
Ethyl (<i>E</i>)-2-butenolate	1	4.71	α -Hydroxyphenylacetone nitrile	4	5.94
Ethyl (<i>E</i>)-2-octenoate	1	3.46	<i>Isothiocyanates</i>		
Ethyl (<i>E</i>)-2-decenoate	1	3.38	Butyl isothiocyanate	1	0.54
Ethyl (<i>E</i>)-4-decenoate	1	2.71	2-Propenyl isothiocyanate	1	0.81
Ethyl (<i>Z</i>)-4-decenoate	1	2.55	2-Phenylethyl isothiocyanate	1	1.73
Vinyl acetate	1	1.50	<i>Furans</i>		
(<i>E</i>)-2-Hexenyl acetate	1	3.52	Menthofuran	1	<0.5
1-Octen-3-yl acetate	1	2.85	<i>Pyridines</i>		
Citronellyl acetate	1	3.80	Pyridine	5	3.50
Geranyl acetate	1	5.07	Quinoline	5	2.26
Linalyl acetate	1	3.38	<i>Pyrroles</i>		
Perillyl acetate	1	5.75	Pyrrole	3	3.90
Carvyl acetate	1	3.51	Indole	4	2.20
Terpinyl acetate	1	3.49			
<i>Aromatic esters</i>					
Benzyl acetate	1	6.90			
2-Phenylethyl acetate	2	3.01			
1-Phenylethyl acetate	1	6.56			
3-Phenylpropyl acetate	2	3.21			
Methyl benzoate	1	3.22			
Ethyl benzoate	1	2.96			
Methyl cinnamate	2	3.38			

(Continued on p. 314)

TABLE IV (continued)

Compound	Mobile phase	k'	Compound	Mobile phase	k'
<i>Pyrazines</i>			<i>Thiazoles</i>		
Pyrazine	5	2.28	Thiazole	4	2.38
Methylpyrazine	4	3.91	2,4-Dimethylthiazole	3	5.19
Ethylpyrazine	4	2.47	2-Isobutylthiazole	3	3.20
2,3-Dimethylpyrazine	4	3.94	4-Methyl-5-vinylthiazole	4	1.77
2,5-Dimethylpyrazine	4	3.42	Benzothiazole	4	1.84
Tetramethylpyrazine	4	2.78	<i>Thiophenes</i>		
Methoxypyrazine	3	3.29	Thiophene	1	<0.5
2-Isobutyl-3-methoxypyrazine	3	1.79	2,5-Dimethylthiophene	1	<0.5

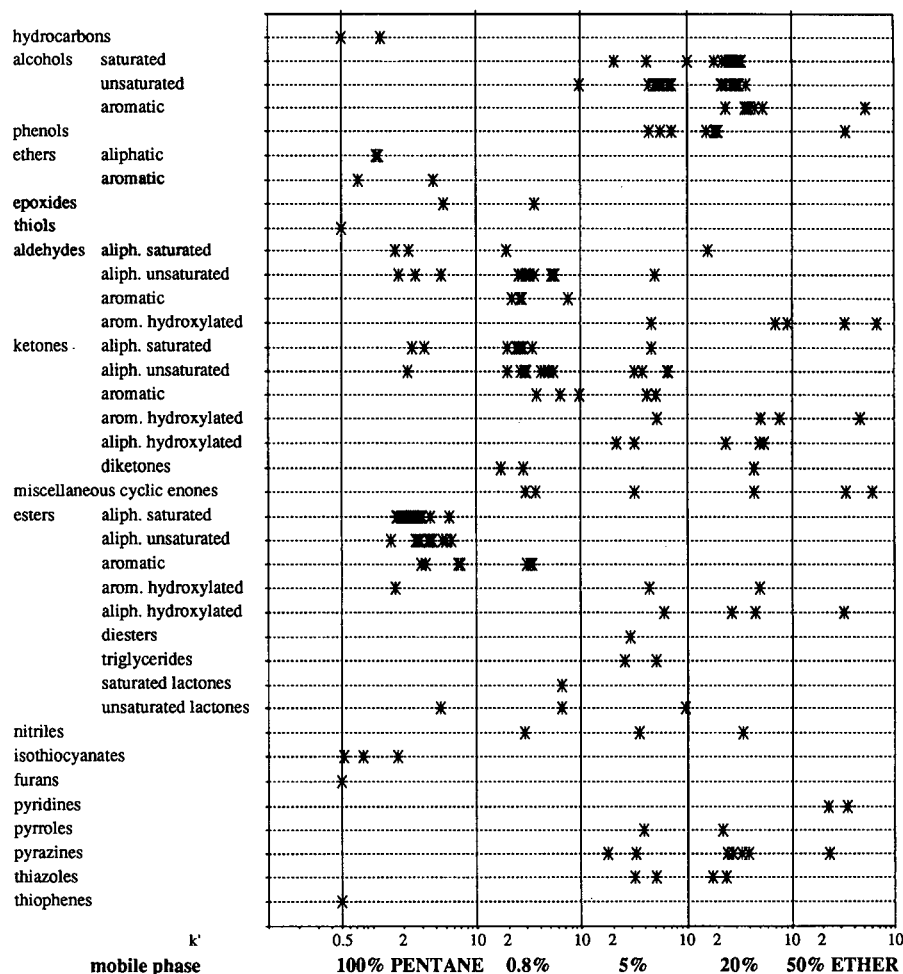


Fig. 1. Subdivision of the capacity factors of the compounds under investigation according to chemical classes. One asterisk corresponds to the capacity factor of one compound. The abscissa shows the mobile phase compositions with increasing polarity. Within each mobile phase, the asterisks are positioned on a scale of k' from 1 to 10 (from 0.5 to 10 for pure pentane). The corresponding values are given in Table IV.

ketones < aldehydes, shows that there are substantial differences in selectivity for aldehydes and nitriles on these two stationary phases.

Within homologous series, as expected, an increase in retention is observed with decreasing alkyl chain length. The “shortest” aldehyde and ketone, formaldehyde and acetone, are strongly retained. The smallest aliphatic esters, apart from the gaseous methyl formate, are methyl acetate and ethyl formate. These two differ markedly in retention, ethyl formate ($k' = 2.47$) being less retained than methyl acetate ($k' = 5.40$). Comparison with ethyl acetate ($k' = 5.42$) (all three values for pure pentane as mobile phase) reveals that the formate does not follow the postulated rule.

On examination of a series of aliphatic esters with equal chain length of nine carbons, differing only in the position of the $-\text{COO}-$ group, a minimum of retention can be found when the carbonyl group is located in the centre of the molecule (Fig. 2). Maximum steric hindrance of the functional group is considered to be responsible for this behaviour.

Branching of an alkyl chain decreases retention (see, *e.g.*, pentyl pentanoate and some of its methyl branched isomers, and 1-pentanol, 2-pentanol and their branched isomers). In addition, retention decreases when the methyl side-chain approaches the functional group. However, the tertiary alcohol 2-methyl-2-butanol is

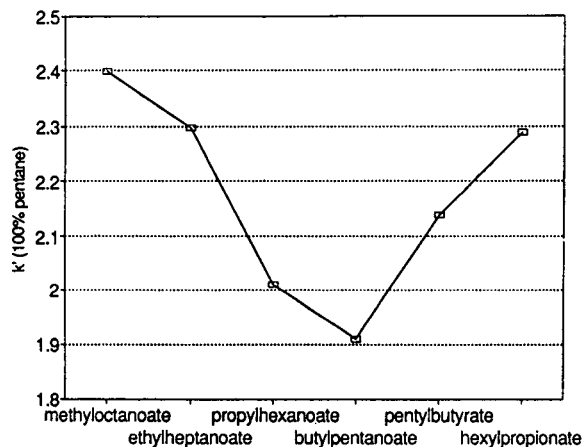


Fig. 2. Capacity factors of a series of aliphatic esters of nine carbons, differing only in the position of the functional group. The mobile phase is pure pentane.

more retained than its secondary homologue, 3-methyl-2-butanol.

The retention of the unsubstituted heterocyclics under investigation follows the order furan \approx thiophene \ll pyrrole < thiazole < pyrazine < pyridine. Only the nitrogen-containing rings are markedly retained.

In order to evaluate the capability of the diol column for the pre-separation of aroma compounds from triglycerides, the retention of tributyrin and tristearin was studied. These two compounds, encompassing approximately the range of triglycerides present in nature, are eluted between aldehydes, ketones, lactones and nitriles on one hand, and alcohols, phenols, nitrogen-containing heterocyclics and hydroxylated compounds on the other, interfering with poorly retained unsaturated alcohols and phenols. With the exception of the latter compounds, aroma extract pre-separation on diol seems to be possible in the presence of larger amounts of triglycerides.

CONCLUSIONS

The diol support is less retentive than silica gel, which means that complete elution under normal-phase conditions is possible even for the most polar compounds usually present in aroma extracts. With the exception of strong acids and strong bases, no irreversible adsorption was observed. Higher selectivity, and hence a higher separation power, is exhibited for compounds containing a hydroxyl group or a nitrogen, followed by those containing a carbonyl group. The lack of retention for non-polar compounds such as hydrocarbons can be advantageous for aroma extract pre-separations. After recovery of this fraction, eluted nearly at the dead time, separation could be achieved on an appropriate support.

Other supports are currently under investigation. The results will be compared with those obtained on the diol support and published later.

ACKNOWLEDGEMENT

We are grateful to Robert Almanza for developing the software allowing the automation of the calculations in this work.

REFERENCES

- 1 C.G. Chappell, C.S. Craeser and M.J. Shepherd, presented at the 19th International Symposium on Chromatography, Aix-en-Provence, September 1992.
- 2 C.L. Teitelbaum, *J. Agric. Food Chem.*, 25 (1977) 466-470.
- 3 J.A. Schmit, R.C. Williams and R.A. Henry, *J. Agric. Food Chem.*, 21 (1973) 551-556.
- 4 L.W. Wulf, C.W. Nagel and A.L. Branen, *J. Chromatogr.*, 161 (1978) 271-278.
- 5 H.H. Wisnieski, R.L. Yates and H.M. Davis, *J. Chromatogr.*, 255 (1983) 455-461.
- 6 M. Benincasa, F. Buiarelli, G.P. Cartoni and F. Coccioli, *Chromatographia*, 30 (1990) 271-276.
- 7 F. Buiarelli, G.P. Cartoni, F. Coccioli and E. Ravazzi, *Chromatographia*, 31 (1991) 489-492.
- 8 D. Barron, *Z. Lebensm.-Unters.-Forsch.*, 193 (1991) 454-459.
- 9 A.M. Siouffi, M. Righiezza and G. Guiochon, *J. Chromatogr.*, 386 (1986) 189-202.
- 10 P.L. Smith and W.T. Cooper, *J. Chromatogr.*, 410 (1987) 249-265.
- 11 P.L. Smith and W.T. Cooper, *Chromatographia*, 25 (1988) 55-60.
- 12 A.W. Salotto, E.L. Weiser, K.P. Caffey, R.L. Carty, S.C. Racine and L.R. Snyder, *J. Chromatogr.*, 498 (1990) 55-65.
- 13 R.J. Smith, C.S. Nieass and M.S. Wainwright, *J. Liq. Chromatogr.*, 9 (1986) 1387-1430.
- 14 A. Aldehai, D.E. Martire and R.P.W. Scott, *Analyst*, 114 (1989) 869-875.
- 15 W.W. Christie and B. Nikolova-Damyanova, presented at the AOCS Annual Meeting, Toronto, May 1992.
- 16 H. Engelhardt and H. Elgass, in C. Horvath (Editor), *High Performance Liquid Chromatography*, Vol. 2, Academic Press, New York, 1980, p. 57.

Use of a porous graphitised carbon column for the high-performance liquid chromatography of oligosaccharides, alditols and glycopeptides with subsequent mass spectrometry analysis

M.J. Davies and K.D. Smith

Glycoconjugates Section, Clinical Research Centre, Watford Road, Harrow HA1 3UJ (UK)

R.A. Carruthers, W. Chai and A.M. Lawson

Clinical Mass Spectrometry, Clinical Research Centre, Watford Road, Harrow HA1 3UJ (UK)

E.F. Hounsell*

Glycoconjugates Section, Clinical Research Centre, Watford Road, Harrow HA1 3UJ (UK)

(First received March 30th, 1993; revised manuscript received June 15th, 1993)

ABSTRACT

HPLC using a porous graphitised carbon (PGC) column eluted in acetonitrile–aqueous trifluoroacetic acid has been shown to give complementary chromatography to reversed-phase (ODS) HPLC for separation of peptides and glycopeptides. The PGC column can also be used for separation of oligosaccharides and oligosaccharide alditols released from protein by enzymes (N-linked chains) or base–borohydride degradation (O-linked chains). The advantages are that peptides, glycopeptides, reducing oligosaccharides, sialylated oligosaccharides and oligosaccharide alditols can be chromatographed under the same conditions. The samples can be readily recovered by evaporation for sensitive liquid secondary ion mass spectrometric (LSI-MS) analysis and there is no contamination or deterioration of chromatography from column leakage. LSI-MS analysis revealed that complete peak separation of all of the possible oligosaccharide components of the standard glycoproteins fetuin and bovine submaxillary mucin was not achieved. However, PGC remains as a useful adjunct to other HPLC profiling and separation techniques in particular where subsequent MS analysis is desired.

INTRODUCTION

Several different methods have been proposed for the purification of reducing oligosaccharides, alditols and glycopeptides which include reversed-phase [RP-HPLC; usually on octadecylsilyl (ODS) columns], normal-phase (NP-HPLC)

chromatography on amino-bonded columns [NH₂, aminopropyl silica (APS), etc] and anion-exchange HPLC (AX-HPLC). Four types of solvent elution have been applied, either (i) aqueous–organic, (ii) buffer–organic, (iii) aqueous buffer gradients, or (iv) mild acid/aqueous acetonitrile, depending on the molecules to be separated. As a generalisation, neutral oligosaccharides and alditols have been eluted by RP- or NP-HPLC with solvent system i [1–3], sialylated oligosaccharides by NP-HPLC with

* Corresponding author.

solvent system ii [4–6] or by AX-HPLC with solvent system iii [7,8], sulphated oligosaccharides by NP-HPLC [9,10] or AX-HPLC [11] with solvent system iv or by the use of RP-HPLC with ion-pairing reagents [12] and glycopeptides by NP- or RP-HPLC with solvent system iv [4,13]. In general initial detection could be achieved by UV absorbance at a sensitivity down to 1 μg but after solvent systems ii or iii a desalting step has to be introduced for further analysis, for example by mass spectrometry (MS). The disadvantage of these methods is the need for more than one column for different applications and their limited ability to isolate isomeric oligosaccharides. Additional systems have therefore been explored.

High pH anion exchange chromatography (HPAEC) with pulsed amperometric detection (PAD) has been shown to separate a wide range of oligosaccharide and alditol isomers both varying in monosaccharide sequence and/or linkage [14–18]. The major drawback of this technique is that it requires high concentrations of sodium hydroxide and sodium acetate which are then difficult to remove sufficiently for further analysis. There is also a risk of epimerisation and degradation of reducing sugars. Ion suppression membranes have been used successfully [19] to desalt monosaccharides separated by HPAEC–PAD with on-line detection by thermospray MS. The separation of oligosaccharides by HPAEC–PAD requires the use of stronger sodium hydroxide and sodium acetate which are difficult to remove completely with these suppression membranes. Separation of malto-oligosaccharides and high-mannose oligosaccharides by HPAEC–PAD with membrane desalting and on-line ionspray MS has been achieved with a custom-packed 2 mm I.D. Carbopac PA1 column but it was reported [20] that acetic acid formed by the desalting process still interfered with the ionisation for MS. Alternative to the use of a membrane, the sugar-containing fractions can be collected and desalted using a cation-exchange column or Bio-Gel P2 minicolumns [21]. All of these desalting mechanisms can result in considerable losses of required material.

We have previously explored porous graphitised carbon (PGC) HPLC as a method of separation of glycopeptides and oligosaccharide alditols

[22]. HPLC with PGC columns exhibits similar properties to RP-HPLC but in addition is able to separate closely related oligosaccharide isomers. We now extend the applications of HPLC with PGC columns to encompass separation of N-linked oligosaccharides and mucin-derived oligosaccharide alditols. The solvent systems used with HPLC on PGC columns do not utilise salts, thus the separated fractions require no clean up prior to further analysis. For example LSI-MS of peptides and native oligosaccharides are readily obtainable. Comparisons are also made with HPAEC–PAD both as a means of separation and as a method of preparing oligosaccharides for MS analysis. We have previously shown that PGC gives more reliable chromatography for neutral oligosaccharide alditols [22] compared to HPAEC as these are eluted away from the solvent front. For sialylated alditols adequate retention is observed on HPAEC [16,17] but an improved HPLC system is required which will separate both sialylated and non-sialylated molecules in one run and which, for preparative purposes, does not require high salt concentrations.

EXPERIMENTAL

Materials

Peptide-N-glycosidase F (PNGase F) was purchased from Boehringer Mannheim (Lewes, UK). Fetuin, asialofetuin, RNAase B, bovine submaxillary mucin (BSM) and L-1-tosylamide-2-phenyl ethyl chloromethyl ketone (TPCK)-treated trypsin were all from Sigma (Poole, UK). The PBA Bond Elut column was from Jones Chromatography (Hengoed, Glamorgan, UK). HPLC-grade trifluoroacetic acid (TFA) was from Pierce (Chester, UK). The PGC column was a Hypercarb S (100 mm \times 6.4 mm) fitted with a Hypercarb guard cartridge, both from Shandon Scientific (Runcorn, UK). HPAEC was performed using a Carbopac PA-1 column (250 mm \times 4 mm) and a PA-1 guard column (50 mm \times 4 mm) both from Dionex (Camberley, UK) with on-line desalting with an anion micromembrane suppressor (AMMS) and autoregen accessory (Dionex).

Methods

Preparation of peptides, glycopeptides, oligosaccharides and oligosaccharide alditols. Peptides and glycopeptides from the bovine serum glycoprotein, fetuin, were generated by trypsin digestion and fractionated by RP-HPLC on an ODS column and HPLC on a PGC column as previously described [13,22].

N-Linked oligosaccharides of asialofetuin, fetuin and RNAase B were prepared by digestion with PNGase F. The glycoproteins were dissolved in 200 μ l 40 mM KH_2PO_4 –10 mM EDTA pH 6.2 with 5 μ l toluene and 1 unit PNGase F per 10 nmol protein. The mixtures were then incubated for 72 h at 37°C. Protein was precipitated with a 2-fold excess of ice-cold ethanol followed by two washes with ice-cold ethanol. The oligosaccharides were retained in the supernatant which was dried for further analysis.

Oligosaccharide alditols were released from BSM by treatment with alkaline borohydride (1 M NaBH_4 in 0.05 M NaOH) for 16 h and at 50°C and purified on a PBA column as described previously [23]. In brief the column was equilibrated consecutively with: 2 \times 1 ml methanol; 1 \times 1 ml 0.1 M HCl; 2 \times 1 ml water; 4 \times 1 ml 0.2 M NH_4OH . The sample was then added in 100 μ l 0.2 M NH_4OH , washes of 2 \times 100 μ l 0.2 M NH_4OH and 2 \times 100 μ l water were carried out and the alditols were then eluted in 6 \times 100 μ l 0.1 M acetic acid and the column washed with 1 \times 1 ml 0.1 M HCl and 2 \times 1 ml water.

HPLC on PGC column. HPLC on a PGC column was carried out using a Gilson system which consisted of two Model 302 pumps, a Model 802C manometric module, a Model 811 dynamic mixer, Model 201 fraction collector and a Model 116 detector (all from Gilson, AnaChem, Luton, UK) controlled by Gilson 715 software (AnaChem) on an IBM personal computer (PS2) model 55 SX. The solvent system for peptides/glycopeptides was a gradient from 0.1% TFA in water–acetonitrile (98:2), pH 2.2 to 0.1% TFA in water–acetonitrile (18:82), pH 2.2 in 80 min. The column was initially equilibrated with 0.1% TFA in water–acetonitrile (98:2), pH 2.2 for 30 min between each run. (The flow-rate was 1 ml/min and detection was by UV absorbance at 206 or 210 nm).

The solvent systems for oligosaccharides and oligosaccharide alditols used a gradient of 0.05% TFA in water to 0.05% TFA in water–acetonitrile (60:40) in 35 min with re-equilibration in 0.05% TFA in water between runs.

HPAEC–PAD

HPAEC–PAD was carried out on a titanium-lined Gilson system consisting of two Model 302 pumps, a Model 802TI manometric module, a Model 811B dynamic mixer and a Model 201-202 fraction collector (all from Gilson, France) controlled by an IBM personal computer (PS2) Model 70 running Gilson 712 software (AnaChem). Detection utilised a pulsed electrochemical detector fitted with a gold working electrode (Dionex) using the following pulse potentials and durations: $E_1 = 0.1$ V ($t_1 = 0.5$ s), $E_2 = 0.6$ V ($t_2 = 0.11$ s), $E_3 = -0.8$ V ($t_3 = 0.11$ s). The oligosaccharide sample was applied to the column equilibrated with the starting eluent at room temperature. Three gradients were run:

(1) Solvent A (water)–solvent B (50 mM NaOH–1.5 mM NaOAc) (98:2) for 20 min followed by a linear gradient of A–B (98:2) to A–B (85:15) over 15 min at a flow-rate of 0.75 ml/min. The limit solvent was then continued for a further 4 min before the column was regenerated in 100 mM NaOH and re-equilibrated in A–B (98:2).

(2) Solvent A (200 mM NaOH)–solvent B (200 mM NaOH–1.0 M NaOAc) (100:0) for 5 min followed by a linear gradient of 100% A to A–B (50:50) over 30 min at a flow-rate of 1 ml/min. The limit solvent was continued for a further 5 min before re-equilibration in 100% A.

(3) Solvent A (100 mM NaOH)–solvent B (100 mM NaOH–500 mM NaOAc) (95:5) for 15 min followed by a linear gradient of A–B (95:5) to A–B (40:60) over 35 min with a flow-rate of 1 ml/min. The limit solvent was continued for a further 5 min before the column was regenerated by moving to 100% A in 3 min and holding for a further 10 min. Thereafter the initial conditions A–B (95:5) were resumed.

On-line desalting was performed with a AMMS ion suppression membrane with a regenerant of 50 mM reagent-grade H_2SO_4 pumped at a flow-rate of 10 ml/min.

Liquid secondary ion mass spectrometry. LSI-MS was carried out on a VG Analytical (Manchester, UK) ZAB2-E mass spectrometer employing a caesium gun operated at 25 keV with an emission current of 0.5 μ A. Mass spectra were obtained at 8 keV accelerating voltage and 1000 resolving power. The data were processed by the 11-250J data system. Mass scans were made at 30 s/decade. Fractions from HPLC were evaporated to dryness, re-evaporated with water ($2 \times 100 \mu$ l) and taken up in 0.5% aqueous TFA pH 2.2 at a concentration of 200 μ M. A 1- μ l (ca. 200 pmol) sample aliquot was loaded onto the MS probe tip containing the matrix, thioglycerol-TFA (10:1) or thioglycerol.

RESULTS AND DISCUSSION

We have previously shown the use of HPLC on a PGC column for the separation of standard oligosaccharide alditols and for the separation of peptides and glycopeptides [22]. During the latter analysis we noted that the order of elution and MS detection of the non-glycosylated peptides separated by chromatography on a PGC column gave complementary information to that obtained from RP-HPLC using an ODS column. A further example of the use of PGC columns to separate glycopeptides and peptides which co-chromatographed in RP-HPLC is described in Fig. 1 for one area of the chromatogram of a protease digest of the standard glycoprotein, fetuin. In brief two glycopeptides (Fig. 1, panel A, peak 1) and also their peptide moieties obtained after PNGase F treatment (Fig. 1, panel B, peak 2), coeluted in each case on an ODS column whereas the original glycopeptides were well separated on a PGC column (Fig. 1, panel C, peaks 3 and 5) and from two peptides (Fig 1, panel C, peaks 4 and 6) enabling the component peptide sequence and oligosaccharide chains to be readily identified. Chromatography on a PGC column was also investigated for preparative separation of the released N-linked chains of the standard glycoprotein fetuin. Fig. 2 shows the superimposed PGC chromatograms of oligosaccharides released by PNGase F from fetuin and asialofetuin. The peaks a–m were fractionated, evaporated to dryness, re-evapo-

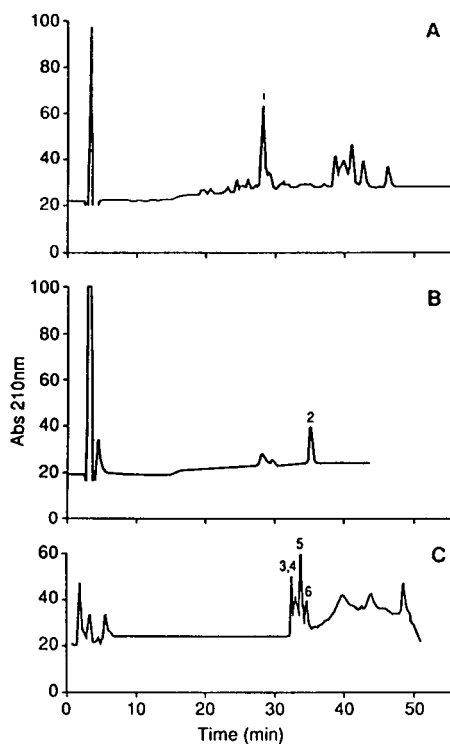


Fig. 1. (A) RP-HPLC of a thermolysin digest of the tryptic glycopeptide LCPDCPLLAPLNDSRVVHAVEVALATFN-AESNGSYLQIVEISR representing amino acids 127 to 169 of bovine serum fetuin where * denotes a glycosylation site. Peak 1 was hexose positive. (B) Analysis of peak 1 from panel A after PNGase F digestion showing the deglycosylated peptides at peak 2 and released oligosaccharides in the solvent front. LSI-MS analysis showed the presence of the sequence LAPLD^{*}DSR (amino acids 134–141) where D is the aspartic acid formed after deglycosylation (m/z 886.7) and peptide sequencing indicated the presence of ALATFNAESDGSY (amino acids 149–161). (C) Analysis of peak 1 in panel A above using a PGC column eluted in the same gradient as the RP-HPLC. Peaks 3 and 5 were hexose positive and shown by peptide sequencing to be amino acids 149–161 and 134–141, respectively. The oligosaccharides released from 3 and 5 gave a similar profile on HPAEC-PAD to the oligosaccharides released from intact fetuin showing that both sites were glycosylated by a mixture of disialo-, trisialo- and tetrasialo-oligosaccharides.

rated once with water and added to the matrix for LSI-MS analysis. Table I shows the molecular ions and the assigned structures of fractions a–d and l–m. No ions consistent with oligosaccharide masses were given in the spectra of fractions e–g. Fig. 3 shows representative spectra of fractions b–d and j–l. High-mannose type

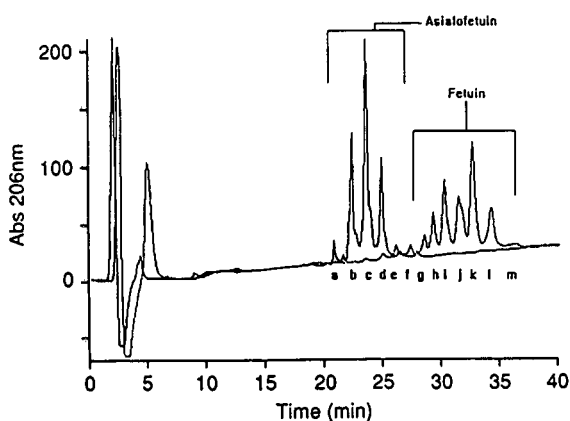


Fig. 2. Superimposed chromatograms of oligosaccharides released from asialofetuin and fetuin by PNGase F and separated by HPLC on a PGC column.

chains of RNAase B were also investigated and these were found to elute between 19 and 29 min (results not shown).

These results show that both non-sialylated and sialylated oligosaccharides can be chromatographed using the same gradient elution on PGC, unlike HPAEC where non-sialylated oligosaccharides are poorly retained compared to sialylated ones. Chromatography on a PGC column could separate biantennary from triantennary non-sialylated oligosaccharides (Table I), although the absence of a Gal from one of the branches could not be distinguished and mono-sialo-oligosaccharides eluted with the same retention time as non-sialylated oligosaccharides. It should be noted that asialofetuin obtained

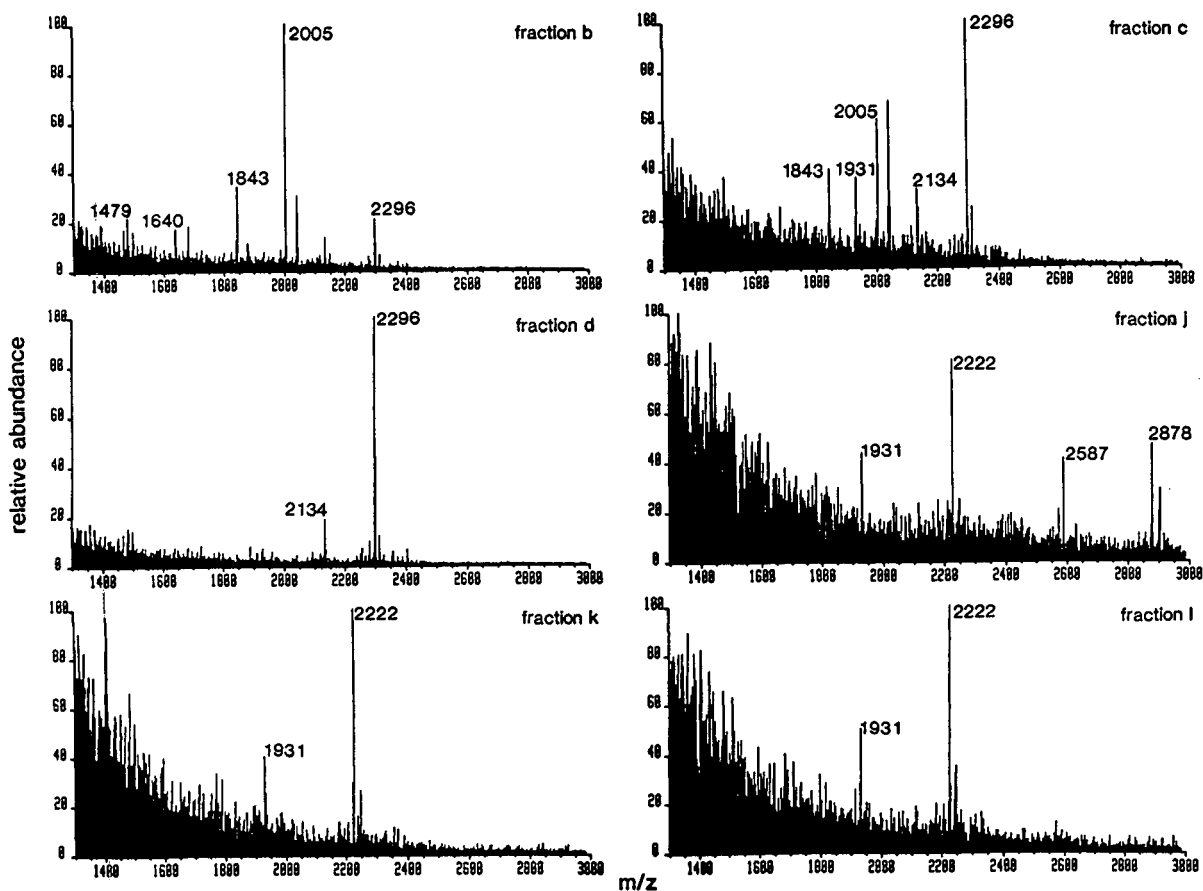


Fig. 3. Representative negative ion LSI-MS spectra of underivatised oligosaccharides obtained by PNGase F digestion of fetuin and asialofetuin analysed after separation by HPLC on a PGC column (Fig. 2) and assigned as shown in Table I.

TABLE I

THE PEAK ASSIGNMENTS AND MOLECULAR IONS FROM LSI-MS ANALYSIS OF THE OLIGOSACCHARIDES RELEASED FROM FETUIN AND ASIALOFETUIN FROM HPLC ON A PGC COLUMN AS SHOWN IN FIG. 2

Structure	M/Z [M - H] ⁻	Peak where present
Gal ₁ $\left\{ \begin{array}{l} \text{GlcNAc-Man} \\ \\ \text{Man-GlcNAc}_2 \\ \\ \text{GlcNAc-Man} \end{array} \right.$	1479	a, b
$\begin{array}{l} \text{Gal-GlcNAc-Man} \\ \\ \text{Man-GlcNAc}_2 \\ \\ \text{Gal-GlcNAc-Man} \end{array}$	1640	a, b
$\begin{array}{l} \text{Gal-GlcNAc-Man} \\ \\ \text{GlcNAc-Man-GlcNAc}_2 \\ \\ \text{Gal-GlcNAc-Man} \end{array}$	1843	b, c
Gal ₂ $\left\{ \begin{array}{l} \text{GlcNAc} \backslash \text{Man} \\ \quad \\ \text{GlcNAc} \quad \text{Man-GlcNAc}_2 \\ \\ \text{GlcNAc-Man} \end{array} \right.$		
$\begin{array}{l} \text{Gal-GlcNAc} \backslash \text{Man} \\ \quad \\ \text{Gal-GlcNAc} \quad \text{Man-GlcNAc}_2 \\ \\ \text{Gal-GlcNAc-Man} \end{array}$	2005	b, c
NeuAc ₁ $\left\{ \begin{array}{l} \text{Gal-GlcNAc} \backslash \text{Man} \\ \quad \\ \text{Gal-GlcNAc} \quad \text{Man-GlcNAc}_2 \\ \\ \text{Gal-GlcNAc-Man} \end{array} \right.$	2296	b, c, d
NeuAc ₁ $\left\{ \begin{array}{l} \text{Gal-GlcNAc-Man} \\ \\ \text{Man-GlcNAc}_2 \\ \\ \text{Gal-GlcNAc-Man} \end{array} \right.$	1931	c, k, l
NeuAc ₁ $\left\{ \begin{array}{l} \text{Gal-GlcNAc} \backslash \text{Man} \\ \quad \\ \text{Gal-GlcNAc} \quad \text{Man-GlcNAc}_2 \\ \\ \text{GlcNAc-Man} \end{array} \right.$	2134	c, d
NeuAc ₁ $\left\{ \begin{array}{l} \text{Gal-GlcNAc-Man} \\ \\ \text{GlcNAc-Man-GlcNAc}_2 \\ \\ \text{Gal-GlcNAc-Man} \end{array} \right.$		

TABLE I (continued)

Structure	M/Z [M - H] ⁻	Peak where present
$\begin{array}{c} \text{NeuAc-Gal-GlcNAc-Man} \\ \\ \text{Man-GlcNAc}_2 \\ \\ \text{NeuAc-Gal-GlcNAc-Man} \end{array}$	2222	h, j, k, l
$\begin{array}{c} \text{NeuAc}_2 \left\{ \begin{array}{l} \text{Gal-GlcNAc} \\ \text{Gal-GlcNAc} \\ \text{Gal-GlcNAc-Man} \end{array} \right. \begin{array}{l} \text{Man} \\ \\ \text{Man-GlcNAc}_2 \\ \\ \text{Man} \end{array} \end{array}$	2588	i, j
$\begin{array}{c} \text{NeuAc-Gal-GlcNAc} \\ \\ \text{NeuAc-Gal-GlcNAc} \left\{ \begin{array}{l} \text{Man} \\ \\ \text{Man-GlcNAc}_2 \\ \\ \text{Man} \end{array} \right. \\ \\ \text{NeuAc-Gal-GlcNAc-Man} \end{array}$	2878	i, j, m

from Sigma has some so-called Gal₀ structures and some remaining sialic acid showing the inefficiency of desialylation with the lability of underlying Gal. The results suggest that the PGC column is capable of distinguishing oligosaccharide isomers varying in sialic acid linkage as monosialo-oligosaccharides eluted in peaks b, c and d. Peak d also contained a disialylated biantennary chain showing that the PGC type separation is not by size or charge alone but also by linkage.

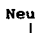
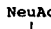

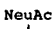
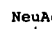

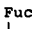

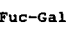
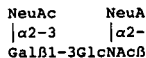
For oligosaccharides released from sialylated fetuin those in peaks i–m had LSI-MS spectra with assignable ions. Peaks i and j contained di- and triantennary-oligosaccharides with two or three sialic acids, whereas k and l contained only biantennary chains but having one or two sialic acids. Only peaks h and m contained single-chain isomers being, respectively, a disialylated biantennary and a trisialylated triantennary chain. From previous studies of fetuin sialyloligosaccharides (reviewed in refs. 13–15) it is known that oligosaccharides with the same composition but varying in linkage positions are present (*i.e.* sialic acid linked either 2–3 or 2–6 to galactose and Galβ1–4GlcNAc sequences linked either β1–2, 4 or 6 to Man) and that these isomers have distinct elution patterns. Minor tetra-

sialylated oligosaccharides which have a Galβ1–3GlcNAc sequences sialylated on both Gal and GlcNAc also present in fetuin [24] were not detected in the present study. The additional variation of mono- or non-sialylated Galβ1–3GlcNAc sequences may be present in either the asialo- or sialo-fetuin derived oligosaccharides.

In order to show the applicability of HPLC on a PGC column for the separation of additional oligosaccharides having blood group-type terminal substituents and N-glycolyl as well as N-acetylneuraminic acid, we have fractionated the oligosaccharide alditols obtained from base-borohydride degradation of BSM. The chromatography was interpreted with knowledge of the oligosaccharides of BSM from detailed structural studies [25,26] Table II shows the molecular ions and structural assignment from analysis of the PGC fractions compared to their HPAEC using three different gradients. Interestingly on PGC, N-glycolylneuraminic acid itself has a slightly reduced retention time compared to N-acetylneuraminic acid whereas the former has twice the retention time on HPAEC. This is reflected in the retention times of the sialylated oligosaccharide alditols present in BSM *e.g.* NeuAc-α2–6[GlcNAcβ1–3]GalNAcol and NeuGcα2–6[GlcNAcβ1–3]GalNAcol had the same retention

TABLE II
RETENTION TIMES OF SIALIC ACIDS AND SIALYLATED OLIGOSACCHARIDE ALDITOLS

Peaks a–f are from HPLC on a PGC column of released chains of bovine submaxillary mucin (BSM).

Structure	M/Z [M - H] ⁻	Retention time (min)			
		PGC	HPAEC		
			Gradient 1	Gradient 2	Gradient 3
<i>BSM-derived alditols</i>					
NeuGc	324	12.5	58	28	35
NeuAc	308	13.2	50	14	12
a 	675	14.3	46	8	20
b { NeuAc-GalNAcol	513	16.4	48	13	23
{ NeuGc-GalNAcol	529	16.4	53	14	23
c { 	716	17.4	39	12	29
{ 	732	17.4	50	15	32
d 	878	20.9	37	15	24
e { 	1024	23.5	NT ^a	12	23
{ 	1040	23.5	NT	14	33
{ Fuc-Gal-GlcNAc-GalNAcol	733	26.4	NR ^b	NR	NR
f { 	879	26.4	NR	NR	NR
{ 	895	26.4	NR	NR	NR
{ 	936	26.4	NR	NR	NR
<i>Non-mucin oligosaccharides</i>					
NeuAc α 2-6Gal β 1-4Glc α 1	634	18.5	34.3	16.0	21
NeuAc α 2-3Gal β 1-4Glc α 1	634	24.6	37.7	19	27
	1290	27.5	39.1	27	30

^a NT = Not tested.

^b NR = Not retained.

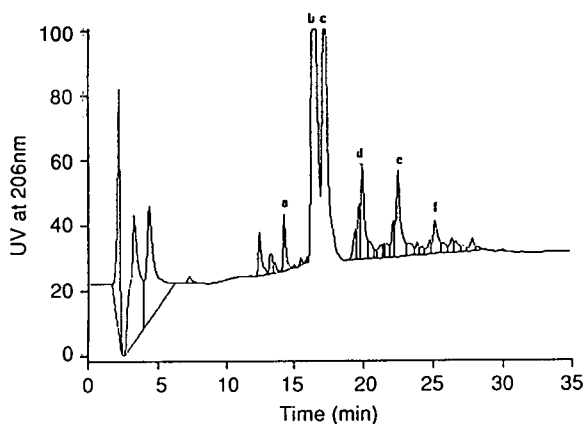


Fig. 4. Chromatography on a PGC column of oligosaccharide alditols obtained from BSM by base-borohydride degradation. Peaks a–f were those identified by LSI-MS as containing oligosaccharide alditols (Fig. 5, Table II).

on PGC but the latter had a greater retention on HPAEC. Identification of the coeluting NeuAc/NeuGc pairs could easily be detected by LSI-MS (Figs. 4 and 5) or by hydrolysis and sialic acid analysis [27]. The advantage of the PGC column was the ability to analyse sialylated and non-sialylated alditols from one HPLC run which cannot be achieved reliably by HPAEC. In particular separation of fucosylated alditols was facilitated which chromatograph near to the solvent front in both HPAEC [15] and RP-HPLC [6]. In addition LSI mass spectra of molecules prepared by chromatography on a PGC column were easily obtained at high sensitivity. PGC has the additional advantages over classical RP-, NP- and HPAEC columns of stability over a large pH range, long column half life, and low day-to-day and column-to-column variability.

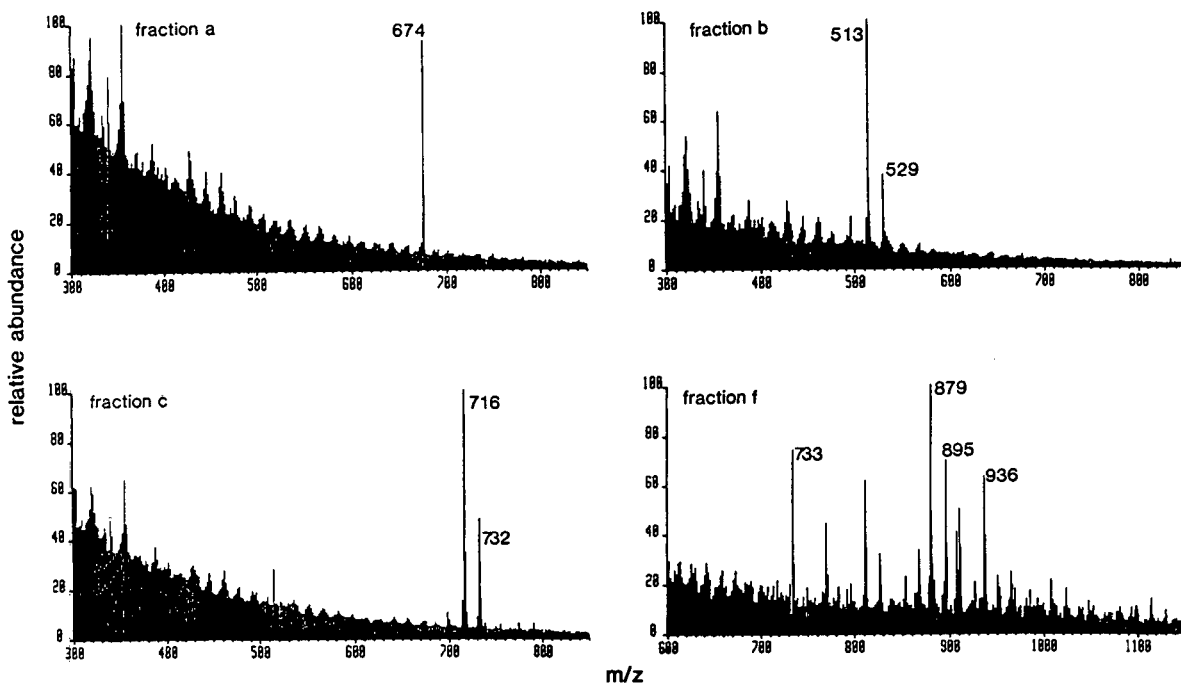


Fig. 5. Representative negative ion LSI-MS of oligosaccharide alditols of BSM as assigned in Table II and Fig. 4.

REFERENCES

- 1 N.P. Arbatsky, M.D. Martynova, A.O. Zheltova, V.A. Dervitskaya and N.K. Kochetkov *Carbohydr. Res.*, 187 (1989) 165–171.
- 2 E.F. Hounsell, A.M. Lawson, J. Feeney, H.C. Gooi, N.J. Pickering, M.S. Stoll, S.C. Lui and T. Feizi, *Eur. J. Biochem.*, 148 (1985) 367–377.
- 3 A. Klein, C. Carnoy, J.-M. Lo-Guidice, G. Lamblin and P. Roussel, *Carbohydr. Res.*, 236 (1992) 9–16.
- 4 N.M.K. Ng Ying Kin and L.S. Wolfe, *Anal. Biochem.*, 102 (1980) 213–219.
- 5 M.L.E. Bergh, P. Koppen and D.H. van den Eijnden, *Carbohydr. Res.*, 94 (1981) 225–229.
- 6 E.F. Hounsell, in C.K. Lim (Editor), *HPLC of Small Molecules*, IRL Press, Oxford, 1986, pp. 49–68.
- 7 T. Tsuji, K. Yamamoto, Y. Konami, T. Irimura and T. Osawa, *Carbohydr. Res.*, 109 (1982) 259–269.
- 8 E.D. Green and J.U. Baenziger, *Anal. Biochem.*, 158 (1986) 42–49.
- 9 A. Hjerpe, C.A. Antonopoulos, B. Engfeldt and M. Nurminen, *J. Chromatogr.*, 242 (1982) 193–195.
- 10 D.C. Seldin, N. Seno, K.F. Austen and R.L. Stevens, *Anal. Biochem.*, 141 (1984) 291–300.
- 11 P. Scudder, P.W. Tang, E.F. Hounsell, A.M. Lawson, H. Mehmet and T. Feizi, *Eur. J. Biochem.*, 157 (1986) 365–373.
- 12 G.J.-L. Lee and H. Tieckelmann, *J. Chromatogr.*, 195 (1980) 402–406.
- 13 K.D. Smith, A.-M. Harbin, R.A. Carruthers, A.M. Lawson and E.F. Hounsell, *Biomed. Chromatogr.*, 4 (1990) 261–266.
- 14 R.R. Townsend, M.R. Hardy and Y.C. Lee, *Methods Enzymol.*, 179 (1989) 65–76.
- 15 Y.C. Lee, *Anal. Biochem.*, 189 (1990) 151–162.
- 16 S. Honda, S. Suzuki, S. Zaiki and K. Kakehi, *J. Chromatogr.*, 523 (1990) 189–200.
- 17 K.O. Lloyd and A. Savage, *Glycoconjugate J.*, 8 (1991) 493–498.
- 18 G.P. Reddy and C.A. Bush, *Anal. Biochem.*, 198 (1991) 278–284.
- 19 R.C. Simpson, C.C. Fenselau, M.R. Hardy, R.R. Townsend, Y.C. Lee and R.J. Cotter, *Anal. Chem.*, 62 (1990) 248–252.
- 20 J.J. Conboy and J. Henion, *Biol. Mass Spectrom.*, 21 (1992) 397–403.
- 21 T.-F. Chen, H. Yu and D.F. Barofsky, *Anal. Chem.*, 64 (1992) 2014–2016.
- 22 M. Davies, K.D. Smith, A.-M. Harbin and E.F. Hounsell, *J. Chromatogr.*, 608 (1992) 125–131.
- 23 M.S. Stoll and E.F. Hounsell, *Biomed. Chromatogr.*, 2 (1988) 249–253.
- 24 D.A. Cumming, C.G. Hellerqvist, M. Harris-Brandts, S.W. Michnick, J.P. Carver and B. Bendiak, *Biochemistry*, 28 (1989) 6500–6512.
- 25 W. Chai, E.F. Hounsell, G.C. Cashmore, J.R. Rosankiewicz, C.J. Bauer, J. Feeney, T. Feizi and A.M. Lawson, *Eur. J. Biochem.*, 203 (1992) 257–268.
- 26 W. Chai, E.F. Hounsell, G.C. Cashmore, J.R. Rosankiewicz, J. Feeney and A.M. Lawson, *Eur. J. Biochem.*, 207 (1992) 973–980.
- 27 A.E. Manzi, S. Diaz and A. Varki, *Anal. Biochem.*, 188 (1990) 20–32.

Study of lectin–ganglioside interactions by high-performance liquid affinity chromatography

M. Caron* and R. Joubert-Caron

Laboratoire de Biochimie et Technologie des Protéines, Université Paris-Nord, 74 Rue M. Cachin, 93012 Bobigny Cedex (France)

J.R. Cartier

Pasteur Mérieux, 1541 Avenue M. Mérieux, 69280 Marcy l'Etoile (France)

A. Chadli and D. Bladier

Laboratoire de Biochimie et Technologie des Protéines, Université Paris-Nord, 74 Rue M. Cachin, 93012 Bobigny Cedex (France)

(First received February 3rd, 1993; revised manuscript received May 14th, 1993)

ABSTRACT

A high-performance affinity column containing immobilized modified GM1 (lyso-GM1) was used to study the binding of an endogenous human brain lectin (HBL) in comparison with other carbohydrate-binding proteins. The proteins are previously converted into biotinylated derivatives. Detection of biotinylated proteins in the eluates by a microtitre plate assay ensures good sensitivity. The maximum binding capacity of the adsorbent for HBL is obtained in Tris buffer supplemented with β -mercaptoethanol. The binding is inhibitable by specific sugar. It is concluded that the use of immobilized glycolipids in analytical high-performance liquid affinity chromatographic methods may serve as models in the study of interactions between gangliosides and carbohydrate-binding proteins.

INTRODUCTION

Surface gangliosides, like membrane glycoproteins, are believed to play a major role in cell recognition and cell to cell interactions [1–3]. Gangliosides can serve as selective receptor sites for several bioeffectors such as neurotransmitters, carbohydrate-binding proteins (lectins) and toxins [4–6]. The interaction between ganglioside GM1 [Gal β 1–3GalNAc β 1–4(NeuAc α 2–3)Gal β 1–4Glc β 1-Cer] and cholera toxin for

example, has been studied in great detail [4,5,7–10].

Although the molecules which recognize these gangliosides *in vivo* are certainly numerous, evidence suggests that complementary carbohydrate-binding proteins may be involved. Previous work has demonstrated the specific recognition by plant lectins of liposomes containing gangliosides and of poly(vinyl chloride)-adsorbed gangliosides [11–13]. The results of these studies clearly depended on the assay system used and on the experimental conditions. Another approach has been to examine the ability of synthetic saccharide derivatives, which can be considered as neoglycolipids [14,15], to interact with

* Corresponding author.

endogenous lectins. In spite of this, however, little is known about the possible interactions between gangliosides and carbohydrate-binding proteins which can co-exist in the same organ, and particularly in brain tissue where glycosphingolipids are particularly abundant.

For many years, we have examined one brain tissue lectin that we particularly characterized in human [16,17]. Hapten inhibition studies and binding of blood group-related synthetic oligosaccharides showed that it is actually specific for structures containing lactose or lactosamine, such as blood group i antigen. However, its possible interaction with brain gangliosides remains to be clarified. To elucidate this aspect, we have now used an analytical high-performance liquid affinity chromatographic (HPLAC) method, based on porous silica beads derivatized with GM1. In addition, some comparisons of the binding activity of the human brain protein with those of plant lectins and cholera toxin are presented.

EXPERIMENTAL

Proteins and derivatives

The main characteristics of the carbohydrate-binding proteins used in this work are summarized in Table I.

HBL was purified as a carboxamidomethylated derivative in a bioactive form as described previously [16,18].

The lectin from *Arachis hypogaea* (peanut agglutinin, PNA) was purified by the Laboratoire de Biochimie et Technologie des Protéines. The B subunit of cholera toxin (CT-B) and the lectins from *Triticum vulgare* (wheat germ agglutinin, WGA) and edible snail (*Helix pomatia* agglutinin, HPA) were obtained from Sigma Chimie (La Verpillière, France). All the carbohydrate-binding proteins were biotinylated according to Avellana-Adalid *et al.* [18].

High-performance liquid affinity chromatography (HPLAC) on Spherosil-DEAE-dextran beads derivatized with GM1

Spherosil beads coated with DEAE-dextran and coupled with lyso-GM1 were prepared as described previously [19,20]. They were packed in a glass column (50 × 5 mm I.D.) of bed volume 1 ml.

Chromatographic experiments were carried out using a high-performance liquid chromatographic (HPLC) system (LKB) consisting of high-precision pump (LKB 2249). Routinely, the concentration of each protein used in a sample was 0.25 mg/ml dissolved in the equilibration buffer. The volume injected was 20 µl and the flow-rate was 0.4 ml/min during the 5 first minutes, then, 0.6 ml/min throughout. The elution of adsorbed proteins was performed using a linear gradient from 0 to 100% elution buffer 1 (50 mM citrate buffer, pH 2.8; 4 min)

TABLE I
CARBOHYDRATE-BINDING PROTEINS USED IN HPLAC EXPERIMENTS

Origin	Common name	M_r	Major sugar specification ^a
Human brain	HBL	14 500 × 2	Galβ1-4GlcNac > Galβ1-4Glc
<i>Vibrio cholerae</i>	CT-B	11 800	Galβ1-3GalNacβ1-4 (NeuNacα2-3)Gal > GalNac β1-4(NeuNacα2-3)Gal
<i>Triticum vulgare</i>	WGA	21 600 × 2	(GlcNacβ1-4) ₃ > NeuNac
<i>Arachis hypogaea</i>	PNA	24 500 × 4	Galβ1-3GalNac > Gal
Edible snail	HPA	13 000 × 6	GalNac, GlcNac

^a Gal = D-galactose; Glc = D-glucose; GalNac = N-acetyl-D-galactosamine; GlcNac = N-acetyl-D-glucosamine; NeuNac = N-acetylneuraminic acid.

followed by 100% elution buffer over 12 min. In some experiments, the bound proteins were eluted by sequential applications of 50 mM Tris-HCl buffer (pH 7.6) containing 0.1 M lactose (elution buffer 2) and of acidic elution buffer 1.

Four different equilibration buffers tested: (1) 50 mM citrate buffer–100 mM NaCl (pH 7.2); (2) 50 mM citrate buffer–100 mM NaCl (pH 4.9); (3) 50 mM Tris-HCl buffer–100 mM NaCl, 0.4 mM β -mercaptoethanol (pH 7.6); and (4) buffer 3 containing 40 mM CaCl_2 .

NaCl was used to suppress ionic adsorption of proteins on the DEAE-dextran monolayer.

Microtitre plate assay

The amount of biotinylated protein in each eluted fraction was determined with streptavidin coupled to horseradish peroxidase (Strep-HRP, Sigma). Microtitre plates (96 wells; Nunc-Immuno Plate Maxisorp, Denmark) were coated with 50 μl of each effluent sample overnight at 4°C. The wells were washed with 10 mM potassium phosphate (pH 7.4), containing 0.05% Tween 20, then blocked with 100 mM potassium phosphate (pH 7.4) containing 3% bovine serum albumin (BSA) and 0.3% Tween 20 for 90 min followed by three further washes. The amount of bound protein was detected by using Strep-HRP as described [21].

RESULTS AND DISCUSSION

As detailed above, we developed a protocol that allows the rapid evaluation of the adsorption of carbohydrate-binding proteins on immobilized gangliosides. This technique used silica beads derivatized with lyso-GM1 ganglioside, a chromatographic support originally developed for the purification of cholera toxin on an industrial scale (1 kg column) [20]. We selected CT-B as the reference protein because it is responsible for binding the toxin to GM1 ganglioside receptors. The binding and the subsequent release of the protein from the HPLAC column were studied by microtitre plate assay detection of the effluent. The use of an HPLC system allowed highly reproducible experimental conditions to be obtained and only analytical amounts (20 μl) of carbohydrate-binding protein to be injected.

Binding of biotinylated cholera toxin B subunit to immobilized lyso GM1

The characteristic binding profile of CT-B to the sorbent is shown in Fig. 1. When the biotinylated derivative prepared from this

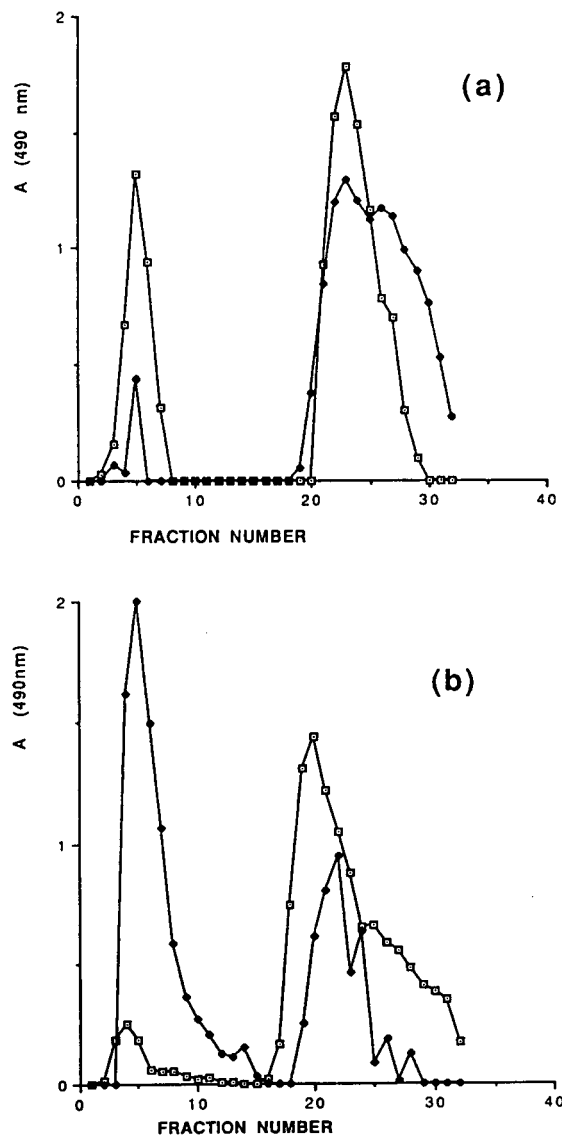


Fig. 1. Chromatograms showing the effect of the equilibration buffer on Spherosil-DEAE-dextran-lyso-GM1 affinity chromatography of cholera toxin B subunit. (a) 50 mM citrate buffer [pH 7.2 (buffer 1) (\square) and pH 4.9 (buffer 2) (\blacklozenge)]; (b) 50 mM Tris-HCl buffer (pH 7.6) containing β -mercaptoethanol (buffer 3) (\square) and CaCl_2 (buffer 4) (\blacklozenge). Sample, 5 μg of protein in equilibration buffer; column, 50 mm \times 5 mm I.D.

subunit was passed through the column in a buffer used on the preparative scale (equilibration buffer 1), *ca.* 78% of this protein was bound to the column (Table II). This is in accordance with the fact that CT-B acts as a biologically inactive structural analogue of cholera toxin by virtue of competition for binding to GM1 [22]. This binding increased to values close to 100% using a more acidic buffer or a Tris-HCl buffer containing β -mercaptoethanol. Conversely, it was significantly decreased in the presence of divalent cations. We interpreted these data by the interactions between Ca^{2+} and the negatively charged saccharidic part of the gangliosides.

Binding of biotinylated human brain lectin

HBL-Biot, when analysed by HPLAC, showed no binding in equilibration buffer 1 (Fig. 2, Table II). In contrast, a significant percentage of the total protein was able to recognize the immobilized ganglioside in more reducing conditions (acidic pH or in the presence of β -mercaptoethanol). These results confirm the thiol dependence of HBL and, more generally, of the lectins belonging to the same protein family [23]. According to the saccharidic specificity of both the lectin and its biotinylated derivative [16–18], one may suggest that the interaction occurs through the internal lactosyl of the ganglioside. The fact that an unbound protein fraction was always found in the effluent indicates either that the lectin was bound with a relatively low affinity or that different conformational forms of the lectin present different affinities for the lyso-

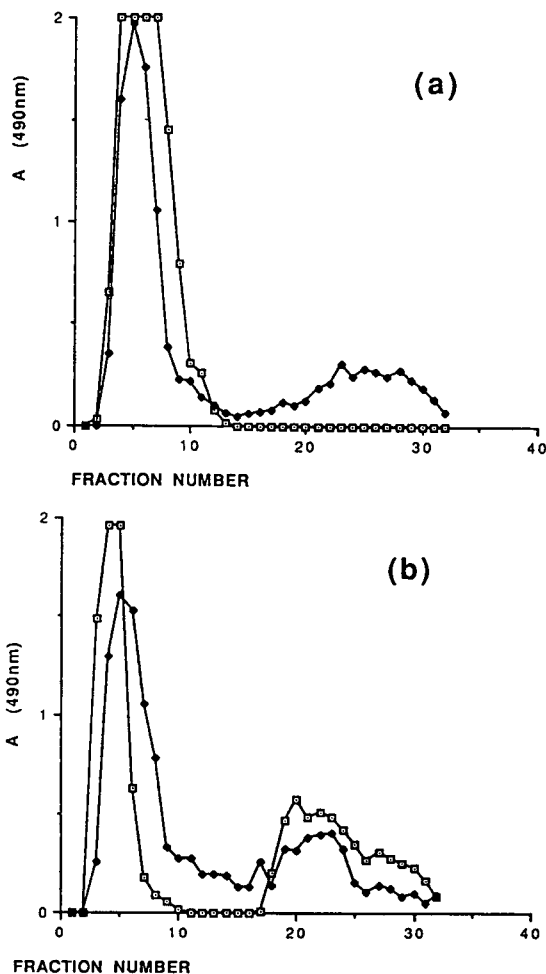


Fig. 2. Chromatograms showing the effect of the equilibration buffer on Spherosil-DEAE-dextran-lyso-GM1 affinity chromatography of human brain lectin and symbols as in Fig. 1.

TABLE II
RECOVERIES (%) OF RETAINED-ELUTED PROTEINS

Equilibration buffer	CT-B	HBL	WGA	PNA	HPA
(1) Citrate buffer (pH 7.2)	77.7	0	47.0	87.7	61.7
(2) Citrate buffer (pH 4.9)	98.8	28.2	24.9	95.6	62.5
(3) Tris buffer containing β -mercaptoethanol	92.6	43.7	41.6	43.2	48.3
(4) Tris buffer containing β -mercaptoethanol and Ca^{2+}	33.9	28.1	5.4	49.7	28.9

GM1 immobilized on the affinity support. Such a microheterogeneity has been reported for HBL. It may be the result of pH-dependent conformational changes, leading to a panel of differently charged molecular species [24].

To test these expectations, the void volume peaks obtained in buffer 3 for CT-B and HBL were rechromatographed. A separation into two peaks was obtained for both proteins in proportions close to those obtained during the first chromatography. These results suggest that, even if the presence of molecular forms showing different affinities cannot be completely excluded, the chromatographic profiles certainly reflect the affinity of the whole protein populations.

Binding profiles of a panel of carbohydrate-binding proteins

We used the protocol established with TC-B and HBL to determine the binding profile of several lectins which are specific for saccharidic constituents of the gangliosides. Table II lists the binding capacities obtained.

Of the proteins, WGA is known to bind to GM1-bearing liposomes [11], certainly by the mediation of N-acetylneuraminic acid, whereas poly(vinyl chloride)-adsorbed GM1 will not bind the lectin [13]. WGA bound only moderately to the affinity support. In particular, a comparison of the relative binding capacities in neutral and acidic citrate buffer showed that among the carbohydrate-binding proteins tested only WGA showed a pH-dependent affinity which could be related to the dissociation of the protein into monomers in acidic media.

Using poly(vinyl chloride)-adsorbed glycosphingolipids, Molin *et al.* [13] reported that PNA showed the highest affinity to asialo-GM1, but also bound, though less strongly, to GM1, whereas Momoi *et al.* [12] found no binding of GM1 to the lectin. Although silica beads derivatized with GM1 bound PNA under a variety of conditions, including Ca^{2+} -containing buffer, the highest binding capacities were obtainable when the sample was applied in citrate buffers. This is especially true for the binding at pH 4.9. As a consequence, it is not necessary to subject the ganglioside to a desialylation prior to obtain a

binding of the lectin under these experimental conditions. However, the affinity and capacity of GM1 for PNA are clearly limited compared with more specific adsorbents such as beads derivatized with lactose.

HPA has been used for the detection of glycolipids with terminal GalNAc residues on thin-layer chromatograms and for the affinity purification of the corresponding glycolipid-derived oligosaccharides [25]. Despite its specificity for GalNAc end-groups, the snail lectin is partially adsorbed on the affinity matrix. Although it has a very low affinity for galactose, one may assume that the large number of galactosyl end-groups must provide sufficient binding loci to cause the lectin to be adsorbed. The same kind of hypothesis has been proposed to explain the fact that HPA can be purified by adsorption to Sephadex followed by elution with galactose or glucose [26]. Another possibility would be the hydrolysis of a small number of $\text{Gal}\beta(1-3)\text{GalNAc}$ linkages leading to some high-affinity sites for the lectin.

Sequential elutions of HBL and cholera toxin

With a view to ascertaining the carbohydrate specificity of the interaction between brain lectin and immobilized GM1, the bound protein was eluted by sequential application of buffer containing 0.1 M lactose and citrate buffer (pH 2.8). An elution peak containing about 82% of the adsorbed lectin was obtained with the 0.1 M lactose solution. That the recognition of GM1 by HBL depends on a different mechanism to the well documented interaction of the same ganglioside with cholera toxin was verified using TC-B instead of the lectin. No elution was obtained with lactose, in accord with the observation that lactosylceramide does not inhibit the binding of cholera toxin to membrane gangliosides [10]. Fig. 3 compares the chromatograms obtained with the two proteins.

CONCLUSIONS

The results reported here established the feasibility of studying protein–glycolipid interactions by use of simple HPLAC procedures. The binding of specific lectins to oligosaccharide

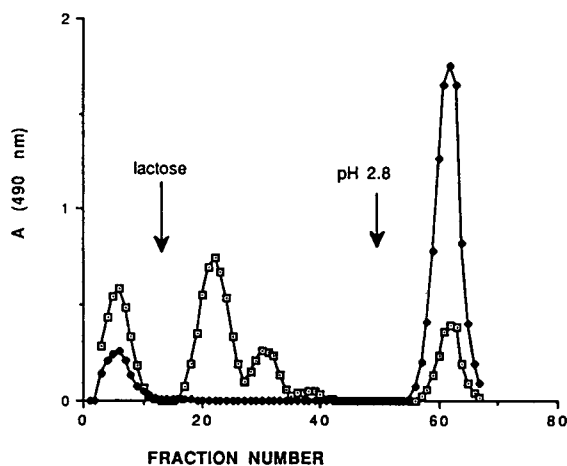


Fig. 3. Chromatogram showing the elution of (□) HBL and (●) cholera toxin subunit B adsorbed on lyso-GM1. Successive elutions were performed (arrows) with Tris-HCl buffer containing 0.1 M lactose and citrate buffer (pH 2.8).

affinity columns was previously used as a relatively simple system to define their carbohydrate specificity [14, 27]. However, protein-glycolipid interactions can be more complex, involving contributions of oligosaccharide and ceramide portions of the ganglioside [10]. We used HPLAC to detect a possible recognition phenomenon between two molecules that co-exist in brain tissue, a soluble lectin and the monosialoganglioside GM1. The binding capacity of the brain protein was compared with those of other carbohydrate-binding proteins, including the well known biological partner of the glycolipid, cholera toxin. All the experiments were conducted in buffers containing a concentration of NaCl previously described to avoid the affinity support to work as an ion-exchange matrix [20].

We can conclude that HBL is able to interact with GM1. However, only half of the molecules were adsorbed during the chromatography. A possible explanation of this result is that it reflects a low affinity between the two partners. This low affinity could be due either to a repulsive effect of the sialic acid or to an inhibitory effect of NaCl [28]. It is interesting that (i) this binding was obtained only in a buffer used during other methods to preserve the activity of the lectin (except NaCl concentration) and (ii) addition of lactose to the buffer is sufficient to

eluate the lectin. It is consistent with the idea that the reaction between HBL and GM1 is carbohydrate specific.

Another point is the differences observed between the results obtained in HPLAC and in other assays. This is not completely surprising as the influence of the experimental conditions during these interactions is well established. An advantage of the HPLAC approach is that it allows this influence to be studied by modifying the composition of the buffers. Further, one may suggest that the interaction of proteins showing a moderate affinity for the ganglioside will be easier than in other assays. A possible explanation is that when the GM1 is present at the end of a spacer arm on an affinity matrix it may be able to rotate more freely and assume a configuration and an orientation that the proteins can recognize.

ACKNOWLEDGEMENTS

The authors thank Philippe Bosset and Xavier Itarrioz for technical assistance and Françoise Berthaud for assistance with manuscript preparation. This work was supported by grants from the INSERM (No. 896001), from the Délégation à la Recherche Clinique de l'Assistance Publique (No. 900012), from the Direction de la Recherche et des Etudes Doctorales (DRED) and from the Association pour la Recherche sur la Sclérose en Plaques (ARSEP).

REFERENCES

- 1 S.I. Hakomori, *Rev. Biochem.*, 50 (1981) 733.
- 2 S. Ando, *Neurochem. Int.*, 5 (1983) 507.
- 3 R. D. Dal Toso, S.D. Skaper, G. Ferrari, G. Vantini, G. Toffano and A. Lear, in D.G. Stein and B.A. Sabel (Editors), *Pharmacological Approaches to the Treatment of Brain and Spinal Cord Injury*, Plenum Press, New York, 1988, pp. 143–164.
- 4 W.E. Van Heyningen, *Nature*, 249 (1974) 415.
- 5 P. Cuatrecasas, *Biochemistry*, 12 (1973) 3558.
- 6 C.C. Blackburn, P. Swank-Hill and R.L. Schnaar, *J. Biol. Chem.*, 261 (1986) 2873.
- 7 P. Cuatrecasas, I. Parikh and M.D. Hollenberg, *Biochemistry*, 12 (1973) 4253.
- 8 C.L. Schengrund and N.J. Ringler, *J. Biol. Chem.*, 264 (1989) 13233.

- 9 K.C. Joseph, A. Stieber and N.K. Gonatas, *J. Cell. Biol.*, 81 (1979) 543.
- 10 P. Cuatrecasas, *Biochemistry*, 12 (1973) 3547.
- 11 D.H. Boldt, S.F. Speckart, R.L. Richards and C.R. Alving, *Biochem. Biophys. Res. Commun.*, 74 (1977) 208.
- 12 T. Momoi, T. Tokunaga and Y. Nagai, *FEBS Lett.*, 141 (1982) 6.
- 13 K. Molin, P. Fredman and L. Svennerholm, *FEBS Lett.*, 205 (1986) 51.
- 14 J.C. Solomon, M.S. Stoll, P. Penfold, W.M. Abbott, R.A. Childs, P. Hanfland and T. Feizi, *Carbohydr. Res.*, 213 (1991) 293.
- 15 A. Chadli, M. Caron, M. Ticha, R. Joubert, D. Bladier and J. Kocourek, *Anal. Biochem.*, 204 (1992) 198.
- 16 D. Bladier, R. Joubert, V. Avellana-Adalid, J.L. Kemeny, C. Doinel, J. Amouroux and M. Caron, *Arch. Biochem. Biophys.*, 269 (1989) 433.
- 17 D. Bladier, J.P. LeCaer, R. Joubert, M. Caron and J. Rossier, *Neurochem. Int.*, 18 (1991) 275.
- 18 V. Avellana-Adalid, R. Joubert, D. Bladier and M. Caron, *Anal. Biochem.*, 190 (1990) 26.
- 19 J.L. Tayot and M. Tardy, in L. Svennerholm, H. Dreyfus and P.F. Urban (Editors), *Structure and Function of Gangliosides*, Plenum Press, New York, 1980, pp. 471–478.
- 20 J.L. Tayot, J. Holmgren, L. Svennerholm, M. Lunblad and M. Tardy, *Eur. J. Biochem.*, 113 (1981) 249.
- 21 H. Eloumami, M. Caron, R. Joubert, C. Doinel and D. Bladier, *J. Neurol. Sci.*, 105 (1991) 6.
- 22 P. Cuatrecasas, *Biochemistry*, 12 (1973) 3577.
- 23 M. Caron, D. Bladier and R. Joubert, *Int. J. Biochem.*, 22 (1990) 1379.
- 24 V. Avellana-Adalid, R. Joubert-Caron, M. Caron and D. Bladier, *Electrophoresis*, 3 (1992) 416.
- 25 B.V. Torres, D.K. McCrumb and D.F. Smith *Arch. Biochem. Biophys.*, 262 (1988) 1.
- 26 I.J. Goldstein and C.E. Hayes, *Adv. Carbohydr. Chem. Biochem.*, 35 (1978) 127.
- 27 H.J. Gabius, *Anal. Biochem.*, 189 (1990) 91.
- 28 N.E. Fink de Cabutti, M. Caron, R. Joubert, M.T. Elola, D. Bladier and J. Herkovitz, *FEBS Lett.*, 223 (1987) 330.

Analysis and configuration assignments of the amino acids in a pyoverdine-type siderophore by reversed-phase high-performance liquid chromatography

Diane K. Hancock* and Dennis J. Reeder

National Institute of Standards and Technology (NIST), Biotechnology Division, Gaithersburg, MD 20899 (USA)

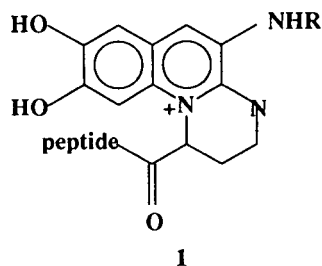
(First received January 19th, 1993; revised manuscript received June 2nd, 1993)

ABSTRACT

The amino acid composition of the siderophore pyoverdine Pf244 was determined by reversed-phase high-performance liquid chromatography (RP-HPLC) of phenylthiocarbamyl derivatives of the acid-hydrolyzed pyoverdine. The siderophore contains an acid-labile amino acid, N^δ-hydroxyornithine, and an amino acid previously unknown in naturally occurring systems, L-threo-β-hydroxyhistidine. Amino acid chirality assignments were determined by RP-HPLC of the β-D-glucopyranosyl isothiocyanate tetraacetate derivatives. Reactions with amino acid oxidases established the L-configuration of threo-β-hydroxyhistidine.

INTRODUCTION

Siderophores are low-molecular-mass peptidic ferric-ion chelators synthesized and secreted by many bacteria and fungi in response to iron deprivation. *Pseudomonas* bacteria produce pyoverdine (also termed pseudobactin) siderophores. Structures of many pyoverdines have been determined using a combination of nuclear magnetic resonance spectroscopy, fast atom bombardment mass spectrometry, and amino acid analysis [1–6]. They all comprise a yellow-green fluorescent chromophore (1) covalently



* Corresponding author.

bound to the N-terminus of a hydrophilic oligopeptide of six to twelve amino acids.

The peptide portion contains two amino acids that function as ferric-specific bidentate ligands, generally either two hydroxamates (as N^δ-hydroxyornithine, present in cyclic form, or as a N^δ-formyl or -acetyl derivative) or one hydroxamate and one β-hydroxyaspartic acid. These bidentate groups and the chromophore catechol unit octahedrally bind the ferric ion through six oxygen atoms. Pyoverdine-type siderophores are strain specific, differing in amino acid configuration, composition and sequence, with amino acid stereochemistry determining the possible coordination isomers. Problems encountered in stereochemical analysis of siderophore amino acids by gas chromatography have been previously addressed [7].

This paper describes (1) Pico-Tag HPLC identification of unusual amino acids (*i.e.*, *allo*-threonine, N^δ-hydroxyornithine and *threo*-β-hydroxyhistidine) present in pyoverdine Pf244, the siderophore expressed by *Pseudomonas fluorescens* 244, and (2) stereochemical assignments of the constituent amino acids by reversed-phase

high-performance liquid chromatography (RP-HPLC) analysis of the amino acids derivatized with the chiral reagent, β -D-glucopyranosyl isothiocyanate tetraacetate (GITC).

EXPERIMENTAL

Chemicals^a

Amino acid standard H, phenylisothiocyanate (PITC) and ninhydrin were obtained from Pierce, GITC from Polysciences, triethylamine (TEA, Gold Label) and (*SS*)-*allo*-threonine (*L-allo*-) from Aldrich, (*RR,SS*)- β -hydroxyaspartic acid (*D,L-threo*-), rhodotorulic acid, (*RR*)-*allo*-threonine (*D-allo*-) and other amino acids from Sigma. Ultrapure hydrochloric acid was prepared at NIST [8]. (*RS,SR*)- β -Hydroxyhistidine (*D,L-erythro*-) and the mother liquors from which (*RR,SS*)- β -hydroxyhistidine (*D,L-threo*-) was recovered were provided by Professor S. Hecht. $\text{CH}_3\text{SiC}^2\text{H}_2\text{C}^2\text{H}_2\text{CO}_2\text{Na}$ (TSP) was obtained from MSD Isotopes, 4-(2-hydroxyethyl)piperazine-1-ethanesulfonic acid (HEPES) from Fluka. Pico-Tag eluents A and B and sample diluent were obtained from Waters or made according to Waters' instructions [9]. Acetonitrile and methanol were HPLC-grade solvents from EM Science. Water was purified with an Organex Milli-Q system (Millipore). The column selectivity test mixture, SRM 869, was obtained at NIST [10]. L-Amino acid oxidase (LAO), supplied in aqueous solution, and D-amino acid oxidase (DAO), supplied dry, were purchased from Worthington Biochemical.

Isolation and purification of pyoverdine

Pyoverdine and ¹⁵N-labelled pyoverdine were isolated from culture media and purified as their ferric chelates by the procedure of Hancock *et al.* [11]. Iron was removed from the ferric pyoverdines by extracting with a 5% (w/v) 8-hydroxyquinoline–chloroform solution.

^a Commercial instruments or materials are identified in this report to specify adequately the experimental procedure. Such identification does not imply recommendation or endorsement by the National Institute of Standards and Technology, nor does it imply that the equipment or materials are the best available for the purpose.

High-performance liquid chromatography

Waters HPLC hardware was used: two Model 501 pumps, U6K injector, 440 detector (254 nm), 660 solvent programmer, TCM temperature control unit and 740 data module. A 150 \times 3.9 mm Pico-Tag column was used for amino acid analysis and a 300 \times 3.9 mm Vydac C₁₈ (218TP5) column (Separations Group) for chiral analysis.

Amino acid analysis by the Pico-Tag method

Pyoverdine samples and amino acid standards were hydrolyzed and derivatized on a Pico-Tag work station equipped with a Varian SD200 vacuum pump. Batch hydrolyses of *ca.* 10-nmol pyoverdine samples were carried out in pyrolyzed (520°C, 24 h) 50 \times 6 mm borosilicate glass tubes. Sample tubes were placed in a reaction vial with a Mininert-type valve (Waters) and vacuum dried. A 200- μ l volume of 6 M ultrapure HCl and a small phenol crystal were added to the reaction vial, which was then alternately evacuated and purged with nitrogen three times, and again evacuated, sealed, and transferred to a 114°C oven for 21 h. Cooled sample tubes were transferred to a clean reaction vial and residual HCl was evaporated under vacuum. To assure basic derivatizing conditions 20 μ l of ethanol–water–TEA (2:2:1) were added to each tube, vortex mixed and evaporated to constant 7 Pa (55 mTorr) pressure. Samples were derivatized with 20 μ l of freshly prepared reagent (ethanol–water–TEA–PITC, 7:2:1:1) for 15 min at 20–25°C, then evaporated to constant pressure of 7 Pa to remove excess derivatizing reagent.

Phenylthiocarbamyl (PTC) derivatives of the amino acids were reconstituted in 200 μ l of sample diluent (Waters) and separated on the Pico-Tag column. A concave gradient, 0–46% B over 8 min at 1 ml/min, was followed by holding the gradient 6 min at 46% B, then increasing to 100% B over 1 min, holding 2 min, reversing to 0% B over 1 min, and reequilibrating for 20 min. Eluent A was (0.14 M NaC₂H₃O₂ + 0.05% TEA, adjusted to pH 6.4 with acetic acid)–CH₃CN (94:6, v/v) and eluent B was CH₃CN–water (60:40, v/v). A 200- μ l volume of 1000 ppm (w/w) aqueous Na₂EDTA was added to each liter of eluents A and B. Column tempera-

ture was maintained at 38°C. Additional analyses were carried out at 45°C with eluent A at pH 5.8. Amino acids in the pyoverdine sample were identified by comparison with PITC-derivatized standards and verified by coinjection of sample and standard under both conditions.

Determination of amino acid configurations

Enantiomeric composition of hydrolyzed pyoverdine samples was determined by RP-HPLC of the GITC-derivatized diastereomers, modifying Nimura *et al.*'s [12] procedure. Amino acids (5 nmol/ μ l) were mixed 1:1:1 (v/v/v) with 50 μ l TEA/ml CH₃CN and 2.2 mg GITC/ml CH₃CN, and kept 30 min at 22°C, then analyzed directly on the same HPLC system used for the PTC-derivatives, except that a polymeric [13] Vydac C₁₈ (218TP5) column was used at 24°C. A linear gradient of 10–75% B over 30 min was run at 1 ml/min, then rapidly increased to 100% B and held 14 min prior to reversing to 10% B with a 3-min linear gradient and reequilibrating 15 min. Eluent A was CH₃OH–10 mM phosphate buffer, pH 2.8 (1:3, v/v) and eluent B was CH₃CN–10 mM phosphate buffer, pH 2.8 (1:1, v/v). A 400- μ l volume of 1000 ppm (w/w) aqueous Na₂EDTA was added to each liter of eluent.

Enantiomer configurations in the hydrolyzed and GITC-derivatized pyoverdines were identified by comparison with GITC-derivatized optically active amino acid standards (commercially available for all except for *threo*- β -hydroxyhistidine) and verified by coinjection. The chirality of *threo*- β -hydroxyhistidine was determined by reacting *threo*- and *erythro*- β -hydroxyhistidine (see below) with LAO in 0.5-ml reaction vials with Mininert caps (Pierce). A 100-nmol amount of hydrolyzed pyoverdine in 75 μ l 0.1 M HEPES buffer, pH 7.2, was treated with 2 μ l of LAO, the vial flushed with oxygen, and incubated at 27°C. The reaction was monitored by HPLC of GITC-derivatized aliquots of the reaction mixture over four days, with additional LAO (10 μ l) added after one day. Another 100-nmol portion of hydrolyzed pyoverdine was treated with 2 μ g of DAO in 100 μ l of 0.05 M sodium pyrophosphate, pH 8.3, and incubated at 37°C.

Isolation and purification of *threo*- β -hydroxyhistidine

threo- β -Hydroxyhistidine was recovered from mother liquors from synthesis of *erythro*- β -hydroxyhistidine [14], known to yield about 10% of the contaminating *threo*-isomer. A 13-g amount of mother liquors, containing mainly glycine and pyruvic acid and less than 0.1% of residual β -hydroxyhistidines, were dissolved in 0.1 M NaC₂H₃O₂, adjusted to pH 3.3, and chromatographed on a 21 \times 2.5 cm SP-Sephadex C-25 cation-exchange column equilibrated with 0.1 M NaC₂H₃O₂, pH 3.3. The column was eluted with the acetate buffer at 1 ml/min, collecting 50-drop fractions. Portions of 1 μ l of each fraction applied to filter paper and dried were spot-tested with 1 μ l of ninhydrin reagent [15] (150 ml of methyl Cellosolve and 50 ml of 4 M NaC₂H₃O₂, pH 5.5, purged with argon before addition of 4 g of ninhydrin and 80 mg of SnCl₂·2H₂O). At ambient temperature, color developed within 30 min. After glycine eluted the eluent was changed to 0.1 M NaC₂H₃O₂, pH 5.4. The β -hydroxyhistidine eluted over many fractions. Representative fractions were adjusted to pH 2, rotoevaporated at 31°C to remove acetate, and then reconstituted in 400 μ l of ²H₂O; 10- μ l aliquots of each were analyzed by HPLC after GITC derivatization. The remaining reconstituted fractions were spiked with an additional 100 μ l of stock ²H₂O–TSP solution and analyzed by NMR, using TSP as an internal standard for relative quantitation of β -hydroxyhistidine.

Fractions were pooled, concentrated, adjusted to pH 4, and applied to 7 \times 1.5 cm SP-Sephadex C-25 columns for desalting and further purification. Columns were eluted with 0.01 M NH₄C₂H₃O₂, pH 4, to remove residual glycine and salts, and then with 1 M NH₄OH. Fractions were monitored with ninhydrin spot tests, pH, and conductivity measurements, and checked for purity by NMR spectroscopy. Finally, pooled fractions were treated with Norit to remove small amounts of colored aromatic contaminants.

Nuclear magnetic resonance

All NMR spectra were measured on a Bruker WM (400 MHz) spectrometer using a 5-mm selective ¹H probe. Intact pyoverdine ¹H–¹H

two-dimensional correlated spectroscopy (COSY) spectra ($^2\text{H}_2\text{O}$, pH 5.3, TSP) were recorded using presaturation, with and without a fixed delay to enhance long-range coupling [16].

Fast atom bombardment mass spectrometry (FAB-MS)

FAB-MS was performed on a Varian MAT 731 double focusing mass spectrometer of Mattauch–Herzog geometry fitted with a Cs^+ gun. A glycerol–thioglycerol (1:1) matrix was used.

RESULTS AND DISCUSSION

Amino acid composition of pyoverdine Pf244

Amino acids derivatized with PITC to give PTC-amino acids were analyzed by RP-HPLC using a modified Pico-Tag method. The RP-HPLC solvent program was empirically determined to resolve all 17 PITC-derivatized amino acids present in the Pierce amino acid standard H preparation (Fig. 1a). Identities of amino acids were confirmed by individual coinjections of PTC derivatives. A chromatogram of the PITC-derivatized pyoverdine hydrolysate (Fig. 1b) indicated that only two of the standard amino acids are present in this pyoverdine—serine and lysine. Three peaks were unidentified.

A COSY NMR spectrum of the intact pyoverdine Pf244 revealed spin systems [$(\alpha\text{CH } 4.30, \beta\text{CH } 4.05, \text{CH}_3 \text{ 1.14 ppm})$, $(\alpha\text{CH } 4.46, \beta\text{CH}_2 \text{ 1.80, 1.99; } \gamma\text{CH}_2 \text{ 1.94, 1.99; } \delta\text{CH}_2 \text{ 3.63 ppm})$, $(\alpha\text{CH } 4.77, \beta\text{CH } 5.18 \text{ ppm})$] suggesting the presence of threonine, ornithine and a β -hydroxyamino acid, respectively. Two additional peaks in the pyoverdine hydrolysate were identified as ornithine and *allo*-threonine by coelution with additional standards.

Analysis of ornithine

Ornithine is found commonly in pyoverdines, often at peptide's C terminus as an internally cyclized N^δ -hydroxyornithine (**2**), or as a N^δ -acyl- N^δ -hydroxyornithine (**3**) where acyl is either formyl or acetyl. Despite common occurrence, verification of the specific form of the ornithine

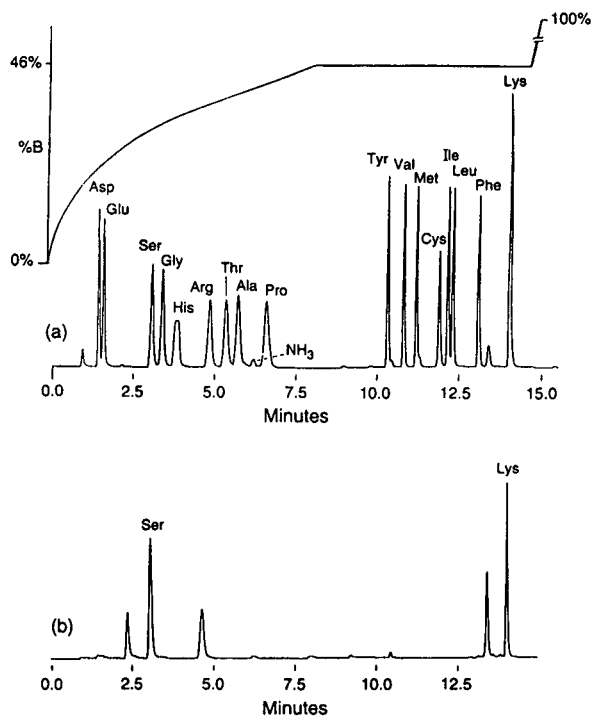
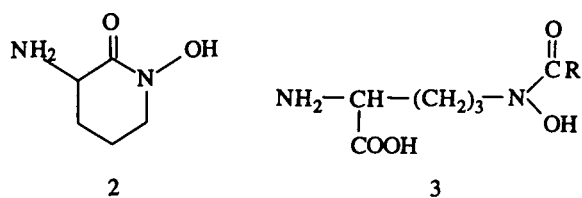


Fig. 1. Amino acid analysis of pyoverdine Pf244. (a) RP-HPLC chromatogram of PITC-derivatized amino acid standards, illustrating mobile phase gradient program: flow-rate 1 ml/min, 38°C, UV-Vis detection, 254 nm; solvent A: sodium acetate–TEA buffer, pH 6.4, and 6% CH_3CN ; solvent B: CH_3CN –water (60:40). (b) RP-HPLC chromatogram of a PITC-derivatized ferric pyoverdine Pf244 hydrolysate, same chromatographic conditions.

is not straightforward due to instability of hydroxamic acids under HCl hydrolysis [7,17–19]. Depending on conditions, hydrolysis of siderophores containing **2** or **3** may give either N^δ -hydroxyornithine or decomposition of the hydroxyamino function and only fractional recovery of ornithine. Iron(III) apparently catalyzes decomposition [18]. The absence of formyl or acetyl peaks in the pyoverdine ^1H NMR spectrum and the presence of a spin system with chemical shifts nearly identical to those reported for pseudobactin [1] suggested that ornithine is present in Pf244 as **2**. Under acid conditions **2** readily undergoes hydrolysis with ring opening to give a N^δ -hydroxyornithine. MS of partially hydrolyzed pyoverdine (6 M HCl, 105°C, 10–120 min) gave $(\text{M} + \text{H} + \text{H}_2\text{O})^+$

and fragmentation peaks corresponding to a C-terminal N^δ-hydroxyornithine residue.



The Pf244 amino acid identified as ornithine coeluted with both PITC-derivatized ornithine and hydrolyzed rhodotorulic acid. Acid hydrolysis of rhodotorulic acid (the diketopiperazine ring dimer of N^δ-acetyl-N^δ-hydroxyornithine) also gives ornithine rather than N^δ-hydroxyornithine. Baseline chromatographic separation of reagent and ornithine peaks, allowing quantitation of ornithine, was achieved on the Pico-Tag column at pH 5.8, 45°C, but not at higher pH and lower temperatures: Both iron-free and ferric pyoverdine, gave *ca.* one-half equivalent of ornithine per pyoverdine hydrolyzed. The PTC derivatives of hydrolyzed rhodotorulic acid and pyoverdine still coeluted with PTC-ornithine, further supporting that the product was PTC-ornithine. Whether the reduction of N^δ-hydroxyornithine to ornithine occurs during acid hydrolysis or during alkaline derivatization was not determined. Though the precise form of ornithine present in Pf244 cannot be established solely by Pico-Tag amino acid analysis, it was readily confirmed as the cyclic N^δ-hydroxy species with MS and NMR data.

Identification of a new amino acid

It was deduced that the unidentified amino acid in pyoverdine Pf244 was probably a bidentate ligand since otherwise iron coordination could be only four-fold —by the quinoline catechol group and the hydroxyornithine hydroxamic acid moiety. However, amino acid analysis had confirmed that *threo*-β-hydroxyaspartic acid, the only other chelating group known in previously studied pyoverdines, was not present. The sequence ions in MS of intact pyoverdine and of a fully ¹⁵N-labelled preparation indicated that the unidentified residue had a mass of 153 u for the non-labelled and 156 u for labelled material,

confirming three nitrogens in the amino acid residue and suggesting it was β-hydroxyhistidine. The β-hydroxy spin system in a two-dimensional COSY NMR spectrum supported this conclusion, revealing extended connectivity from the αCH and βCH to singlets at 7.21 and 8.14 ppm.

The siderophore literature has no record of β-hydroxyhistidine. β-Hydroxyhistidine has been found naturally only as the *erythro*-isomer in the bleomycin family of anti-tumor antibiotics [20]. Amino acid analyses of a sample of DL-*erythro*-β-hydroxyhistidine containing a trace of the *threo*-isomer [14, gift of S. Hecht] showed that the *erythro*-isomer was not the amino acid present in pyoverdine, but the small (≤1%) contaminant did have the same retention time as the unidentified pyoverdine amino acid. Cation-exchange column chromatography of the concentrated mother liquors from Hecht *et al.*'s synthesis of the DL-*erythro*-β-hydroxyhistidine [14] yielded 0.01% (w/w) of the *threo*-isomer in isomeric mixtures. One cut of column fractions that by ¹H NMR contained a 1:1 mixture of *threo*- and *erythro*-isomers was PITC-derivatized and the derivatives could then be separated on the Pico-Tag column (Fig. 2b). Comparison with

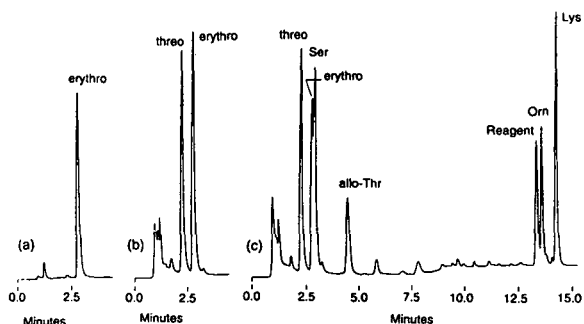
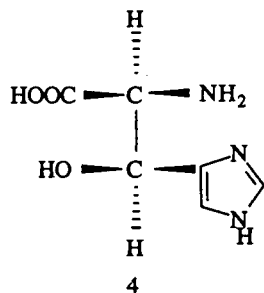


Fig. 2. Amino acid analyses to verify that the β-hydroxyhistidine in pyoverdine Pf244 is the *threo* isomer. Mobile phase solvent program as in Fig. 1 except eluent A at pH 5.8 and temperature at 45°C to resolve ornithine from reagent peak. (a) Chromatogram of PITC-derivatized DL-*erythro*-β-hydroxyhistidine. (b) Chromatogram of *ca.* 1:1 mixture of PITC-derivatized *threo*- and *erythro*-β-hydroxyhistidine isolated from mother liquors. (c) Chromatogram of coinjected PITC-derivatized hydrolyzed pyoverdine Pf244 and the β-hydroxyhistidines from the mother liquors. The *threo*-β-hydroxyhistidine coelutes with the pyoverdine β-hydroxyhistidine.

the retention time in the chromatogram of an *erythro*-standard (Fig. 2a), allowed identification of the PTC-*threo*-isomer. Coinjection of PTC-derivatized pyoverdine Pf244 and the *threo*- and *erythro*- β -hydroxyhistidine mixture (Fig. 2c) confirmed the identity of the remaining unidentified amino acid as *threo*- β -hydroxyhistidine (4).



Quantitation of the amino acids in pyoverdine

Absorbance measurements of the PTC derivatives were employed to quantify the amino acid composition of pyoverdine Pf244. PTC reacts quantitatively with both primary and secondary amino acids, giving derivatives with nearly identical molar extinction coefficients at 254 nm on a per amino group basis [21]. Table I summarizes the relative response factors for the PTC-amino acids obtained from analyses of standards, and the experimental results for the

TABLE I

MOLAR RESPONSE FACTORS FOR CHROMATOGRAPHIC ANALYSIS OF PTC-DERIVATIZED AMINO ACIDS AND THEIR APPLICATION TO AMINO ACID ANALYSIS OF IRON-FREE PYOVERDINE

Amino acid	Response factor normalized to lysine ^a	Amino acid composition of pyoverdine (mol)
β -Hydroxyhistidine	0.58 ^b	1.05
Serine	0.96	1.80
<i>allo</i> -Threonine	0.97	0.96
Ornithine	1.93	0.55
Lysine	2.00	1.00
Rhodotorulic acid ^c	0.43	

^a Determined at pH 5.8, 45°C.

^b Determined on *erythro*-isomer.

^c Hydrolyzed in 6 M HCl, 114°C, 21 h; molarity based on molecular mass of monomer.

composition of pyoverdine Pf244: 1 mol equivalent each of β -hydroxyhistidine, *allo*-threonine and lysine; 2 mol of serine; and one-half equivalent of ornithine. Response factors for β -hydroxyhistidine and hydrolyzed rhodotorulic acid are aberrant. The extinction coefficient for PTC- β -hydroxyhistidine does, in fact, appear to be different. However, the PTC derivative of hydrolyzed rhodotorulic acid is PTC-ornithine which arises from reduction of the HCl hydrolysis intermediate, N⁸-hydroxyornithine. Acid-catalyzed degradation of this intermediate, also present in the pyoverdine hydrolysis, accounts for both the low response factor for rhodotorulic acid and the low ornithine value for pyoverdine. The amino acid composition determined by 254-nm absorbance of the component PTC derivatives is consistent with the MS observation of a molecular (M + H)⁺ ion at *m/z* 1044 for non-chelated pyoverdine Pf244, where the R group on the chromophore (1) is a succinic acid moiety.

Configuration of amino acids in pyoverdine Pf244

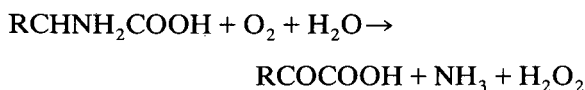
Stereochemical analysis of the component amino acids employed RP-HPLC with GITC as the precolumn chiral derivatizing agent. Separation was accomplished on a polymeric Vydac column with 30-nm pore size, following Sander and Wise [13], who reported that polymeric C₁₈ phases with large pore sizes showed enhanced shape selectivity. Parallel efforts with a monomeric (selectivity coefficient 1.7 [10,22]) Beckman Ultrasphere ODS column and a methanol-phosphate buffer mobile phase [23,24] were unsuccessful. Using a methanol-acetonitrile-phosphate buffer gradient system adapted from a system of Nimura *et al.* [12], separation on the Vydac column at 24°C provided nearly baseline resolution of both enantiomers of GITC-derivatized DL-serine, -*allo*-threonine, -ornithine, -lysine and hydrolyzed pyoverdine with L enantiomers eluting before D.

Excepting *threo*- β -hydroxyhistidine, enantiomer configurations in the pyoverdine sample were easily identified as: one D-serine, one L-serine, one L-lysine, one L-ornithine and one D-*allo*-threonine. Assignment of configuration to

the remaining *threo*- β -hydroxyhistidine was not straightforward because no optically pure standards were available. Although elution order for the other amino acid enantiomers was L before D, Nimura *et al.* [12] had observed inversion of this order for histidine and arginine.

Determination of configuration of *threo*- β -hydroxyhistidine by amino acid oxidase reactivity

Absolute assignment of amino acid configuration was accomplished by reactions with LAO and DAO, which catalyze the oxidative deamination of many L- and D-amino acids:



Since GITC couples with both primary and secondary amines, reaction of LAO or DAO with a given amino acid enantiomer provides configuration identification that is detected as a decrease in its peak size and an increase in the ammonia peak in chromatograms of the GITC-derivatized reaction products. However, these oxidase enzymes are unreactive to some amino acids and enzyme activity is often species-specific [25].

For the β -hydroxyhistidines, LAO/DAO analyses were complicated by overlapping chromatographic peaks, despite extensive variation of solvent gradients, eluents and temperatures. The chromatogram of GITC-derivatized *DL*-*erythro*- β -hydroxyhistidine showed well-resolved D- and L-peaks (Fig. 3a). However, a GITC-derivatized *threo*-*erythro* (2:1) mixture gave only three, not the expected four, peaks because of overlap of one *threo* and one *erythro* isomer (Fig. 3b). *threo*- β -Hydroxyhistidine in GITC-derivatized hydrolyzed pyoverdine coeluted with the first of the *erythro*- β -hydroxyhistidine peaks (Fig. 3c), verifying coelution of one *threo* enantiomer with one *erythro* enantiomer.

LAO and DAO enzyme reaction variables (pH, temperature, buffer system, oxygen level) [25–27], were selected to maximize reaction rates and yet permit direct HPLC analysis of the reaction mixture after GITC derivatization. RP-

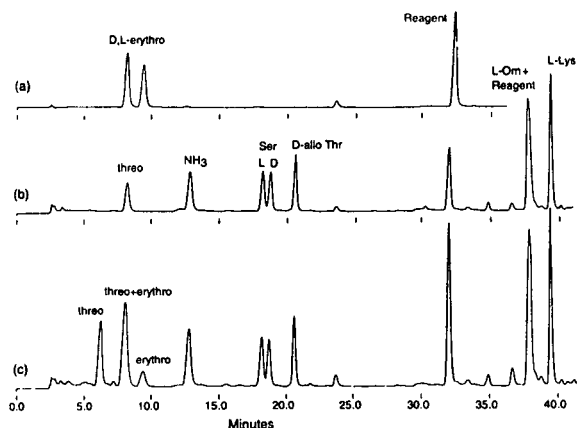


Fig. 3. Chiral amino acid analyses on a Vydac C_{18} column to confirm the identity of the β -hydroxyhistidine enantiomer in pyoverdine Pf244. (a) Chromatogram of GITC-derivatized *DL*-*erythro*- β -hydroxyhistidine. (b) Chromatogram of GITC-derivatized pyoverdine hydrolysate. (c) Chromatogram of GITC-derivatized mother liquor 2:1 *threo*- to *erythro*- β -hydroxyhistidine isolate coinjecting with GITC-derivatized pyoverdine hydrolysate. See text for D,L-assignments.

HPLC chromatograms of GITC derivatives of LAO-treated and non-treated *DL*-*erythro*- β -hydroxyhistidine showed disappearance of the second *erythro* peak in the treated sample after 66 h and concomitant appearance of a peak corresponding to GITC-ammonia. This indicates that the second of the GITC *erythro* peaks is the L-enantiomer, in accord with the D-before-L inverted elution order for GITC-*erythro*- β -hydroxyhistidine previously observed for histidine [12]. Treatment of *DL*-*erythro*- β -hydroxyhistidine with DAO showed no chromatographic changes, signifying that DAO was inactive towards the D-enantiomer under the conditions used, although under the same conditions it fully reacted with D-alanine.

RP-HPLC of a GITC-derivatized β -hydroxyhistidine mother liquor isolate that had been treated with LAO for 48 h, showed a 68% reduction in the L-*erythro* peak, and no decrease in the other two peaks, indicating that the L-*erythro* isomer was more reactive than the L-*threo* isomer. Treatment of a mother liquor preparation with DAO showed no chromatographic changes.

Results of RP-HPLC analyses of hydrolyzed pyoverdine incubated with increased amounts of

TABLE II
REACTION OF L-AMINO ACID OXIDASE WITH
HYDROLYZED PYOVERDINE

Amino acid	HPLC peak areas of GITC-derivatized reaction mixture ^a			
	0 h	15 h	60 h	80 h ^c
<i>threo</i> - β -OH-His	0.59	0.53	—	0.34 \pm 0.01
L-Ser	0.84	0.69	0.16	0.13 \pm 0.001
D-Ser	0.82	0.79	0.82	0.82 \pm 0.002
D- <i>allo</i> -Thr	1.00	1.00	1.00	1.00
L-Orn ^b	5.47	3.96	3.00	3.02 \pm 0.2
L-Lys	2.12	0.92	0.42	0.37 \pm 0.03
NH ₃	1.35	2.44	3.79	4.73 \pm 0.4

^a Peak areas normalized to *allo*-threonine.

^b A reagent peak coelutes with ornithine.

^c Values shown are the averages of two determinations and the standard deviation of the mean.

LAO in an oxygen atmosphere are summarized in Table II and illustrated in Fig. 4a and b. RP-HPLC of pyoverdine solutions showed that without oxygen blanketing both D- and L-serine enantiomers were unstable in 0.1 M HEPES buffer, pH 7.5, in the presence or absence of LAO. However after 80 h in an oxygenated system, analyses showed significant reduction in *threo*- β -hydroxyhistidine, L-serine, L-lysine and

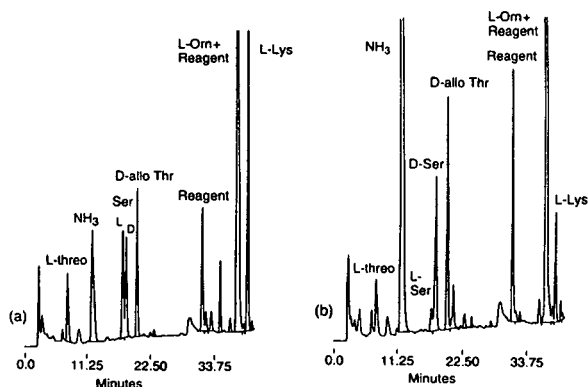


Fig. 4. Analyses of products from the reaction of L-amino acid oxidase on pyoverdine Pf244. (a) Chromatogram of GITC-derivatized reaction mixture at 0 h. (b) Chromatogram of reaction mixture after 80 h. Comparison of the 0 h and 80 h chromatograms confirms that the *threo*- β -hydroxyhistidine in pyoverdine Pf244 has the L-configuration.

L-ornithine peaks and no change in the D-serine or D-*allo*-threonine peaks. Although reaction of LAO with the *threo*- β -hydroxyhistidine was slow, heavy oxidation confirmed that the *threo*- β -hydroxyhistidine amino acid had the L-configuration.

CONCLUSIONS

Elucidation of the structure of a new pyoverdine containing a previously unseen amino acid demonstrates the potential of RP-HPLC for identification and stereochemical analysis of unusual amino acids found in small oligopeptide structures. Such approaches could be extended, for example, to other bacterial and fungal proteins. RP-HPLC of phenylthiocarbamyl derivatives of the amino acid constituents of pyoverdine hydrolysates may be used to identify and quantitate the peptide chain components, except where an N-hydroxylated form of ornithine requires confirmation by MS analysis of non-hydrolyzed material. Stereochemical configurations of the amino acids may be assigned with the chiral derivatizing agent, GITC, and RP-HPLC of the derivatized amino acids components on a Vydac 30-nm pore column. Reactivity with amino acid oxidases can be used to establish the configuration of unknown amino acids when preparations of pure enantiomers are lacking.

REFERENCES

- 1 M. Teintze and J. Leong, *Biochemistry*, 20 (1981) 6457.
- 2 S.B. Philson and M. Llinás, *J. Biol. Chem.*, 257 (1982) 8086.
- 3 P. Demange, S. Wendenbaum, A. Bateman, A. Dell and M.A. Abdallah, in G. Winkelmann, D. van der Helm and J.B. Neilands (Editors), *Iron Transport in Microbes, Plants and Animals*, VCH, Weinheim, 1987, pp. 167–187.
- 4 G. Mohn, K. Taraz and H. Budzikiewicz, *Z. Naturforsch. B: Chem. Sci.*, 45 (1990) 1437.
- 5 M. Persmak, T. Frejd and B. Mattiasson, *Biochemistry*, 29 (1990) 7348.
- 6 P. Demange, A. Bateman, C. Mertz, A. Dell, Y. Piémont and M.A. Abdallah, *Biochemistry*, 29 (1990) 11041.
- 7 P. Demange, M.A. Abdallah and H. Frank, *J. Chromatogr.*, 438 (1988) 291.
- 8 J.R. Moody and E.S. Beary, *Talanta*, 29 (1982) 1003.
- 9 S.A. Cohen, M. Meyes and T.L. Tarvin, *The Pico-Tag Method, a Manual of Advanced Techniques for Amino Acid Analysis*, Waters Publications, Milford, MA, 1989.

- 10 W.P. Reed, *NIST Certificate—Standard Reference Material 869*, Standard Reference Material Program, National Institute of Standards and Technology, Gaithersburg, MD, 1990.
- 11 D.K. Hancock, B. Coxon, E. White V, S.Y. Wang, D.J. Reeder, and J.M. Bellama, in preparation.
- 12 N. Nimura, A Toyama and T. Kinoshita, *J. Chromatogr.*, 316 (1984) 547.
- 13 L.C. Sander and S.A. Wise, *LC·GC*, 8 (1990) 378.
- 14 S.M. Hecht, K.M. Rupprecht and P.M. Jacobs, *J. Am. Chem. Soc.*, 101 (1979) 3982.
- 15 D.H. Spackman, W.H. Stein and S. Moore, *Anal. Chem.*, 30 (1958) 1190.
- 16 K. Nagayama, A. Kumar, K. Wüthrich and R.R. Ernst, *J. Magn. Reson.*, 40 (1980) 321.
- 17 G.A.J.M. van der Hofstad, J.D. Marugg, G.M.G.M. Verjans and P.J. Weisbeck, *NATO ASI Ser., Ser A.*, 117 (1986) 71–75.
- 18 T. Emery and J.B. Neilands, *J. Am. Chem. Soc.* 83 (1961) 1626.
- 19 K. Poppe, K. Taraz and H. Budzikiewicz, *Tetrahedron*, 42 (1987) 2261.
- 20 G. Koyama, H. Nakamura, Y. Muraoka, T. Takita, K. Maeda and H. Umezawa, *J. Antibiotics*, 26 (1973) 109.
- 21 R.L. Heinrikson and S.C. Meredith, *Anal. Biochem.*, 136 (1984) 65.
- 22 L.C. Sander and S.A. Wise, *J. High Resolut. Chromatogr. Chromatogr. Commun.*, 11 (1988) 383.
- 23 T. Kinoshita, Y. Kasahara and N. Nimura, *J. Chromatogr.*, 210 (1981) 77.
- 24 T. Nambara, in W.S. Hancock (Editor), *CRC Handbook of HPLC for the Separation of Amino Acids, Peptides, and Proteins*, Vol. 1, CRC Press, Boca Raton, FL, 1984, pp. 383–389.
- 25 J.P. Greenstein and M. Winitz, *Chemistry of the Amino Acids*, Vols. I, II and III, Wiley, New York, 1961.
- 26 C.C. Worthington (Editor), *Worthington Enzyme Manual*, Worthington Biochemical Corp., Freehold, NJ, 1988.
- 27 D.S. Page and R.L. Van Etten, *Biochim. Biophys. Acta*, 191 (1969) 38.

Characterisation of the photochemotherapeutic agent disulphonated aluminium phthalocyanine and its high-performance liquid chromatographic separated components

S.M. Bishop*, B.J. Khoo, A.J. MacRobert, M.S.C. Simpson and D. Phillips

Department of Chemistry, Imperial College, Kensington, London SW7 2AY (UK)

A. Beeby

Department of Chemistry, Durham University, South Road, Durham DH1 3LE (UK)

(First received January 25th, 1993; revised manuscript received June 7th, 1993)

ABSTRACT

Disulphonated aluminium phthalocyanine (AlPc₂), a potential clinical photosensitiser, has been synthesised in a reproducible form and shown by reversed-phase HPLC to consist of at least eight components which are believed to be individual AlPc₂ regioisomers. These components have been isolated either as single bands or mixtures of two using preparative reversed-phase HPLC methods. The number and position of sulphonate groups per phthalocyanine macromolecule for each component has been determined using a chemical degradation and HPLC assay. Results suggest that the bulk AlPc₂ material consists mostly (> 60%) of an amphiphilic α -, α -disubstituted regioisomer, with both sulphonate groups substituted to the same side of the molecule (adjacent form). Possible structures for some of the other separated components of AlPc₂ are also presented.

INTRODUCTION

Photodynamic therapy (PDT) is a treatment for neoplastic disease that involves the selective destruction of tumours using light-activated sensitiser compounds (photosensitisers) that preferentially accumulate in target tissue areas [1–3]. Phthalocyanines (Pc) are one of the second generation photosensitisers that show significant therapeutic advantages over the presently used hematoporphyrin-based compounds owing to superior light absorption at longer wavelengths and lower skin photosensitivity [4–6]. Much interest has centred around the use of water-

soluble sulphonated metallophthalocyanines (Fig. 1), MPcS_n (where M = Al, Zn, Ga and n = 1, 2, 3 or 4). The disulphonated compound AlPcS₂ has shown particularly promising results in biological studies [7–9] and is under investigation as a potential clinical candidate.

Chromatographic analysis of symmetric sulphonated metallophthalocyanines, such as GaPcS₂ and AlPcS₂, shows them to consist of many components [8–11]. These have proven difficult to isolate and identify by HPLC and other analytical techniques. Recently a method for the analysis of asymmetric sulphophthalocyanines using a diode array HPLC detector has been reported that identifies components of synthetic fractions based on their spectral properties [12].

* Corresponding author.

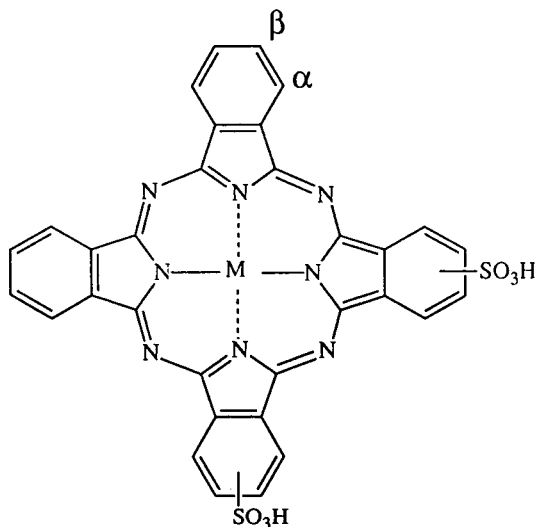


Fig. 1. The structure of disulphonated metallophthalocyanine ($MPCs_2$) showing the two possible positions (α and β) of substitution per Pc ring.

A mixture of differently sulphonated aluminium phthalocyanines ($AlPcS_{1-4}$) can be synthesised either by direct sulphonation of aluminium phthalocyanine chloride ($AlPcCl$) with oleum or by the condensation of phthalic and sulphophthalic acids with aluminium chloride [10]. $AlPcS_2$ is then obtained from $AlPcS_{1-4}$ using preparative reversed-phase medium-pressure liquid chromatography (MPLC). Material prepared in this way is composed of several components as demonstrated by reversed-phase HPLC. It is believed that these components are all disulphonated but differ in the location of sulphonate substitution around the phthalocyanine ring. The $AlPcS_2$ fraction obtained from the oleum reaction and MPLC process has been shown to be highly reproducible [10] and for this reason this material has been synthesised in bulk for evaluation as a clinical photosensitiser. A knowledge of the properties of the individual components of this $AlPcS_2$ fraction is essential in order to fully characterise it for future studies. Due to the low volatility and tendency to aggregate in solution of these compounds usual methods of structural analysis (NMR and mass spectroscopy) are inconclusive. This paper describes the separation and isolation of these components from the $AlPcS_2$ fraction using preparative reversed-phase

HPLC methods, their subsequent reversed-phase HPLC analysis and characterisation of each using a chemical degradation and HPLC assay technique.

EXPERIMENTAL

Aluminium disulphonated phthalocyanine

Disulphonated aluminium phthalocyanine was prepared in our laboratory via the sulphonation of $AlPcCl$ with oleum and preparative-scale MPLC (elution with water–methanol, 30:70), as described elsewhere [10]. An analytical HPLC trace of this material is shown in Fig. 2 with the major component peaks labelled a–h.

Preparative and analytical HPLC

The chromatograph used for both analytical and preparative operations was a Gilson Auto-prep System consisting of a Model 305 and two Model 306 piston pumps, an 806 manometric module, an 811B dynamic mixer with 1.5-ml mixing chamber, a Rheodyne 7125 injection valve fitted with a 20- μ l loop, an Applied Biosystems 759A absorbance detector and a Gilson Model 201 fraction collector. The apparatus incorporated a Rheodyne 7030 switching valve allowing both analytical and preparative columns to be connected to the system. Automatic control of the system and collection and analysis of data was facilitated through a Gilson 506B system interface using a Gilson 712 software package on an Elonex 286M computer.

Analytical separations were achieved on a

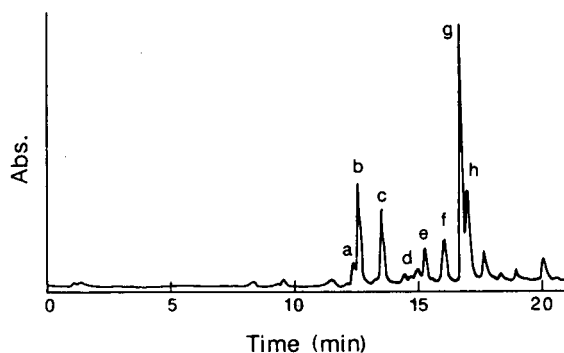


Fig. 2. Chromatogram of bulk $AlPcS_2$ material composed of components a–h which are probably different regioisomers.

Nova Pak Radial-Pak C₁₈ 6 μ m 100 \times 8 mm Waters radial compression column contained within an RCM 8 \times 10 cartridge holder with a guard column of the same packing material. In a typical analysis a 20- μ l sample of analyte (of concentration *ca.* 30–1000 μ g/ml) in water was injected onto the column and eluted with a linear gradient of 100% 20 mM phosphate buffer (pH 7.0) changing to 80% methanol over 20 min, running at a flow-rate of 2 ml/min. The eluted phthalocyanine components were detected by their absorption at 360 nm.

Preparative separations of the AlPcS₂ components were carried out on a Prep Nova Pak HR Prep Pak 6 μ m 100 \times 25 mm Waters radial compression column with a Guard Pak insert, both contained within a RCM 25 \times 10 cartridge holder and using a mobile phase of 20 mM ammonium acetate (pH 6.4) and methanol at a flow-rate of 10 ml/min. Gradient elution methods developed to separate the components are described in the Results and discussion section.

In a typical preparative run 100–300 μ l of a 5 mg/ml solution of AlPcS₂ was injected onto the column using one of the Model 306 pumps. Milligram quantities of each individual eluted component were collected by running the apparatus over many cycles. Samples were evaporated to dryness at 120°C and re-dissolved in water at a concentration of *ca.* 50 μ g/ml prior to assay using the analytical method described above.

Chemical degradation and HPLC assay

This method is a modification of a procedure described elsewhere [11] and is used to determine both the average number of sulphonate groups per phthalocyanine molecule and ratio of α : β sulphonate substitution, from the HPLC peak ratios of the three degradation products 3- and 4-sulphophthalimide and phthalimide. A similar method used for the trace analysis of insoluble phthalocyanine pigments has recently also been described [13]. Briefly, a small quantity of phthalocyanine material was dissolved in a minimal quantity of concentrated nitric acid (Fisons, analytical-reagent grade) and heated to 50°C until the characteristic phthalocyanine green colour disappeared (1–3 min). The re-

sulting solution was then neutralised with 1 M sodium hydroxide (BDH, AristaR grade) and analysed by HPLC. The HPLC method was adapted to allow for more sensitive detection using typically <100 μ g analyte. Separation of the degradation products was achieved using a Spherisorb S5ODS2 25 cm \times 4.6 mm column and a binary mobile phase of 0.1% trifluoroacetic acid in water and methanol running an elution programme of 0% methanol for 10 min followed by a linear gradient to 70% methanol by 35 min at a flow-rate of 1 ml/min. The eluent was monitored at 220 nm. Elution times of degraded components were: 3-sulphophthalimide, 7 min; 4-sulphophthalimide, 11 min; phthalimide, 29 min, as determined from the standard compounds 3- and 4-sulphophthalimide (prepared as described in ref. 14) and phthalimide (Aldrich). Ratios of sulphonated to unsulphonated and 3-sulpho to 4-sulpho substitution were calculated from the peak areas of 3-sulphophthalimide + 4-sulphophthalimide:phthalimide and 3-sulphophthalimide:4-sulphophthalimide respectively.

UV-visible spectroscopy

UV-visible spectra of the AlPcS₂ fraction and its separated components were obtained over the range 300–800 nm using a Perkin-Elmer Lambda 2 spectrophotometer. Concentrations of the methanolic and aqueous solutions was *ca.* 1 μ M.

RESULTS AND DISCUSSION

The chromatogram of the bulk AlPcS₂ fraction is shown in Fig. 2 and is seen to consist of at least eight components (labelled a–h) with one of the more lipophilic components, g, comprising over 60% of the material (by peak area). The profile of this chromatogram was seen to be unchanged over a range of injected AlPcS₂ concentrations indicating it unlikely that any of the peaks are due to dimers or higher aggregates. Two reversed-phase preparative methods were developed to isolate these components: (a) Components a, b, c and d ; 100% 20 mM ammonium acetate (pH 6.4), then linear gradient to 40% methanol over 8 min which was then held isocratically for a further 20 min.

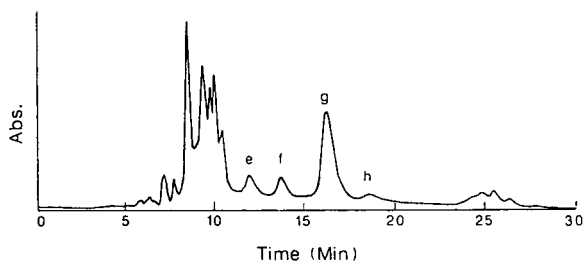


Fig. 3. Example chromatogram from the preparative reversed-phase HPLC method (conditions described in the text) used to isolate components e, f, g and g/h from the bulk AlPcS₂ material.

Elution times: a = 13.8 min, b = 14.3 min, c = 16.2 min and d = 19.8 min. (b) Components e, f, g and h; 100% 20 mM ammonium acetate (pH 6.4) then linear gradient to 52% methanol over 6 min which was then held isocratically for a further 22 min. A typical chromatogram from this method is shown in Fig. 3. Elution times: e = 12.0 min, f = 13.8 min, g = 16.2 min and h = 18.6 min.

Single-peak components were obtained with >90% purity (by peak area) but components a and b were inseparable (Fig. 4A) on a prepara-

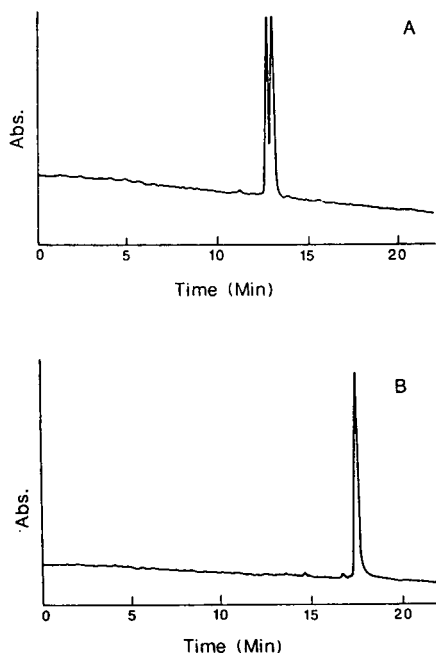


Fig. 4. Chromatograms of the isolated components a/b (A) and g (B). HPLC conditions and retention times of other components are described in the text.

tive scale and isolation of h from g was not possible. These were therefore isolated as mixed fractions a/b and g/h, respectively. A typical analytical HPLC chromatogram for a single-peak component is shown in Fig. 4B. Retention times for each component are a = 12.5 min, b = 12.9 min, c = 13.6 min, d = 14.4 min, e = 15.4 min, f = 16.1 min, g = 16.9 min, h = 17.1 min. A 3-mg loading of AlPcS₂ per run for the preparative chromatography was found to give the optimum recovery of each component. Increased loading caused peak broadening in the chromatography resulting in poor separation. Solubility of these component fractions was found to be lower in water compared to that of the bulk AlPcS₂ starting material. The UV-visible spectra of these species showed the formation of typical phthalocyanine aggregates and dimers ($\lambda_{\max} = 640$ nm [15]). This increased aggregation following HPLC is probably due to reductions in electrostatic repulsions between phthalocyanine molecules caused by either a change of the axial ligands of aluminium phthalocyanine from OH/H₂O to acetate, or a change in the salt form of the sulphonated substituents from SO₃Na to SO₃H induced by the acidic nature of the eluent. The UV-visible spectra of all components in methanol, except component fractions a/b and f which still showed the some aggregate, were typical of monomeric metallated phthalocyanine species ($\lambda_{\max} = 670$ nm [15]).

The results from the chemical degradation and HPLC assay of the bulk AlPcS₂ fraction and some of the individual components are shown in Table I. Figure 5 shows a typical chromatogram from a degraded sulphonated phthalocyanine sample. Each component was assayed at least twice, the error in the results obtained being $\pm 15\%$. Both the bulk AlPcS₂ fraction and its major component g show evidence of being disulphonated species with the sulphonate groups predominantly substituted on the α positions of the phthalocyanine ring. Components a/b, d and f are also consistent with disulphonated species, though component c had a sulphonated:unsulphonated ratio indicating some monosulphonate character. In general, as lipophilicity of the component fractions increased (*i.e.* as retention time increased) then the sul-

TABLE I

RATIOS DETERMINED FROM THE PEAK AREAS OF THE CHEMICALLY DEGRADED PRODUCTS OF AlPcS₂ AND ISOLATED COMPONENTS SHOWING DEGREE OF SULPHONATION (A RATIO OF 1:1 UNSULPHONATED: SULPHONATED INDICATES A DISULPHONATED PHTHALOCYANINE) AND POSITION OF SULPHONATE SUBSTITUTION, ON ORIGINAL PHTHALOCYANINE RING (FROM RATIO OF 3-SULPHOPHTHALIMIDE:4-SULPHOPHTHALIMIDE)

Component	a/b	c	d	f	g	AlPcS ₂
Sulphonated:unsulphonated	1:1.1	1:1.7	1:1.1	1:1.2	1:0.9	1:0.8
3-Sulphophthalimide:4-sulphophthalimide	1.75:1	1.6:1	2.1:1	9.0:1	7.4:1	6.4:1

phonate substitution changed from α/β to almost pure α .

There are sixteen possible regioisomers of AlPcS₂ (Fig. 6 shows three of the possibilities) of which five are β -, β -disubstituted, five are α -, α -disubstituted and six are α -, β -disubstituted. Further, of all sixteen possibilities there are ten isomers with sulphonate groups on the same side (adjacent form) and six with groups on opposite sides of the ring (opposite form). Previous chromatographic studies with GaPcS₂ [16] and AlPcS₂ [8,9] by other workers have shown them to also be composed of a number of components. These studies have postulated single isomer structures for these components based on their amphiphilic properties and *in vitro* photobiological efficacy. The more lipophilic components are suggested to be the adjacent form isomers. Using the same reasoning it would also be expected that isomers with α -sulphonate substitution would show increased lipophilicity over

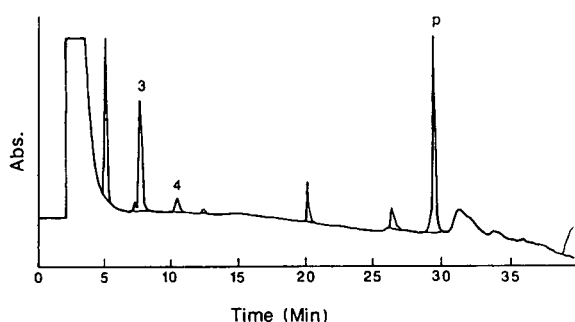


Fig. 5. The separation of the degradation products 3-sulphophthalimide (3), 4-sulphophthalimide (4) and phthalimide (p) from the AlPcS₂ component g. Table I shows the peak area ratios determined for unsulphonated:sulphonated and 3:4 sulphonate substitution.

those with β -substitution. Based on this previous work and upon the lipophilicity (elution time) and degradation assay presented here, structures for the isolated components of AlPcS₂ can be proposed. The major component g is therefore probably an adjacent α -, α -disubstituted regioisomer (e.g. Fig. 6A) and similarly, the components corresponding to f, d and a/b, for example, are consistent with opposite α -, α -, adjacent α -, β - and opposite α -, β -disubstituted species, respectively.

The bulk AlPcS₂ fraction used in these studies has previously been shown to be a very effective photosensitiser *in vitro* and *in vivo* [7,17]. This is most probably related to the amphiphilic nature of its major components which would be expected to have excellent cell penetrating prop-

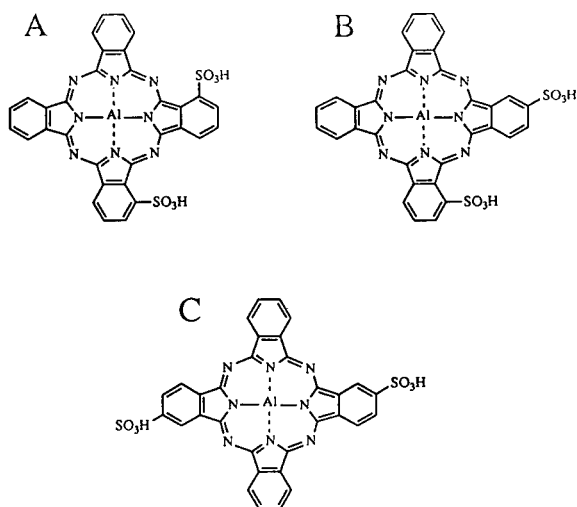


Fig. 6. Examples of possible AlPcS₂ isomeric structures for the isolated components: (A) adjacent α -, α -, (B) adjacent α -, β - and (C) opposite β -, β -.

erties. It is possible that a photosensitiser comprising of only this major component would be more efficacious and photobiological studies are underway using isolated component g. However, recent work [18] has suggested that a mixture of sulphonated metallophthalocyanine compounds varying in lipophilicity may have advantages *in vivo* by targeting different areas of the tumour (*i.e.* more lipophilic taken up by cells and more hydrophilic residing in the vascular stroma) and potentially increasing tumour kill. Clearly if this is the case then the role played by the different fractions may now be studied and compared to the mixture. The bulk AlPcS₂ material described in this paper may demonstrate such an effect and this is also under investigation.

CONCLUSIONS

An AlPcS₂ mixture synthesised via the oleum method for potential clinical use has been separated into seven component fractions by preparative HPLC. The direct sulphonation of aluminium phthalocyanine chloride with oleum results in the production of phthalocyanine species with predominantly α -substituted groups. The analysis of these component fractions using a chemical degradation and HPLC assay has suggested that this clinical AlPcS₂ material consists of different regioisomers that vary in lipophilicity, though it most resembles the major lipophilic component. Isomeric structures for these component fractions have been proposed based on their lipophilicity and degree and position of sulphonate substitution. Further work to assess the *in vitro* and *in vivo* phototoxicity and uptake of these individual component fractions compared to the clinical AlPcS₂ material is underway.

ACKNOWLEDGEMENTS

We would like to thank the Science and Engineering Research Council (SERC), the Im-

perial Cancer Research Fund, the Nuffield Foundation and the Waldberg Trust for their financial support for this work. We are also indebted to Mrs. Ann Crane of the Department of Chemistry at Leicester University, UK for reproduction of the chromatograms.

REFERENCES

- 1 T.J. Dougherty, *Photochem. Photobiol.*, 45 (1987) 879.
- 2 A.J. MacRobert, S.G. Bown and D. Phillips, *Photosensitising Compounds: their Chemistry, Biology and Clinical Use (Ciba Foundation Symposium, Vol. 146)*, Wiley, Chichester, 1989, p. 4.
- 3 J. Moan and K. Berg, *Photochem. Photobiol.*, 55 (1992) 931.
- 4 J.D. Spikes, *Photochem. Photobiol.*, 43 (1986) 691.
- 5 I. Rosenthal, *Photochem. Photobiol.*, 53 (1991) 859.
- 6 W.S. Chan, J.F. Marshall, R. Svenson, D. Phillips and I.R. Hart, *Photochem. Photobiol.*, 45 (1987) 757.
- 7 W.S. Chan, C.M.L. West, J.V. Moore and I.R. Hart, *Br. J. Cancer*, 64 (1991) 827.
- 8 B. Paquette, H. Ali, R. Langlois and J.E. van Lier, *Photochem. Photobiol.*, 47 (1988) 215.
- 9 K. Berg, J.C. Bommer and J. Moan, *Cancer Lett. (Shannon, Irel.)*, 44 (1989) 7.
- 10 M. Ambroz, A. Beeby, A.J. MacRobert, M.S.C. Simpson, R.K. Svenson and D. Phillips, *J. Photochem. Photobiol. B: Biol.*, 9 (1991) 87.
- 11 H. Ali, R. Langlois, R. Wagner, N. Brasseur, B. Paquette and J.E. van Lier, *Photochem. Photobiol.*, 47 (1988) 713.
- 12 P. Margaron, S. Gaspard and J.E. van Lier, *J. Chromatogr.*, 634 (1993) 57.
- 13 C. Fischer, *J. Chromatogr.*, 592 (1992) 261.
- 14 J. Horyna, M. Holub and K. Mach, *Czech. Pat.*, CS244 748(Cl.C07D209/48), Aug. 14, 1987, *Appl.* 85/2305, March 29, 1985.
- 15 J.R. Darwent, I. McCubbin and D. Phillips, *J. Chem. Soc., Faraday Trans. 2*, 78 (1982) 347.
- 16 N. Brasseur, H. Ali, R. Langlois and J.E. van Lier, *Photochem. Photobiol.*, 46 (1987) 739.
- 17 W.S. Chan, J.F. Marshall, R. Svenson, J. Bedwell and I.R. Hart, *Cancer Res.*, 50 (1990) 4533.
- 18 Q. Peng, J. Moan, J.M. Nesland and C. Rimington, *Int. J. Cancer*, 46 (1990) 719.

Hydrogen bonding

XXVIII. Comparison of the solvation theories of Abraham and Poole, using a new acidic gas–liquid chromatography stationary phase

Michael H. Abraham* and Jenik Andonian-Haftvan

Department of Chemistry, University College London, 20 Gordon Street, London WC1H 0AJ (UK)

Ian Hamerton

Department of Chemistry, University of Surrey, Guildford, Surrey GU2 5XH (UK)

Colin F. Poole and Theophilus O. Kollie

Department of Chemistry, Wayne State University, Detroit, MI 48202 (USA)

(First received February 2nd, 1993; revised manuscript received May 21st, 1993)

ABSTRACT

The solvation theories of Abraham and of Poole have been applied to gas–liquid partition coefficients, $\log K$, for 62 varied solutes on bis(3-allyl-4-hydroxyphenyl)sulphone, with all K values corrected for interfacial adsorption. Application of the general solvation equation of Abraham, $\log K = c + rR_2 + s\pi_2^H + a\alpha_2^H + b\beta_2^H + l \log L^{16}$, to $\log K$ values at 121 and 176°C shows that the new phase has considerable hydrogen-bond acidity.

The solvation equation of Poole, $\Delta G_s^{\text{SOLN}}(X) = \Delta G_s^{\text{CAV+DISP}}(X) + \Delta G_s^{\text{INT}}(X)$, was also applied to $\log K$ values at 121°C. It was shown that the terms $(rR_2 + s\pi_2^H + a\alpha_2^H + b\beta_2^H)$ and $-\Delta G_s^{\text{INT}}(X)/RT$ agreed to within 0.12 log unit for the total interaction effect for 23 varied solutes. Likewise, the combined cavity plus dispersion terms $(c + l \log L^{16})$ and $-\Delta G_s^{\text{CAV+DISP}}(X)/RT$ agreed to within 0.11 log unit for the same 23 solutes.

It is concluded that the solvation theories of Abraham and of Poole are entirely compatible and, indeed, yield essentially the same qualitative and quantitative results.

INTRODUCTION

Two of the most widely used solvation models in gas–liquid chromatography (GLC) are those of Abraham and co-workers and of Poole and co-workers. Since these have been described in detail [1,2] we give only a summary of these

models. Both are derived from a cavity model of solvation [3–5], in which the process of solvation of a gaseous solute is broken down into three stages: (1) A cavity of suitable size to accommodate the solute must be created in the solvent; work is required in order to disrupt solvent–solvent interactions and hence this process is endoergic. (2) Solvent molecules round the cavity are reorganised; the Gibbs energy change for

* Corresponding author.

this process is generally assumed to be negligible [4], but we note that this is not the case in terms of enthalpy or entropy. (3) The solute is introduced into the cavity, and various solute–solvent interactions are set up, all of which are exoergic. The dissolution of a gaseous solute into a solvent or GLC stationary phase, as measured by K (or L), the gas–liquid partition coefficient (eqn. 1), will therefore depend on the balance between the endoergic stage (1) opposing solution and the exoergic stage (3) that aids solution. In both the Abraham and the Poole models, the system for analysis consists of a set of retention data, preferably as $\log K$ values, for a series of solutes on a given stationary phase. Hence the solvent properties remain constant, and a major task is to define suitable solute properties or descriptors, through which some understanding of the solvation process can be obtained.

$$K \text{ (or } L) = \frac{\text{concentration of solute in solution}}{\text{concentration of solute in the gas phase}} \quad (1)$$

Abraham and co-workers [5–10] attempted to find descriptors that would reflect the ability of a solute to take part in the various solute–solvent interactions that could be set up in stage (3) above. The general solvation equation of Abraham contains the solute descriptors R_2 (an excess molar refraction [6] that reflects some general dispersion interactions), π_2^H (a dipolarity/polarisability parameter [7]), and α_2^H and β_2^H (the solute hydrogen-bond acidity and hydrogen-bond basicity respectively [7,8]). It should be noted that α_2^H and β_2^H are the effective or summation acidity and basicity ($\Sigma \alpha_2^H$ and $\Sigma \beta_2^H$) appropriate for the situation in which a solute is surrounded by an excess of solvent molecules [10]. The final solute descriptor is $\log L^{16}$, where L^{16} is the gas–liquid partition coefficient on hexadecane at 25°C [9], and includes the important cavity term plus a general dispersion interaction term. All these descriptors are included in eqn. 2, where the coefficients c , r , s , a , b and l are found by the method of multiple linear regression analysis and serve as constants that characterise the solvent or stationary phase under investigation.

$$\log K = c + rR_2 + s\pi_2^H + a\alpha_2^H + b\beta_2^H + l \log L^{16} \quad (2)$$

In the approach of Poole and co-workers [2,11] the standard Gibbs energy change for solvation of a solute X , in a solvent s ,

$$\Delta G_s^{\text{SOLN}}(X) = -RT \ln K(X) \quad (3)$$

is considered to be made up of a cavity term, a non-polar term and a polar term,

$$\Delta G_s^{\text{SOLN}}(X) = \Delta G_s^{\text{CAV}}(X) + \Delta G_s^{\text{NP}} + \Delta G_s^{\text{P}} \quad (4)$$

Once again, it is not possible to obtain the cavity term, $\Delta G_s^{\text{CAV}}(X)$ separately, and so Poole et al. [2] deconvoluted $\Delta G_s^{\text{SOLN}}(X)$ into an experimentally more accessible form,

$$\Delta G_s^{\text{SOLN}}(X) = \Delta G_s^{\text{SOLN}}(\text{HC})^V + \Delta G_{\text{SQ}}^{\text{P}}(X) + \Delta G_s^{\text{INT}}(X) \quad (5)$$

where $\Delta G_s^{\text{SOLN}}(\text{HC})^V$ is the Gibbs energy change for solvation of a hydrocarbon, of the same Van der Waals volume as X , into solvent s , and $\Delta G_{\text{SQ}}^{\text{P}}(X)$ is the polar contribution to solvation of solute X in squalane. The latter is experimentally obtained through

$$\Delta G_{\text{SQ}}^{\text{P}}(X) = \Delta G_{\text{SQ}}^{\text{SOLN}}(X) - \Delta G_{\text{SQ}}^{\text{SOLN}}(\text{HC})^V \quad (6)$$

and so only the term $\Delta G_s^{\text{INT}}(X)$ in eqn. 5 is unknown, and hence can be obtained by difference [11]. In eqn. 5, the sum of $\Delta G_s^{\text{SOLN}}(\text{HC})^V$ and $\Delta G_{\text{SQ}}^{\text{P}}(X)$ represents the cavity term plus a general dispersion interaction term and so can be represented as

$$\Delta G_s^{\text{SOLN}}(X) = \Delta G_s^{\text{CAV+DISP}}(X) + \Delta G_s^{\text{INT}}(X) \quad (7)$$

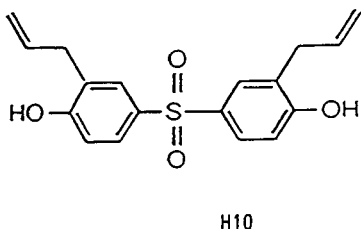
A simple rearrangement of the general solvation equation, eqn. 2, shows clearly the connection between eqns. 2 and 7,

$$\log K = (c + l \log L^{16}) + (rR_2 + s\pi_2^H + a\alpha_2^H + b\beta_2^H) \quad (8)$$

The cavity plus dispersion term of eqn. 7 is equivalent to the constant plus the $l \log L^{16}$ term of eqn. 2, and the interaction term of eqn. 7 is equivalent to the sum of all the individual interaction terms in eqn. 2.

Kollie *et al.* [1] used the carefully obtained $\log K$ values of Kollie and Poole [11,12] to test these supposed equivalences. They showed that for 30 various solutes on 25 stationary phases there was excellent agreement between $(c + l \log L^{16})$ [13] and $\log K$ (CAV + DISP), the latter being used instead of the Gibbs energy term in eqn. 7. For the same sets of solutes and phases, there was again excellent agreement between the two interaction terms $(rR_2 + s\pi_2^H + a\alpha_2^H)$ [13] and $\log K$ (INT). In this analysis of Poole and Abraham, the interaction term of eqn. 8 was reduced to the term $(rR_2 + s\pi_2^H + a\alpha_2^H)$ because none of phases studied was a significant hydrogen-bond acid: hence the solute hydrogen-bond basicity was unnecessary.

It seemed important to compare the two equations of Abraham and Poole for the more general case when all the interaction terms in eqn. 8 are significant. Although all the commercially available GLC stationary phases are either non-acidic or only poorly acidic, Abraham *et al.* [14] showed in a preliminary survey that bis(3-allyl-4-hydroxyphenyl)sulphone, which we denote as H10, had significant hydrogen-bond acidity at 175°C, *i.e.* some 30°C above its melting point. We have therefore prepared a further quantity of H10 in order to investigate its chromatographic properties more thoroughly, and in order to compare the methods of Abraham and Poole with a stationary phase that has considerable hydrogen-bond acidity.



EXPERIMENTAL

The stationary phase H10 was prepared exactly as described before [14]. Its density was determined using a micro Lapkin bicapillary pycnometer over the range 145–180°C, and the density values fitted to the equation

$$\rho(\text{H10}) = 1.3602 - 0.001119 T (\text{°C}) \quad (9)$$

Column packings containing from 8 to 20% (w/w) of H10 on Chromosorb W AW (60–80 mesh, 0.18–0.25 mm) were prepared using the rotary evaporator technique. The damp packing was dried in a fluidized bed drier and packed into 2.0 m × 2 mm glass columns with the aid of suction and gentle vibration. Columns were conditioned at the temperature used in the investigation until a stable baseline and invariant retention times and symmetrical peaks for a test mixture of compounds was obtained. Accurate phase loadings were determined by Soxhlet extraction for 72 h of an aliquot of the used packing with the same solvent selected for coating. For column evaluation a 3700 gas chromatograph (Varian Instruments, Palo Alto, CA, USA) with heated on-column injectors and a flame ionization detector was used. Column temperatures were measured with a NIST-certified (National Institute of Standards, USA) mercury thermometer to $\pm 0.2^\circ\text{C}$ and averaged over the column cavity. The column pressure drop was measured with a mercury manometer to ± 1 mmHg (1 mm Hg = 133.322 Pa). The carrier gas was helium, adjusted to a known flow-rate of about 20 ml/min using a thermostated soap-film bubble meter. Samples of 1–10 μl of headspace vapours were injected onto the column by a gas-tight syringe. Several injections at different amounts were made to ensure that the conditions for infinite dilution/zero surface coverage were met.

The gas-liquid partition coefficients were calculated [15–17] by linear extrapolation to infinite phase volume of plots of the net retention volume per gram of column packing/volume of liquid phase against the reciprocal of the volume of liquid phase. A minimum of four column packings was used to span the phase loading of 8–20% (w/w) in reasonably equal increments. This procedure was carried out in order to correct the observed net retention volumes for any contribution due to interfacial adsorption.

Retention data were obtained at 176.2°C and at 121.2°C, where H10 at the latter temperature exists as a supercooled liquid. The corrected gas → liquid partition coefficients are listed in Table I together with corresponding standard deviations (S.D.).

TABLE I
VALUES OF *K* AND log *K* ON PHASE H 10 AT 176°C AND 121°C

Solute	<i>K</i> (176)	S.D.	log <i>K</i> (176)	<i>K</i> (121)	S.D.	log <i>K</i> (121)
Dodecane	13.68	0.87	1.136	52.88	0.44	1.723
Tridecane	24.95	3.70	1.397	97.35	0.66	1.988
Tetradecane	34.54	7.00	1.538	176.28	1.43	2.246
Pentadecane	55.83	4.70	1.747	291.06	3.05	2.464
Hexadecane	82.65	10.90	1.917	506.82	1.07	2.705
cis-Hydrindane	24.92	1.60	1.397	45.44	0.95	1.657
Oct-2-yne				34.37	0.96	1.536
Dodec-1-yne	34.16	4.60	1.534	259.96	0.96	2.415
1,1,2,2-Tetrachloroethane	46.47	3.62	1.667	223.91	1.03	2.350
Di-n-hexylether	93.58	1.06	1.971	709.76	0.97	2.851
1,2-Diethoxyethane	212.00	41.60	2.326	6526.14	0.98	3.815
1,4-Dioxane	54.54	0.19	1.737	228.22	0.95	2.358
Nonanal	145.58	0.21	2.163	866.23	0.96	2.938
Pentan-2-one	39.04	1.25	1.592	167.33	0.95	2.224
Hexan-2-one	52.22	3.61	1.718	196.46	0.98	2.293
Heptan-2-one	84.56	2.58	1.927	476.98	0.97	2.679
Octan-2-one	123.01	6.93	2.090	716.68	0.99	2.855
Nonan-2-one				1231.95	2.25	3.091
Methyl heptanoate	71.39	5.23	1.854	462.65	0.98	2.665
Methyl octanoate	109.17	8.66	2.038	679.00	1.00	2.832
Methyl nonanoate	160.28	9.70	2.205	1152.93	1.03	3.062
Methyl decanoate	224.25	17.60	2.351	2208.02	1.01	3.344
Methyl undecanoate	323.11	27.85	2.509	3273.47	1.11	3.515
1-Nitropropane	42.85	2.49	1.632	215.21	0.96	2.333
1-Nitropentane	92.04	1.87	1.964	572.69	0.95	2.758
1-Nitrohexane	143.40	0.74	2.157	924.91	0.98	2.966
Nitrocyclohexane				1575.14	1.01	3.197
Dimethylformamide	1032.00	24.60	3.014	3739.66	0.97	3.573
Dimethylacetamide	2601.00	13.50	3.415			
Butan-1-ol	38.34	3.25	1.584	199.85	0.96	2.301
Pentan-1-ol	73.55	1.16	1.867	352.21	0.97	2.547
Hexan-1-ol	111.07	0.29	2.046	617.07	0.96	2.790
2-Methylpentan-2-ol	39.61	1.07	1.598	199.85	0.96	2.301
Heptan-1-ol	164.75	1.83	2.217	1077.74	1.07	3.033
Octan-1-ol	237.51	0.97	2.376	1488.48	0.96	3.173
Nonan-1-ol	346.87	4.73	2.540	1806.63	0.96	3.257
Dimethylsulphoxide	6009.60	16.80	3.779			
Benzene	7.96	0.10	0.901	27.81	0.96	1.444
Toluene	15.36	0.38	1.186	45.15	0.96	1.655
Ethylbenzene	24.54	0.86	1.390	79.72	0.95	1.902
Butyl benzene	41.23	4.30	1.615	137.86	0.97	2.139
Chlorobenzene	33.81	1.92	1.529	95.38	0.95	1.979
<i>o</i> -Dichlorobenzene	109.13	1.55	2.038	251.97	0.23	2.401
Bromobenzene	67.93	0.64	1.832	159.78	0.95	2.204
Iodobenzene	131.86	0.12	2.120	373.89	0.95	2.573
Anisole	64.89	3.06	1.812	253.01	0.96	2.403
Benzaldehyde	260.14	1.21	2.415	1012.55	0.98	3.005
Acetophenone	531.76	0.29	2.726	2410.16	1.03	3.382
Benzonitrile	312.03	0.75	2.494	1207.82	0.97	3.082
2,6-Dimethylaniline	549.20	2.61	2.740	3483.72	1.21	3.542

TABLE I (Continued)

Solute	$K(176)$	S.D.	$\log K(176)$	$K(121)$	S.D.	$\log K(121)$
N-Methylaniline	304.34	0.53	2.483	1997.25	1.01	3.300
N,N-Dimethylaniline	191.29	1.65	2.282	1119.13	1.00	3.049
Nitrobenzene	395.38	0.93	2.597	1713.06	0.97	3.234
Phenol	289.30	0.68	2.461	1756.01	0.98	3.245
<i>m</i> -Cresol	426.70	1.51	2.630			
<i>p</i> -Cresol	429.90	0.01	2.633	2783.37	1.04	3.445
2,5-Dimethylphenol				4634.74	0.97	3.666
2,6-Dimethylphenol				2913.68	0.97	3.464
3,5-Dimethylphenol				4908.81	1.05	3.691
4-Chlorophenol	945.80	2.19	2.976	7802.55	1.02	3.892
1,4-Benzodioxane				2225.62	0.96	3.347
Pyridine	181.68	15.80	2.259	352.66	0.94	2.547

RESULTS AND DISCUSSION

The useful liquid range for the stationary phase H10 is 150–220°C, but it can also be used in the supercooled state from 150°C down to around 100°C. There is some loss in efficiency at these lower temperatures due to the high viscosity of the material, but it is very useful to obtain retention data at 121°C in order to compare present results with those previously obtained at 121.4°C [11,12]. We found that contributions from interfacial adsorption were considerable, especially at 121°C rather than 176°C, and especially with alkanes as solutes. Some examples of the contribution of gas–liquid partition and interfacial adsorption to the obtained specific retention volumes, V_G , are given in Table II. The large contribution of interfacial adsorption in the case of alkanes on the polar phase H10 reinforces the previous warning of Poole and co-workers [18,19] of the deficiencies of the McReynolds system, which relies on retention data for alkanes. On the other hand, the approach of Poole is not tied to alkane data on polar phases at all, and in the method of Ab-

raham, data on alkanes are not essential—all that is required for the application of eqn. 2 is a set of retention data for any wide range of solutes.

Characterisation of H10 by the method of Abraham is straightforward. The necessary solute descriptors [6–10,13] are in Table III, and application of the general solvation equation, eqn. 2 yields an excellent equation for $\log K$ at 121.2°C. In eqn. 10 and elsewhere, n is the number of solutes, r is the overall correlation coefficient, S.D. is the regression standard deviation, and F is the Fisher F -statistic. The standard deviation of each coefficient is given below the coefficient. There are no outliers in eqn. 10, and for the one solute missing, that is 1,2-diethoxyethane, we lack the required descriptors. Eqn. 10 confirms that H10 is, indeed, a reasonably strong hydrogen-bond acid, with a b constant of 1.457 units at 121°C. It is also quite dipolar, with the s constant at 1.323 units near that for OV-225 or Carbowax 20M [13], and quite basic with the a constant at 1.266 units larger [13] than that for OV-225 (0.964) and nearly as large as that for tetrabutylammonium picrate (1.424).

$$\log K (121.2^\circ\text{C}) = -0.568 - 0.051R_2 + 1.323\pi_2^H + 1.266\alpha_2^H + 1.457\beta_2^H + 0.418 \log L^{16}$$

$$0.060 \quad 0.044 \quad 0.052 \quad 0.052 \quad 0.070 \quad 0.010$$

$$n = 58, r = 0.9940, \text{S.D.} = 0.069, F = 856$$

(10)

TABLE II

EXAMPLES OF CONTRIBUTIONS FROM GAS-LIQUID PARTITION AND INTERFACIAL ADSORPTION TO V_G VALUES FOR SOLUTES ON H10 AT 121°C

V_G values in $\text{cm}^3 \text{g}^{-1}$. Phase loading 8.9% (w/w) H10.

Solute	V_G (exp)	V_G (partition)	V_G (adsorption)	% (adsorption) ^a
<i>n</i> -Dodecane	64.59	29.91	34.68	53.7
<i>n</i> -Tridecane	112.01	55.06	56.95	50.8
<i>n</i> -Tetradecane	194.72	99.71	95.01	48.8
<i>n</i> -Pentadecane	330.46	164.63	165.83	50.2
<i>n</i> -Hexadecane	567.17	286.67	280.50	49.5
<i>cis</i> -Hydrindane	27.79	25.70	2.09	7.5
Oct-2-yne	27.25	19.44	7.81	28.7
Heptan-2-one	312.59	269.79	42.80	13.7
Methyl nonanoate	828.23	652.13	176.10	21.3
1-Nitropentane	333.49	323.93	9.56	2.9
N,N-Dimethylformamide	2159.34	2115.25	44.09	2.0
Heptan-1-ol	746.64	609.60	137.04	18.4
Toluene	31.66	25.54	6.12	19.3
Anisole	161.55	143.11	18.44	11.4
Bromobenzene	94.49	90.37	4.12	4.4
Acetophenone	1528.49	1363.25	165.24	10.8
Phenol	1059.18	993.24	65.94	6.2
4-Chlorophenol	4585.81	4413.33	172.48	3.8

^a This is the % contribution of adsorption to V_G (exp) with a phase loading of 8.9%. The V_G (partition) values used to obtain the log K values, are those extrapolated as described in the text to zero contribution from adsorption.

TABLE III

DESCRIPTORS USED IN EQN. 2

Solute	R_2	π_2^H	α_2^H	β_2^H	log L^{16}
Dodecane	0.000	0.00	0.00	0.00	5.696
Tridecane	0.000	0.00	0.00	0.00	6.200
Tetradecane	0.000	0.00	0.00	0.00	6.705
Pentadecane	0.000	0.00	0.00	0.00	7.209
Hexadecane	0.000	0.00	0.00	0.00	7.714
<i>cis</i> -Hydrindane	0.439	0.25	0.00	0.00	4.635
Oct-2-yne	0.225	0.30	0.00	0.10	3.850
Dodec-1-yne	0.133	0.23	0.13	0.10	5.657
1,1,2,2-Tetrachloroethane	0.595	0.76	0.16	0.12	3.803
Di- <i>n</i> -hexylether	0.000	0.25	0.00	0.45	5.938
1,2-Diethoxyethane	0.008		0.00		
1,4-Dioxane	0.329	0.75	0.00	0.64	2.892
Nonanal	0.150	0.65	0.00	0.45	4.856
Pentan-2-one	0.143	0.68	0.00	0.51	2.755
Hexan-2-one	0.136	0.68	0.00	0.51	3.262
Heptan-2-one	0.123	0.68	0.00	0.51	3.760
Octan-2-one	0.108	0.68	0.00	0.51	4.257

TABLE III (Continued)

Solute	R_2	π_2^H	α_2^H	β_2^H	$\log L^{16}$
Nonan-2-one	0.119	0.68	0.00	0.51	4.735
Methyl heptanoate	0.079	0.60	0.00	0.45	4.356
Methyl octanoate	0.065	0.60	0.00	0.45	4.838
Methyl nonanoate	0.056	0.60	0.00	0.45	5.321
Methyl decanoate	0.053	0.60	0.00	0.45	5.803
Methyl undecanoate	0.050	0.60	0.00	0.45	6.285
1-Nitropropane	0.242	0.95	0.00	0.31	2.894
1-Nitropentane	0.212	0.95	0.00	0.29	3.938
1-Nitrohexane	0.203	0.95	0.00	0.29	4.416
Nitrocyclohexane	0.441	0.97	0.00	0.31	4.826
N,N-Dimethylformamide	0.367	1.31	0.00	0.74	3.173
N,N-Dimethylacetamide	0.363	1.33	0.00	0.78	3.717
Butan-1-ol	0.224	0.42	0.37	0.48	2.601
Pentan-1-ol	0.219	0.42	0.37	0.48	3.106
Hexan-1-ol	0.210	0.42	0.37	0.48	3.610
2-Methylpentan-2-ol	0.169	0.30	0.31	0.60	3.081
Heptan-1-ol	0.211	0.42	0.37	0.48	4.115
Octan-1-ol	0.199	0.42	0.37	0.48	4.619
Nonan-1-ol	0.193	0.42	0.37	0.48	5.124
Dimethylsulphoxide	0.522	1.74	0.00	0.89	3.459
Benzene	0.610	0.52	0.00	0.14	2.786
Toluene	0.601	0.52	0.00	0.14	3.325
Ethylbenzene	0.613	0.51	0.00	0.15	3.778
n-Butylbenzene	0.600	0.51	0.00	0.15	4.730
Chlorobenzene	0.718	0.65	0.00	0.07	3.657
o-Dichlorobenzene	0.872	0.78	0.00	0.04	4.518
Bromobenzene	0.882	0.73	0.00	0.09	4.041
Iodobenzene	1.188	0.82	0.00	0.12	4.502
Anisole	0.708	0.75	0.00	0.29	3.890
Benzaldehyde	0.820	1.00	0.00	0.39	4.008
Acetophenone	0.818	1.01	0.00	0.48	4.501
Benzonitrile	0.742	1.11	0.00	0.33	4.039
2,6-Dimethylaniline	0.972	0.89	0.20	0.46	5.028
N-Methylaniline	0.948	0.90	0.17	0.45	4.478
N,N-Dimethylaniline	0.957	0.84	0.00	0.41	4.701
Nitrobenzene	0.871	1.11	0.00	0.28	4.557
Phenol	0.805	0.89	0.60	0.30	3.766
m-Cresol	0.822	0.88	0.57	0.34	4.310
p-Cresol	0.820	0.87	0.57	0.31	4.312
2,5-Dimethylphenol	0.840	0.79	0.54	0.37	4.774
2,6-Dimethylphenol	0.860	0.79	0.39	0.39	4.680
3,5-Dimethylphenol	0.820	0.84	0.57	0.36	4.856
4-Chlorophenol	0.915	1.08	0.67	0.20	4.775
1,4-Benzodioxan	0.874	1.07	0.00	0.35	4.971
Pyridine	0.631	0.84	0.00	0.52	3.022

The corresponding equation for $\log K$ (176.2°C) is disappointing, with a correlation

$$\log K(176.2^\circ\text{C}) = -0.749 + 0.165R_2 + 1.160\pi_2^H + 0.808\alpha_2^H + 1.290\beta_2^H + 0.332\log L^{16}$$

$$\begin{array}{cccccc} 0.123 & 0.088 & 0.096 & 0.105 & 0.139 & 0.020 \end{array}$$

$$n = 54, r = 0.9738, \text{S.D.} = 0.134, F = 176$$

(11)

coefficient lower than usual, and a standard deviation higher than usual, in this type of work. The rather poor equation can hardly be due to poorly-determined descriptors, because eqn. 10 is quite reasonable. Neither are there any obvious outliers—dimethylacetamide (but not dimethylformamide) is out by just over two standard deviations, but removal of this solute has little effect, with F increasing from 176.2 to only 178.5. However, the trend in the main constants, s , a , b and l is as expected. All of these are lower at 176.2°C than at 121.2°C.

It is of considerable interest to compare the acidic phase H10 with a phase recently studied at 80°C by Li *et al.* [20] 4-dodecyl- α,α -bis(trifluoromethyl)benzyl alcohol, which we denote as BOH. Li *et al.* [20] did not actually characterise BOH, because their intention was to use this phase to obtain solute hydrogen-bond basicities. However, we have [6–10] all the necessary descriptors for 143 out of 146 solutes studied by Li *et al.* [20] leading to the regression equation (eqn. 12), where K' is a relative partition coefficient.

Although eqn. 12 is very poor, it does show that BOH has zero hydrogen-bond basicity, but is a very strong hydrogen-bond acid. Even though eqn. 12 refers to 80°C, rather than to 121°C as does eqn. 11, it is likely that BOH is a considerably stronger hydrogen-bond acidic phase than is H10. Unfortunately, the poor quality of eqn. 12 precludes the use of BOH, at 80°C, to determine further values of β_2^H since the projected error in any back-calculated β_2^H value is too large (estimated as S.D./ $b = 0.099$).

We thought it useful also to characterise the corresponding ether of Li *et al.* [20], BOMe, and

if carboxylic acids and n -hexylamine are excluded we obtain eqn. 13. As found by Li *et al.* [20] using either 59 or 87 solutes, BOMe is slightly polar, non-basic, but is a weak hydrogen-bond acid, again at 80°C.

The method of Poole starts with the total standard Gibbs energy of solvation, $\Delta G^{\text{SOLN}}(\text{X})$, which at 121.2°C can be transformed into a $\log K(\text{T})$ term through the factor $\Delta G^{\text{SOLN}} = -1.804 \log K(\text{T})$, where the parenthesised T denotes the total solvation energy term. The $\Delta G^{\text{INT}}(\text{X})$ term and the $\Delta G^{\text{CAV+DISP}}(\text{X})$ term can similarly be transformed into a $\log K(\text{INT})$ and a $\log K(\text{C} + \text{D})$ term, and are given in Table IV for the set of test solutes used previously by Kollie and Poole [11,12]. Depending on the solute, either the interaction term or the (cavity plus dispersion) term can be the larger. However, the latter composite term will include a rather large cavity term that would result in positive values of ΔG_s^O , and hence in negative values of $\log K(\text{C} + \text{D})$, together with a dispersion term that favours solution and would lead to positive $\log K(\text{C} + \text{D})$ values. Clearly the dispersion term always outweighs the cavity effect, and probably is the most important single solute-solvent interaction. The $\log K(\text{INT})$ values for the alcohols are amongst the largest interaction terms, and show clearly the effect of the acidic and basic stationary phase on these amphoteric compounds.

The analysis of Abraham can be used to breakdown the total interaction term ($rR_2 + s\pi_2^H + a\alpha_2^H + b\beta_2^H$) into component parts, as shown also in Table IV. The dipolar and polarisable aromatic compounds such as benzonitrile and nitrobenzene give rise to large $s\pi_2^H$ terms, the phenols (as expected) show the largest $a\alpha_2^H$

$$\log K'(\text{BOH}) = -1.598 - 0.223R_2 + 0.447\pi_2^H + 2.686\beta_2^H + 0.678 \log L^{16}$$

0.095	0.121	0.119	0.125	0.026
-------	-------	-------	-------	-------

$$n = 143, r = 0.9598, \text{S.D.} = 0.265, F = 402.9 \quad (12)$$

$$\log K'(\text{BOMe}) = -1.440 + 0.411\pi_2^H + 0.166\beta_2^H + 0.691 \log L^{16}$$

0.018	0.016	0.024	0.005
-------	-------	-------	-------

$$n = 140, r = 0.9977, \text{S.D.} = 0.053, F = 9761.6 \quad (13)$$

TABLE IV
BREAKDOWN OF SOLUTE-SOLVENT EFFECTS ACCORDING TO THE METHODS OF ABRAHAM AND POOLE

Solute	Poole ^a		Abraham ^b					$\log K(\text{INT})$	$\log K(\text{C} + \text{D})$	$\log K(\text{T})$	c	rR_2	$\sigma\pi_2^H$	$\alpha\alpha_2^H$	$b\beta_2^H$	$f \log L^{16}$	INT ^c	(C + D) ^c	T ^d
	$\log K(\text{INT})$	$\log K(\text{C} + \text{D})$																	
cis-Hydrindane	0.275	1.382	-0.57	-0.02	0.33	0.00	0.00	1.94	0.33	1.35	1.68								
Oct-2-yne	0.626	0.910	-0.57	-0.01	0.40	0.00	0.15	1.61	0.54	1.03	1.57								
Dodec-1-yne	0.688	1.727	-0.57	-0.01	0.30	0.16	0.15	2.36	0.61	1.79	2.40								
1,1,2,2-Tetrachloroethane	1.278	1.072	-0.57	-0.03	1.01	0.20	0.17	1.59	1.38	0.99	2.37								
Di-n-hexylether	0.998	1.854	-0.57	0.00	0.33	0.00	0.66	2.48	0.99	1.91	2.90								
1,4-Dioxane	1.888	0.471	-0.57	-0.02	0.99	0.00	0.93	1.21	1.92	0.62	2.55								
Nonanal	1.537	1.401	-0.57	-0.01	0.86	0.00	0.66	2.03	1.52	1.45	2.97								
Octan-2-one	1.722	1.134	-0.57	-0.01	0.90	0.00	0.74	1.78	1.64	1.21	2.85								
1-Nitropropane	1.849	0.484	-0.57	-0.01	1.26	0.00	0.45	1.21	1.71	0.63	2.34								
1-Nitropentane	1.764	0.994	-0.57	-0.01	1.26	0.00	0.42	1.65	1.68	1.07	2.75								
Butan-1-ol	2.072	0.229	-0.57	-0.01	0.56	0.47	0.70	1.09	1.72	0.51	2.23								
2-Methylpentan-2-ol	1.823	0.478	-0.57	-0.01	0.40	0.39	0.87	1.29	1.66	0.71	2.37								
Octan-1-ol	1.870	1.303	-0.57	-0.01	0.56	0.47	0.70	1.93	1.72	1.35	3.08								
Benzene	0.954	0.490	-0.57	-0.03	0.69	0.00	0.20	1.16	0.89	0.57	1.46								
n-Butylbenzene	0.688	1.452	-0.57	-0.03	0.67	0.00	0.22	1.98	0.89	1.38	2.27								
Anisole	1.304	1.100	-0.57	-0.04	0.99	0.00	0.42	1.63	1.41	1.02	2.44								
Benzonitrile	1.918	1.164	-0.57	-0.04	1.47	0.00	0.48	1.69	1.95	1.08	3.03								
2,6-Dimethylamine	1.828	1.714	-0.57	-0.05	1.18	0.25	0.67	2.10	2.10	1.48	3.58								
N-Methylamine	1.843	1.458	-0.57	-0.05	1.19	0.22	0.66	1.87	2.06	1.26	3.32								
N,N-Dimethylaniline	1.496	1.553	-0.57	-0.05	1.11	0.00	0.60	1.97	1.71	1.35	3.06								
Nitrobenzene	1.741	1.493	-0.57	-0.04	1.47	0.00	0.41	1.90	1.88	1.29	3.17								
Phenol			-0.57	-0.04	1.18	0.76	0.44	1.57	2.37	0.97	3.34								
4-Chlorophenol	1.654	1.694	-0.57	-0.05	1.43	0.85	0.29	2.00	2.57	1.38	3.95								
1,4-Benzodioxan	1.913	0.635	-0.57	-0.04	1.42	0.00	0.51	2.08	1.93	1.47	3.39								
Pyridine			-0.57	-0.03	1.11	0.00	0.76	1.26	1.87	0.66	2.53								

^a According to eqn. 7, with $\log K$ instead of Gibbs energy.

^b According to eqn. 2.

^c Terms summed as shown in eqn. 8.

^d Total of the previous two columns.

terms, and compounds such as dioxane and the nitrogen bases give large $b\beta_2^H$ terms. In all cases however, the composite $l \log L^{16}$ term is larger than any given interaction term; since, again, the $l \log L^{16}$ term includes a general dispersion interaction favouring solution, and a cavity effect opposing solution, it may be deduced that the general dispersion interaction must be by far the largest individual interaction.

If the total interaction term ($rR_2 + s\pi_2^H + a\alpha_2^H + b\beta_2^H$) is summed and denoted INT, and the dispersion plus cavity effects ($c + l \log L^{16}$)^a are summed and denoted as (C + D), then it is possible to make a straight comparison between the results of Poole's analysis and those of the analysis of Abraham. In Table IV, the entries under $\log K(\text{INT})$ can be compared directly with those under the heading INT. There is very good agreement between the two sets of data, the average difference being only 0.12 log unit. Similarly, the average difference between the Poole term, $\log K(\text{C} + \text{D})$, and the Abraham term (C + D) is only 0.11 log units.

The approaches of Poole and Abraham are rather different. In the Poole system, the term $\Delta G_s^{\text{CAV} + \text{DISP}}$, corresponding to $\log K(\text{C} + \text{D})$ in Table IV, is obtained using retention data on squalane, and the ΔG_s^{INT} term, corresponding to $\log K(\text{INT})$ in Table IV, is obtained by difference through eqn. 7. In the Abraham system, a breakdown of observed $\log K$ values into various interactions is obtained through multiple linear regression analysis, using eqn. 2 and solute descriptors as outlined in the Introduction. However, when the various terms in eqn. 2 are summed so as to correspond to Poole's INT and (CAV + DISP) terms, there is excellent agreement between the two sets of data for 23 varied solutes on a phase, bis(3-allyl-4-hydroxyphenyl)-sulphone, that can interact through a number of

effects including two types of hydrogen-bonding (solute acid–solvent base, and solute base–solvent acid). Taken together with our previous results using 25 non-acidic stationary phases [1], our overall conclusion is that the solvation models of Abraham and Poole are entirely compatible, and when applied to experimental retention data, as outlined in this work, yield essentially the same qualitative and quantitative results.

REFERENCES

- 1 T.O. Kollie, C.F. Poole, M.H. Abraham and G.S. Whiting, *Anal. Chim. Acta*, 259 (1992) 1.
- 2 C.F. Poole, T.O. Kollie and S.K. Poole, *Chromatographia*, 34 (1992) 281.
- 3 R.A. Pierotti, *Chem. Revs.*, 76 (1976) 717.
- 4 M.H. Abraham and J. Liszi, *J. Chem. Soc., Faraday Trans. 1*, 74 (1978) 1604.
- 5 M.H. Abraham, P.L. Grellier, I. Hamerton, R.A. McGill, D.V. Prior and G.S. Whiting, *Faraday Disc. Chem. Soc.*, 85 (1988) 107.
- 6 M.H. Abraham, G.S. Whiting, R.M. Doherty and W.J. Shuely, *J. Chem. Soc., Perkin Trans. 2*, (1990) 1451.
- 7 M.H. Abraham, G.S. Whiting, R.M. Doherty and W.J. Shuely, *J. Chromatogr.*, 587 (1991) 213.
- 8 M.H. Abraham and G.S. Whiting, *J. Chromatogr.*, 594 (1992) 229.
- 9 M.H. Abraham, P.L. Grellier and R.A. McGill, *J. Chem. Soc., Perkin Trans. 2*, (1987) 797.
- 10 M.H. Abraham, *Chem. Soc. Rev.*, 22 (1993) 73.
- 11 T.O. Kollie and C.F. Poole, *J. Chromatogr.*, 556 (1991) 457.
- 12 T.O. Kollie and C.F. Poole, *J. Chromatogr.*, 550 (1991) 213.
- 13 M.H. Abraham, G.S. Whiting, R.M. Doherty and W.J. Shuely, *J. Chromatogr.*, 587 (1991) 229.
- 14 M.H. Abraham, I. Hamerton, J.B. Rose and J.W. Grate, *J. Chem. Soc., Perkin Trans. 2*, (1991) 1417.
- 15 B.R. Kersten, S.K. Poole and C.F. Poole, *J. Chromatogr.*, 468 (1989) 235.
- 16 S.K. Poole and C.F. Poole, *J. Chromatogr.*, 500 (1990) 329.
- 17 C.F. Poole, K.G. Furton, R.M. Pomaville, S.K. Poole and B.R. Kersten, *Molten Salt Techniques*, 4 (1990) 41.
- 18 B.R. Kersten, C.F. Poole and K.G. Furton, *J. Chromatogr.*, 411 (1987) 43.
- 19 S.K. Poole, B.R. Kersten and C.F. Poole, *J. Chromatogr.*, 471 (1989) 91.
- 20 J. Li, Y. Zhang, H. Ouyang and P.W. Carr, *J. Am. Chem. Soc.*, 114 (1992) 9813.

^a We include the constant c , in order to be able to compare these effects with the $\log K(\text{C} + \text{D})$ term of Poole. Note that in the Poole summation, there is no constant term at all.

Evaluation of the polarity of packed and capillary columns by different classification methods

G. Castello*, G. D'Amato and S. Vezzani

Istituto di Chimica Industriale, Corso Europa 30, 16132 Genova (Italy)

(Received April 15th, 1993)

ABSTRACT

The behaviour of packed gas chromatographic columns filled with 30 different stationary phases was compared by using various polarity indicators: the difference in apparent carbon number of linear alkanes and alcohols with the same retention time, ΔC , the sum of the first five McReynolds constants, Σ_{MR}^5 , Snyder's selectivity parameters, the Kováts coefficient, K_c , and the retention polarity, RP . The correlation between these different systems for polarity evaluation is discussed. The polarity of some wide- and narrow-bore capillary columns, filled with non-polar, polar and modified carbon layer phases, was also evaluated as a function of temperature, in the range 60–120°C for Σ_{MR}^5 and selectivity parameters and in the range 60–190°C for ΔC .

INTRODUCTION

In previous papers [1,2], a method for the classification of the polarity order of gas chromatographic columns, based on the difference in apparent carbon number of linear alkanes and alcohols with the same retention time, ΔC , was introduced and compared with other polarity indicators, such as the McReynolds constants [3] and Snyder's selectivity parameters [4–6].

Twenty-three liquid stationary phases, six Porapak types and polar and non-polar wide-bore bonded-phase capillary column were tested, and the effect of the series connection of different capillary columns on the overall polarity was investigated.

In order to evaluate the correspondence between the polarity values obtained by ΔC measurement with those given by other methods for the classification of polarity, experiments were carried out by using packed columns filled with the liquid phases tested previously [2] and with

other columns. The polarity values obtained with the ΔC , the McReynolds constants [3,7], Snyder's triangle [4–6], the Kováts coefficient, K_c [8,9], and the retention polarity, RP [10], values were compared.

EXPERIMENTAL

The characterization of the packed columns was carried out by injecting samples of *n*-alkanes (C_4 – C_{12}) and *n*-alkanols (C_2 – C_8), of the first five McReynolds probes (benzene, *n*-butanol, 2-pentanone, nitropropane and pyridine) and, for the determination of Snyder's constants, dioxane. The columns were prepared with a concentration of 20% of liquid phase on Chromosorb W (80–100 mesh) in order to permit a comparison with previously published values [2,7] and to reduce the interfacial and adsorption effects on the solid support. Phase loadings of 10% were also tested, with no significant influence on the results.

In Table I, the liquid phases used in the experiments are denoted "e" and those for which V_g values at 120°C previously published by

* Corresponding author.

McReynolds [7] were used in order to evaluate the applicability of the classification method to literature data are denoted "m".

Some of the columns whose ΔC values were previously calculated by using literature data [2] were tested experimentally and the results agreed fairly well. The best fitting between experimental and literature data was obtained by using liquid phases of definite chemical composition (e.g., esters), whereas columns prepared with silicone polymers or with hydrocarbon mixtures (e.g., Apiezon) showed an appreciable fluctuation of ΔC and the other polarity indicators (up to $\pm 2\%$), owing to the different distributions of molecular masses in the various commercially available products.

Varian (Palo Alto, CA, USA) Model 3700 and 1220 gas chromatographs equipped with thermal conductivity detectors were used. The analyses were performed at 100, 120 and 140°C on columns of various diameters, lengths and tubing material. Helium was used as the carrier gas at a flow-rate of 30 cm³ min⁻¹.

The capillary columns used were narrow-bore Supelcowax-10 and SPB-1 bonded phases (30 m × 0.32 mm I.D.), film thickness 0.25 μm, and a Carbowax B carbon layer open-tubular (CLOT) column, modified with polyethylene glycol liquid phase (Supelco, Bellefonte, PA, USA), a narrow-bore DB-1 (30 m × 0.32 mm I.D.), 0.25 μm film thickness (J & W Scientific, Folsom, CA, USA), and wide-bore Supelcowax-10 and SPB-1 (60 m × 0.75 mm I.D.) (Supelco).

The wide-bore glass columns were installed in a Varian Model 3700 and the fused-silica narrow-bore columns in a Varian Model 3600 gas chromatograph. Both instruments were equipped with flame ionization detectors; nitrogen and helium were used as the carrier gases. The same standard substances as used for characterization of the packed columns, obviously in less concentrated solutions, were injected in splitless (wide-bore columns) and split (narrow-bore columns) modes. The carbon number range of *n*-alkanes and *n*-alkanols was increased to C₂₂ and C₁₃, respectively.

The various polarity indicators were calculated from experimental V_g and t'_R values as follows. The difference in apparent carbon number be-

tween linear alkanes and alkanols with the same retention, ΔC , was determined both graphically, by measuring the horizontal distance between the two straight lines having the equation

$$\ln V_g = a + bZ \quad (1)$$

obtained by plotting $\ln V_g$ as a function of the number of carbon atoms, Z , for *n*-alkanes and *n*-alkanols, and mathematically, with the equation

$$\Delta C = (a_{OH} - a_P) / [(b_{OH} + b_P) / 2] = \Delta a / b^0 \quad (2)$$

where the subscripts OH and P refer to the coefficients of eqn. 1 for alkanols and alkanes, respectively, and b^0 is the average slope value [2]. The adjusted retention times, t'_R , can be used instead of V_g , mainly when the polarity of capillary columns is measured.

The overall McReynolds polarity, Σ_{MR}^5 , was obtained as the sum of the McReynolds' constants, ΔI , of the first five polarity probes listed above, *i.e.*, the difference between the retention index values of the probes on each liquid phase and those on squalane.

Snyder's selectivity parameters, x_b for *n*-butanol, x_n for nitropropane and x_d for dioxane, were calculated with the equation

$$x_i = \frac{\Delta I_i}{\Delta I_b + \Delta I_n + \Delta I_d} \quad (3)$$

and give a measure of the relative importance of hydrogen bonding (*n*-butanol having an active hydrogen atom, dioxane two electron-donor oxygen atoms) and of dipole interactions (nitropropane showing a large dipole moment of 3.7 D) [4–6].

For solute–solvent pairs whose polar interaction depends only on hydrogen bonding (e.g., alkanols with polyethylene glycols), the relative importance of the active hydrogen *vs.* donor oxygen atom was evaluated by normalization of the values of the selectivity parameters x_b for *n*-butanol and x_d for dioxane:

$$y_b = \frac{x_b}{x_b + x_d} = \frac{\Delta I_{\text{butanol}}}{\Delta I_{\text{butanol}} + \Delta I_{\text{dioxane}}} \quad (4)$$

The Kováts coefficient, K_c , was calculated as

$$K_c = -100a_p/b_p \quad (5)$$

where a_p and b_p are the two coefficients of the straight line representing eqn. 1 for the n -alkanes [8,9].

The retention polarity, RP , was calculated with the equation

$$RP = 20 \sum_{i=1}^5 (\Delta I/I_{sq})_i \quad (6)$$

where ΔI is the McReynolds constant and I_{sq} the retention index of the probe i on squalane, being the summation calculated with the values for the first five McReynolds probes [10].

RESULTS AND DISCUSSION

Table I gives the values obtained with the above-described methods. Some of the ΔC , Σ_{MR}^5 and selectivity parameters have been published previously [2] and are reported here to permit a direct comparison with the other polarity parameters. For some of the ester-type liquid phases, the new experimental values are reported instead of those calculated from literature data. The differences in ΔC values are about $\pm 1\%$ (change in the second decimal figure). Some of the liquid phases tested are nowadays of reduced interest, as they are often replaced with silicone polymers modified with a suitable number of polar groups.

TABLE I
VALUES OF ΔC AND OF OTHER POLARITY INDICATORS

No.	Liquid phase	ΔC	Σ_{MR}^5	x_b	x_n	x_d	K_c	RP	y_b	Source ^a
1	Squalane	1.48	0				157	0.00		e
2	Apiezon L	1.90	143	0.260	0.376	0.365	214	4.38	0.416	e
3	SE-52	2.43	334	0.304	0.413	0.283	212	10.42	0.518	e
4	SE-30	2.48	217	0.329	0.398	0.273	200	6.78	0.547	e
5	OV-101	2.51	229	0.335	0.394	0.270	202	7.18	0.554	e
6	DC-200	2.52	227	0.337	0.390	0.272	201	7.10	0.553	e
7	DC-550	2.90	660	0.279	0.420	0.300	238	19.26	0.482	e
8	Di-2-ethylhexyl sebacate	3.40	653	0.369	0.396	0.235	197	20.38	0.611	e
9	Dioctyl sebacate	3.42	651	0.370	0.396	0.233	201	20.38	0.614	e
10	Diisodecyl phthalate	3.43	767	0.332	0.418	0.249	247	23.92	0.571	e
11	Didecyl phthalate	3.45	1150	0.326	0.415	0.260	248	36.14	0.556	e
12	Dioctyl phthalate	3.50	835	0.331	0.420	0.249	246	25.92	0.571	e
13	Di-2-ethylhexyl adipate	3.59	709	0.364	0.396	0.239	204	22.20	0.604	e
14	QF-1	3.67	1500	0.239	0.474	0.287	230	46.54	0.454	e
15	Castorwax	4.16	1023	0.384	0.332	0.284	261	31.92	0.575	e
16	Hallcomid M-18	4.46	845	0.450	0.372	0.178	198	26.62	0.717	e
17	Pluronic L-81	4.90	1183	0.385	0.355	0.260	273	36.98	0.597	m
18	Tricresyl phosphate	5.00	1420	0.338	0.394	0.268	335	44.28	0.558	e
19	Neopentyl glycol adipate	5.62	1849	0.342	0.368	0.290	348	57.57	0.541	e
20	Pluronic P 85	5.75	1561	0.367	0.365	0.268	323	48.74	0.578	m
21	Pluronic P 65	5.90	1581	0.366	0.365	0.268	332	49.36	0.577	m
22	Neopentyl glycol succinate	6.14	2115	0.328	0.378	0.294	382	65.82	0.527	e
23	Pluronic F-68	6.55	1949	0.353	0.371	0.276	374	60.76	0.561	m
24	Carbowax 20M	6.93	2308	0.348	0.371	0.281	395	71.90	0.553	e
25	Pluronic F-88	6.97	1931	0.354	0.371	0.276	352	60.20	0.562	m
26	Carbowax 6000	7.28	2320	0.347	0.371	0.281	423	72.26	0.553	e
27	Ethylene glycol adipate	7.37	2689	0.326	0.367	0.306	492	83.66	0.516	e
28	Diethylene glycol adipate	7.69	2760	0.330	0.365	0.305	516	85.92	0.520	e
29	Carbowax 1000	7.85	2587	0.352	0.363	0.286	445	80.60	0.552	e
30	Diethylene glycol succinate	9.89	3430	0.323	0.367	0.310	649	106.64	0.510	e

^a e = experimental data; m = taken from ref. 7.

Notwithstanding this, as many of these phases were available in our laboratory, we tested them because they have a reproducible chemical composition and the polarity indicators are not influenced by the molecular mass distribution, number of specific groups bonded to the polydimethylsiloxane backbone, chain branching, etc. It is therefore possible to compare the experimental data with previously published values.

Fig. 1 shows that the values of ΔC establish a polarity order corresponding fairly well with that obtained with the Σ_{MR}^5 method, mainly when stationary phases whose interaction is due to hydrogen bonding are considered.

The greatest deviation is shown by solvents whose interaction depend on dipole moment, such as the fluorinated silicone QF-1. For this liquid phase, both the ΔI for nitropropane (462) and Snyder's x_n (0.474) are very high, as shown by the position near the right-hand side of the polarity triangle in Fig. 2. It was previously observed [6,11,12] that the use of 1-nitropropane as one of the probes may overestimate the contribution of the polarizability term, owing to its large dipole moment. This is confirmed by the excessive change in position on the selectivity triangle of some silicon liquid phases, indicated with numbers 3, 4, 5, 6 and 7 in Table I and in Figs. 2 and 3, which show similar behaviour in practice.

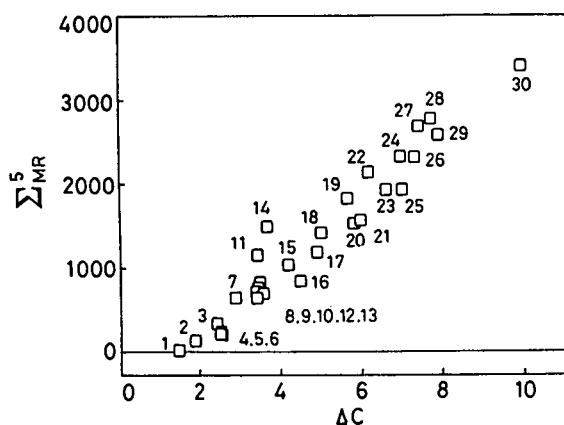


Fig. 1. Trend of the Σ_{MR}^5 values for liquid phases with respect to their ΔC values at 120°C. Numbers refer to the list in Table I.

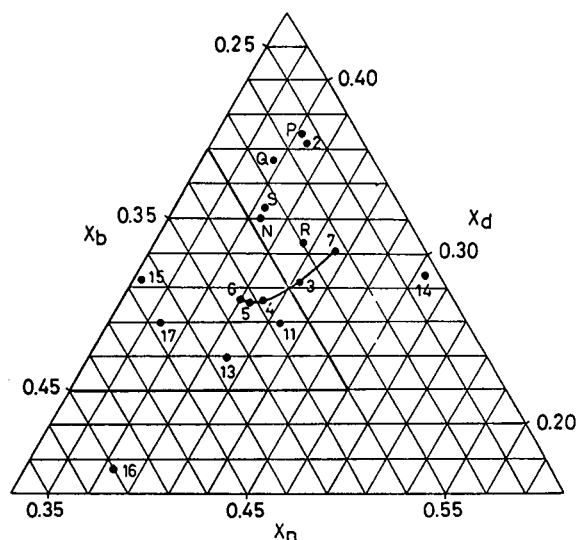


Fig. 2. Selectivity triangle where the values of x_b , x_n and x_d for the various columns at 120°C are shown. Numbers refer to Table I. The positions of Porapak porous polymers are also shown and indicated with identifying letters (from ref. 2). Methyl- and phenylsilicone phases are connected. An enlarged inner portion of the triangle is shown in Fig. 3.

An increasing influence of polarizability is expected on changing from methylsilicones (SE-30, OV-101, DC-200) to methylphenylsilicones (SE-52, DOW-550), but the shift towards in-

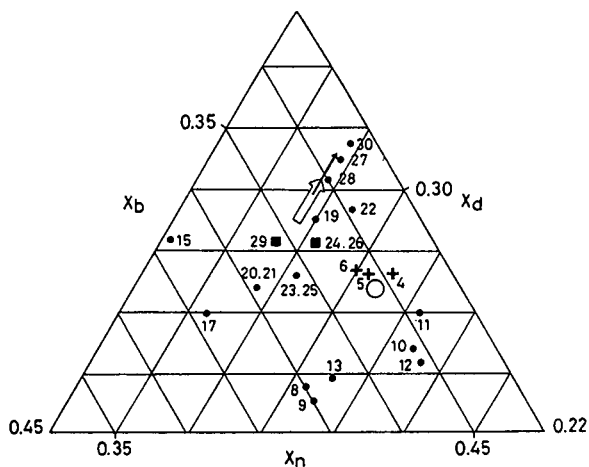


Fig. 3. Enlarged part of the selectivity triangle in Fig. 2. ■ = Carbowax columns; + = methylsilicone columns; ○ = position of capillary DB-1 and SPB-1 columns in the temperature range 60–120°C. The shift of the CLOT and Supelcowax-10 positions in the same range is indicated with arrows (white = Supelcowax-10; black = CLOT).

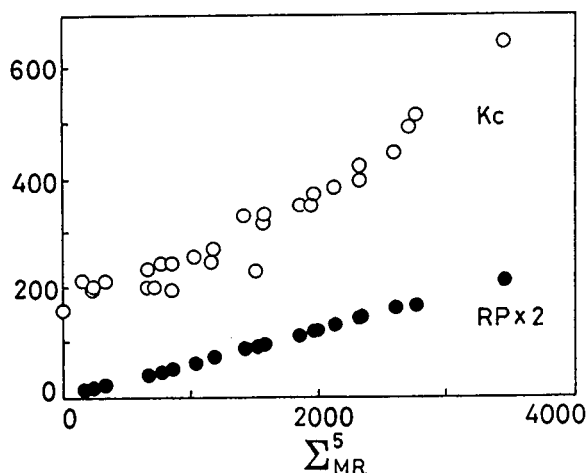


Fig. 4. K_c and RP values at 120°C (the latter multiplied by 2) as a function of Σ_{MR}^5 for the liquid phases listed in Table I.

creasing x_n values seems too large, while the position of all these liquid phases is low on all the other polarity scales: ΔC , Σ_{MR}^5 , RP and K_c .

The dependence of RP on Σ_{MR}^5 is perfectly linear, as these two polarity indicators have the same origin, *i.e.*, the ΔI of the same probes, whereas the plot of K_c as a function of Σ_{MR}^5 shows appreciable curvature (Fig. 4). If plotted as a function of ΔC , both RP and K_c show good linearity (Fig. 5).

The values of x_b and x_d are a measure of the interaction of 1-butanol and dioxane with the stationary phase: as the active hydrogen of the OH group interacts with the lone electron pairs

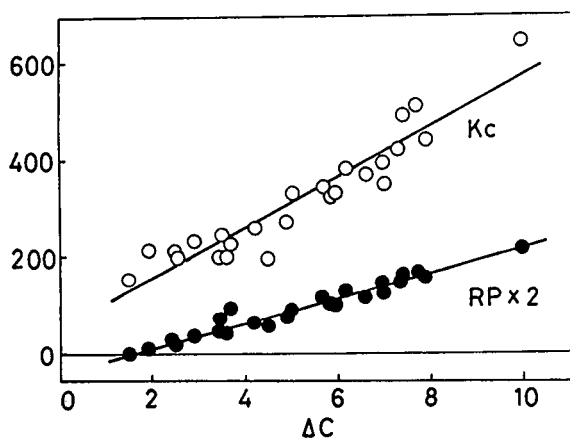


Fig. 5. Linear dependence of K_c and RP on the ΔC values at 120°C for the liquid phases listed in Table I.

of the liquid phase, while the $-O-$ bridges in the dioxane molecules react with active hydrogen atoms of the liquid phase, the values of $\Delta I_{n\text{-butanol}}$ and $\Delta I_{\text{dioxane}}$ are a measure of the relative influence of the two mechanisms. The parameter y_b , calculated with eqn. 4 and reported in Table I, summarizes this effect, and increases with increasing tendency of the liquid phase to behave as an electron donor (Class III following Ewell *et al.*'s classification [13]).

Capillary columns

Some of the polarity indicators listed above cannot be applied to capillary columns: K_c cannot be calculated as it depends on a knowledge of V_g values; other indicators (RP , Snyder's selectivity parameters, McReynolds constants) require a knowledge of the ΔI values with respect of squalane, which cannot be used at temperatures above 120°C. Another problem connected with the determination of these values is the choice of the polarity probes: the boiling points of the McReynolds and Snyder probes is low and therefore the retention times at column temperatures above 120°C are so short as to be subject to appreciable errors that impair the accuracy of the calculation of the polarity. The polarity indicators suitable up to 120°C are Σ_{MR}^5 and Snyder's selectivity parameters. ΔC can be used up to the maximum allowable temperature of the columns (in this instance 190°C); the ΔC values at 120°C measured on wide-bore columns (SPB-1 and Supelcowax-10; 0.75 mm I.D.) were 2.53 and 7.75, respectively, similar to the values in Table I for methylsilicones (SE-30, OV-101, DC-200) and polyethylene glycol liquid phases (Carbowax 6000 and 1000).

The narrow-bore columns were used to investigate the dependence of ΔC , Σ_{MR}^5 and selectivity parameters on the column temperature. ΔC could be measured without problems in the range 60–190°C, as it does not require any reference column, and the n -alkanes and n -alkanols used for the determination of the difference in apparent carbon number can be selected in order to give suitable and well measurable retention times at any temperature.

The determination of Σ_{MR}^5 , x_b , x_n and x_d values was only possible in the range 60–120°C,

owing to the very short and scattered t'_R values of the polarity probes at higher temperatures.

As no suitable bonded-phase squalane column with the same length, diameter and film thickness as for the columns used is available, the ΔI value may be experimentally measured by comparing the Supelcowax-10 and CLOT data with those obtained on the non-polar methylpolysiloxane column. This procedure, if used to compare highly polar columns, is correct enough as the ΔI values of methylsilicone columns are low with respect to those of, e.g., polyethylene glycols; average values on various SE-30, OV-101 and DC-200 columns are $\Delta I_{\text{benzene}} = 16$, $\Delta I_{\text{butanol}} = 55.7$, $\Delta I_{2\text{-pentanone}} = 44.6$, $\Delta I_{\text{nitropropane}} = 65.7$ and $\Delta I_{\text{pyridine}} = 42.3$.

The ΔI values for McReynolds probes on the two non-polar capillary columns tested were calculated with respect of the average I values obtained in the range 60–120°C on various packed squalane columns (stationary phase concentration between 5 and 20%). An accuracy of about $\pm 10\%$ of the absolute polarity values can therefore be expected but this is of relatively little significance because the aim of the determination was to establish the relative difference between DB-1 and SPB-1 and the effect of temperature.

The Σ_{MR}^5 values measured in this way cannot be used for the determination of the absolute

polarity of methylsilicone columns, whereas ΔC , being an absolute parameter, permits this determination.

Table II gives the values of ΔC and Σ_{MR}^5 on DB-1, SPB-1, CLOT and Supelcowax-10 columns. The difference in Σ_{MR}^5 between the two polydimethylsiloxane columns is of the same order of magnitude observed at 120°C on various packed silicone columns: SF-96 = 208, SE-30 = 217, OV-1 = 223, DC-200 = 227, OV-101 = 229.

The change with temperature of the same parameter in the range 60–120°C is about 2% for methylsilicones, 3% for polyethylene glycol and 11% for the CLOT column, which, the carbon substrate being covered with a layer of polyethylene glycol, show an intermediate behaviour between gas–solid and gas–liquid mechanisms, changing in polarity with increasing temperature [14,15].

The change with temperature of the Σ_{MR}^5 values for purely gas–liquid chromatographic columns is not justified by a true change in polarity, but depends on the choice of the polarity probes and on the dependence on temperature of their retention values with respect to the reference column and *n*-alkane series. This is confirmed by the constant value of ΔC over a very extended temperature range for polydimethylsiloxane and pure polyethylene glycol columns, whereas the change in the behaviour of

TABLE II

VALUES OF ΔC AND Σ_{MR}^5 AT VARIOUS TEMPERATURES ON NARROW-BORE CAPILLARY COLUMNS

Column temperature (°C)	DB-1		SPB-1		CLOT		Supelcowax-10	
	ΔC	Σ_{MR}^5	ΔC	Σ_{MR}^5	ΔC	Σ_{MR}^5	ΔC	Σ_{MR}^5
60	2.596	207	2.690	219	6.002	1595	7.505	2307
70	2.599	207	2.705	205	6.030	1624	7.518	2315
80	2.595	209	2.698	221	6.068	1685	7.520	2354
90	2.596	210	2.693	222	6.095	1707	7.511	2370
100	2.591	211	2.690	223	6.162	1735	7.515	2359
120	2.597	213	2.698	224	6.205	1778	7.531	2373
140			2.690		6.266		7.534	
150			2.704		6.302		7.532	
160			2.698		6.328		7.511	
170			2.715		6.379		7.501	
180			2.693		6.399		7.523	
190			2.711		6.445		7.522	

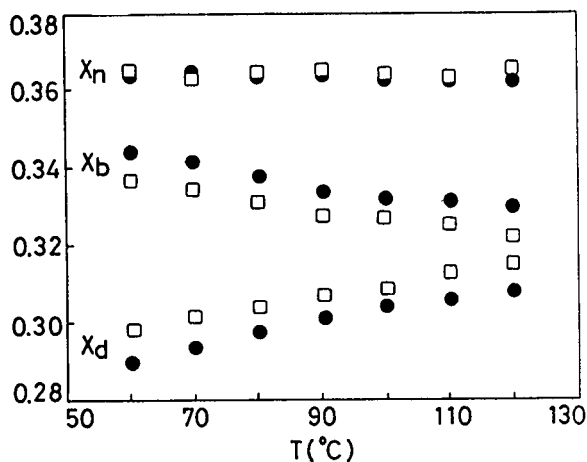


Fig. 6. Change of selectivity parameters of polar capillary columns as a function of temperature. \square = Supelcowax-10; \bullet = CLOT.

the CLOT column depends linearly on temperature. Three decimal figures are given for ΔC in Table II in order to permit an evaluation of the experimental fluctuations.

The values of Snyder's selectivity parameter of polar columns are shown in Fig. 6 as a function of temperature. Owing to the change in ΔI of *n*-butanol and dioxane on these columns, the x_b and x_d values, showing the influence of hydrogen bonding, change in an inversely proportional way, whereas no appreciable effect on the x_n value is observed, as temperature has no effect on dipole interactions. For the same reason, no hydrogen bonding being possible on non-polar columns, their selectivity parameters remain unchanged within the considered temperature range (60–120°C); for SPB-1 $x_b = 0.334$, $x_n = 0.395$ and $x_d = 0.271$; for DB-1 $x_b = 0.333$, $x_n = 0.398$ and $x_d = 0.269$.

The position of the four narrow-bore columns tested is compared in the selectivity triangle portion of Fig. 3 with that of packed columns, and the change with increasing temperature of the position of CLOT and Supelcowax-10 is indicated with arrows.

CONCLUSIONS

The results show how the various polarity indicators give comparable results in the tem-

perature range where the standard reference phase, squalane, can be used. The polarity order of the tested liquid phases is similar on all the polarity scale tested. Above 120°C, however, where it is impossible to use squalane as the reference phase, some of the polarity systems cannot be used.

Further, owing to the low boiling points of the various polarity probes, the determination of their retention times at high column temperatures is subject to excessive errors.

The difference in the apparent carbon number of *n*-alkanes and *n*-alkanols, ΔC , can be used over a wider temperature range as a suitable range of alkanes and alcohols can be selected at every temperature; no reference column is necessary and an absolute polarity value is obtained. Whereas in previously published papers the dependence of ΔC on temperature could not be exactly determined as packed columns with a restricted temperature range were examined, the use of various capillary columns here permitted it to be confirmed that ΔC can be applied to this type of separation system and that its value remains constant over a wide temperature range when a gas-liquid separation mechanism is involved. On the other hand, when mixed gas-solid, gas-liquid-solid and gas-liquid mechanisms are simultaneously present, as in the carbon black columns modified with a layer of polar liquid phase, the ΔC values change linearly with temperature, indicating the regular variation of the separation mechanism.

ACKNOWLEDGEMENTS

The authors thank Supelchem, Milan, the Italian representative of Supelco, who kindly supplied some of the capillary columns used. The work was supported by the Italian Ministry of University and Scientific Research (MURST), 60% research funds.

REFERENCES

- 1 G. Castello, A. Timossi and T.C. Gerbino, *J. Chromatogr.*, 582 (1990) 329.
- 2 G. Castello and G. D'Amato, *J. Chromatogr.*, 623 (1992) 289.

- 3 W.O. McReynolds, *J. Chromatogr. Sci.*, 8 (1970) 685.
- 4 L.R. Snyder, *J. Chromatogr.*, 92 (1974) 223.
- 5 L.R. Snyder, *J. Chromatogr. Sci.*, 16 (1979) 223.
- 6 M.S. Klee, M.A. Kaiser and K.B. Laughlin, *J. Chromatogr.*, 279 (1983) 681.
- 7 W.O. McReynolds, *Gas Chromatographic Retention Data*, Preston Technical Abstracts, Evanston, IL, 1966.
- 8 G. Tarjan, S. Nyiredi, M. Györ, E.R. Lombasi, T.S. Lombasi, M.V. Budaheygi, S.J. Meszdaros and J.M. Takács, *J. Chromatogr.*, 472 (1982) 1.
- 9 E. Fernandez-Sanchez, A. Fernandez-Torres, J.A. Garcia-Dominguez and J.M. Santiuste, *Chromatographia*, 31 (1991) 75.
- 10 Z. Szentirmai, G. Tarjan and J. Takács, *J. Chromatogr.*, 73 (1972) 11.
- 11 M.A. Hepp and M.S. Klee, *J. Chromatogr.*, 404 (1987) 145.
- 12 T.J. Betts, *J. Chromatogr.*, 504 (1990) 186.
- 13 R.N. Ewell, J.M. Harrison and L. Berg, *Ind. Eng. Chem.*, 30 (1944) 871.
- 14 L.M. Sidisky and M.V. Robillard, in P. Sandra and M. Lee (Editors), *Proceedings of the 14th International Symposium on Capillary Chromatography, Baltimore, 25–29 May, 1992*, p. 110.
- 15 G. Castello and S. Vezzani, in P. Sandra (Editor), *Proceedings of the 15th International Symposium on Capillary Chromatography, Riva del Garda, 24–27 May, 1993*, Alfred Hüthig Verlag, Heidelberg, p. 68.

Development of a high-temperature gas chromatography–inductively coupled plasma mass spectrometry interface for the determination of metalloporphyrins

W.G. Pretorius, L. Ebdon and S.J. Rowland*

Department of Environmental Sciences, University of Plymouth, Drake Circus, Plymouth PL4 8AA (UK)

(First received March 9th, 1993; revised manuscript received May 18th, 1993)

ABSTRACT

The development of a high-temperature gas chromatography–inductively coupled plasma mass spectrometry interface is reported. The method is applied to the analysis of synthetic and geological metalloporphyrins and detection limits and retention indices are given.

INTRODUCTION

Metallated porphyrins (geoporphyrins) are common, and sometimes abundant, constituents of many crude oils, oil shales, coals and sedimentary rocks [1] and they have been proposed as useful maturity indicators in such substrates [2,3]. Geoporphyrins have also been shown to be important in an industrial context where they effect catalytic upgrading of crude oils by reducing catalyst lifetime or by catalysing the formation of unwanted byproducts [4]. The development of methods suitable for analysis of geoporphyrins is therefore an important goal for geochemists and petroleum chemists.

Most studies of geoporphyrins have focused on structural elucidation of the demetallated porphyrin macrocycle [5]. However, recent developments in high-performance liquid chromatography (HPLC) and gas chromatography (GC) have led to a number of reports of the metallated

species in geochemical samples [6,7]. This has the advantage that the selective decompositions which are observed during demetallation are avoided [8]. In addition, the study of intact metallospecies may extend reports beyond the common nickel and vanadyl compounds, leading to increased geochemical information. Notable amongst more recent reports is that of Boreham [8] who described high-resolution reversed-phase HPLC of nickel and vanadyl geoporphyrins in marine rocks from the Toolebuc Formation, Australia. An impressive resolution of the major classes of metalloporphyrin macrocycles was obtained but the detection method used (UV–Vis spectrophotometry) was not designed to provide information about metals other than nickel or vanadium. In contrast, the use of inductively coupled plasma (ICP) mass spectrometry (MS) as a metal-selective detector in our recent studies of metalloporphyrins in coals allowed us to demonstrate the distribution of gallium porphyrins but no detailed study of the macrocycle was possible [9].

GC separation of metalloporphyrins has at-

* Corresponding author.

tracted attention for a considerable time [10,11]. However, the advent of so-called high-temperature gas chromatography (HTGC) columns has seen some impressive advances. Thus, Blum and co-workers [12,13] were able to demonstrate the distributions of nickel and vanadyl porphyrins in Julia Creek and Serpiano oil shales by GC-flame ionization detection (FID) and GC-MS [electron impact and ammonia chemical ionization (CI)]. The latter has the advantage of providing both structural information as well as confirmation of the metal content. However modern GC-MS systems are not well-suited to the use of HTGC columns and aggressive CI reagent gases [13] and, to our knowledge no detection limits or quantitative analyses have been reported.

In the present report we describe the modification of a recently described GC-ICP-MS [14] system to allow quantitative determination of synthetic nickel, vanadyl, manganese, iron, copper and zinc metalloporphyrins and metalloporphyrins in samples of coals and oil shale. "Working limits" for quantitation are given and the practical retention range of organometallic compounds has been greatly extended. The method has considerable potential for the rapid metal profiling of geoporphyryns.

EXPERIMENTAL

Gas chromatography

A Carlo Erba HRGC 5300 Mega Series gas chromatograph equipped with a constant-pressure, constant-flow unit (Fisons, UK) was used. A 10 m × 0.32 mm, HT-5 (0.1 μm film thickness) aluminium clad high-temperature column (S.G.E., UK), with a helium (high purity, Air Products, UK) flow-rate of 3 cm³ min⁻¹ was used. Typical the temperature programme was from 60 to 410°C at 15 or 20°C min⁻¹ with a 5–10-min isothermal hold.

Inductively coupled plasma mass spectrometry

A VG Plasmaquad 2 (VG Elemental, UK) instrument was used under the operating conditions given in Table I. Commercially available software (VG Elemental) was used for data acquisition and a BASIC programme was used

TABLE I
ICP-MS OPERATING CONDITIONS

Cooling gas	15 l min ⁻¹
Auxiliary gas	1.01 min ⁻¹
Injector gas	1.33 l min ⁻¹
Forward power	1500 W
Reflected power	<5 W
Mode	Time resolved analysis
Dwell time	Typically 1280 μs
No. of scans	Typically < 900
Data acquisition time	Typically < 10 min

for data processing and conversion. The ICP-MS system was tuned using a continuous cold vapour ²⁰²Hg signal [15].

Reagents

Synthetic metalloporphyrins. Synthetic nickel octaethylporphyrin (OEP), iron OEP chloride, vanadyl OEP, copper OEP, zinc OEP chloride and manganese OEP chloride were obtained from Aldrich, UK. Solutions were prepared in dichloromethane (Rathburn, UK) and examined on the same day.

Geoporphyryn samples. Bagworth coal was obtained from the British Coal Bank (Stoke Orchard, UK). The iron porphyrins were isolated as the chloride complexes using TLC [16]. Green River Shale was extracted (Soxhlet, 24 h) and porphyrins separated by flash column chromatography [17]. Nickel and vanadyl porphyrins were isolated by column chromatography. A Marl Slate nickel porphyrin fraction was obtained from Dr. A.J.G. Barwise (BP Research Centre, Sunbury-on-Thames, UK).

RESULTS AND DISCUSSION

Development of the HTGC-ICP-MS interface

The construction of the GC-ICP-MS interface and its application to the analysis of low- and medium-molecular-mass organometallic compounds has been described recently [14,15]. The GC retention index of the most retained analyte was ca. 3400 [15]. Metalloporphyrins typically have retention indices of ca. 5000 [18]. Thus, modification of the published interface was

needed before metalloporphyrins could be examined. The limitation of the GC–ICP–MS method to *ca.* 3400 retention index was thought to be due to the cooling effects of the argon injector gas (typical flow-rates 1.4–1.5 l min⁻¹).

Modifications of the GC–ICP–MS interface were made as shown in Fig. 1, which shows three major components; an argon heater, the heated transfer line and the demountable torch. The modifications to the ICP–MS system itself have already been described [14]. The main problem associated with heating argon is its low heat capacity. Therefore aggressive heating was needed and all tubing between the argon heater and ICP–MS injector insert was reduced to a minimum.

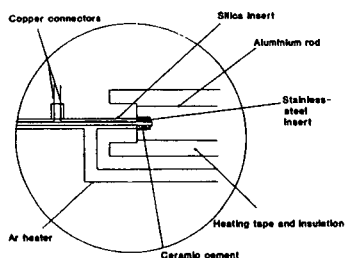
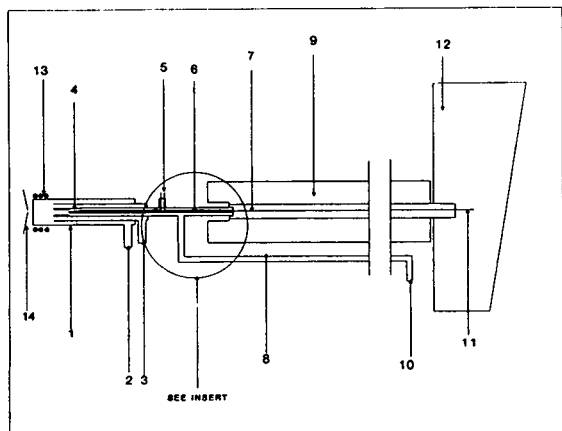


Fig. 1. HTGC–ICP–MS interface design. 1 = Plasma demountable torch; 2 = cooling gas inlet; 3 = auxiliary gas inlet; 4 = stainless-steel inset; 5 = outlet for copper leads (sealed with ceramic paste); 6 = copper wire leads; 7 = aluminium rod; 8 = argon heater; 9 = insulation; 10 = injector gas inlet; 11 = capillary column; 12 = GC oven; 13 = RF load coil; 14 = ICP–MS interface.

The argon heater consisted of nichrome wire inside a silica tube. The nichrome wire was heated to red heat with a suitable power supply (power requirement *ca.* 200 W) and the argon injector gas passed through the silica tube. The heater was insulated with Dalfratex cord (Darchem, UK) and further insulation was provided by industrial pipe lagging (Encon, UK).

The transfer line consisted of an aluminum rod through which the capillary column was threaded [14]. The transfer line and argon heater were grounded to the torch box.

A demountable torch with a 3 mm ICP injector insert (Baumbach and Co., UK) was used. A stainless-steel tube (1 mm × 12 mm) was mounted concentrically in the injector insert. The stainless-steel insert was introduced into a 2.5-mm hole in the aluminium rod. This not only provided support for the GC column, but ensured that the temperature was maintained above 400°C along the entire cross-section of the tube. The stainless-steel tube was resistively heated using a laboratory-made low-voltage power supply (power requirement *ca.* 150 W).

The GC column could only be extended to the end of the stainless-steel tube (24 mm from plasma), resulting in a dead volume of 0.70 cm³. Extending the capillary further (within 2 mm of plasma) resulted in a lower sensitivity and poor peak shape. Further extension of the stainless-steel tube would probably result in arcing from the RF load coil and was not attempted.

Evaluation of HTGC–ICP–MS interface

Fig. 2 shows a chromatogram obtained from HTGC–ICP–MS of five synthetic metalloporphyrins using the modified interface described above. The components eluted within a reasonable time (*ca.* 15–20 min) and had acceptable peak shapes. Furthermore, the specificity of ICP–MS as, effectively, a multielement chromatographic detection method, allowed all five metals to be monitored virtually simultaneously by selected ion recording (SIR; Fig. 2). The loss in resolution when comparing the HTGC–ICP–MS system to HTGC–FID was < 1% (calculated on peak base width).

The detection limits for these porphyrins, and the estimated detection limit for vanadyl oc-

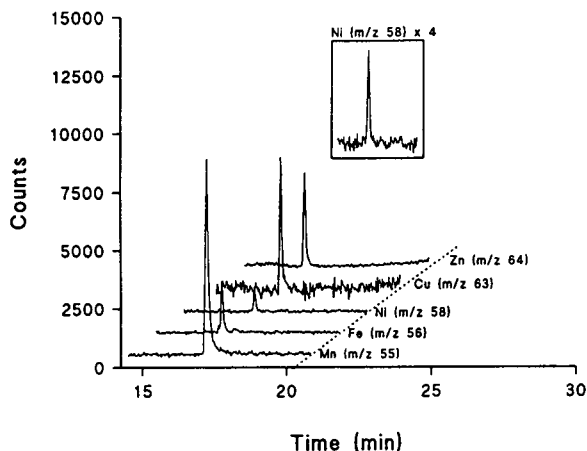


Fig. 2. Selected ion recording chromatograms of m/z 55 (Mn), m/z 56 (Fe), m/z 58 (Ni), m/z 63 (Cu) and m/z 64 (Zn). GC programme 60 to 350°C at 20°C min⁻¹, 350 to 410°C at 12°C min⁻¹, 1-min isothermal hold.

taethylporphyrin, are shown in Table II. These detection limits are “working limits”, calculated using temperature programmes that would normally be employed for geoporphyrin analyses. The method of tuning with ²⁰²Hg is not optimum. Alternative methods are currently being investigated and these may lead to improved limits.

TABLE II

DETECTION LIMITS FOR SYNTHETIC METAL-LOPORPHYRINS

Metalloporphyrin	Retention index ^a	Detection limits ^b (ng on column)
Vanadyl OEP	6280	0.51
Manganese OEP Cl	6022	0.10
Iron OEP Cl	6213	0.30
Nickel OEP	6266	0.51
Copper OEP	6692	0.55
Zinc OEP Cl	6114	0.14

^a Calculated from *n*-alkane standards.

^b Calculated at 3 σ .

Analysis of geoporphyrins

Figs. 3–5 show HTGC–FID and HTGC–ICP–MS chromatograms of porphyrin-containing extracts from coal and oil shales. These figures clearly illustrate the specificity of the HTGC–ICP–MS method over HTGC–FID and show a considerable simplification of the chromatograms by SIR. For example, Fig. 3b shows selected ion HTGC–ICP–MS chromatograms of the porphyrin fraction isolated from the Green River Shale. The chromatographic peak shape of the vanadyl species is quite poor, whilst that of the

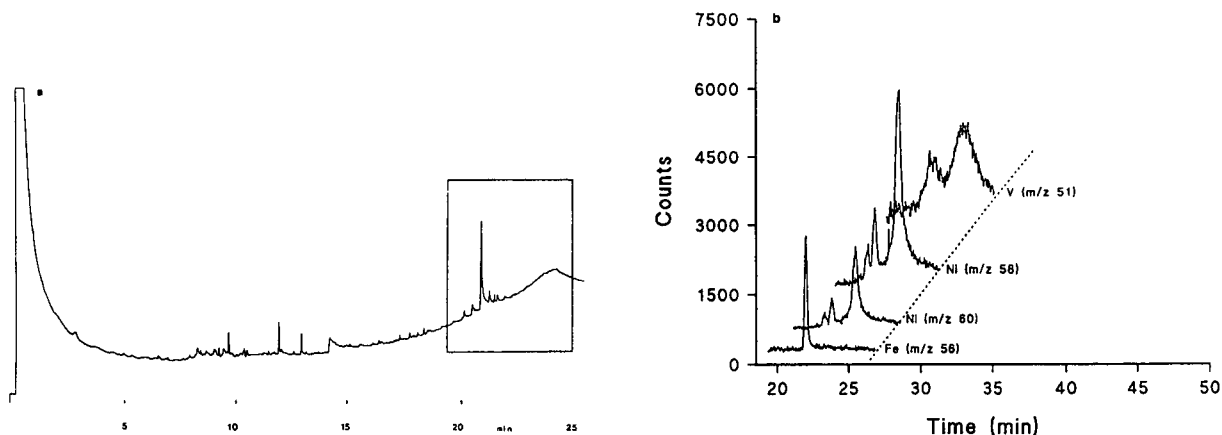


Fig. 3. (a) HTGC–FID chromatogram of Green River Shale porphyrin fraction, GC programme 60 to 410°C at 15°C min⁻¹, followed by an isothermal hold. Box indicates HTGC–ICP–MS chromatogram range. (b) HTGC–ICP–MS chromatogram (m/z 51, 56, 58, 60) of Green River Shale porphyrin fraction, GC programme 60 to 350°C at 15°C min⁻¹, 350°C at 10°C min⁻¹, 1.5 min-isothermal hold.

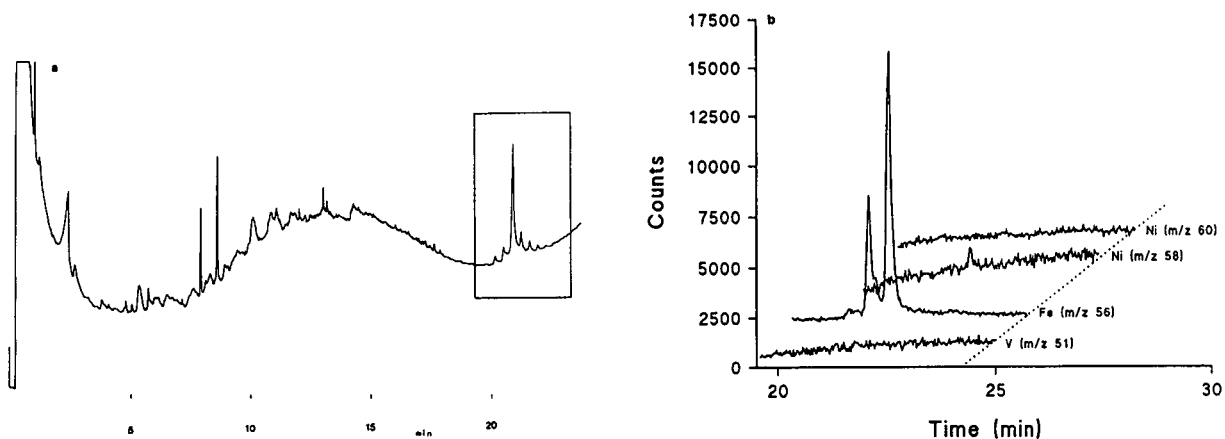


Fig. 4. (a) HTGC-FID chromatogram of iron porphyrin fraction from Bagworth coal, GC programme 60 to 410°C at 15°C min⁻¹, followed by an isothermal hold. Box indicates HTGC-ICP-MS chromatogram range. (b) HTGC-ICP-MS chromatogram (*m/z* 51, 56, 58, 60) of iron porphyrin fraction extracted from Bagworth coal, GC programme 60 to 350°C at 15°C min⁻¹, 350°C at 10°C min⁻¹.

nickel species is acceptable. Both nickel and vanadyl species could be quantified by reference to the added synthetic iron porphyrin internal standard (10 ng as iron).

The iron porphyrins isolated from a “standard” UK coal (Bagworth) [16] were also monitored by SIR (*m/z* 56) (Fig. 4b). The gallium porphyrins of this coal have been the subject of previous studies including HPLC-ICP-MS analysis [9], but to our knowledge this is the first

instrumental chromatographic technique applied to iron porphyrins in a coal. The only previous report of a chromatographic technique being applied to these porphyrins, used TLC [16].

Analysis of the so-called “nickel” porphyrin fraction from the Marl Slate by HTGC-ICP-MS (Fig. 5b) also revealed the presence of titanium porphyrins which co-elute with the nickel compounds but which could easily be distinguished by SIR (*m/z* 48). The close similarity in chro-

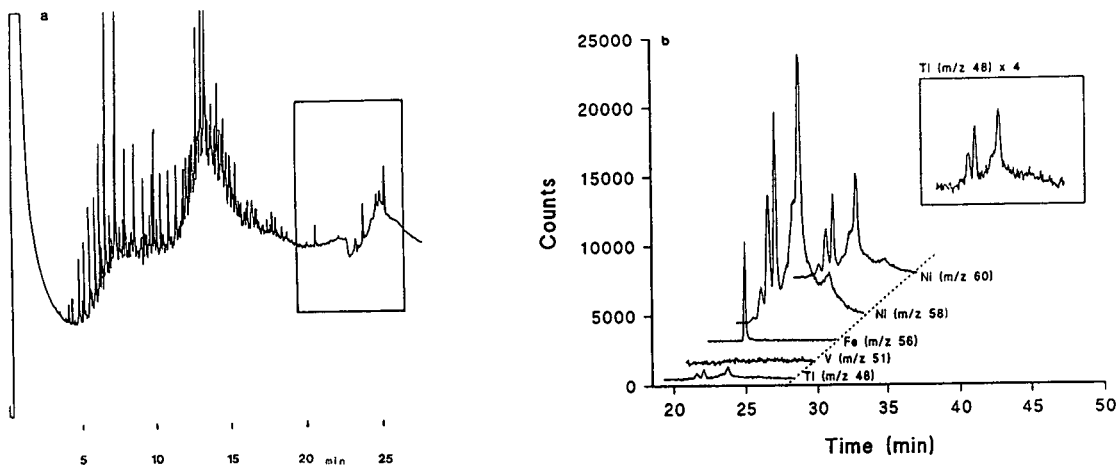


Fig. 5. (a) HTGC-FID chromatogram of Marl Slate nickel porphyrin fraction, GC programme 60 to 410°C at 15°C min⁻¹, followed by an isothermal hold. Box indicates HTGC-ICP-MS chromatogram range. (b) HTGC-ICP-MS chromatogram (*m/z* 48, 51, 56, 58, 60) of Marl Slate nickel porphyrin fraction, GC programme 60 to 350°C at 15°C min⁻¹, 350°C at 10°C min⁻¹, 2.8-min isothermal hold.

matographic behaviour of the nickel and titanium porphyrins possibly explains the lack of previous reports since less selective detection methods would not reveal their presence.

Titanium porphyrins have not been reported in geological samples previously, although Chicarelli *et al.* [17] speculated on their presence in several shales on the basis of off-line liquid chromatography followed by direct nebulization ICP-MS. Mango [19] commented on the catalytic activity of transition metals in catalysing reactions under conditions of diagenesis and mentioned titanium as one of the possible transition metal catalysts. Other workers have suggested that the poisoning of coal liquefaction catalysts was due in part to the presence of titanium porphyrins [20].

The gas chromatograms obtained for all of the geological porphyrin distributions were quite simple, as expected from previous studies [12,13,21,22]. This contrasts with the complexity revealed by HPLC methods [9] and reflects the greater resolving power of HPLC where variations in mobile phase and stationary phases allow separations to be maximized [5,6]. Hence the improved HPLC resolution of geoporphyrins mixtures over the last 12 years [8,23]. Whilst the lack of GC resolution is a disadvantage, the simplicity of the metal ion chromatograms does allow rapid metal profiles of geoporphyrins to be obtained and compared, and this is potentially valuable for screening source rocks or oils in petroleum exploration, petroleum refining or even oil pollution studies (*e.g.* tarball fingerprinting [24]).

The simple nature of the high-temperature gas chromatograms which typically consist of two or three peaks, may reflect the distributions of the major macrocycle types (*e.g.* deoxophyllerythroetioporphyrins and etioporphyrins) but this remains to be tested by coinjection of pure metalloporphyrins.

CONCLUSIONS

HTGC-ICP-MS is a selective and sensitive method for the rapid profiling of metalloporphyrins in geological samples. The method should find wide application in petroleum explo-

ration geochemistry, industrial petroleum refining and oil pollution studies.

ACKNOWLEDGEMENTS

The authors would like to thank Mr. A.W. Kim for advice on interface design and Dr. A.J.G. Barwise and BP for funding early stages of the project. W.G.P. would like to thank Professor H. Snyman, Mr. R. Venter and The Foundation for Research Development (South Africa) and the University of Plymouth for funding.

REFERENCES

- 1 E.W. Baker and S.E. Palmer, in D. Dolphin (Editor), *The Porphyrins*, Vol. 1A, Academic Press, New York, 1978, Ch. 11, p. 486.
- 2 G. Eglinton, J.R. Maxwell, R.P. Evershed and A.J.G. Barwise, *Interdiscip. Sci. Rev.*, 10 (1985) 222.
- 3 A.J.G. Barwise and P.J.D. Park, in M. Bjoroy, P. Albrecht, C. Cornford, K. de Groot, G. Eglinton, E. Galimov, D. Leyhäuser, R. Pelet, J. Rullkotter and G. Speers (Editors), *Advances in Organic Geochemistry*, Wiley, Chichester, 1981, p. 668.
- 4 J.F. Branthaver, in R.H. Filby and J.F. Branthaver (Editors), *Metal Complexes in Fossil Fuels (ACS Symposium Series, No. 344)*, American Chemical Society, Washington, DC, 1987, Ch. 12, p. 188.
- 5 A.J.G. Barwise, R.P. Evershed, G.A. Wolff, G. Eglinton and J.A. Maxwell, *J. Chromatogr.*, 368 (1986) 1.
- 6 P. Sandararaman, W.R. Biggs, J.G. Reynolds and J.C. Fetzer, *Geochim. Cosmochim. Acta*, 52 (1988) 2337.
- 7 C.J. Boreham and C.J.R. Fookes, *J. Chromatogr.*, 467 (1989) 195.
- 8 C.J. Boreham, in J.M. Moldowan, P. Albrecht and R.P. Philp (Editors), *Biological Markers in Sediments and Petroleum*, Prentice-Hall, Englewood Cliffs, NJ, 1992, Ch. 15, p. 301.
- 9 W.G. Pretorius, M.E. Foulkes, L. Ebdon and S.J. Rowland, *J. High Resolut. Chromatogr.*, 16 (1993) 157.
- 10 P.J. Gill, R.P. Evershed, M.I. Chicarelli, G.A. Wolff, J.R. Maxwell and G. Eglinton, *J. Chromatogr.*, 350 (1985) 37.
- 11 P.J. Gill, R.P. Evershed and G. Eglinton, *J. Chromatogr.*, 369 (1986) 281.
- 12 W. Blum, W.J. Richter and G. Eglinton, *J. High Resolut. Chromatogr. Chromatogr. Commun.*, 11 (1988) 148.
- 13 W. Blum, P. Ramstein and G. Eglinton, *J. High Resolut. Chromatogr.*, 13 (1990) 85.
- 14 A. Kim, M.E. Foulkes, S. Hill, L. Ebdon, R.L. Patience, A.J.G. Barwise and S.J. Rowland, *J. Anal. At. Spec.*, 7 (1992) 1.

- 15 A. Kim, S. Hill, L. Ebdon and S.J. Rowland, *J. High Resolut. Chromatogr.*, 15 (1992) 665.
- 16 Bonnett, F. Czechowski and P.S. Hughes, *Chem. Geol.*, 91 (1991) 193.
- 17 M.I. Chicarelli, C.B. Eckardt, C.R. Owen, J.R. Maxwell, G. Eglinton, R.C. Hutton and A.N. Eaton, *Org. Geochem.*, 15 (1990) 267.
- 18 P.J. Gill, *Ph.D. Thesis*, Bristol University, Bristol, 1984.
- 19 F.D. Mango, *Geochim. Cosmochim. Acta*, 56 (1992) 553.
- 20 A.W. Lynch, *Appl. Catal.*, 24 (1986) 227.
- 21 B.D. Quimby, P.C. Dryden and J.J. Sullivan, *J. High Resolut. Chromatogr.*, 15 (1991) 110.
- 22 Y. Zeng, J.A. Seeley, T.M. Dowling, P.C. Uden and M.Y. Khuhawar, *J. High Resolut. Chromatogr.*, 15 (1992) 669.
- 23 S.K. Hajibrahim, P.J.C. Tibbetts, C.D. Watts, J.R. Watts, G. Eglinton, H. Colin and G. Guiochon, *Anal. Chem.*, 50 (1978) 549.
- 24 S.K. Hajibrahim, in J. Albaiges, R.W. Frei and E. Merian (Editors), *Chemistry and Analysis of Hydrocarbons in the Environment*, Gordon & Breach Science, London, 1983, p. 117.

Electrophoretic behavior of aromatic-containing organic acids and the determination of selected compounds in water and soil by capillary electrophoresis

William C. Brumley* and Cynthia M. Brownrigg

US Environmental Protection Agency, Environmental Monitoring Systems Laboratory, P.O. Box 93478, Las Vegas, NV 89193-3478 (USA)

(First received February 19th, 1993; revised manuscript received May 25th, 1993)

ABSTRACT

The behavior of 56 aromatic-containing organic acids (ACOAs) was obtained under free zone electrophoresis and under micellar electrokinetic chromatography using cholic acid as the micellar agent. The compound classes encompass phenoxy acid herbicides, phenylalkanoic acids, aromatic carboxylic acids, aromatic sulfonic acids, azo and other dyes, and ACOAs containing nitrogen. Seven compounds were studied with respect to extraction and cleanup from spiked water and soil at levels of 1.0 and 0.1 $\mu\text{g/g}$ and 100 and 20 $\mu\text{g/g}$, respectively. A general scheme of isolation and cleanup was developed that used extraction disks and solid-phase extraction cartridges. Average recoveries for three determinations ranged from 26.5 to 98.2% with relative standard deviations ranging from 6.7 to 55%.

INTRODUCTION

Aromatic-containing organic acids (ACOAs) are important compounds in commerce, pharmaceuticals, biochemistry and the environment. Typical examples of ACOAs from these respective areas include phthalic acid, a precursor to phthalate esters; acetylsalicylic acid, a drug; nicotinic acid, a vitamin; and 2,4-dichlorophenoxyacetic acid, a herbicide. Analytical interest in the determination of ACOAs in various matrices may be concerned with waste streams, drinking water, biological activity, quality control of drugs, and hazardous waste, among others.

Our focus is the environmental occurrence and determination of specific ACOAs. Azo dyes are an important subset of such compounds because of the large amounts produced and the potential for the production of toxic by-products. The dyes

are essential to the textile industry and are used in food and cosmetics as well, where concern has been raised about their potential carcinogenicity. One dye, trypan blue, is listed as an Appendix VIII RCRA analyte [1]. The dyes themselves or their breakdown products, which may be toxic, have been the subject of studies assessing their environmental distribution, occurrence and fate [2]. Herbicides also constitute an important subset of ACOAs that are of intense analytical interest [3,4]. The levels of such compounds as 2,4-dichlorophenoxyacetic acid in hazardous waste, for example, are of special concern under RCRA [1].

Even relatively simple ACOAs can present chromatographic problems for techniques such as capillary gas chromatography. It is, therefore, not surprising that such compounds have not received as thorough a treatment in existing US Environmental Protection Agency methodology such as the SW-846 manual [5] as have volatile and semivolatile analytes. Recent updates plan-

* Corresponding author.

ned for SW-846 include methods for non-volatile compounds such as aromatic sulfonic acids (Method 8350) [6].

Because ACOAs are often highly polar and may occur as salts, rendering them non-volatile, liquid chromatography (LC) is an obvious choice for effecting their separation. Gradient elutions in reversed-phase (RP) LC are possible if ionization can be suppressed by appropriate buffers [4]. Alternatively, RP separations using ion-pairing reagents can be carried out [7]. Azo dyes are sufficiently retained in C_{18} RPLC to allow separation with methanol–water gradients [2]. Ion chromatography has often been the technique of choice for ACOAs [8], but even supercritical fluid chromatography has been used [9,10].

Hyphenated techniques of LC with mass spectrometry (MS) are a powerful means to the identification and quantitation of ACOAs in various contexts [11]. Usually, LC–MS is carried out with relatively large bore columns (> 2 mm I.D.) using particle-beam MS [4] and thermospray MS [12]. Problems with decomposition using particle-beam interfaces have been addressed [4]. Applications of spray ionization techniques are highly relevant to ACOAs [13]. These compounds may also be determined by open tubular capillary LC [14] and packed column capillary LC [15].

Thin-layer chromatography (TLC) is also highly applicable to the determination of ACOAs. Several reviews have been published and the review by Sherma [16] may be consulted. Recent TLC applications involving ACOAs include separations involving phenylglyoxylic acids [17], dihydroxybenzoic acids [18,19], and arylsulfonyl alkanic and arylsulfonylcycloalkanecarboxylic acids [20].

Recently, high-performance capillary electrophoresis (HPCE) has emerged as a powerful technique for the separation of many types of compounds sufficiently soluble in aqueous buffer solutions. A comparison of ion chromatography with CE revealed the greater efficiency of CE [21]. A comprehensive review by Kuhr and Monnig [22] may be consulted for further references. The coupling of CE to MS has been described [23]. Aromatic sulfonic acids were studied under free zone capillary electrophoresis

(CZE) conditions [24] as were isomers of benzoic acid [25,26]. Sulfonated azo dyes were subjected to CE–MS [2]. The application of micelles in HPCE has been described by Terabe [27] and Nishi *et al.* [28], and has resulted in increased selectivity in many separations.

In this work we present a scheme for the isolation of ACOAs from water and soil based on extraction disks and solid-phase extraction (SPE) cartridges. The electrophoretic behavior of 56 ACOAs is tabulated under CZE and micellar electrokinetic chromatography (MEKC) conditions. Seven compounds are studied in detail with regard to recovery and determination in water and soil by MEKC.

EXPERIMENTAL

Chemicals

Compounds were used as received, and came from Aldrich (Milwaukee, WI, USA) unless otherwise noted. Trypan blue was obtained from Pfalz & Bauer (Stamford, CT, USA). Dodecylbenzenesulfonic acid, cumenesulfonic acid, xylenesulfonic acid and toluenesulfonic acid were obtained from Chem Service (West Chester, PA, USA). Analytical standards of seven compounds (1–7, Fig. 1) were made up in water–methanol solution at a concentration of about 0.2 to 0.4 mg/ml in a mixed standard referred to as the 7-STD. This solution was used for matrix spiking and for response factor determinations. An internal standard solution of 4-hydroxyphenylacetic acid (IS1) and anthraquinone-2,6-disulfonic acid (IS2) was prepared at a concentration of about 0.2 mg/ml. A 1-ml volume each of the 7-STD and of the internal standard solution was combined with buffer and diluent in the 4-ml sample vials. This constituted the center of the working concentration range for these analytes (*i.e.*, about 0.05–0.1 mg/ml in the sample vials).

Deionized water was produced (Barnstead/Thermolyne, Dubuque, IA, USA) for all aqueous solutions. The organic solvents, methanol and acetone, were distilled in glass (Burdick & Jackson, Muskegon, MI, USA). Boric acid–sodium borate buffer was made to a nominal concentration of 50 mM by titrating 100 mM

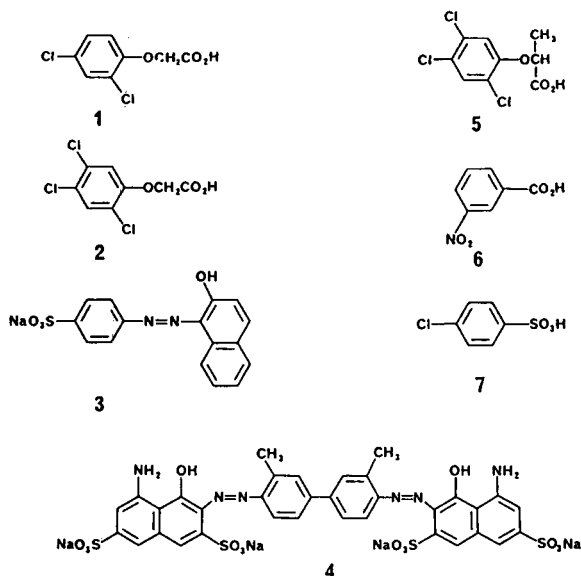


Fig. 1. Structures of seven compounds used in recovery studies: 1 = 2,4-dichlorophenoxyacetic acid; 2 = 2,4,5-trichlorophenoxyacetic acid; 3 = orange II; 4 = trypan blue; 5 = 2,4,5-trichlorophenoxypropionic acid; 6 = 3-nitrobenzoic acid; 7 = 4-chlorobenzenesulfonic acid.

solutions to a pH 8.3 endpoint. The micellar solution was made up of 0.1722 g of cholic acid sodium salt monohydrate in each 4-ml sample vial, giving a solution approximately 100 mM in the cholic acid (total volume 4.4 ml) [28]. Solutions in all vials were filtered through 0.2- μ m pore size disposable nylon filters (Alltech, Deerfield, IL, USA). The 6 M HCl and 6 M NaOH were made from concentrated HCl (Mallinckrodt, Paris, KY, USA) and sodium hydroxide pellets (Fisher Scientific, Fair Lawn, NJ, USA).

HPCE

A P/ACE Model 2100 instrument (Beckman, Fullerton, CA, USA) was used for all CE experiments. A 57 cm (50 cm to the detector) \times 50 μ m I.D. capillary was used at 25 kV for MEKC separations and 30 kV for CZE separations. Injections were by pressure for 5 to 10 s at the anode (positively charged) end. Detection was by UV at 214 nm.

Spiking/extraction studies

Water. Deionized water of 250- and 1000-ml volumes was spiked at nominal concentrations of 1.0 and 0.1 μ g/g with the 7-STD. The water was

adjusted to pH 2 and extracted by means of extraction disks (Varian version of Empore, 3M, St. Paul, MN, USA). We followed the manufacturer's recommendation of adding 5 ml of methanol per 1000 ml water to be extracted and of using a drip rate no greater than 5 min per 1000 ml of water (usually 10 min per 250 ml). The disks were prepared according to the manufacturer's instructions that accompany the disks. This consisted of rinsing with 10 ml of methanol, 10 ml of water, and 10 ml of water-methanol (95:5, v/v). The first fraction of retained analytes (OR fraction) was eluted with two 7-ml portions of basic methanol (pH 8–9); the eluate comprised analytes 1–6. Compounds that were not retained under these acidic conditions were isolated by readjusting the pH to 6 and adding 0.050 g of cetyldiethylmethylammonium bromide (CEMA) per 250 ml of aqueous sample. A new disk extraction was carried out with the disk activated as above but with an additional 10 ml of water-methanol (95:5) containing CEMA at 0.025 g per 100 ml. The second fraction of retained analytes was eluted twice with two 10-ml volumes of methanol and contained analytes 6 and 7 (CL fraction). The OR fraction was readjusted to pH 6 and then the OR and CL fractions were each passed through an SCX (Bond Elut; Varian, Harbor City, CA, USA) cartridge followed by a 1-ml methanol rinse. The SCX cartridge was activated with 3 ml of water, 3 ml of 0.1 M sodium sulfate, 1 ml of water, and finally 2 ml of methanol. A drip rate of about 3 ml per 15 s was used. The eluates were concentrated as appropriate under a nitrogen stream and subjected to MEKC.

Soil. A 10-g portion of soil was spiked by pipet with the 7-STD, mixed, and allowed to sit overnight. The spiked soil was extracted by either sonication or Soxhlet methods [5] using a water-methanol (25:75, v/v) solvent mixture. The extract was concentrated to about 25 ml and diluted with deionized water to 250 ml, and then treated exactly as the spiked water sample.

Additional cleanup

TLC. Silica gel 60 plates (E. Merck, Darmstadt, Germany) were spotted and then developed with the solvent mixture isopropanol-

tetrahydrofuran-ammonia-water (100:50:4:1, v/v). Typical R_F values were as follows: 1-3 and 5-7 were found in the range 0.30-0.55; 4 was essentially unmoved at 0.02; polar neutrals were found at 0.80 or greater.

Ion-pairing on C_{18} SPE cartridges. The cartridges were activated with 5 ml of methanol followed by 3 ml of water-methanol (95:5) containing 0.025 g CEMA per 100 ml. The CL fraction was diluted to 50 ml with deionized water, 0.010 g of CEMA was added, and this solution was passed through the cartridge. The cartridge was washed with 3 ml of water-methanol (95:5) containing 0.025 g CEMA per 100 ml and then eluted with methanol-water (75:25) containing 0.025 g CEMA per 100 ml.

RESULTS AND DISCUSSION

Migration times

Tables I-VI tabulate the CZE and MEKC migration times (MT_c and MT_e , respectively) for 56 ACOAs at pH 8.3 using the boric acid-sodium borate buffer. This system was chosen as a generally applicable system for the determination of ACOAs. The basic pH conditions avoid, to a large extent, activity and adsorption effects than can affect peak shape when acidic pH values are used. As such, these conditions are likely a good compromise for multiresidue environmental analysis and analytes such as dyes.

TABLE I

CORRECTED MIGRATION TIMES OF PHENOXY ACIDS UNDER MEKC AND CZE CONDITIONS

Buffer, borate pH 8.3; MEKC with cholic acid.

Phenoxy acids	MT_c	MT_e
2,4-Dichlorophenoxyacetic acid	8.87	3.46
2-Methyl-4-chlorophenoxyacetic acid	9.03	3.45
2,3-Dichlorophenoxyacetic acid	9.08	3.50
3,4-Dichlorophenoxyacetic acid	9.21	3.48
2,4,5-Trichlorophenoxypropionic acid	9.23	3.29
2,4,5-Trichlorophenoxyacetic acid	9.37	3.40
2,4-Dichlorophenoxybutyric acid	9.93	3.28
2-Methyl-4-chlorophenoxybutyric acid	9.93	3.46

TABLE II

CORRECTED MIGRATION TIMES OF AROMATIC CARBOXYLIC ACIDS UNDER MEKC AND CZE CONDITIONS

Buffer, borate pH 8.3; MEKC with cholic acid.

Aromatic carboxylic acids	MT_c	MT_e
9-Anthracenecarboxylic acid	8.65	3.41
4-Hydroxybenzoic acid	8.95	3.73
3-Hydroxybenzoic acid	9.17	3.77
4-Aminobenzoic acid	9.19	3.78
2-Chlorobenzoic acid	9.46	3.77
4-Cyanobenzoic acid	9.54	4.24
2-Hydroxybenzoic acid	9.57	3.81
4-Nitrobenzoic acid	9.64	3.78
4-Chlorobenzoic acid	9.66	3.75
3-Nitrobenzoic acid	9.70	3.89

The tables group the compounds according to a common structural feature, which is indicated in the titles. Within the tables, compounds are sorted by increasing MT_c . The MT_c and MT_e values are corrected to a standard set of conditions to facilitate comparison among the many compounds using data accumulated over several months; a short discussion of a convenient approach to the correction will be given (see *Corrections to migration times*).

Of the 56 compounds, more than 80% of them have an MT_c that falls between 3.0 and 4.0 min. We estimate that under these conditions, we could reasonably expect to resolve about 10 compounds based on observed peak widths. Therefore, the contention that CZE is a technique of high efficiency but limited selectivity is supported [29] within this context. In contrast, examination of the MT_c reveals considerably more selectivity at pH 8.3. As pointed out by Terabe *et al.* [30], the optimum pH for separation of acids is in the vicinity of their pK_a . Therefore, the implications of our comparison of CZE and MEKC is limited in view of the one pH value used.

MEKC also exhibits wider applicability to complex ions such as dyes because of improved peak shape. We estimate that of the nearly 40

TABLE III

CORRECTED MIGRATION TIMES OF AROMATIC SULFONIC ACIDS UNDER MEKC AND CZE CONDITIONS

Buffer, borate pH 8.3; MEKC with cholic acid.

Aromatic sulfonic acids	MT _c	MT _e
Cumenesulfonic acid	9.04	3.57
Anthraquinone-2-sulfonic acid	9.37	3.52
Xylenesulfonic acid	9.55, 9.24, 9.45, 9.07	3.75, 3.30, 3.56, 3.70
Naphthalenesulfonic acid	9.70	3.75
4-Hydroxybenzenesulfonic acid	9.99	3.74
Toluenesulfonic acid	10.51	3.90
4-Chlorobenzenesulfonic acid	10.51	3.95
3-Nitrobenzenesulfonic acid	10.65	3.98
Dodecylbenzenesulfonic acid	11.34 (center)	3.13 (center)
Anthraquinone-2,6-disulfonic acid	14.92	5.31
1,2-Benzenedisulfonic acid	28.14	7.24

compounds (about 70% of the total) with MT_c in the range of 8.0 to 10.0 min, nearly half could be separated. About 30% of the compounds have MT_c greater than 10.0. Therefore, HPCE under these conditions is a technique of high efficiency and relatively high selectivity. In the context of a given separation, the additional flexibility of choosing the surfactant compound for micellar formation enhances the separation power of the technique. Further modifications based on the

use of additives such as ion-pair agents and organic modifiers are discussed by Terabe and co-workers [27,28].

Corrections to migration times

A convenient approach was used to correct MT values to a standard set of conditions based on the use of two internal standards for assessing changes in the apparent mobility. From the basic equation of electrophoresis, the apparent mobili-

TABLE IV

CORRECTED MIGRATION TIMES OF ARYL ALIPHATIC ACIDS UNDER MEKC AND CZE CONDITIONS

Buffer, borate pH 8.3; MEKC with cholic acid.

Aryl aliphatic acids	MT _c	MT _e
4-Hydroxyphenylacetic acid	8.43	3.54
3-Hydroxyphenylacetic acid	8.46	3.55
7-Hydroxycoumarin-4-acetic acid	8.82	3.74
4-Chlorophenylacetic acid	8.92	3.58
4-Nitrophenylacetic acid	8.94	3.78
2-Hydroxyphenylacetic acid	8.98	3.73
Pyrenebutyric acid	10.86	3.76

TABLE V

CORRECTED MIGRATION TIMES OF SELECTED DYES UNDER MEKC AND CZE CONDITIONS

Buffer, borate pH 8.3; MEKC with cholic acid. N.O. = Not observed.

Dyes	MT _c	MT _e
Erioglaucine	9.16	6.05
Acid Blue 113	10.17	N.O.
Erythrosin	10.26	3.61
Acid Blue 25	10.69	3.78
Orange II	10.78	3.41
Indigo Carmine	11.05	4.59
Trypan Blue	12.96	3.39
Tartrazine	15.67	3.33

TABLE VI

CORRECTED MIGRATION TIMES OF NITROGEN-CONTAINING ACOAs UNDER MEKC AND CZE CONDITIONS

Buffer, borate pH 8.3; MEKC with cholic acid.

Nitrogen-containing ACOAs	MT _c	MT _e
2-Quinolinecarboxylic acid	7.72	3.55
9-Acridinecarboxylic acid	7.87	3.35
4-Quinolinecarboxylic acid	8.52	3.48
3-Quinolinecarboxylic acid	8.75	3.55
2,3-Pyridinedicarboxylic acid	8.79	6.04
2-Pyridineethanesulfonic acid	8.80	3.69
2-Pyridylacetic acid	8.87	3.69
2,4-Pyridinedicarboxylic acid	9.76, 10.61	3.84
Picolinic acid	9.78	3.65
Nicotinic acid	10.17	3.90
Isonicotinic acid	10.18	3.91
4,9-Acridinedicarboxylic acid	10.71	3.39

ty of a substance can be calculated based on its observed MT; its apparent mobility is the combination of the mobility of the electroosmotic flow (EOF) and the mobility of the substance as modified by the capacity factor under MEKC conditions. Mobility is proportional to $1/MT$ so that corrections can be developed from the use of a single internal standard (IS) by relating $1/MT(\text{sample})$ to $1/MT(\text{IS})$. The inclusion of two internal standards allows the immediate assessment of changes in conditions independent of an EOF marker via the difference $\delta = 1/MT(\text{IS}_1) - 1/MT(\text{IS}_2)$. This is particularly convenient under MEKC conditions where EOF may be difficult to determine exactly. All MT values in the tables are corrected to an EOF of 2.30 min (determined by pyridine) under CZE conditions and MT of 8.43 and 14.92 for IS1 and IS2, respectively, under MEKC conditions. Generally, we have found that corrections via IS1^a alone usually bring the MT within a 1% reproducibility. Additional corrections based on scaling the δ values could further reduce variability

^a $MT(\text{corr}) = 1 / \{1/MT(\text{IS}_1, S) - [1/MT(\text{IS}_1) - 1/MT(S)]\}$, where $MT(\text{IS}_1, S) = 8.43$ and $MT(\text{IS}_1)$ and $MT(S)$ are the particular MT of the internal standard and substrate, respectively, observed in a given run.

but were not used for the corrected MT given in the tables.

Difficult separations achieved

A number of separation problems are implicitly solved by the experimental data reported in Tables I–VI. For example, a useful approach to the separation and determination of phenoxy acid herbicides, aromatic carboxylic acids and aromatic sulfonic acids (Tables I–III) is provided under MEKC conditions. The MT_c reveal that many of the compounds would be separated. MEKC also provides a general approach to the separation of azo dyes (Table V) and the analysis of the purity of dye standards. Fig. 2 presents the electropherogram of trypan blue, which reveals nine major peaks for the standard. This equates to 72% purity based on the assumption of equal molar absorptivity among the compounds. The first peak, because of its early MT, is probably a neutral compound.

Certain kinds of separations difficult to carry out by RPLC can be directly effected using MEKC. For example, the electropherogram of nicotinic, isonicotinic and picolinic acids is shown in Fig. 3. Nicotinic and isonicotinic acids are not resolved, but peak shapes of all acids are sharp without extreme measures to prevent peak tailing [31]. Under CZE conditions, nicotinic and isonicotinic acids are also unresolved. We have observed (shown as an inset in Fig. 3) a partial separation of nicotinic and isonicotinic acids with acetone as a 5% additive under MEKC conditions.

Spiked water and soil samples —isolation and recovery

Seven compounds, 1–7, were chosen to evaluate a general analytical scheme for the determination of ACOAs in water and soil (Tables VII–IX). The compounds encompass phenoxy acid herbicides, aromatic carboxylic acids and sulfonic acids, and azo dyes. The separation of 1–7 is shown in Fig. 4 under MEKC conditions. The compounds are well resolved in a relatively short time in view of the wide differences in molecular structure. The electropherograms generally display between 200 000 and 250 000 theoretical plates based on peak

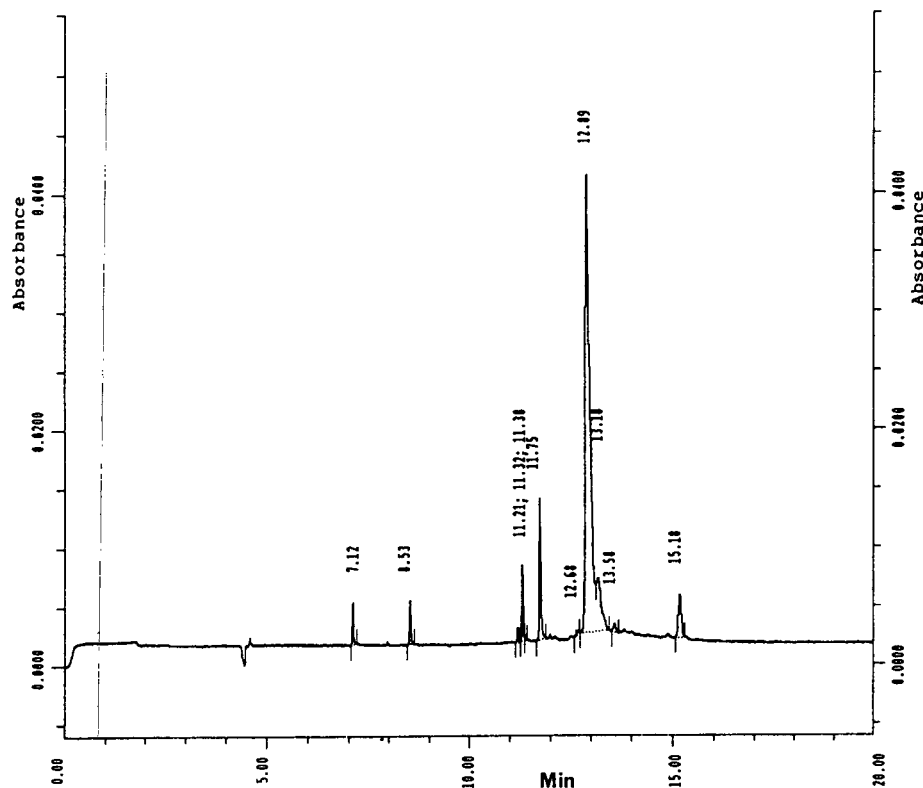


Fig. 2. Electropherogram of trypan blue standard under micellar conditions (pH 8.3, boric acid–sodium borate 50 mM, 100 mM sodium cholate). Main component MT = 12.89.

widths. The peak corresponding to 2,4,5-trichlorophenoxypropionic acid (**5**) is broadened and at times we have observed the slight separation of two peaks. We attribute this to a partial resolution of optical isomers of **5** in view of the chiral nature of cholic acid [28].

The isolation of the compounds from spiked water and soil is a unified approach that depends on SPE using extraction disks and SPE cartridges. All but the most strongly acidic, water-soluble acids are isolated at pH 2 on the C_{18} disks. This pH was chosen to remain within the operating range of stability (pH 2–7) recommended by the manufacturer^a. The non-retained acids at pH 2 are, nevertheless, retained on disk at pH 6 using the ion-pairing agent CEMA when the aqueous acid filtrate is reextracted with a

new disk. Alternatively, acid labile compounds can be extracted exclusively using the ion-pairing approach.

Extraction from soil requires the presence of water in the solvent in order to recover **4**. We found that a water–methanol (25:75, v/v) solvent was adequate to ensure reproducible recovery. Once the analytes are extracted, a reduced volume of the extracting solvent is diluted in water and subjected to the SPE isolation given previously.

Compounds 1–7 were studied at nominal levels of 1.0 and 0.1 $\mu\text{g/g}$ for water and 100 and 20 $\mu\text{g/g}$ for soil. The percent recoveries are fairly good, ranging from 38 to 101% for water and 26.5 to 94.4% for soil. Trypan blue (**4**) was particularly difficult to recover, a fact not surprising in view of its complex structure. It should also be pointed out that overall recovery is dependent on both extraction efficiency and recovery efficiency from the disk. Trypan blue is

^a A referee has commented that pH 1 may be used to improve retention of analytes that are not fully retained at pH 2 (Yoo *et al.* [36]).

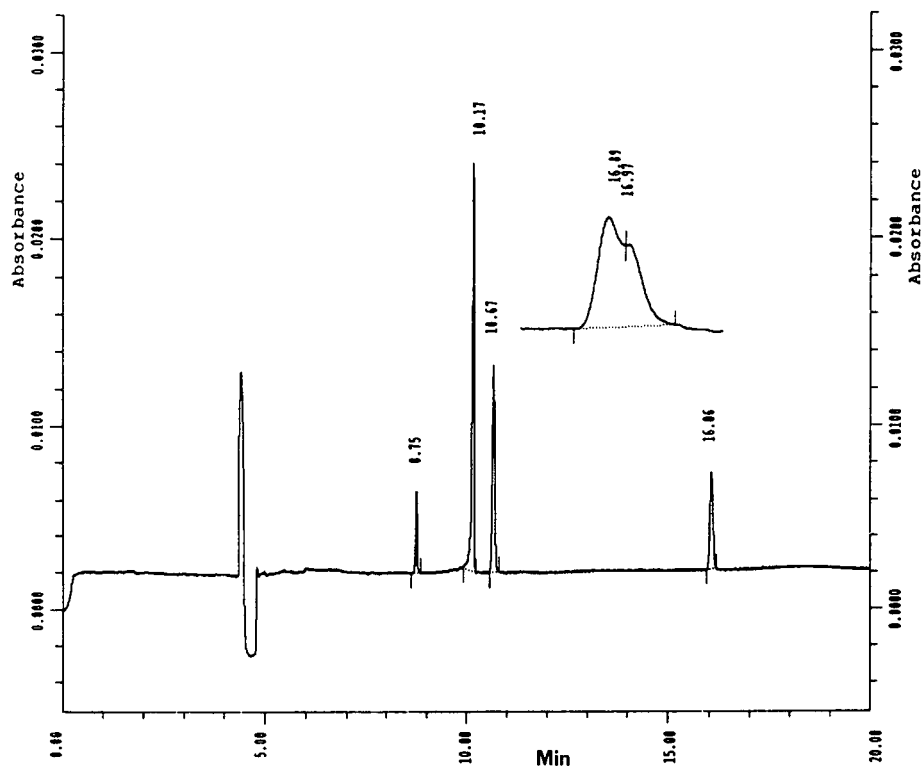


Fig. 3. Electropherograms of nicotinic, isonicotinic and picolinic acids under micellar conditions (pH 8.3, boric acid-sodium borate 50 mM, 100 mM sodium cholate). Picolinic acid MT = 10.17; isonicotinic and nicotinic MT = 10.67. Inset: nicotinic and isonicotinic acids partially resolved using 5% acetone additive in the buffer.

difficult to recover completely from the disk. The reason for the lower recovery of 5 in water is not clear to us. Again, factors related to recovery from the disk could be involved. The coextrac-

tives and minute soil particles retained on the disk apparently aided subsequent recovery of 5 from a soil matrix.

The precision of recovery indicated by the

TABLE VII
RECOVERY OF 7-STD IN SPIKED WATER

Analyte	Spike level 1.0 $\mu\text{g/g}$ ^a			Spike level 0.1 $\mu\text{g/g}$ ^b		
	Recovery (%)	Average	R.S.D.	Recovery (%)	Average	R.S.D.
1	88.9, 49.5, 88.1	75.5	30	42.2, 90.0, 77.3	69.8	36
2	86.0, 65.2, 44.4	65.2	32	45.3, 82.2, 74.6	67.4	29
3	101, 110, 93.0	101	8.4	44.4, 91.8, 88.7	75.0	35
4	109, 45.3, 91.5	81.9	40	48.0, 95.4, 89.5	77.6	33
5	50.8, 43.4, 20.2	38.1	42	64.9, 76.6, 42.1	61.2	29
6	91.4, 105, 98.3	98.2	6.9	36.4, 51.6, 89.1	59.0	46
7	81.9, 74.5, 72.2	76.2	6.7	41.0, 75.4, 82.7	66.4	34

^a Exact spike level for 1-7, respectively, in $\mu\text{g/g}$: 0.764; 0.92; 0.816; 1.592; 0.80; 1.024; 0.892.

^b Exact spike level for 1-7, respectively, in $\mu\text{g/g}$: 0.0955; 0.115; 0.102; 0.199; 0.100; 0.128; 0.1115.

TABLE VIII
RECOVERY OF 7-STD IN SPIKED SOIL

Analyte	Spike level 100 $\mu\text{g/g}^a$			Spike level 20 $\mu\text{g/g}^b$		
	Recovery (%)	Average recovery (%)	R.S.D. (%)	Recovery (%)	Average recovery (%)	R.S.D. (%)
1	93.1, 88.0, 102	94.4	7.5	89.5, 82.9, 104	92.1	12
2	90.3, 86.3, 101	92.5	8.2	80.3, 87.4, 105	90.9	14
3	89.2, 71.1, 80.7	80.3	11	90.9, 103, 76.2	89.9	15
4	25.8, 21.0, 37.5	28.1	30	11.2, 40.3, 28.1	26.5	55
5	92.7, 86.0, 103	93.9	9.1	83.2, 83.5, 105	90.6	14
6	74.7, 68.2, 41.4	61.4	29	82.9, 93.3, 93.2	89.8	6.7
7	83.3, 57.9, 41.6	60.9	34	83.3, 76.3, 86.7	83.1	7.1

^a Exact spike level for 1-7, respectively, in $\mu\text{g/g}$: 111; 106; 104; 226; 105.5; 117; 130.5.

^b Exact spike level for 1-7, respectively, in $\mu\text{g/g}$: 22.2; 21.2; 20.8; 45.2; 21.1; 23.4; 26.1.

R.S.D.s was higher for water than for soil, and reflects a variability that is not entirely understood. The lower recovery for water is also curious. The presence of free silanol groups on the bonded silica may be playing a role in retention and subsequent elution. These data, however, are comparable to extraction efficiencies and precision obtained with analytes as routine as organophosphorus pesticides [32]. In

TABLE IX
RECOVERY OF 7-STD IN SPIKED SOIL USING SOXHLET EXTRACTION AND REEXTRACTION AFTER SONICATION EXTRACTION

Analyte	Recovery (%)	
	100 $\mu\text{g/g}^a$	Soxhlet reextraction of sonicated soil 100 $\mu\text{g/g}^b$
1	96.7	13.1
2	96.5	12.4
3	112	13.1
4	48.8	10.1
5	55.3	10.3
6	113	6.9
7	96.3	6.2

^a Exact spike level for 1-7, respectively, in $\mu\text{g/g}$; see footnote *a* in Table VIII. ^b Exact spike level for 1-7, respectively, in $\mu\text{g/g}$; see footnote *a* in Table VIII.

that study, 17 organophosphorus pesticides recovered from water ranged in recovery from 7 to 98% and the R.S.D. from 7 to 38%. Further studies published on the application of SPE to a variety of semivolatile analytes using multiresidue methodology show a great variety of recoveries and precision that are not entirely understood [33,34]. It was postulated that the presence of other analytes affects recoveries in certain compound classes. This factor may be important in understanding the better recoveries we obtained from a soil matrix. Method variability from laboratory to laboratory is a well known and not always explicable phenomenon.

An example of an electropherogram of the OR fraction and the CL fraction is given in Fig. 5 for a spiked soil. Compound 6 is recovered in both fractions and is an example of breakthrough at pH 2. The peaks that result from analyzing the finished sample extract are less sharply focussed in a 10-s injection than those for the 7-STD. This is presumably due to the higher ionic strength of the finished extract that results in less focussing effect by field amplification [35] than that observed with standards. Drift in MT seen in comparing Figs. 4 and 5 was observed when comparing samples and standards run on different days. These variations can be minimized by doing complete changeouts of inlet and outlet buffer vials regularly. Use of internal standards

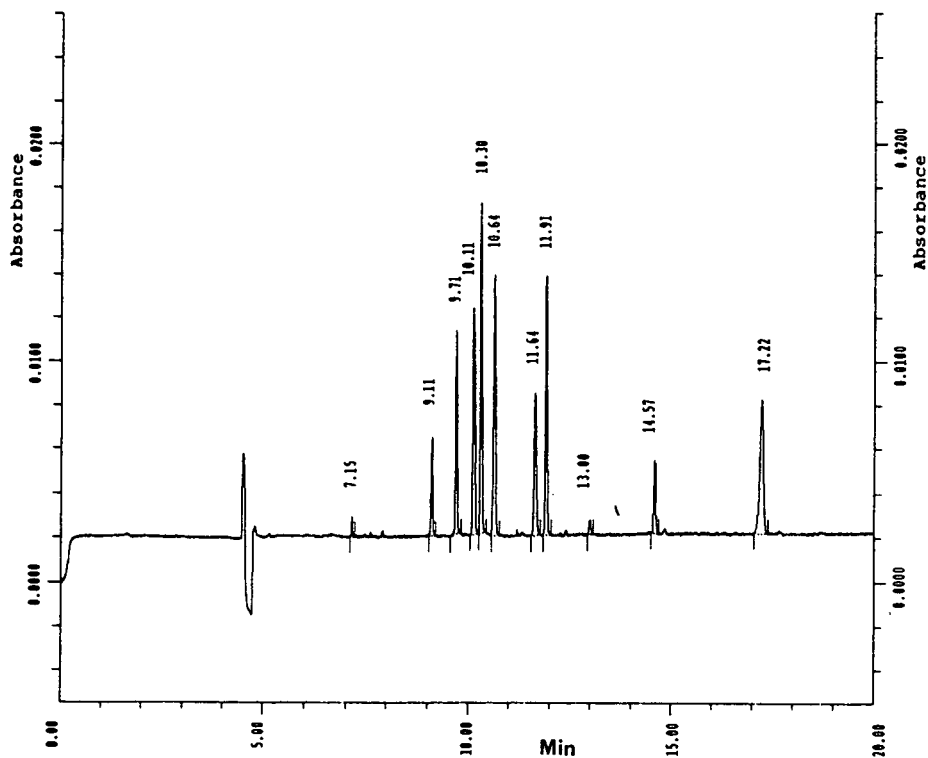


Fig. 4. Electropherogram of the 7-STD under micellar conditions. Identification of peaks: MT 9.11 = IS1; MT 9.71 = 1; MT 10.11 = 5; MT 10.30 = 2; MT 10.64 = 6; MT 11.64 = 7; MT 11.91 = 3; MT 14.57 = 4; MT 17.22 = IS2.

adequately compensates for observed variations which for IS2 varied over about a 3-min window before regular changeouts of buffer were instituted.

Compounds 1-7 encompass a wide range of structures and complexity. Extraction by SPE in this work depends upon controlling pH and modifying retention via ion-pairing reagents. The critical nature of any experimental parameters including the source of the disks and effects of coextractives may need to be assessed in a more systematic way. Although specialized procedures have been developed for specific classes of compounds, such as herbicides, the general approach that we present provides the foundation for a broad monitoring tool. It integrates the procedure for both water and soil determinations based on SPE from water and determination by MEKC. Where anticipated ACOAs are unstable at pH 2, the ion-pairing procedure used for 6 and 7 should result in an efficient isolation. Although

the OR and CL fractions may be combined and determined simultaneously, we feel the two-fraction determination increases the likelihood of obtaining good separations and recovery for complex samples.

Extraction comparison

Compounds were extracted from soil using a sonication method [5]. For comparison, recoveries from Soxhlet extraction of a soil are given in Table IX; both methods are comparable. In addition, a soil that was first extracted by sonication was reextracted by the Soxhlet method to estimate residues remaining. The sonication extraction performs well in terms of recovery, because we expected higher efficiency from the Soxhlet method. Trypan blue presents special difficulties as it even adheres to the final filter used before HPCE determination. It must be removed with methanol containing buffer.

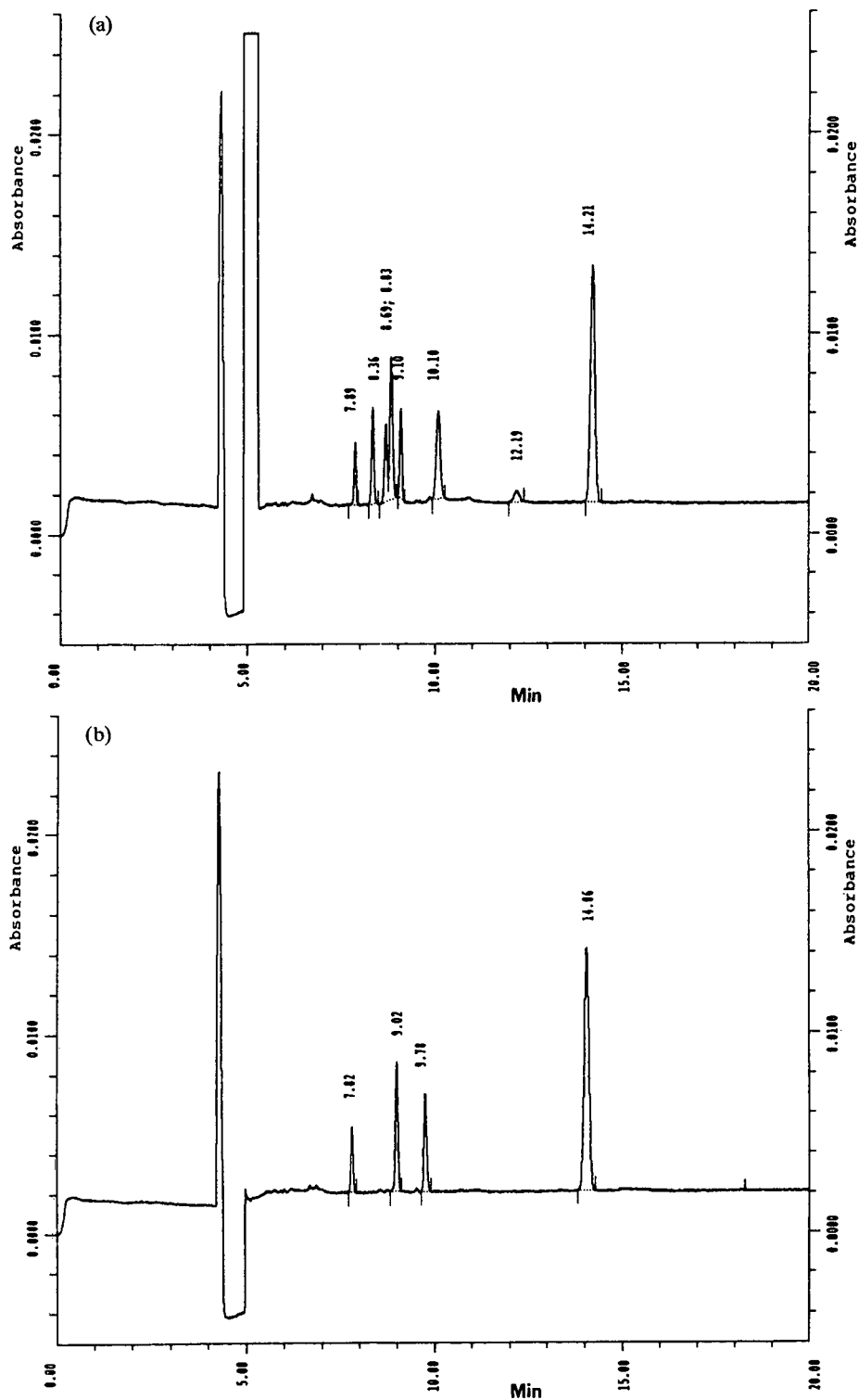


Fig. 5. Electropherogram of (a) OR fraction (1-6 from C₁₈ SPE, pH 2) and (b) CL fraction (6 and 7 from ion pairing, pH 6) after extraction/cleanup of a 20.0 μg/g spiked soil and run under micellar conditions. Peaks (a): MT 7.89 = IS1; MT 8.36 = 1; MT 8.69 = 5; MT 8.83 = 2; MT 9.10 = 6; MT 10.10 = 3; MT 12.19 = 4; MT 14.21 = IS2. Peaks (b): MT 9.02 = 6; MT 9.78 = 7.

Interferences to MEKC determination

The UV detection under MEKC is relatively non-specific. Therefore, a number of potential interferences to the determination of ACOAs exist. Under MEKC conditions using cholate as the micellar agent, neutral compounds will usually elute before IS1. This is due to the limited affinity of hydrophobic compounds and the enhanced affinity of anions for cholic acid micelles relative to micelles of sodium dodecyl sulfate (SDS). This particular specificity of cholic acid micelles makes them particularly applicable to anionic analytes. Presumably, the great difference in aggregation numbers between micelles of SDS and cholate affect anion affinities via charge repulsion [27].

Although further cleanup is not required at the levels studied, other matrices and soil types and lower detection levels may dictate the need for additional cleanup steps. Two complementary approaches are suggested. The first employs TLC separation of dyes, herbicides, and aromatic acids from polar and non-polar neutrals. Analytes may be recovered from the TLC plates, which can also serve as a sample screening technique. A second cleanup approach can be based on an ion-pairing technique using C₁₈ SPE cartridges (see Experimental section).

Cationic surfactants are removed in the SCX cleanup step. Anionic surfactants will be recovered in this scheme. If anionic surfactants interfere with the determination of ACOAs by MEKC, a separation based on RP C₁₈ cartridges, ion-pairing with C₁₈ cartridges, or TLC on silica should effect the necessary additional cleanup.

NOTICE

Although the research described in this report has been funded by the US Environmental Protection Agency, it has not been subjected to Agency review and, therefore, does not necessarily reflect the views of the Agency and no official endorsement should be inferred. Mention of trade names or commercial products does not constitute endorsement or recommendation for use.

REFERENCES

- 1 Appendix VIII; Resource Conservation and Recovery Act (RCRA), Part 261; Fed. Reg., 45, No. 98, May 19 (1980) 33132.
- 2 E.D. Lee, W. Muck, J.D. Henion and T.R. Covey, *Biomed. Environ. Mass Spectrom.*, 18 (1989) 844–850.
- 3 I.S. Kim, F.I. Sasinos, R.D. Stephens, J. Wang and M.A. Brown, *Anal. Chem.*, 63 (1991) 819–823.
- 4 L.D. Betowski, C.M. Pace and M.R. Roby, *J. Am. Soc. Mass Spectrom.*, 3 (1992) 823–830.
- 5 *Test Methods for Evaluating Solid Waste (SW-846)*, Vol. 1B, US Environmental Protection Agency, Washington, DC, 3rd ed., November 1986.
- 6 B. Lesnik, *Environ. Lab.*, Dec.–Jan. (1992–1993) 43–49.
- 7 C.F. Poole and S.A. Schuette, *Contemporary Practice of Chromatography*, Elsevier, Amsterdam, 1984, pp. 526–537.
- 8 M.A. Brown, I.S. Kim, R. Roehl, F.I. Sasinos and R.D. Stephens, *Chemosphere*, 19 (1989) 1921–1927.
- 9 T.A. Berger and J.F. Deye, *J. Chromatogr. Sci.*, 29 (1991) 26–30.
- 10 T.A. Berger and J.F. Deye, *J. Chromatogr. Sci.*, 29 (1991) 141–146.
- 11 M.A. Brown (Editor), *Liquid Chromatography/Mass Spectrometry (ACS Symposium Series, No. 420)*, American Chemical Society, Washington, DC, 1990.
- 12 T.L. Jones, L.D. Betowski and J. Yinon, in M.A. Brown (Editor), *Liquid Chromatography/Mass Spectrometry (ACS Symposium Series, No. 420)*, American Chemical Society, Washington, DC, 1990, pp. 62–74.
- 13 E.C. Huang and J.D. Henion, *Anal. Chem.*, 63 (1991) 732–739.
- 14 J.S.M. deWit, C.E. Parker, K.B. Tomer and J.W. Jorgenson, *Anal. Chem.*, 59 (1987) 2400–2404.
- 15 M.A. Mosely, L.J. Deterding, K.B. Tomer and J.W. Jorgenson, *Anal. Chem.*, 63 (1991) 1467–1473.
- 16 L.J. Sherma, *Anal. Chem.*, 64 (1992) 134R–147R.
- 17 J. Gartzke, D. Burch and R. Grahl, *J. Pharm. Biomed. Anal.*, 8(1990) 1087–1090.
- 18 G.P. Tomkinson, I.D. Wilson and R.J. Ruane, *J. Planar Chromatogr. Mod. TLC*, 2 (1989) 224–227.
- 19 G.P. Tomkinson, I.D. Wilson and R.J. Ruane, *J. Planar Chromatogr. Mod. TLC*, 3 (1990) 491–494.
- 20 J. Polanski and A. Ratajczak, *J. Chromatogr.*, 543 (1991) 195–200.
- 21 P. Jandik, W.R. Jones, A. Weston and P.R. Brown, *LC·GC*, 9 (1991) 634–645.
- 22 W.G. Kuhr and C.A. Monnig, *Anal. Chem.*, 64 (1992) 389R–407R.
- 23 M.A. Mosely, L.J. Deterding, K.B. Tomer and J.W. Jorgenson, *J. Chromatogr.*, 516 (1990) 167–173.
- 24 W.C. Brumley, *J. Chromatogr.*, 603 (1992) 267–272.
- 25 S. Fujimana and S. Honda, *Anal. Chem.*, 59 (1987) 487–490.
- 26 M.J. Nielen, *J. Chromatogr.*, 542 (1991) 173–183.
- 27 S. Terabe, *Micellar Electrokinetic Chromatography*, Beckman Instruments, Fullerton, CA, 1992.

- 28 H. Nishi, T. Fukuyama, M. Matsuo and S. Terabe, *J. Chromatogr.*, 513 (1990) 279–295.
- 29 S.A. Swedberg, *J. Chromatogr.*, 503 (1990) 449–452.
- 30 S. Terabe, T. Yashima, N. Tanaka and M. Araki, *Anal. Chem.*, 60 (1988) 1673–1677.
- 31 T.L. Ascah, *The Supelco Reporter*, XI (1992) 23–24.
- 32 *US Environmental Protection Agency (EPA) Report 600/4-87/009, Single Laboratory Validation of EPA Method 8140*, Environmental Monitoring Systems Laboratory, Las Vegas, NV, March 1987.
- 33 P.R. Loconto, *LC·GC*, 9 (1991) 460–465.
- 34 P.R. Loconto, *LC·GC*, 9 (1991) 752–760.
- 35 R.L. Chien and D.S. Burgi, *Anal. Chem.*, 64 (1992) 489A–496A.
- 36 L. Yoo, Y. Shen and S. Fitzsimmonds, presented at the *Division of Environmental Chemistry, 203rd National ACS Meeting, San Francisco, CA, April 5–10, 1992.*

The analysis of multiple phosphoseryl-containing casein peptides using capillary zone electrophoresis

Nicholas Adamson, Peter F. Riley and Eric C. Reynolds*

Biochemistry and Molecular Biology Unit, School of Dental Science, The University of Melbourne, 711 Elizabeth Street, Melbourne 3000 (Australia)

(First received February 18th, 1993; revised manuscript received June 1st, 1993)

ABSTRACT

Multiple phosphoseryl-containing sequences of peptides and proteins stabilize amorphous calcium phosphate at neutral and alkaline pH and have been implicated in the nucleation/regulation of biomineralization. In an approach to analyze these peptides using capillary zone electrophoresis (CZE) we have attempted to relate the absolute electrophoretic mobility of various casein phosphopeptides to their physicochemical properties. Multiple phosphoseryl-containing peptides were selectively precipitated from enzymic digests of sodium caseinate and further purified using RP-HPLC and anion-exchange fast protein liquid chromatography. Purified fractions were then analyzed by CZE. Absolute electrophoretic mobilities of 13 peptides were determined by measurement of migration times relative to that of a neutral marker, mesityl oxide. A linear relationship ($r^2 = 0.993$) was obtained between absolute electrophoretic mobility and $q/M_r^{2/3}$ where q is the net negative charge of the peptide calculated using relevant pK_a values and M_r is the molecular mass. $M_r^{2/3}$ is a measure of the surface area of a sphere that has a volume proportional to the M_r of the peptide and relates to the frictional drag exerted on the peptide during electrophoretic migration. As absolute electrophoretic mobility is influenced by charge and size CZE can be used to monitor peptide phosphorylation, dephosphorylation, deamidation and truncation. This technique therefore would be suitable for quantitative analysis of peptide substrates in kinase and phosphatase studies. In conclusion CZE is a rapid and efficient technique for the resolution of multiple phosphoseryl-containing peptides from enzymic digests of casein.

INTRODUCTION

Multiple phosphoseryl-containing sequences of peptides and proteins stabilize amorphous calcium phosphate at neutral and alkaline pH and have been implicated in the nucleation/regulation of biomineralization [1–3]. Casein tryptic peptides containing multiple phosphoseryl residues have potential as toothpaste, mouthwash and food additives for the prevention of dental caries [4]. The structure of these sequences and the relationship between structure and function, particularly in calcium phosphate stabilization, anticariogenicity and biomineralization is as yet

unclear. To obtain insight into the structure and function of these peptides it is first essential to develop analytical techniques for their purification and characterization.

Capillary zone electrophoresis (CZE) has been used extensively in the separation and characterization of proteins and peptides. The advantages of CZE are high resolution, rapid automated analyses and minimal sample requirements [5–11]. CZE has also shown potential as a useful tool for the determination of structure when used to exploit the orientation of molecules in free solution under the influence of an electric field [12]. Relatively few workers however have attempted to relate the absolute electrophoretic mobilities (μ) of peptides and proteins to their physicochemical properties. Offord [13] has shown a linear relationship between

* Corresponding author.

paper electrophoretic mobilities of a series of charged peptides and their molecular mass to the power of $-2/3$. Grossman *et al.* [5] proposed a semi-empirical model which related the electrophoretic mobilities of a range of positively charged peptides to their size, charge and hydrophobicity. The effects of size and charge were determined independently and then combined to show a linear relationship between μ and $\ln(q + 1)/n^{0.43}$ where n is the number of amino acids in the polypeptide chain and q is the net negative charge of the peptide. Rickard *et al.* [11] using CZE have recently shown a linear correlation of absolute electrophoretic mobility for various peptides with $q/M_r^{2/3}$ over a range of pH values. The correlation was the best of three relationships investigated proving more suitable than mobility against $q/M_r^{1/3}$ or $q/M_r^{1/2}$.

Absolute electrophoretic mobility (μ) is proportional to the net charge and inversely proportional to the frictional properties of a molecule, the latter being determined by its size and shape [11,12]. Assuming that the structure of the peptides in the capillary can be approximated by a sphere of constant density, then the radius of the sphere would be proportional to the molecular mass raised to the $1/3$ power ($M_r^{1/3}$). Hence, if frictional drag is governed by Stokes law then absolute electrophoretic mobility would be related to the radius of the species *i.e.* proportional to $M_r^{1/3}$ [11]. However, if frictional drag is related to the surface area (or cross-sectional area) of the molecule absolute electrophoretic mobility would be proportional to $M_r^{2/3}$ [13].

From studies of synthetic polymers it has been shown that the average radius of gyration is proportional to the square root of the number of polymer units multiplied by the length of a single unit [14]. Rickard *et al.* [11] concluded from this that if the frictional drag were proportional to the average radius of gyration it would be proportional to the square root of the number of residues (*ca.* $M_r^{1/2}$).

In an approach to characterize multiple phosphoserine-containing peptides using capillary zone electrophoresis we have related the absolute electrophoretic mobility of various casein phosphopeptides to their physicochemical properties.

MATERIALS AND METHODS

Sodium caseinate was obtained from Murray Goulburn (Melbourne, Australia). Trypsin (E.C. 3.4.21.4) was purchased from Sigma (St. Louis, MO, USA) and pancreatin from Southern Cross Laboratories (Dural, NSW, Australia). Mesityl oxide was obtained from BDH (Melbourne, Australia), disodium tetraborate from AJAX (Sydney, Australia) and trifluoroacetic acid (TFA) from Pierce (Rockford, IL, USA). All other chemicals were of the highest purity analytical grade available.

Preparation of multiple phosphoserine-containing casein peptides

Multiple phosphoserine-containing peptides were selectively precipitated from enzymic digests of casein using calcium and ethanol as described previously [4,15]. Sodium caseinate [96% (w/w) protein, 20 mg/ml] was dissolved in 20 mM Tris-HCl pH 8.0 to which trypsin or pancreatin was added at 0.4 mg/ml. Hydrolysis was carried out at 50°C for 2 h and stopped by the addition of 1 M HCl to pH 4.6. Insoluble material was removed by centrifugation (12000 g, 15 min) and the multiple phosphoserine-containing peptides selectively precipitated from the hydrolysate by the addition of CaCl_2 to 1.0% (w/v) and ethanol to 50% (v/v). The selectively precipitated casein phosphopeptides were further purified using reversed-phase HPLC (Brownlee AQUAPORE RP-300, 220 × 4.6 mm, C_8 column, ABI, Australia) and anion-exchange fast protein liquid chromatography (FPLC) (Mono Q HR 5/5, Pharmacia-LKB, Australia) and characterized using amino acid composition and sequence analyses [4].

The multiple phosphoserine-containing casein peptides obtained and used in this study are listed in Table I together with their physicochemical properties.

Analysis of multiple phosphoserine-containing casein peptides by capillary zone electrophoresis

Peptides were dissolved in Milli Q water or 0.1% TFA (1 mg/ml) and analyzed by capillary zone electrophoresis (CZE) using an Applied

TABLE I

PHYSICO-CHEMICAL PROPERTIES AND ABSOLUTE ELECTROPHORETIC MOBILITIES OF VARIOUS MULTIPLE PHOSPHOSERYL-CONTAINING PEPTIDES FROM CASEIN TRYPTIC AND PANCREATIC DIGESTS

Peptide ^a	M_r ^b	Net negative charge ^c pH 9.2	μ ^d (cm ² /Vs) · 10 ⁴
$\beta(1-25)$	3125	13.91	3.223 ± 0.069
$\beta(2-25)$	2969	14.91	3.487 ± 0.111
$\alpha_{s1}(59-79)$	2721	15.04	3.629 ± 0.017
[Glp ⁵⁹] $\alpha_{s1}(59-79)$	2721	15.07	3.660 ± 0.016
[Glu ⁵⁹] $\alpha_{s1}(59-79)$,	2721	16.04	3.785 ± 0.015
[Glu ⁷⁸] $\alpha_{s1}(59-79)$			
$\alpha_{s2}(46-70)$	3009	16.06	3.629 ± 0.017
$\alpha_{s2}(3-21)$	2505	12.00	3.223 ± 0.069
$\alpha_{s2}(2-21)$	2619	12.06	3.193 ± 0.009
$\beta(7-24)$	2200	12.99	3.596 ± 0.013
$\alpha_{s1}(61-76)$	2076	14.91	4.082 ± 0.022
$\alpha_{s1}(64-75)$	1648	12.99	4.236 ± 0.026
$\alpha_{s1}(61-75)$	1977	14.91	4.267 ± 0.009

^a Primary structure of peptides $\beta(1-25)$, RELEELNVPGEIVEΣLΣΣΣEESITR; $\alpha_{s1}(59-79)$, QMEAEΣIΣΣΣEEIVPNΣVEQK; $\alpha_{s2}(46-70)$, NANEEEYISIGΣΣΣEEΣAEVATEEVK; $\alpha_{s2}(2-21)$, NTMEHVΣΣΣEESIIΣQETVK where Σ = Ser(P).

^b Calculated using free acid residue masses.

^c Calculated using Ser(P) pK_{a1} 1.5, pK_{a2} 6.48 [16]; Lys pK_{aε} 10.30; Arg pK_a(guanidino) 12.50 [17]; Glu pK_{aγ} 4.85; Asp pK_{aβ} 4.85 [18]; N-terminus and C-terminus pK_a values from Rickard *et al.* [11].

^d cm = Capillary length (72 cm), V = volts applied (30 kV), s = seconds.

Biosystems 270A instrument. Separation conditions consisted of 30 kV applied voltage at 30°C with 20 mM sodium tetraborate pH 9.2 as the running buffer. Samples were introduced at the anode into a capillary of length 72 cm by creating an intracapillary vacuum (17 kPa) for a specified time (0.5–1.0 s). Peptides were detected by UV absorbance at 200 nm using a variable wavelength detector situated 50 cm along the capillary. The instrument was hardwired to an IBM AT compatible PC and data were collected by a Galactic LAB CALC. data processing and acquisition software package. Absolute electrophoretic mobility of the purified peptides was calculated from measurement of migration time relative to that of a neutral marker, mesityl oxide. Absolute electrophoretic mobility, μ is defined as migration velocity per unit electrical field strength. Measurements made by CZE result in the determination of apparent electrophoretic mobility, μ_{app} which is dependent upon the electrophoretic migration of the analyte (μ) as

well as the electroosmotic flow of the buffer. μ_{app} is defined by the equations

$$\mu_{app} = \mu + \mu_{eo} \quad (1)$$

$$\mu_{app} = v_{net}/E = L_d L_t / t_m V \quad (2)$$

where μ_{eo} is the electroosmotic component of the apparent mobility, v_{net} is the net (measured) migration velocity, E is the electrical field strength, L_d is the length of the capillary from the injection end to the detector, L_t is the total length of the capillary, V is the applied voltage over that length, and t_m is the measured electrophoretic migration time in seconds. Similarly μ_{eo} is defined by the relationship

$$\mu_{eo} = v_{eo}/E = L_d L_t / t_{eo} V \quad (3)$$

where v_{eo} is the electroosmotic velocity and t_{eo} is the migration time for a neutral molecule whose motion through the capillary is due solely to electroosmosis. Measurement of the migration time for a neutral molecule hence allows

the calculation of μ_{e0} from eqn. 3. Absolute electrophoretic mobility of each multiple phosphoserine-containing casein peptide was calculated from its measured electrophoretic migration time using eqns. 1, 2 and 3. Net charge of the peptides at pH 9.2 was calculated using Ser(P) pK_{a1} 1.5, pK_{a2} 6.4 [16]; Lys pK_{ae} 10.30; Arg pK_a (guanidino) 12.50 [17]; Glu $pK_{a\gamma}$ 4.85; Asp $pK_{a\beta}$ 4.85 [18]; N-terminus and C-terminus pK_a values from Rickard *et al.* [11].

RESULTS

Representative electropherograms obtained from CZE of selectively precipitated multiple phosphoserine-containing peptides from a tryptic (A) and pancreatic (B) digest of casein are shown in Fig. 1. Thirteen peptides were purified from these selective precipitates using anion-exchange FPLC and reversed-phase HPLC and the electrophoretic migration times measured relative to that of a neutral marker, mesityl oxide using CZE. The peptides obtained were $\beta(1-25)$ and truncated forms, $\alpha_{s1}(59-79)$ and its deamidated and truncated forms and minor amounts of

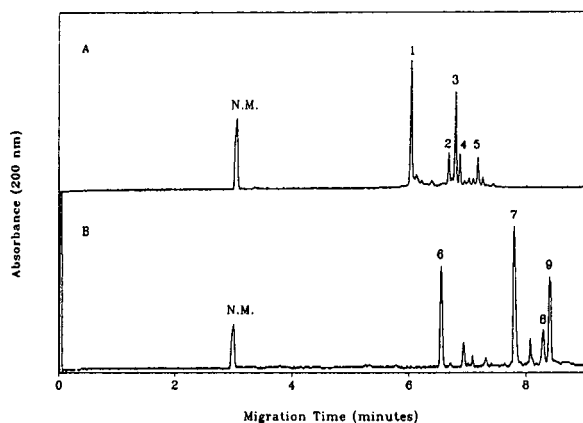


Fig. 1. Electropherogram from CZE of a mixture of multiple phosphoserine-containing peptides purified from (A) casein tryptic and (B) pancreatic digests. Peak 1 = $\beta(1-25)$ and $\alpha_{s2}(3-21)$; peak 2 = $\beta(2-25)$; peak 3 = $\alpha_{s1}(59-79)$ and $\alpha_{s2}(46-70)$; peak 4 = $[\text{Glp}^{59}]\alpha_{s1}(59-79)$; peak 5 = $[\text{Glu}^{59}]\alpha_{s1}(59-79)$ and $[\text{Glu}^{78}]\alpha_{s1}(59-79)$; peak 6 = $\beta(7-24)$; peak 7 = $\alpha_{s1}(61-76)$; peak 8 = $\alpha_{s1}(64-75)$ and peak 9 = $\alpha_{s1}(61-75)$. Peak "N.M." is the neutral marker peak, mesityl oxide. Conditions: 30 kV applied voltage, 30°C, 20 mM sodium tetraborate pH 9.2, capillary length = 72 cm, detection $\lambda = 200$ nm, detector 50 cm along capillary.

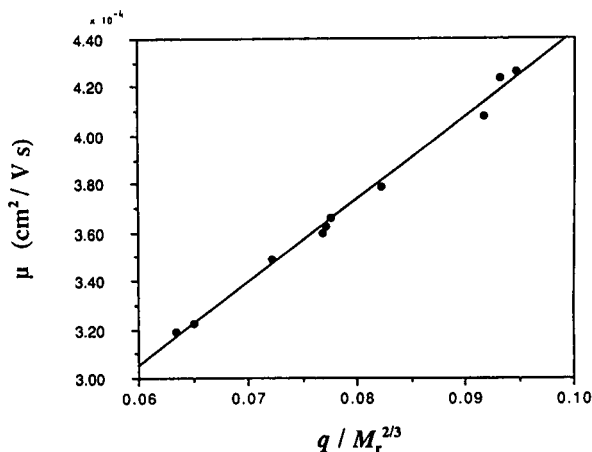


Fig. 2. The relationship between absolute electrophoretic mobility (μ) and $q/M_r^{2/3}$ for 13 multiple phosphoserine-containing peptides purified from casein tryptic and pancreatic digests.

the multiple phosphoserine-containing peptides from α_{s2} -casein, $\alpha_{s2}(46-70)$ and $\alpha_{s2}(2-21)$. The truncation presumably resulted through exopeptidase activity in the crude pancreatin. Absolute electrophoretic mobilities (μ) were calculated using the migration times obtained for the purified peptides and are presented in Table I along with the net negative charge and molecular mass of each peptide. Absolute electrophoretic mobility was related to $q/M_r^{2/3}$ (Fig. 2), $q/M_r^{1/2}$ (Fig. 3), $\ln(q+1)/n^{0.43}$ (Fig. 4) and $q/M_r^{1/3}$

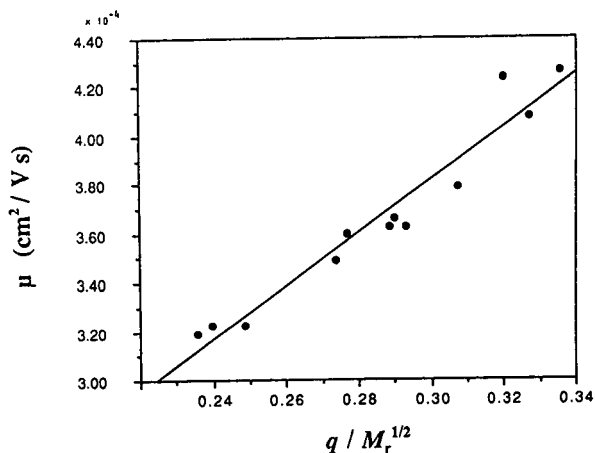


Fig. 3. The relationship between absolute electrophoretic mobility (μ) and $q/M_r^{1/2}$ for 13 multiple phosphoserine-containing peptides purified from casein tryptic and pancreatic digests.

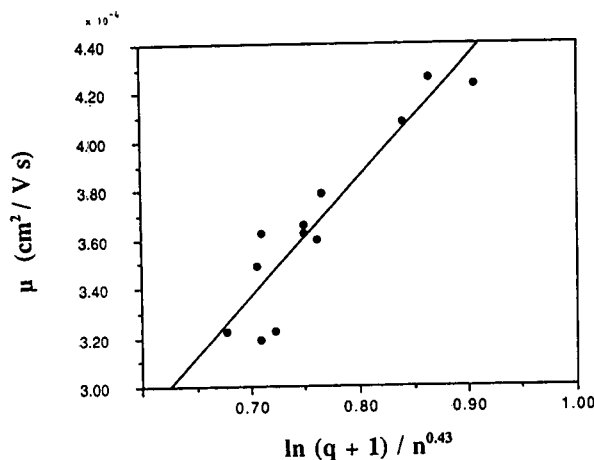


Fig. 4. The relationship between absolute electrophoretic mobility (μ) and $\ln(q+1)/n^{0.43}$ for 13 multiple phosphoserine-containing peptides purified from casein tryptic and pancreatic digests.

(Fig. 5). All relationships were linear, however absolute electrophoretic mobility was most closely correlated ($r^2 = 0.993$) with $q/M_r^{2/3}$, followed by $q/M_r^{1/2}$ ($r^2 = 0.941$), $\ln(q+1)/n^{0.43}$ ($r^2 = 0.861$) and then $q/M_r^{1/3}$ ($r^2 = 0.755$).

DISCUSSION

In this study we have shown capillary zone electrophoresis (CZE) to be a rapid method for

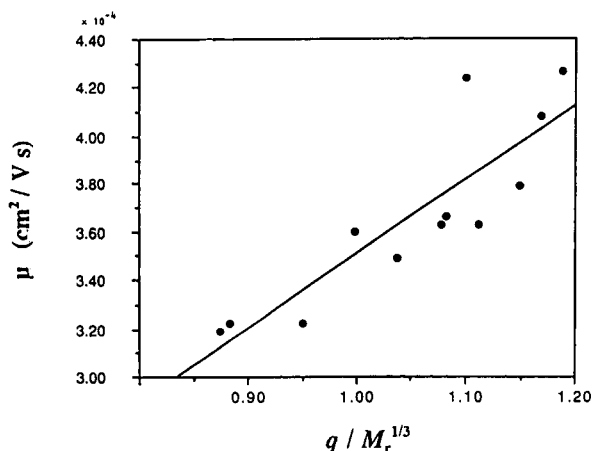


Fig. 5. The relationship between absolute electrophoretic mobility (μ) and $q/M_r^{1/3}$ for 13 multiple phosphoserine-containing peptides purified from casein tryptic and pancreatic digests.

the resolution and characterization of multiple phosphoserine-containing casein peptides. Analysis of a selective precipitate of phosphorylated peptides from a tryptic casein hydrolysate revealed baseline resolution of 5 major peaks (Fig. 1A) in less than 8 min. The peptides of this selective precipitate were purified using a combination of reversed-phase HPLC and anion-exchange FPLC into 8 different phosphopeptides however this proved a much more complex and time consuming procedure [4].

Absolute electrophoretic mobility (μ) of the multiple phosphoserine-containing peptides was most closely correlated with $q/M_r^{2/3}$. Rickard *et al.* [11] also found that the absolute electrophoretic mobility of a set of non-phosphorylated peptides with isoelectric points of 3.35–13.10 correlated closely with $q/M_r^{2/3}$. The results presented here therefore confirm and extend this relationship to include multiple phosphoserine-containing peptides with isoelectric points of 2.0 and less. It is interesting to note however that we obtained a closer association between, $q/M_r^{1/2}$ and μ with the casein phosphopeptides than did Rickard *et al.* [11] with non-phosphorylated peptides. Spectroscopy studies on multiple phosphoserine-containing proteins, for example phosphovitin [19] and phosphophoryn [20] indicate that multiple phosphorylation appears to destabilize secondary and tertiary structure promoting flexibility. Although little work has been done on the conformation of the multiple phosphoserine-containing casein peptides some information is available on the structures of the caseins. Optical rotatory dispersion, circular dichroism and $[^{31}\text{P}]\text{NMR}$ measurements all indicate that α_{s1} -casein and β -casein have a rather open structure in solution with many amino acid side chains exposed to solvent and relatively flexible [21]. $[^{31}\text{P}]\text{NMR}$ relaxation measurements indicate that Ser(P) residues are relatively mobile in β -casein [19]. Further, Chaplin *et al.* [22] have reported the secondary structure of the casein phosphopeptide $\beta(1-28)$ to be composed of β -structure and random coil. It is possible that the better correlation obtained between μ and $q/M_r^{1/2}$ with multiple phosphoserine-containing casein peptides relates to their relative flexibility during capillary migration compared with the

structures of the peptides studied by Rickard *et al.* [11].

The results of this study show that the absolute electrophoretic mobility of multiple phosphoserine-containing peptides is influenced by charge and size such that CZE is an efficient technique for monitoring peptide phosphorylation, dephosphorylation, deamidation and truncation. The ability of CZE to rapidly resolve peptides which exhibit varying degrees of phosphorylation would make it ideal for the rapid and quantitative analysis of peptide substrates in kinase and phosphatase studies. In conclusion CZE is a rapid and efficient technique for the resolution of multiple phosphoserine-containing peptides from a tryptic digest of casein.

ACKNOWLEDGEMENTS

N.A. is the recipient of a Dairy Research and Development Corporation fellowship award. The financial assistance of the Victorian Dairy Industry Authority is gratefully acknowledged.

REFERENCES

- 1 R.E. Reeves and N.G. Latour, *Science*, 128 (1958) 472.
- 2 M.E. Marsh, *Biochemistry*, 28 (1989) 346–352.
- 3 T. Negata, C.G. Bellows, S. Kasugai, W.T. Butler and J. Sodek, *Biochem. J.*, 247 (1991) 513–520.
- 4 E.C. Reynolds, *US Pat.*, 5 015 628 (1991).
- 5 P.D. Grossman, J.C. Colburn and H.H. Lauer, *Anal. Biochem.*, 179 (1989) 28–33.
- 6 P.D. Grossman, J.C. Colburn, H.H. Lauer, R.G. Nielsen, R.M. Riggan, G.S. Sittampalam and E.C. Rickard, *Anal. Chem.*, 61 (1989) 1186–1194.
- 7 R.G. Nielsen, R.M. Riggan and E.C. Rickard, *J. Chromatogr.*, 480 (1989) 393–401.
- 8 R.G. Nielsen, G.S. Sittampalam and E.C. Rickard, *Anal. Biochem.*, 177 (1989) 20–26.
- 9 M. Zhu, R. Rodriguez, D. Hansen and T. Wehr, *J. Chromatogr.*, 516 (1990) 123–31.
- 10 R.G. Nielsen and E.C. Rickard, *J. Chromatogr.*, 516 (1990) 99–114.
- 11 E.C. Rickard, M.M. Strohl and R.G. Nielsen, *Anal. Biochem.*, 197 (1991) 197–207.
- 12 P.D. Grossman and D.S. Soane, *Anal. Chem.*, 62 (1990) 1592–1596.
- 13 R.E. Offord, *Nature*, 211 (1966) 591–593.
- 14 C.H. Tanford, *Physical Chemistry of Macromolecules*, Wiley, New York, 1961, Ch. 3.
- 15 R.F. Peterson, L.W. Nauman and T.L. McMeekin, *J. Am. Chem. Soc.*, 80 (1958) 95–99.
- 16 L.K. Creamer, *Biochim. Biophys. Acta*, 271 (1972) 252–261.
- 17 H.E. Swaisgood, in P.F. Fox (Editor), *Developments in Dairy Chemistry-1. Proteins*, Applied Science Publishers, New York, London, 1982, Ch. 1.
- 18 C. Ho and D.F. Waugh, *J. Am. Chem. Soc.*, 87(1) (1965) 110–117.
- 19 B. Prescott, V. Renugopalakrishnan, M.J. Glimcher, A. Bhushan and G.J. Thomas Jr., *Biochemistry*, 25 (1986) 2792–2798.
- 20 D.J. Cookson, B.A. Levine, R.J.P. Williams, M. Jantell, A. Linde and B. Bernard, *Eur. J. Biochem.*, 110 (1980) 273–278.
- 21 R.S. Humphrey and K.W. Jolley, *Biochim. Biophys. Acta*, 208 (1982) 294–299.
- 22 L.C. Chaplin, D.C. Clark and L.J. Smith, *Biochim. Biophys. Acta*, 956 (1988) 162–172.

Micellar electrokinetic capillary chromatography of haematoporphyrin, protoporphyrin and their copper and zinc complexes

Chikara Kiyohara, Koichi Saitoh* and Nobuo Suzuki

Department of Chemistry, Faculty of Science, Tohoku University, Sendai, 980 Miyagi (Japan)

(First received November 17th, 1992; revised manuscript received May 14th, 1993)

ABSTRACT

The micellar electrokinetic chromatographic separation of haematoporphyrin IX (HP) and protoporphyrin IX (PP) in the forms of free acids and of metal complexes with zinc or copper is successful in a mixture of a micellar solution of sodium dodecyl sulphate (SDS) at pH 11 and dimethylformamide (10:2, v/v). All the porphyrins migrate in the direction of the electric field, *i.e.*, from the positive end towards the grounded end of the capillary. The migration time of each porphyrin increases with increasing concentration of DMF in the carrier solution. The capacity factor calculated for the distribution of each porphyrin compound between the SDS micelles and the bulk solution varies nearly linearly with the concentration of the SDS micelles. The migration sequence, that is, the increasing order of migration time, for the porphyrins is Zn(HP) < H₂HP < Cu(HP) < Zn(PP) < H₂PP < Cu(PP).

INTRODUCTION

There are two types of separation for porphyrins and metalloporphyrins: (1) their separation in either the free acid form or the complexed form with a certain metal in accordance with the difference in the molecular structure of the porphyrin and (2) their separation in accordance with the complexing metal ion. The latter type of separation is generally the more difficult because each metal ion is surrounded by a bulky macrocyclic structure of porphyrin. High-performance thin-layer chromatography (HPTLC) [1,2] and column high-performance liquid chromatography (HPLC) [3,4] have been promising methods for both types of separation of metalloporphyrins and porphyrins.

Recently, there has been increased interest in the high separation ability of capillary zone

electrophoresis (CZE) and also its expanded mode, micellar electrokinetic capillary chromatography (MEKC) [5]. The applicability of MEKC to the separation of metal complexes was previously confirmed for non-charged bis- and trisacetylacetonato complexes of di- and trivalent metals using a micellar solution of sodium dodecyl sulphate (SDS) as the carrier solution [6,7].

This work was undertaken in order to examine the feasibility of MEKC for the separation of metalloporphyrins in accordance with both their central metal ions and their porphyrin structures. With regard to the metal-free forms of porphyrins, MEKC separation of urinary porphyrins has already been reported by Weinberger *et al.* [8]. Two typical bioporphyrins, *viz.*, haematoporphyrin IX (HP) and protoporphyrin IX (PP), were considered in this work. The migration behaviour of the respective porphyrins in the free acid forms and the complexed forms with copper(II) and zinc(II) was investigated using

* Corresponding author.

different conditions of the electrophoretic carrier solution.

EXPERIMENTAL

Materials

Fig. 1 shows the structures of free acid forms of HP and PP (H_2HP and H_2PP , respectively) and the corresponding metal complexes $[M(HP)]$ and $M(PP)$, in general.

H_2HP (Wako, Osaka, Japan) was purified as detailed elsewhere [9]. Copper haematoporphyrin $[Cu(HP)]$ and zinc haematoporphyrin $[Zn(HP)]$ were prepared by reaction of H_2HP with copper chloride and zinc acetate in mixtures of dimethyl sulphoxide (DMSO) and water, respectively [10].

H_2PP was purified from its sodium salt (Green Cross, Osaka, Japan) as follows. The sodium salt of the porphyrin (120 mg) was taken in 40 ml of acetone–water (7:3, v/v), and the non-dissolved fraction was removed by centrifugation. A 20-ml portion of this solution was diluted with 240 ml of buffer solution (3.5 mM H_3PO_4 –19.9 mM NaH_2PO_4 , pH 3), followed by shaking with 320 ml of ethyl acetate. The organic phase was washed with 200 ml of water, then H_2PP was precipitated by adding 2,2,4-trimethylpentane. The purified H_2PP was dried under vacuum.

Copper protoporphyrin $[Cu(PP)]$ was prepared by the reaction of H_2PP (8.6 μ mol) and copper acetate (38 μ mol) in 4 ml of *N,N*-dimethylformamide (DMF) at 80°C for 1 h. After

been cooled near to the room temperature, the reaction mixture was shaken with a mixture of 50 ml of ethyl acetate and 40 ml of 2.4 M hydrochloric acid for several minutes. The organic phase was washed four times with 30 ml each of water and then concentrated by removal of the solvent under vacuum. Finally, $Cu(PP)$ was precipitated by addition of 2,2,4-trimethylpentane. Zinc protoporphyrin $[Zn(PP)]$ was synthesized by the reaction of H_2PP (6.8 μ mol) with zinc acetate (20.1 μ mol) in 2 ml of DMSO at 80°C for 15 h. The reaction mixture was shaken with a mixture of 50 ml of ethyl acetate and 40 ml of water. $Zn(PP)$ was precipitated from the organic phase by procedures similar to those for the preparation of $Cu(PP)$. Identification of the final products of $Cu(PP)$ and $Zn(PP)$ was performed by UV–visible and mass spectrometry.

CAPS buffer (pH 11) was prepared so as to contain 20 mM 3-cyclohexylaminopropanesulphonic acid (CAPS) (Dojin Labs., Kumamoto, Japan) and 17 mM sodium hydroxide.

The hydrophobic pigment Oil Yellow OB [α -(*o*-tolylazo)- β -naphthylamine] (Tokyo Kasei, Tokyo, Japan) was used as a reference substance for monitoring the migration of the SDS micelle.

Apparatus and conditions

A Model CE890 capillary electrophoretic separation system (JASCO, Tokyo, Japan) was used with a fused-silica capillary (70 cm \times 50 μ m I.D.). Spectrophotometric detection was carried out 50 cm from the positive end of the capillary. The carrier solution was prepared by mixing, immediately before use, the desired amounts of DMF and the CAPS buffer (pH 11) containing SDS at a certain concentration, unless indicated otherwise. A typical composition of the carrier solution was 40 mM SDS in CAPS buffer–DMF (10:2, v/v). The sample solution of a porphyrin or a porphyrin mixture was prepared at a concentration of 10^{-4} M for each porphyrin in an identical solution to the carrier solution. Introduction of sample solution (about 4 nl) into the capillary was performed with the aid of an electroinjection technique. Electrophoretic experiments were carried out with an applied voltage of 30 kV (electric field strength along the

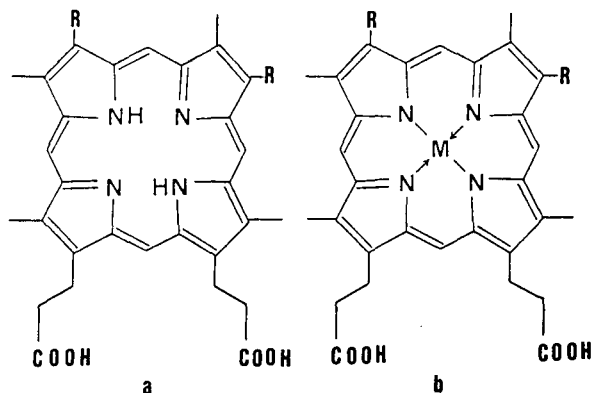


Fig. 1. Structural formulae of (a) porphyrin and (b) its metal (M) complex. R = $-CH(OH)CH_3$ for H_2HP and $M(HP)$ and $-CH=CH_2$ for H_2PP and $M(PP)$.

capillary 429 V/cm) and at a detection wavelength of 405 nm.

RESULTS AND DISCUSSION

Carrier solution

The electroosmosis of an aqueous solution occurring in a fused-silica capillary generally takes place in the direction of the electric field, *i.e.*, from the positive end towards the grounded end of the capillary, and the velocity of the electroosmotic flow increases with increasing pH of the solution. In this study, the carrier solution filled in the capillary was CAPS buffer of pH 11 (20 mM CAPS–17 mM NaOH), so that a strong electroosmotic flow of the solution would occur.

All the porphyrin compounds studied were regarded as anionic in a basic solution owing to the dissociation of carboxylic protons from respective molecules. It was reasonable to consider that the migration of the anionic form of each porphyrin compound would be governed by its electrophoretic motion toward the positive end of the capillary in addition to the electroosmotic flow of the carrier solution in the opposite direction. When the feasibility of the CZE separation of H₂HP, Cu(HP) and Zn(HP) was preliminarily examined simply using the CAPS buffer alone, these three HP compounds moved towards the negative end of the capillary and were detected at migration times of 6.5, 6.8 and 5.6 min, respectively, at an electric field strength of 269 V/cm. This implied that the velocity components of the electrophoresis for these negatively charged HP species were smaller than that of the electroosmosis of the solution.

When SDS was added to the buffer solution noted above, the solubility of each porphyrin was improved. The addition of SDS, however, resulted in a decrease in the reproducibility of the migration velocities (and times) of porphyrins. The migration times (t_s) of H₂HP and Cu(HP) in particular increased successively with repetition of the CZE runs. For example, the t_s values for H₂HP were 9.83, 10.39, 11.26 and 14.50 min in the first, third, fifth and eighth runs, respectively, with CAPS buffer containing 25 mM SDS and at an applied voltage of 30 kV. Such undesirable effects were not observed with

Zn(HP) and Oil Yellow OB. However, the migration velocity of these two compounds also decreased after the sample solution containing H₂HP and/or Cu(HP) had been injected into the capillary. These undesirable phenomena were presumably caused by the adsorption of H₂HP and/or Cu(HP) on the inner surface of the capillary.

When DMF was added at levels up to 10% (v/v), instead of SDS, to the buffer solution, the reproducibility was not improved, although the solubility of each porphyrin was improved. It was found that the problems of both the reproducibility of the migration velocity and low solubility of these HP compounds could be solved by using buffer solution containing both SDS and DMF. For example, the t_s values for H₂HP were 7.14 and 7.16 min in the first and third runs, respectively, when using the DMF–CAPS buffer (pH 11) (20:80, v/v) containing 25 mM SDS and an applied voltage of 30 kV.

Effect of DMF concentration

In this study DMF was used as an organic additive to the carrier solution, considering its high dissolving capability for porphyrins, high dielectric constant (36.7 D) and low viscosity (0.80 cP).

When a buffer solution (pH 11) containing 50 mM SDS was used as the carrier solution, the migration times of each porphyrin (t_s), carrier solution (t_0) and SDS micelle (t_{mc}) increased with increasing concentration of DMF in the carrier solution, as shown in Fig. 2, where t_0 and t_m were estimated from the migration times of a non-retained system peak and Oil Yellow OB, respectively. It is obvious that the difference in t_s values among the porphyrin compounds increases with increasing DMF content.

Effect of SDS concentration

The formation of micelles of SDS in a DMF-containing solution was examined by conductivity. Fig. 3 shows the variation of the specific conductivity change ($\Delta\kappa$) and the molar conductivity (Λ) of SDS with the total concentration of SDS (C_{SDS}) in CAPS buffer (pH 11)–DMF (10:2, v/v). The break of the proportionality between the specific conductivity change ($\Delta\kappa$)

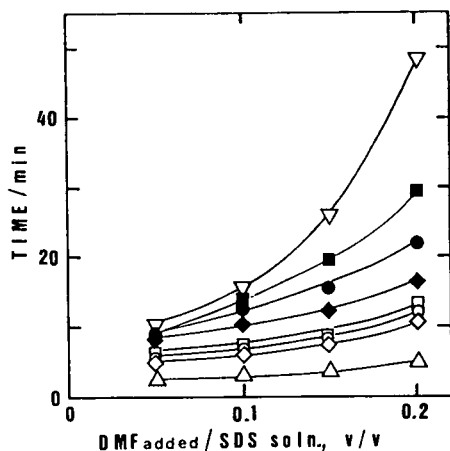


Fig. 2. Effect of addition of DMF to a carrier solution (volume ratio) on t_s of porphyrin compounds, t_0 and t_{mc} . Carrier solution, 50 mM SDS-20 mM CAPS-17 mM NaOH; capillary, 70 cm \times 50 μ m I.D.; effective migration length, 50 cm; applied voltage, 30 kV. $\circ = t_{s,H_2HP}$; $\square = t_{s,Cu(HP)}$; $\diamond = t_{s,Zn(HP)}$; $\bullet = t_{s,H_2PP}$; $\blacksquare = t_{s,Cu(PP)}$; $\blacklozenge = t_{s,Zn(PP)}$; $\triangle = t_0$; $\nabla = t_{mc}$.

and C_{SDS} indicates the formation of micelles of SDS in the solution. From the break point, the critical micelle concentration (CMC) of SDS is estimated to be about 8 mM in this instance.

When the solution contained SDS micelles, the partitioning phenomenon between the micelles and the bulk aqueous solution was taken into account for a non-charged solute having hydrophobic characteristics [5]. The capacity factor, k' , defined as the ratio of the amount of a

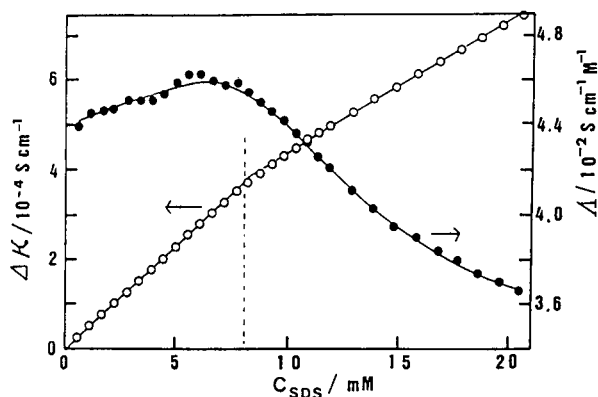


Fig. 3. Variation of conductivity with total concentration of SDS (C_{SDS}) in CAPS buffer (pH 11)-DMF (10:2, v/v) at 25°C. Λ = Molar conductivity of SDS; $\Delta\kappa$ = specific conductivity change.

solute in the micelle phase to that in the bulk aqueous phase, is given as a combined function of t_s , t_0 and t_{mc} [11]:

$$k' = (t_s - t_0) / [t_0(1 - t_s/t_{mc})] \quad (1)$$

and in that case k' varies with the total concentration of SDS (C_{SDS}) in the solution, according to the following approximate equation:

$$k' = KV_{SDS}(C_{SDS} - CMC) \quad (2)$$

where K is the distribution coefficient, defined as the concentration ratio of the solute in the micelle phase to that in the bulk aqueous phase, V_{SDS} is the partial molar volume of SDS in the micelle and CMC is the critical micelle concentration of SDS. It is noted that eqn. 2 is valid in principle under the condition $C_{SDS} > CMC$.

The effect of the SDS concentration on the migration behaviour of porphyrins was investigated using CAPS buffer (pH 11)-DMF (10:2, v/v). It was found that the k' values calculated for the porphyrins according to eqn. 1 did not always increase with increasing C_{SDS} , as shown in Fig. 4. This result is reasonable when it is considered that a considerable proportion of each porphyrin compound is not electrically

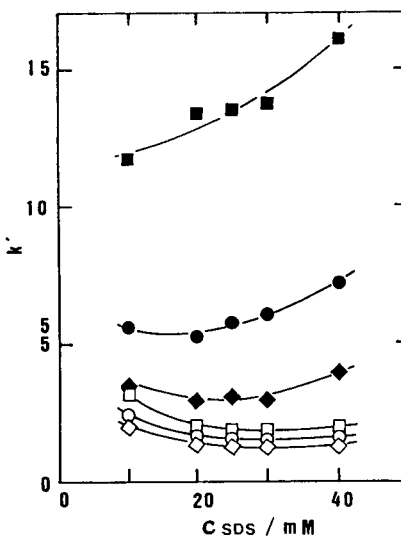


Fig. 4. Plot of capacity factor (k') calculated from eqn. 1 versus total concentration of SDS in the carrier solution CAPS buffer [(pH 11)-DMF (10:2, v/v)]. $\circ = t_{s,H_2HP}$; $\square = t_{s,Cu(HP)}$; $\diamond = t_{s,Zn(HP)}$; $\bullet = t_{s,H_2PP}$; $\blacksquare = t_{s,Cu(PP)}$; $\blacklozenge = t_{s,Zn(PP)}$.

neutral but negatively charged owing to the dissociation of carboxylic protons under such basic conditions as pH 11. Accordingly, the contribution of the electrophoretic motion occurring in the bulk aqueous phase should be taken into account in the calculation of k' . In such a case, eqn. 2 should be altered by using the distribution ratio (D) in the place of the partition coefficient (K) because the solute distribution phenomenon is not related to the concentration of a particular species (C_i) but to those of all (n) species of the solute:

$$k' = DV_{\text{SDS}}(C_{\text{SDS}} - \text{CMC}) \quad (3)$$

where

$$k' = \frac{\sum_{i=1}^n C_{i, \text{ micelle phase}}}{\sum_{i=1}^n C_{i, \text{ bulk aqueous phase}}}$$

Capacity factor

Under the practical experimental conditions of CZE, the bulk aqueous solution and SDS micelles moved towards the negative end of the capillary at apparent velocities v_{eo} and v_{mc} , respectively. When the migration of a solute is a combined function of the electrophoresis in the bulk aqueous phase and the distribution between the SDS micelle phase and the bulk aqueous phase, the velocity of the solute, v_s , is given by the following equation:

$$\begin{aligned} v_s &= [n_{\text{aq}}/(n_{\text{aq}} + n_{\text{mc}})](v_{\text{eo}} + v_{\text{s,ep}}) \\ &\quad + [n_{\text{mc}}/(n_{\text{aq}} + n_{\text{mc}})]v_{\text{mc}} \\ &= [1/(1 + k')](v_{\text{eo}} + v_{\text{s,ep}}) + [1/(1 + k')]v_{\text{mc}} \end{aligned} \quad (4)$$

where n_{aq} and n_{mc} are the numbers of solute molecules in the bulk aqueous phase and the SDS micelle phase, respectively, and $v_{\text{s,ep}}$ is the electrophoretic velocity vector of the solute in the bulk aqueous phase. By rearranging this equation, the capacity factor, k' , is represented by

$$k' = (v_{\text{eo}} - v_s + v_{\text{s,ep}})/(v_s - v_{\text{mc}}) \quad (5)$$

The k' values of the porphyrins and their

metal complexes were calculated from eqn. 5. The values of v_{eo} , v_s and v_{mc} were calculated from the values of t_0 , t_s and t_{mc} , respectively, measured in the experiments using a micellar solution of SDS, and $v_{\text{s,ep}}$ was approximately estimated from the values of v_s and v_{eo} that were measured in an SDS-free carrier solution. It was found that the capacity factor increased with increasing C_{SDS} in the solution, as shown in Fig. 5. When the result of the plot of k' versus C_{SDS} was fitted to a linear relationship, the intercepts on the C_{SDS} axis were found to be in the range 5–10 mM.

When the linear relationship given by eqn. 3 is fitted to the experimental plots (k' versus C_{SDS}) shown in Fig. 5, the slope and the intercept on the C_{SDS} axis correspond to the product DV_{SDS} and the CMC of SDS in the carrier solution, respectively. The values of the intercept on the C_{SDS} axis for the plots for the porphyrin compounds of interest are in the range 5–10 mM, which agrees with the value of the CMC of SDS estimated by conductimetry (*ca.* 8 mM; see Fig. 3). It has been clarified at this stage that the capacity factor of each porphyrin compound depends little on the concentration of the free (*i.e.*, not aggregated) form of SDS but considerably on the concentration of the micellar

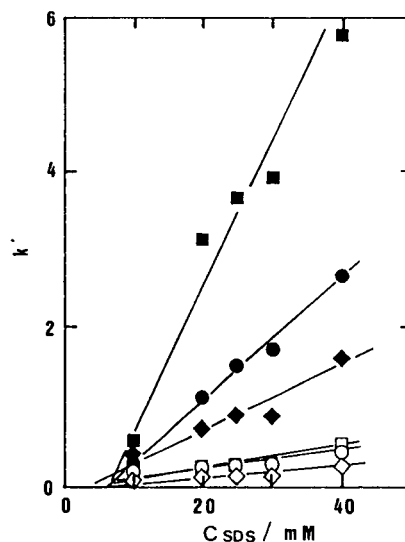


Fig. 5. Plot of capacity factor (k') calculated from eqn. 5 versus total concentration of SDS in the carrier solution. Carrier solution and symbols as in Fig. 4.

form of SDS in the solution. According to the slopes of the k' versus C_{SDS} plots shown in Fig. 5, the distribution ratio (D) increases in the order $\text{Zn(HP)} < \text{H}_2\text{HP} < \text{Cu(HP)} < \text{Zn(PP)} < \text{H}_2\text{PP} < \text{Cu(PP)}$.

Separation of haematoporphyrin, protoporphyrin and their copper and zinc complexes

It was found in both series of haematoporphyrin and protoporphyrin that the migration time increased in the order Zn complex < free acid form < Cu complex. This migration sequence agrees with the retention sequences observed for various porphyrin families in reversed-phase HPLC [1–3].

The feasibility of the CZE separation of six porphyrin compounds, viz., H_2HP , Cu(HP) , Zn(HP) , H_2PP , Cu(PP) and Zn(PP) , was examined using a solution containing 20–40 mM SDS in CAPS buffer (pH 11)–DMF (10:2, v/v). All the porphyrin compounds could be detected within 30 min. When the SDS concentration was increased, the time span from t_0 to t_{mc} in which all sample components should be detected was extended and accordingly the resolution for each pair of adjacent peaks was improved. The separation of these six porphyrin compounds using the recommended conditions is demonstrated in Fig. 6.

The separation of Zn(HP) , H_2HP and Cu(HP) was successful, with elution in that order, using an octadecyl-bonded silica gel (ODS) column (25 cm \times 4 mm I.D.) with a methanol–phosphate buffer (pH 3) (85:15, v/v) within 5 min at a flow-rate of 1 ml/min [12]. Using MEKC, complete separation of these three HP compounds was possible in less than 2 min (see Fig. 6). Few data are available at this stage for comparing MEKC with HPLC with respect to sensitivity.

CONCLUSION

It has been confirmed that MEKC is a promising method for the separation of haematoporphyrin and protoporphyrin and their complexes with copper and zinc. A micellar solution of SDS containing DMF is an effective carrier solution.

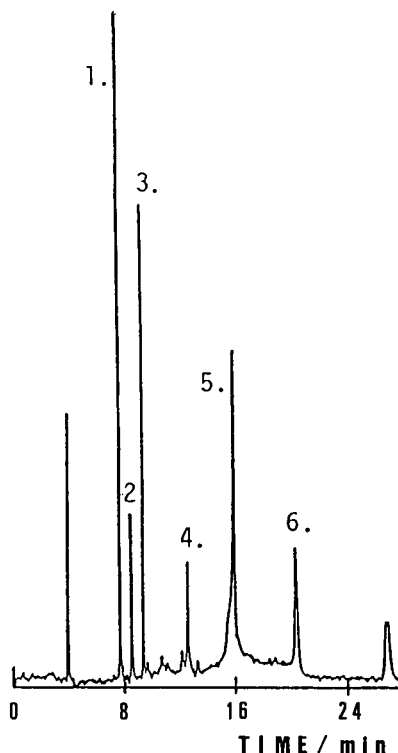


Fig. 6. MEKC separation of porphyrin compounds. Carrier solution, 40 mM SDS in CAPS buffer (pH 11)–DMF (10:2, v/v). Applied voltage, 30 kV (429 V/cm); UV detection at 405 nm. Peaks: 1 = Zn(HP) ; 2 = H_2HP ; 3 = Cu(HP) ; 4 = Zn(PP) ; 5 = H_2PP ; 6 = Cu(PP) .

For the successful separation of the six porphyrin compounds, a 40 mM SDS solution in CAPS buffer (pH 11)–DMF (10:2, v/v) is recommended.

ACKNOWLEDGEMENT

This work was supported by a Grant-in-Aid for Scientific Research from the Ministry of Education, Science and Culture.

REFERENCES

- 1 K. Saitoh, M. Kobayashi and N. Suzuki, *Anal. Chem.*, 53 (1981) 2309.
- 2 K. Adachi, K. Saitoh and N. Suzuki, *J. Chromatogr.*, 457 (1988) 99.
- 3 K. Saitoh, M. Kobayashi and N. Suzuki, *J. Chromatogr.*, 243 (1982) 291.

- 4 K. Saitoh, Y. Shibata and N. Suzuki, *J. Chromatogr.*, 542 (1991) 351.
- 5 S. Terabe, K. Otsuka, K. Ichikawa, A. Tsuchiya and T. Ando, *Anal. Chem.*, 56 (1984) 111.
- 6 K. Saitoh, C. Kiyohara and N. Suzuki, *J. High Resolut. Chromatogr.*, 14 (1991) 245.
- 7 K. Saitoh, C. Kiyohara and N. Suzuki, *Anal. Sci.*, 7, Suppl. (1991) 269.
- 8 R. Weinberger, E. Sapp and S. Moring, *J. Chromatogr.*, 516 (1990) 271.
- 9 K. Saitoh and Y. Sugiyama and N. Suzuki, *J. Chromatogr.*, 358 (1986) 307.
- 10 N. Suzuki, K. Saitoh and Y. Sugiyama, *Chromatographia*, 21 (1986) 509.
- 11 A.S. Cohen, S. Terabe, J.A. Smith and B.L. Karger, *Anal. Chem.*, 59 (1987) 1021.
- 12 N. Suzuki, K. Saitoh and Y. Sugiyama, *Chromatographia*, 22 (1986) 132.

Investigation of vanadate as a pH sensitive analyte anion using capillary zone electrophoresis

T. Groh and K. Bächmann*

Technische Hochschule Darmstadt, Fachbereich Chemie, Hochschulstrasse 10, D-64289 Darmstadt (Germany)

(First received March 4th, 1993; revised manuscript received May 18th, 1993)

ABSTRACT

Inorganic anions were determined using capillary zone electrophoresis with UV detection. 1,2-Dihydroxybenzene-3,5-disulphonic acid disodium salt (Tiron) was used as the electrolyte. The determination of vanadate as the analyte ion resulted in two peaks which depended on the pH of the analyte solution. The two vanadate peaks showed opposite behaviour. A pH range of 2.3–11.8 was investigated. The relative standard deviation of the peak areas was 8%. Spectroscopic investigations showed that the vanadate anions interact with the electrolyte.

INTRODUCTION

Capillary zone electrophoresis (CZE) is being used to an increasing extent for the determination of inorganic cations and anions [1–8]. In addition to the determination of the ions of interest, the simultaneous determination of the pH of the analyte solution is desirable, especially in routine analysis, so that no additional pH measurement is necessary. When only small sample volumes are available, the determination of either the ions or the pH value is possible, but not both. Even when using microelectrodes, measurement of the pH of samples in a volume smaller than 1 μ l is not feasible [9].

In principle, two approaches are possible to determine the pH of the analyte solution integrated in the electrophoretic process. The first is by the determination of the protons together with the analyte cations. However, problems arise because of the high ionic mobility of the

protons in comparison with those of the electrolyte and the analyte cations. Further, the proton concentration will be changed by a factor of 10 per pH unit. This implies a system having low limits of detection for the protons (e.g., 1 μ M H^+ at pH 6.0).

On the other hand, the determination of pH is possible by adding a pH-sensitive species to the analyte solution. The species must fulfil the condition of showing a sensitive pH dependence of detector response (e.g., absorbance), which must remain in a steady state until detection. Further, the species should not co-migrate with the ions of interest. Isopolyanions seem to be an interesting group of species that can be used as analyte additives for pH determination. Our experiments with different isopolyanions show that vanadate is the most pH-sensitive anion.

In aqueous solution, vanadates undergo a series of complex hydrolysis–polymerization reactions in a system of changing pH value [10,11]. The different pH-dependent species show different UV absorptivities [12].

In this work, the determination of vanadate at

* Corresponding author.

different pH values and concentrations was investigated. The peak area of the observed two vanadate signals depends on the pH of the analyte solution. 1,2-Dihydroxybenzene-3,5-disulphonic acid disodium salt (Tiron) was used as an electrolyte and UV detection was carried out.

EXPERIMENTAL

A Dionex (Idstein, Germany) CES 1 capillary electrophoresis instrument was used for analysis. UV detection was carried out at 293 nm. A high voltage of 25 kV with a negative voltage mode was applied. The separations were carried out using conventional fused-silica capillaries from Scientific Glass Engineering (Weiterstadt, Germany). The dimensions of the capillaries were 75 μm I.D. and 60 cm total length, with 55 cm from the point of injection to the detector cell. Before starting the separation the capillaries used were washed with the electrolyte. Hydrostatic injection (10 cm, 30 s) and electrokinetic injection (3 kV, 10 s) were used for sample introduction.

All solutions were prepared each day from 50 mM stock solutions, filtered through a 0.22- μm

membrane from Millipore (Eschborn, Germany) and degassed under vacuum for 10 min.

Spectroscopic investigations were carried out on a Hewlett-Packard model (Bad Homburg, Germany) 8451A diode-array spectrophotometer.

Chemicals

All solutions, standards and the electrolyte were prepared with purified water obtained from a Milli-Q system (Millipore). 1,2-Dihydroxybenzene-3,5-disulphonic acid disodium salt (99%), 2,5-dihydroxy-1,4-benzenedisulphonic acid dipotassium salt (98%) and 1,3-benzenedisulphonic acid disodium salt (90%) was obtained from Aldrich (Steinheim, Germany). Sodium metavanadate (NaVO_3) (98%) (Fluka, Neu-Ulm, Germany) was used for the preparation of the vanadate standards. All other reagents were of analytical-reagent grade from Merck (Darmstadt, Germany).

RESULTS AND DISCUSSION

Fig. 1 shows an electropherogram of an anion standard solution including vanadate. The van-

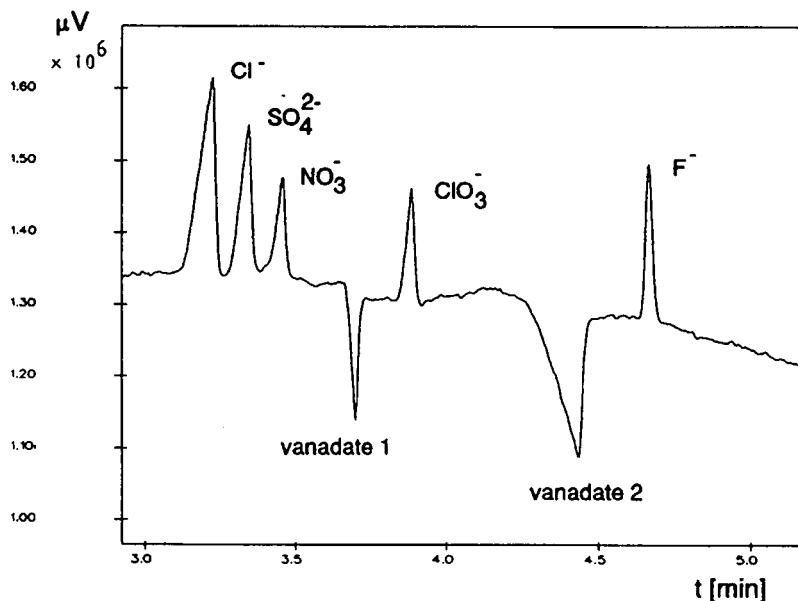


Fig. 1. Electropherogram of an anion standard including vanadate. Concentration of each anion = 0.1 mM, except for vanadate (0.4 mM). Electrolyte, 5 mM 1,2-dihydroxy-3,5-disulphonic acid disodium salt, (pH 5.3); capillary, fused silica (60 cm total length, 55 cm to the detector, 75 μm I.D.); voltage, -25 kV; detection, UV (293 nm), range 0.01 absorbance; injection hydrostatic (30 s, 10 cm).

adate anion gives two positive signals without co-migration with the main anions chloride, nitrate and sulphate. The second vanadate peak is extremely broad and shows fronting, possibly due to the adsorption of the vanadate species by the capillary surface, which results in peak distortion [13,14].

The vanadate samples were measured at different times after sample preparation. In Table I the ratio of the peak areas of the two vanadate peaks and the time after sample preparation (from 15 min to 10 h) are summarized. As can be seen, the ratio of the peak areas shows no significant changes. The same results were achieved by measurement of vanadate using different capillary lengths.

Experiments with molybdate and tungstate as analyte additives did not show the same significant pH dependence as vanadate. Niobate and tantalate, which also form isopolyanions, were

not investigated because both species show precipitation at pH 7 [10].

Both vanadate peaks have an interesting dependence on the pH of the analyte solution, as demonstrated in Fig. 2a where three electropherograms of a vanadate standard (0.4 mM) with different pH values of the analyte solution are shown.

At acidic pH (3.5) (Fig. 2a), the first vanadate peak shows a greater absorbance than the second peak. At higher pH (5.3), both peaks have nearly the same height (Fig. 2b). The second peak becomes dominant when the pH of the analyte solution is increased to 8.8 (Fig. 2c).

This pH-dependent behaviour is clearly demonstrated in Fig. 3, which shows the relationship between the pH of the analyte solution in the range 2.3–11.8 and the areas of the vanadate peaks. The two vanadate peaks show opposite behaviour.

The opposite behaviour of the vanadate peaks as demonstrated in Fig. 2 can be seen at pH 3.8. The first vanadate peak increases with decreasing pH whereas the second peak decreases. In the acidic pH region a stronger pH dependence of the peak areas can be observed than at pH > 5.0, where the peak areas are change only slightly with change in pH. At pH 11 only the second peak can be observed, the first peak having disappeared. The observed migration times of both peaks were constant over the pH range investigated.

The ratio of the peak areas (peak 2/peak 1) of the vanadate peaks as a function of pH is shown in Fig. 4. With increasing pH from pH 3.8 the peak-area ratio increases, whereas at lower pH the peak-area ratio decreases. This behaviour restricts the application of vanadate as an analyte additive at this concentration to samples with pH > 4.0.

With fifteen consecutive injections by hydrostatic injection of a vanadate standard (0.4 mM), the relative standard deviation (R.S.D.) of the peak areas was 8%. The limit of detection for vanadate depends on the pH and is about 40 μ M.

Measurements were also carried out with other Tiron and vanadate concentrations. Experiments with Tiron concentrations from 1 to 9 mM (at a constant pH of 5.3) and a vanadate

TABLE I

RATIO OF THE PEAK AREAS (VANADATE 2/VANADATE 1) DEPENDING ON THE TIME AFTER SAMPLE PREPARATION

pH of the vanadate solution = 6.5. Experimental conditions as in Fig. 1.

Time after sample preparation [min]	Ratio of peak areas
15	3.3
45	3.1
85	3.2
100	3.4
124	3.6
150	3.4
161	3.1
172	3.2
180	3.3
189	3.2
203	3.4
232	3.1
290	3.0
361	3.6
404	3.2
455	3.3
541	3.5
620	3.6
629	3.2

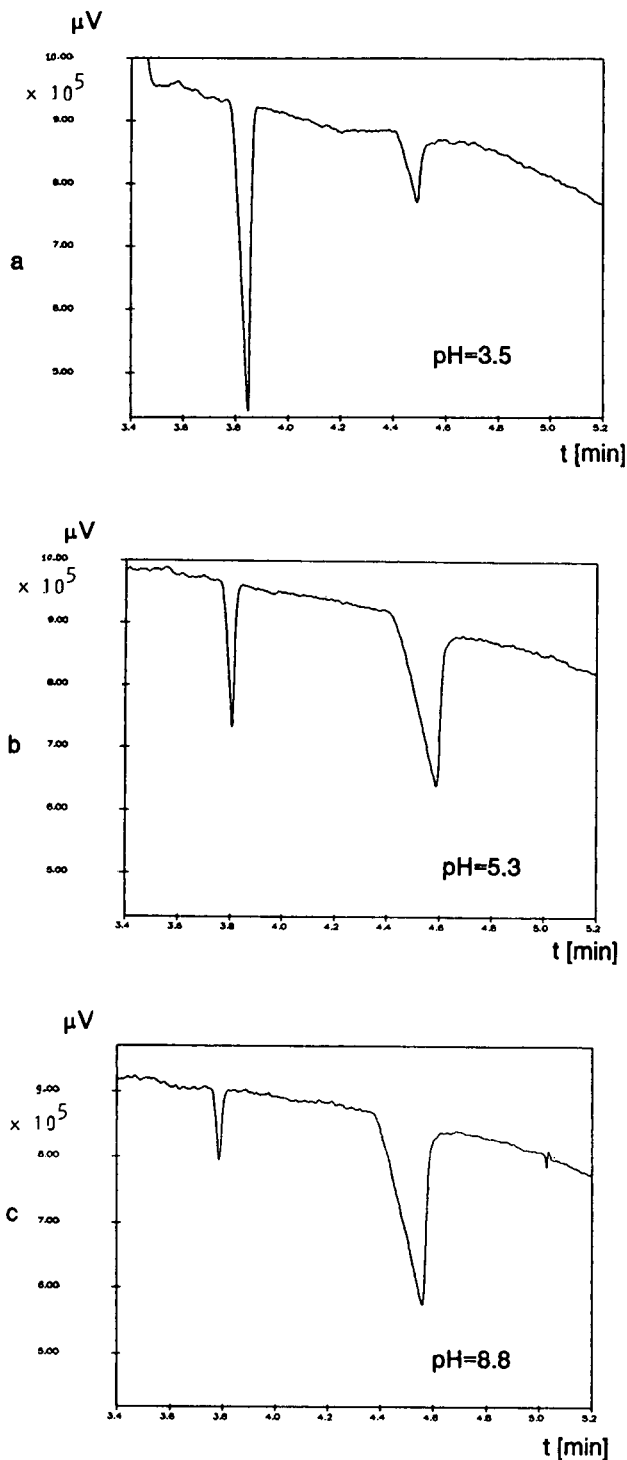


Fig. 2. Electropherograms of vanadate at different pH values of the analyte solution: (a) 3.5; (b) 5.3; (c) 8.8. Experimental conditions as in Fig. 1.

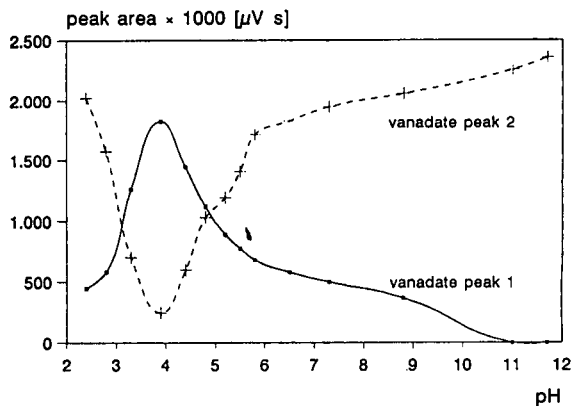


Fig. 3. Dependence of the areas of the two vanadate peaks on the pH of the analyte solution. Experimental conditions as in Fig. 1.

concentration of 0.4 mM showed no significant changes in the pH dependence of the two vanadate peaks, probably caused by the concentration excess of Tiron in all instances. For example, Fig. 5 shows the areas of the vanadate peaks as a function of the concentration of Tiron. The pH of the vanadate solution was 7.0. Only the separation efficiency will be influenced by the concentration of Tiron. The best separation results were obtained with a Tiron concentration of about 5 mM.

Different vanadate concentrations (0.2–0.8 mM) with a fixed Tiron concentration (5 mM, pH 5.3) were also investigated. Fig. 6 shows the ratio of the areas of the two vanadate peaks

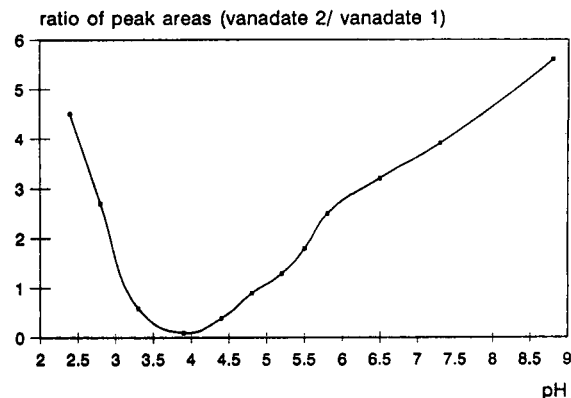


Fig. 4. Dependence of the ratio of the peak areas (vanadate 2/vanadate 1) on the pH of the analyte solution. Experimental conditions as in Fig. 1.

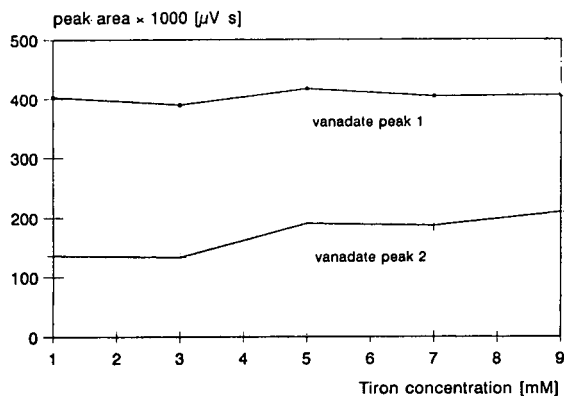


Fig. 5. Dependence of the areas of the two vanadate peaks on the concentration of Tiron. Vanadate concentration, 0.4 mM (pH 7.0); electrolyte, 1–9 mM 1,2-dihydroxy-3,5-disulphonic acid disodium salt (pH 5.3); other conditions as in Fig. 1.

using 0.2 and 0.8 mM vanadate at different pH values. The curve for 0.8 mM vanadate is comparable to that in Fig. 4, whereas the curve for 0.2 mM vanadate differs and shows great variations in the pH range 3–8. Therefore, this concentration is not useful for pH determination. Better results are obtained at higher vanadate concentrations (e.g., 0.4 mM), but limited by problems of separating vanadate from the other anions of interest if the vanadate concentration is too high.

Investigations with different pH values of the electrolyte were also carried out. Using 5 mM Tiron, the pH range was varied from 3 to 7. The

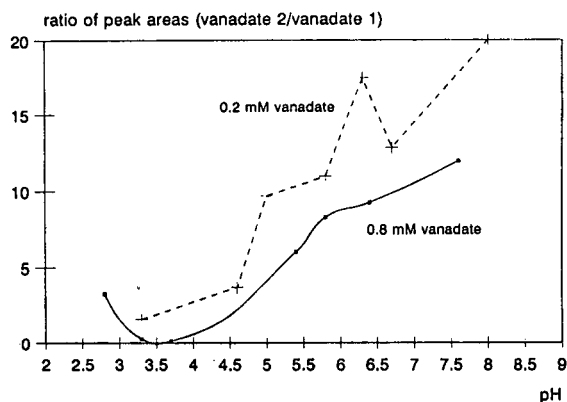


Fig. 6. Dependence of the ratio of the peak areas (vanadate 2/vanadate 1) on the pH of the analyte solution. Vanadate concentration 0.2 and 0.8 mM; other conditions as in Fig. 1.

analyte solution was 0.4 mM vanadate at different pH values. The experiments showed that with electrolyte pH values below 5 the pH dependence of vanadate, as shown in Fig. 4, cannot be observed. Fig. 7 shows the ratio of the vanadate peak areas as a function of the pH of the vanadate solutions. The electrolyte pH value was 3.0.

In the pH range 5.0–7.0 the pH dependence for vanadate is comparable to that in Fig. 4. Above pH 7.0 the velocity of the electroosmotic flow is higher than the velocity of the vanadate ions in the opposite direction so that no measurements can be carried out.

The experiments were carried out with hydrostatic injection. With this injection mode, the ionic strength of the analyte solution shows no influence on the vanadate peaks. Electrokinetic injection with different vanadate concentrations and different pH values was also used.

Fig. 8 shows the ratio of the areas of the vanadate peaks as a function of pH using three vanadate concentrations and electrokinetic injection. The plots shows a maximum between pH 6 and 7. Hydrostatic injection is to be preferred because of discrimination effects when using the electrokinetic injection mode. The amount of sample injected varies with the total ionic concentration of the sample [4]. Therefore, the use of internal standards is necessary [15].

Identification of the structures of the species

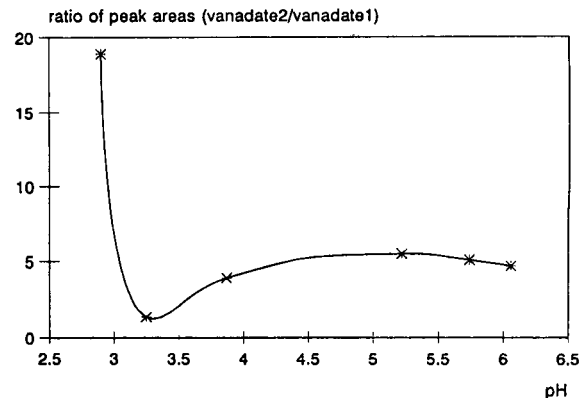


Fig. 7. Dependence of the ratio of the peak areas (vanadate 2/vanadate 1) on the pH of the analyte solution. Vanadate concentration, 0.4 mM; electrolyte, 5 mM 1,2-dihydroxy-3,5-disulphonic acid disodium salt (pH 3.0); other conditions as in Fig. 1.

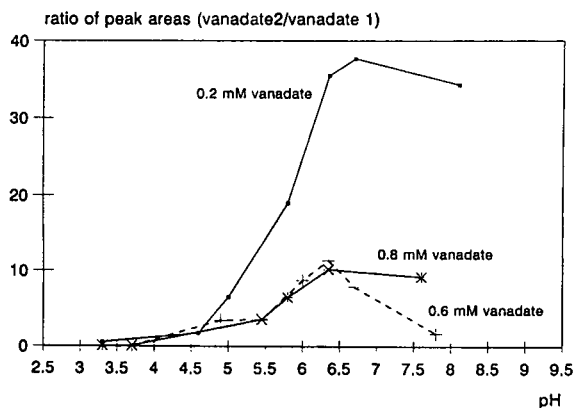


Fig. 8. Dependence of the ratio of the peak areas (vanadate 2/vanadate 1) on the pH of the analyte solution. Vanadate concentration, 0.2, 0.6 and 0.8 mM; injection, electrokinetic (10 s, 3 kV); other conditions as in Fig. 1.

giving the two vanadate peaks is difficult. The nature of the vanadate species existing in the acidic pH range is controversial and has not been clearly resolved [16]. The complex reactions (polymerization, condensation and protonation) of vanadates in aqueous solutions depend on pH and the vanadate concentration [12,17]. Further, the vanadate anions can be influenced by the electrolyte because two positive vanadate peaks were obtained. At 293 nm Tiron has a molar absorptivity of $5000 \text{ l mol}^{-1} \text{ cm}^{-1}$. At the same wavelength the molar absorptivity of vanadate is only $1200 \text{ l mol}^{-1} \text{ cm}^{-1}$. These results indicate that the vanadate anions interact with the aromatic electrolyte so that Tiron–vanadate species are formed with a higher UV absorbance than Tiron. This conclusion is supported by spectroscopic investigations because the absorbance of Tiron at 293 nm increases and the absorbance maximum will be shifted to longer wavelengths (from 293 to 299 nm) by adding vanadate to the aromatic compound.

Other electrolytes without the two hydroxy groups in the *ortho* position were also investigated. The experiments were carried out with 1,3-benzenedisulphonic acid disodium salt and 2,5-dihydroxy-1,4-benzenedisulphonic acid di-

potassium salt. The results showed that only one vanadate peak will be observed. This peak shows a pH dependence similar to that of the first vanadate peak with the Tiron system. The second vanadate peak appears only with Tiron as electrolyte.

The application of vanadate for the pH determination of real samples and further spectroscopic investigations will be carried out.

ACKNOWLEDGEMENT

We thank the Deutsche Forschungsgemeinschaft for financial support of this work.

REFERENCES

- 1 P. Jandik and W.R. Jones, *J. Chromatogr.*, 546 (1991) 431.
- 2 P. Jandik and W.R. Jones, *J. Chromatogr.*, 546 (1991) 445.
- 3 E.S. Yeung and L. Gross, *Anal. Chem.*, 62 (1990) 427.
- 4 E.S. Yeung and L. Gross, *J. Chromatogr.*, 480 (1989) 169.
- 5 W. Beck and H. Engelhardt, *Chromatographia*, 33 (1992) 313.
- 6 J. Boden, I. Haumann and K. Bächmann, *J. Chromatogr.*, 626 (1992) 259.
- 7 T. Groh and K. Bächmann, *Electrophoresis*, 13 (1992) 458.
- 8 A. Weston, P.R. Brown, P. Jandik, W.R. Jones and A.L. Heckenberg, *J. Chromatogr.*, 593 (1992) 289.
- 9 *Biotechnology Update*, Vol. 2, No. 2, Lazar Research Laboratories, Los Angeles, CA, 1993.
- 10 M.T. Pope and B.W. Dale, *Q. Rev. Chem. Soc.*, 22 (1968) 527.
- 11 L.G. Sillén, *Q. Rev. Chem. Soc.*, 12 (1959) 146.
- 12 K. Schiller and E. Thilo, *Z. Anorg. Chem.*, 319 (1961) 261.
- 13 H.H. Lauer and D. McManigill, *Anal. Chem.*, 58 (1986) 166.
- 14 S.F.Y. Li, *Capillary Electrophoresis*, Elsevier, Amsterdam, 1992.
- 15 E.V. Dose and G.A. Guiochon, *Anal. Chem.*, 63 (1991) 1155.
- 16 K.F. Jahr and J. Fuchs, *Angew. Chem.*, 15 (1966) 725.
- 17 J.O. Hill, I.G. Worsley and L.G. Hepler, *Chem. Rev.*, 71 (1971) 127.

Short Communication

Behaviour of polyhydroxyethyl methacrylate sorbent with dextran-filled macropores in dye-affinity chromatography of proteins

Danica Mislovičová*

Institute of Chemistry, Slovak Academy of Sciences, Dúbravská cesta 9, 842 38 Bratislava (Slovak Republic)

Miroslav Petro

Department of Analytical Chemistry, Faculty of Sciences, Comenius University, Mlynská dolina CH-2, 842 15 Bratislava (Slovak Republic) and Polymer Institute, Slovak Academy of Sciences, Dúbravská cesta 9, 842 38 Bratislava (Slovak Republic)

Dušan Berek

Polymer Institute, Slovak Academy of Sciences, Dúbravská cesta 9, 842 38 Bratislava (Slovak Republic)

(First received December 11th, 1992; revised manuscript received May 27th, 1993)

ABSTRACT

A series of composite sorbents based on the rigid macroporous polyhydroxyethyl methacrylate (HEMA)-based support filled with soft dextran gel was prepared. The affinity dyes Cibacron Blue and Remazol Brilliant Blue were then immobilized on both the original HEMA and the composite (HEMA-D) sorbents. The properties of HEMA and HEMA-D sorbents, such as hydrophobic interactions with proteins and recovery of chromatographed enzymes (lactate dehydrogenase and malate dehydrogenase), in both original and dyed forms were studied. Important advantages of using HEMA-D supports in dye-affinity chromatography as compared with only HEMA supports were found.

INTRODUCTION

The Separon polyhydroxyethyl methacrylate (HEMA) sorbents are based on a rigid, macroporous polymer matrix prepared by the suspension copolymerization of 2-hydroxyethylmethacrylate with ethylenedimethacrylate [1]. Column packings based on HEMA seem to

be very suitable for biopolymer separations in various LC modes including high-performance affinity chromatography (HPAC) [2,3]. However, the hydrophobic interactions of unmodified HEMA sorbents with proteins often prevent their direct application in affinity-based separations. A suitable sorbent for affinity ligand immobilization can be prepared by glycosylation of the HEMA surface [4] or by modifying the HEMA support with polysaccharides [5].

This paper describes the preparation and ap-

* Corresponding author.

plication of the HEMA sorbent with pores filled with dextran gels of various cross-linking density. The permeation and sorption properties of the supports prepared were examined. After subsequent derivatization with the reactive dyes Cibacron Blue 3G-A and Remazol Brilliant Blue R, the materials were applied in dye-affinity chromatography of the enzymes lactate dehydrogenase (LDH) and malate dehydrogenase (MDH).

EXPERIMENTAL

Materials

Macroporous Separon HEMA S 10 000, 25–40 μm (Tessek Prague, Czech Republic), was used as support. The exclusion limit of this material for dextrans is about $M_r \cdot 10^7$. Dextran D-40, $M_r \cdot 4 \cdot 10^4$ was obtained from Biotika (Slovenská L'upča, Slovak Republic). The cross-linking reagent 1,4-butanediol diglycidyl ether (BDGE) was from Aldrich (Milwaukee, WI, USA). The dye Cibacron Blue 3G-A (CB) was purchased from Ciba-Geigy (Basle, Switzerland), Remazol Brilliant Blue R (RBB) was from Hoechst (Frankfurt, Germany) and Coomassie Blue G-250 from Serva (Heidelberg, Germany). LDH (E.C. 1.1.1.27) from beef flank muscle was prepared as crude lyophilizate [6]. Other enzymes, such as LDH from rabbit muscle (Fluka, Buchs, Switzerland) and MDH (E.C. 1.1.1.37) from pig heart, were purchased from Boehringer Mannheim (Mannheim, Germany). NADH was from Reanal (Budapest, Hungary). CB-dextran T 10 was prepared according to the procedure previously described [7]. Dextran standards were from Pharmacosmos (Viby, Denmark). Other chemicals were purchased from commercial sources and were of analytical grade.

Apparatus

Spekol 11 and Specord 40 (both from Carl Zeiss Jena, Germany) were used for spectrophotometric determinations of dyes, enzymes and proteins. Gradient HPAC equipment consisted of a GP3 gradient programmer, an LCI 30 manual loop injector, an LCD 2040 UV detec-

tor, an FCC 61 fraction collector and a TZ 4620 line recorder (all from Laboratory Instruments, Prague, Czech Republic) and of a VCR 40 high-pressure pump (from Workshops of the Czechoslovak Academy of Sciences, Prague, Czech Republic). Gel permeation chromatographic (GPC) equipment consisted of a Waters 510 HPLC pump (Waters, Division of Millipore, Milford, MA, USA), a Rheodyne 7120 injector (Rheodyne, Berkeley, CA, USA), an RIDK 101 differential refractometric detector and a TZ 4620 line recorder (both from Laboratory Instruments). A Baseline 810 chromatography workstation, (Dynamic Solutions, Division of Millipore, Ventura, CA, USA) was used for data collection and processing.

Methods

The activities of LDH and MDH were determined spectrophotometrically [8] and the protein content was determined according to the method of Bradford [9].

Synthesis of HEMA S 10 000 with dextran-filled pores

HEMA S 10 000 dried overnight at 120°C was treated with an alkaline solution of dextran (4.67 g of D-40 dissolved in 10 ml of 0.5 M aqueous NaOH) containing the appropriate amount of cross-linking agent. The mass ratio of BDGE vs. dextran was $0.74 \cdot 10^{-3}$ mol/g for HEMA-D1, $0.56 \cdot 10^{-3}$ mol/g for HEMA-D2 and $0.15 \cdot 10^{-3}$ mol/g for HEMA-D3. The amount of dextran incorporated into HEMA pores was 0.56 g/g, 0.33 g/g or 0.20 g/g for HEMA-D1, HEMA-D2 or HEMA-D3, respectively. The cross-linking reaction was stopped by neutralizing the system with 2% (v/v) nitric acid after 48 h. Afterwards the HEMA-dextran composite sorbent was allowed to swell in water for 5 h at 40°C and was then washed with deionized water.

Preparation of dyed HEMA sorbents

The technique used originally for the attachment of dyes to cellulose beads [7] was applied to the preparation of the dyed derivatives of HEMA sorbents: 1 g of HEMA sorbent was suspended in 25 ml of water and then the

appropriate amounts of dye (25–80 mg) and sodium chloride (0.3 g) were added. After dissolution of the latter compounds, alkaline conditions in the reaction mixture were adjusted with 5 ml of 6% Na₂CO₃ (CB) or 5 ml of 8% NaOH (RBB). The reaction time was 2 h at 80°C (CB) or at ambient temperature (RBB). The reaction was stopped by neutralization and the unbound dye was washed out with distilled water until the filtrate was colourless. The degree of substitution was determined spectrophotometrically at 610 nm (CB) and at 595 nm (RBB) from the difference between the initial amount of the dye in the reaction mixture and the residual amount of dye in the washing solution.

Packing the columns

Glass minicolumns for elution and loading experiments were packed with the sorbents swollen in water. Stainless-steel columns for GPC and HPAC experiments were packed with the sorbents from water slurry under the maximum pressure of 20 MPa. The fines generated during preparation of composite HEMA-D sorbents were removed by repeatedly decanting them in water and methanol.

Chromatographic experiments

GPC characterization. GPC characterization of HEMA–dextran composite sorbents was performed with degassed distilled water as mobile phase. Columns of 25 × 0.8 cm I.D. were used. The flow-rate was 3 ml/min. A 20- μ l aliquot of sample solution containing dextran standards, saccharose, glucose and deuterium oxide (1 mg/ml total amount) was injected.

Elution experiments. These were performed using glass minicolumns (1 × 1.1 cm I.D.) filled with 0.2 g of dyed sorbents and equilibrated with 50 mM phosphate buffer, pH 7. The enzyme solution (50 μ l; ca. 10 U) was loaded. The unbound proteins were washed out with the equilibration buffer followed by elution with 2 M potassium chloride in equilibration buffer and finally with 1 mM NADH in equilibration buffer. The flow-rate was 0.2 ml/min and both the total enzyme activity and the protein content (in the case of crude preparation) were determined in 1-ml fractions. The non-specific interactions of

HEMA sorbents with LDH were determined using a column (2.5 × 1.1 cm I.D.) containing 0.5 g of undyed support after loading about 10 U (1.8 mg of proteins) of crude LDH enzyme while the elution was performed only with the equilibration buffer.

Loading experiments. The same dyed support columns as for elution experiments were used. After equilibration with 50 mM phosphate buffer, the columns were loaded with the solution of crude LDH (3 mg/ml) in the equilibration buffer at a flow-rate of 0.2 ml/min. The activity of LDH in effluent was determined as above. After the column had been saturated, the excess enzyme was washed out with the equilibration buffer and the bound LDH was eluted with 50 μ M CB–dextran T 10 [10].

HPAC-experiments. The steel column (10 × 0.6 cm I.D.) filled with 2.8 ml of CB–HEMA-D2 containing 8.5 μ mol dye per g of sorbent was used. A 20- μ l aliquot of enzyme solution (about 5 U) was applied on the equilibrated column with 50 mM phosphate buffer, pH 7. The enzyme was eluted with equilibration buffer and then with a concentration gradient of KCl (0–3 M) or NADH (0–0.5 mM). The experiment was performed at a flow-rate of 0.2 ml/min, pressure 2 MPa and at ambient temperature. The activities of both enzyme and proteins were determined in 1-ml effluent fractions.

RESULTS AND DISCUSSION

The pore structure of HEMA-D composite sorbents and bare HEMA support was characterized by inverse GPC. Fig. 1 shows the GPC calibration curves of dextran standards observed for HEMA sorbents with and without dextran gel filling. The permeation properties of prepared sorbents correlates well with the conditions of dextran cross-linking, mainly with the molar ratio of cross-linking agent to dextran. HEMA-D1 represents material with an exclusion limit of $M_r \approx 4 \cdot 10^3$ for dextran standards. Therefore the proteins are excluded from its pores. In the case of HEMA-D2 and HEMA-D3, with exclusion limits of $M_r 2 \cdot 10^5$ and $4 \cdot 10^5$, respectively, the proteins that are small enough to penetrate the dextran gel can interact with the

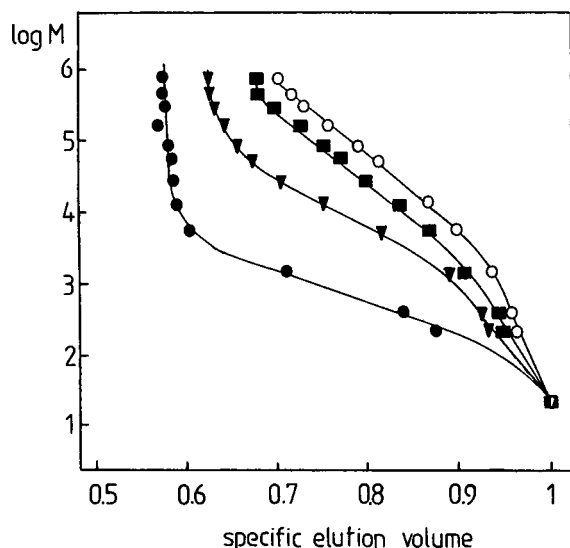


Fig. 1. GPC calibration curves of HEMA and HEMA-D sorbents. Columns, 25×0.8 cm, were packed with HEMA-D1 (●), HEMA-D2 (▼), HEMA-D3 (■) and bare HEMA (○). A $20\text{-}\mu\text{l}$ aliquot of calibration standard solution (dextrans, saccharose, glucose and deuterium oxide; 1 mg/ml) was injected onto the column with distilled water as eluent at a flow-rate of 3 ml/min . The specific elution volume was determined as elution volume of injected standard relative to the elution volume of deuterium oxide. M is (weight average) molar mass of injected standard.

HEMA surface. The highest reproducibility was achieved in the case of HEMA-D1 synthesis because the exclusion properties of the resulting sorbent were less sensitive to variation in the reaction conditions. The synthesis of HEMA-D2 and HEMA-D3 sorbents needed more precisely controlled reaction conditions [5].

The activities of LDH eluted from applied HEMA and HEMA-D sorbents were close to 100% of loaded enzyme activities, and no important differences in enzyme recoveries among the sorbents were revealed. Higher non-specific interactions were observed in the case of accompanying proteins. About 25–31% of loaded proteins was adsorbed on bare HEMA and on HEMA with pores filled with slightly cross-linked dextran (HEMA-D2 and HEMA-D3). In the case of composite containing the most densely cross-linked dextran network (HEMA-D1) the recovery of proteins reached 90% because there was no contact between proteins and the inside surface of the HEMA-matrix.

All described sorbents were derivatized with two kinds of dyes: CB and RBB. The concentration of immobilized RBB necessary was more than ten times higher than the concentration of CB required to bind the same amount of enzyme. As described in our previous papers [7,11], the interaction of LDH with CB is stronger than with RBB because of its different nature (CB is pseudobiospecific, RBB is mainly hydrophobic). The higher hydrophobicity of LDH–RBB interaction was expressed as difficulty in eluting bound enzyme with KCl solution as the elution agent. Thus it is preferable to use an affinity sorbent containing the immobilized CB dye.

Table I shows the results of affinity chromatography experiments with the crude preparation of LDH on the dyed sorbents. The loaded enzymes elute more easily from filled than from non-filled HEMA containing the same amount of a particular dye. The existence of hydrophobic interactions between solute and substrate is evident from the lack of elution of bound LDH with KCl solution. It seems that these non-specific enzyme–sorbent interactions play a major role in the case of dyed non-filled HEMA sorbent and they are partially reduced in the case of dyed dextran-filled HEMA. The presence of very small pores in HEMA-D1 causes only a negligible amount of enzyme to be bound on both CB- and RBB-dyed HEMA-D1. From the point of view of desired sorbent affinity to the LDH the dyed HEMA-D2 sorbents have the best properties for our purposes.

Sorbent CB–HEMA-D2 ($8.5\ \mu\text{mol}$ of CB per g) was used for the HPAC of LDH (beef muscle) with a concentration gradient of KCl and NADH. The same experiments were done with pure commercial MDH (pig heart) and LDH (rabbit muscle). It is demonstrated in Fig. 2 that enzymes can be selectively separated from accompanying proteins on HEMA–dextran with immobilized dyes. The optimum concentrations of eluting agent (KCl and NADH) as determined from HPAC gradient chromatograms are similar for all three enzymes (1.3 M KCl and 0.2 mM NADH). The decrease in the concentration of KCl in eluent down to the optimum in isocratic experiments caused an increase in the

TABLE I

ELUTION OF BOVINE LDH FROM RBB-DYED AND CB-DYED SORBENTS

Support	Dye content ($\mu\text{mol/g}$)	LDH activity (%)		
		Elution with		
		Equilibr. buffer	2 M KCl	1 mM NADH
RBB-HEMA	48.0	35.4	–	22.5
RBB-HEMA-D1	51.4	94.2	–	–
RBB-HEMA-D2	50.8	91.7	3.0	0.8
	73.3	38.8	32.6	25.5
RBB-HEMA-D3	50.9	88.8	–	11.1
	71.9	13.0	–	85.3
CB-HEMA	8.3	–	–	93.2
CB-HEMA-D1	7.6	78.6	20.2	5.0
CB-HEMA-D2	7.8	6.7	66.7	22.0
CB-HEMA-D3	9.0	6.8	33.7	59.4
CB-HEMA-D3	30.1	–	–	100.0

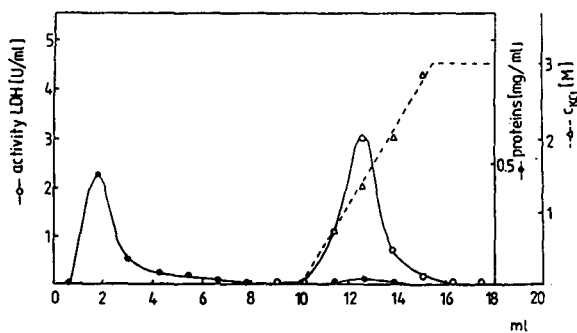


Fig. 2. Affinity chromatography of bovine muscle LDH on CB-dyed HEMA-dextran sorbent. Column: CB-HEMA-D2 (10×0.6 cm I.D., $8.5 \mu\text{mol}$ of CB per g). Mobile phase: 50 mM phosphate buffer, pH 7. Concentration gradient of KCl (c_{KCl}): 0–3 M. A $20\text{-}\mu\text{l}$ aliquot of lyophilizate solution, 11 U of LDH, 1.6 mg of protein, was injected. Flow-rate: 0.2 ml/min. Pressure: 2 MPa.

amount of bound LDH eluted from 66.7% (with 2 M KCl) to 78.6% (with 1.3 M KCl).

The loading capacities (activity of bound LDH/mass of sorbent) of CB-dyed HEMA-dextran composite sorbent and CB-dyed HEMA with about the same content of immobilized affinity ligands are not significantly different (Table II). However, the recovery of LDH from CB-HEMA-D2 obtained at maximum loading of LDH is several times higher than from CB-HEMA. In the case of CB-HEMA the small distance between affinity ligands bonded on the HEMA matrix surface probably results in the irreversible binding of LDH (multivalent interaction). On the other hand, the affinity ligands in CB-HEMA-D2 can be distributed throughout

TABLE II

THE RECOVERIES OF LDH OBTAINED ON CB-HEMA AND CB-HEMA-D2 SORBENTS

Sorbent	Dye content ($\mu\text{mol/g}$)	LDH activity (U per g of sorbent)		Recovery (%)
		Loaded	Eluted	
CB-HEMA	8.3	190.85	47.5	24.9
CB-HEMA-D2	8.5	224.05	184.00	82.1

the whole dextran network incorporated into HEMA pores. This results in better accessibility of affinity ligands to LDH molecules. Also, for this reason, the enzymes can be easily eluted from dyed HEMA–dextran composites with aqueous KCl with the same purification effect as with NADH.

CONCLUSIONS

New packing materials for liquid chromatography based on solid macroporous HEMA matrix filled with dextran gels were prepared. The incorporated dextran network acts as a suitable medium for immobilization of CB and RBB dyes. HEMA–dextran composites with immobilized affinity dyes show suppressed non-specific interactions with applied enzymes and improved recovery of specifically bound enzyme in comparison with dyed non-filled HEMA.

ACKNOWLEDGEMENTS

We thank Mrs. A. Bičanová for excellent technical assistance and Dr. J.-C. Janson (Phar-

macia, Uppsala) for providing us with 1,4-butanediol diglycidyl ether and dextran standards.

REFERENCES

- 1 J. Čoupek, M. Kriváková and S. Pokorný, *J. Polym. Sci. Polym. Symp.*, 42 (1973) 185.
- 2 O. Mikeš, P. Štrop and J. Čoupek, *J. Chromatogr.*, 153 (1978) 23.
- 3 O. Mikeš, J. Čoupek, in K.M. Gooding and F. Regnier (Editors), *HPLC of Biological Macromolecules — Methods and Applications (Chromatographic Science Series, Vol. 51)*, Marcel Dekker, New York, 1990, p. 25.
- 4 K. Filka, J. Čoupek and J. Kocourek, *Biochim. Biophys. Acta*, 539 (1978) 518.
- 5 M. Petro, *Ph.D. Thesis*, Polymer Institute of the Slovak Academy of Sciences, Bratislava, 1993.
- 6 A. Pesce, R.H. Mc Kay, F. Stalzenbach, R.D. Cahn and N.O. Kaplan, *J. Biol. Chem.*, 239 (1964) 1753.
- 7 P. Gemeiner, D. Mislovičová, J. Zemek and L. Kuniak, *Collect. Czechoslov. Chem. Commun.*, 46 (1981) 419.
- 8 H.U. Bergmeyer, *Methoden der Enzymatischen Analyse*, Vol. 1, Verlag Chemie, Weinheim, 2nd ed., 1970.
- 9 M.M. Bradford, *Anal. Biochem.*, 72 (1976) 248.
- 10 D. Mislovičová, P. Gemeiner, E. Stratilová and M. Horváthová, *J. Chromatogr.*, 510 (1990) 197.
- 11 D. Mislovičová, P. Gemeiner and A. Breier, *Enzyme Microb. Technol.*, 10 (1988) 568.

Short Communication

Identification of lichen substances by a standardized high-performance liquid chromatographic method

G.B. Feige* and H.T. Lumbsch

Botanical Institute, University of Essen, P.O. Box 103 764, 45117 Essen (Germany)

S. Huneck

Institute of Plant Biochemistry, Weinberg 3, 06018 Halle (Germany)

J.A. Elix

Department of Chemistry, The Faculties, Australian National University, Canberra, ACT 0200 (Australia)

(First received March 9th, 1993; revised manuscript received May 24th, 1993)

ABSTRACT

A method for the identification of secondary aromatic lichen substances using high-performance liquid chromatography (HPLC) with reversed-phase columns, gradient elution and benzoic and solorinic acids as standards has been developed. A retention index (I), calculated from the elution time of the appropriate peak with reference to the standards, is used in identification. I values are recorded for 331 compounds chromatographed in this standard system.

INTRODUCTION

Lichens are well known for the diversity of secondary metabolites that they produce, and the identification of these substances has become an integral part of modern taxonomic investigations of these organisms [1]. Out of a total of ca. 550 lichen compounds so far reported, over 450 are aromatic derivatives.

Standardized methodology and further refinement of routine analytical TLC procedures for detecting and comparing lichen metabolites have been reported by Culberson and co-workers [2–

6]. Further, two-dimensional TLC has considerably improved rate of flow values (R_F) discrimination of structurally similar compounds and has enabled the identification of minor constituents present in complex mixtures [7].

Recently, high-performance liquid chromatography (HPLC) has become more widely used as an effective analytical tool for the separation and identification of lichen substances. Early attempts to apply this method to lichen chemotaxonomy were made using normal-phase silica columns [8,9], but better results are obtained with bonded reversed-phase columns. While Culberson and Culberson [10] used a methanol–water–acetic acid solvent system, Lumbsch and

* Corresponding author.

Elix [11] used a mobile phase consisting of methanol, water and orthophosphoric acid.

Although these isocratic methods produced excellent results, gradient elution is an even more effective method for HPLC analyses of lichen extracts, since such extracts frequently contain metabolites of wide-ranging hydrophobicity. Methods using gradient elution for various analyses in the genera *Cladina*, *Cladonia*, *Placopsis*, *Rhizocarpon* and the Roccellaceae and other groups of lichenized ascomycetes have been reported [12–18]. Here we propose a new standardized method of gradient elution for the identification of lichen products in chemotaxonomic investigations. The new solvent gradient devised in this study maximizes the resolution of a large number of the compounds that are found in lichens and has already been used successfully in a number of lichen genera belonging to different families, namely the Agyriaceae [19], Lecanoraceae [20,21], Pertusariaceae [22] and Roccellaceae [23].

MATERIALS AND METHODS

Sources of compounds

In general, authentic samples of lichen substances were used when available, and each compound was injected separately to determine its retention index (*I*). Otherwise, herbarium specimens with established chemistry were used as standards. In these cases 10 mg of lichen material were extracted in 1 ml of cool acetone for 60 min.

Equipment, solvent systems and internal standards

A Kontron HPLC system connected to a Data System 450 instrument with a 430 UV detector and a 360 autosampler was used. A Spherisorb 5 ODS 2 column (Kontron), 5 μm , 250 \times 4.6 mm, at room temperature was used.

Two solvent systems were employed. Solvent system A was Aqua bidest containing 1% orthophosphoric acid and solvent system B was 100% methanol (Baker). The solvents were degassed for 30 min in an ultrasonic vibrator prior to use.

The substances were dissolved in acetone to which the two standards were added (20 mg of

benzoic acid and 20 mg of solorinic acid per 1000 ml of acetone). Benzoic acid elutes very rapidly and solorinic acid elutes slowly. Only orsellinic acid, consalazinic acid and the phthalides elute more rapidly than benzoic acid and the *I* values (detailed later) of these compounds are given as negative numbers. Only one lichen metabolite (hierridin) eluted more slowly than solorinic acid in our gradient system.

The programmed run

The run started with 30% B and continued isocratically for 1 min at a flow-rate of 0.7 ml/min. After 1 min, 20 μl were injected and solvent system B was increased to 70% within 14 min, then up to 100% in 30 min, and then isocratically in 100% B for a further 18 min. At the end of the run the solvent system B was decreased to 30% within 1 min and the column flushed with 30% B for 16 min before a new run was started.

The compounds were detected at $\lambda = 245$ nm and the UV spectra ($\lambda = 200$ –400 nm) of each peak eluted were recorded automatically.

The retention index value

Benzoic and solorinic acids were used as internal standards by their addition to the extraction liquid (acetone). Benzoic acid was utilized previously by Huovinen *et al.* [17] as a substance that elutes more rapidly than most but not all lichen compounds. Bis-(2-ethylhexyl)-phthalide was employed as a second internal standard [17]. However, this compound elutes at the same time as some chlorolichexanthenes and is therefore not recommended as a standard for the identification of lichen extracts containing chloroxanthenes or long-chain depsides. We therefore sought a more hydrophobic compound and found solorinic acid to be ideal. This compound is present in large quantities in the Arctic–alpine lichen *Solorina crocea* and can be readily isolated because of its hydrophobicity. The *I* value of an unknown peak is calculated as follows:

$$I = \frac{t_{\text{R}} \text{ of peak} - t_{\text{R}} \text{ of benzoic acid}}{t_{\text{R}} \text{ of solorinic acid}} \times 100$$

The *I* values as defined here are very stable over the lifetime of a column.

TABLE I

RETENTION INDICES OF THE EXAMINED LICHEN SUBSTANCES AND THEIR SUBSTANCE CLASS

<i>I</i>	Examined substance	Substance class
–3	5,7-Dihydroxy-6-methylphthalide	Monocyclic phenol derivatives
–3	6-Formyl-5,7-dihydroxyphthalide	Monocyclic phenol derivatives
–2	Orsellinic acid	Monocyclic phenol derivatives
–1	Consalazinic acid	Depsidones
1	Constictic acid	Depsidones
2	Montagnetol	Monocyclic phenol derivatives
3	Connorstictic acid	Depsidones
3	Conporphyrilic acid	Dibenzofuranes
3	Variolaric acid	Depsidones
4	Canarione	
4	Cryptostictic acid	Depsidones
5	6-Hydroxymethyleugenitin	Chromones
5	Galapagin	Chromones
5	Menegazzaic acid	Depsidones
5	Methyl orsellinate	Monocyclic phenol derivatives
5	Salazinic acid	Depsidones
6	Pannaric acid	Dibenzofuranes
6	Pulvinic acid	Pulvinic acid derivatives
6	Stictic acid	Depsidones
7	Decarboxythamnolic acid	Depsides
7	Erythrin	Depsides
7	Hypoconstictic acid	Depsidones
7	Porphyrilic acid	Dibenzofuranes
7	Strepsilin	Dibenzofuranes
8	Eugenitol	Chromones
8	Hyposalazinic acid	Depsidones
8	Methyl 4-O-methylorsellinate	Monocyclic phenol derivatives
8	Roccellin	Chromones
9	Galbinic acid	Depsidones
9	Virensic acid	Depsidones
10	Barbatolin	Benzyl ester
10	Diploschistesic acid	Depsides
10	Lepraric acid	Chromones
10	Methyl β -orsellinate	Monocyclic phenol derivatives
10	Siphulellic acid	Depsidones
10	Succinprotocetraric acid	Depsidones
11	4-O-Demethylnotatic acid	Depsidones
11	Chiodectonic acid	Anthraquinones
11	Norlobariol	Diphenyl ether
11	Pannaric acid 6-methyl ester	Dibenzofuranes
11	Protosiphulin	Chromones
12	4-O-Demethylglomellic acid	Depsides
12	Norstictic acid	Depsidones
13	2'-O-Demethylpsoromic acid	Depsidones
13	2-O-Methylsquamatic acid	Depsides
13	Alectorialin	Benzyl ester
13	Epiphorellic acid 2	Diphenyl esters
13	Hypostictic acid	Depsidones
13	Pannaric acid 2-methyl ester	Dibenzofuranes
13	Sordidone	Chromones

(Continued on p. 420)

TABLE I (continued)

<i>I</i>	Examined substance	Substance class
14	4-O-Demethylloxodellic acid	Depsides
14	Lecanoric acid	Depsides
14	Protocetraric acid	Depsidones
15	Confumarprotocetraric acid	Depsidones
15	Hypothamnolic acid	Depsides
15	Norlichexanthon	Xanthones
16	2,4'-Di-O-methylnorsekikaic acid	Depsides
15	Subpicrolichenic acid	Depsones
16	3-Hydroxyumbilicic acid	Depsides
16	Barbatolic acid	Benzyl ester
16	Echinocarpic acid	Unknown
16	Methyl evernate	Depsides
16	Norlobariol methyl ester	Diphenyl ether
16	Schizopeltic acid	Dibenzofuranes
17	Arthonin	
17	2-O-Methylhiassic acid	Depsides
17	3'-Dechlorolecideiodin	Depsidones
17	4-O-Demethyldiffractaic acid	Depsides
17	Conorlobaridone	Depsidones
17	Fumarprotocetraric acid	Depsidones
17	Malonprotocetraric acid	Depsidones
17	Oxyphysodic acid	Depsidones
17	Paludosic acid	Depsides
18	Alectorialic acid	Benzyl ester
18	Arthoniaic acid	Depsides
18	Contortin	Biphenyl
18	Glomellic acid	Depsides
18	Glomellonic acid	Depsidones
18	Methyl lecanorate	Depsides
18	Physodalic acid	Depsidones
18	Pulvinic acid	Pulvinic acid derivatives
18	Thamnolic acid	Depsides
19	5-Chloronorlichexanthon	Xanthones
19	Crustinic acid	Depsides
19	Eugenitin	Chromones
19	Hiassic acid	Depsides
19	Hypoprotocetraric acid	Depsidones
19	Leprolomin	Diphenyl ether
19	Notatic acid	Depsidones
19	Submerochlorophaeic acid	Depsides
19	Vittatolic acid	Depsidones
20	2-Chloronorlichexanthon	Xanthones
20	4'-O-Methylnorsekikaic acid	Depsides
20	4-O-Demethylglomelliferic acid	Depsides
20	Conloxodin	Depsidones
20	Hypothallin	Amino acid derivatives
20	Isonorlobaridone	Diphenyl ether
20	Lividic acid	Depsidones
20	Orcinyl lecanorate	Depsides
21	2'-O-Methylphysodic acid	Depsidones
21	3-Methoxyumbilicic acid	Depsides
21	4'-O-Demethylsekikaic acid	Depsides
21	4-Chloronorlichexanthon	Xanthones

TABLE I (continued)

<i>I</i>	Examined substance	Substance class
21	Gangaleoidin	Depsidones
21	Normiriquidisäure	Depsides
21	Psoromic acid	Depsidones
22	2'-O-Methylanziaic acid	Depsides
22	2-O-Methylobtusatic acid	Depsides
22	Aspicilin	Macrocyclic lactone
22	Loxodellic acid	Depsides
22	Nordivaricatic acid	Depsides
22	Norgangaleoidin	Depsidones
22	Parietic acid	Anthraquinones
22	Picrolichenic acid	Depsidones
22	Siphulin	Chromones
22	Squamatic acid	Depsides
23	3-O-Demethylscenscidin	Depsidones
23	4-O-Demethylmicrophyllinic acid	Depsides
23	Buellolide	Diphenyl ether
23	Cryptochlorophaeic acid	Depsides
23	Ovoic acid	Depsides
24	4'-O-Methylnorhomosekikaic acid	Depsides
24	4-O-Demethylbarbatic acid	Depsides
24	4-O-Demethylplanaic acid	Depsides
24	5-O-Methylhiascic acid	Depsides
24	7-Chloronorlichexanthone	Xanthenes
24	Epiphorellic acid 1	Diphenyl esters
24	Isonotatic acid	Depsidones
24	Lecideoidin	Depsidones
24	Methyl 3,5-dichlorolecanorate	Depsides
24	Teloschistin	Anthraquinones
25	2'-O-Methylmicrophyllinic acid	Depsides
25	2-O-Methylsekikaic acid	Depsides
25	Gyrophoric acid	Depsides
25	Methyl 2,2'-di-O-methylesteriodermate	Depsides
25	Physodic acid	Depsidones
25	Pseudoplacodiolic acid	Usnic acids
25	Umbilicic acid	Depsides
25	Vulpinic acid	Pulvinic acid derivatives
26	2-O-Methylnorstenosporic acid	Depsides
26	3-Methoxy-2,4-di-O-methylgyrophoric acid	Depsides
26	4'-O-Methylcryptochlorophaeic acid	Depsides
26	4,5-Dichloronorlichexanthone	Xanthenes
26	Ålectronic acid	Depsidones
26	Evernic acid	Depsides
26	Glomelliferonic acid	Depsidones
26	Haemothamnolic acid	Depsides
26	Hirtifructic acid	Unknown
26	Merochlorophaeic acid	Depsides
26	Norlobaridone	Depsidones
26	α -Collatolic acid	Depsidones
27	2,5-Dichloronorlichexanthone	Xanthenes
27	Euplectin	Anthraquinones
27	Glomelliferic acid	Depsides
27	Methyl 3'-methyllecanorate	Depsides

(Continued on p. 422)

TABLE I (continued)

<i>I</i>	Examined substance	Substance class
27	Olivetoric acid	Depsides
27	Placodiolic acid	Usnic acids
28	2,7-Dichloronorlichexanthone	Xanthonnes
28	2-O-Methylconfluentic acid	Depsides
28	2-O-Methyldivaricatic	Depsides
28	4-O-Demethylstenosporic acid	Depsides
28	4-O-Methylhypoprotocetraric acid	Depsidones
28	Baeomycesic acid	Depsides
28	Chlorolecideoidin	Depsidones
28	Leprapinic acid	Pulvinic acid derivatives
28	Loxodin	Depsidones
28	Oxostenosporic acid	Depsides
28	Sekikaic acid	Depsides
28	Subdidymic acid	Dibenzofuranes
29	2'-O-Methylanziaic acid	Depsides
29	2,4-Dichloronorlichexanthone	Xanthonnes
29	2,4-Di-O-Methylgyrophoric acid	Depsides
29	4-O-Demethylimbricatic acid	Depsides
29	Confluentic acid	Depsides
29	Methyl sekikaiate	Depsides
29	Pinastric acid	Pulvinic acid derivatives
29	Wrightiin	Depsides
29	<i>m</i> -Scrobiculin	Depsides
30	4,7-Dichloronorlichexanthone	Xanthonnes
30	4-O-Methylisocryptochlorophaeic acid	Depsides
30	5,7-Dichloronorlichexanthone	Xanthonnes
30	DiffRACTaic acid	Depsides
30	Glaucophaeic acid	Depsides
30	Isoobtusatic acid	Depsides
30	Lobaric acid	Depsidones
30	Methyl 2'-O-methyleriodermate	Depsides
30	Methyl gyrophorate	Depsides
30	Miriquidic acid	Depsides
30	Pseudocyphellarin B	Depsides
31	2',2''-Di-O-methyltenuiorin	Depsides
31	2-Chloro-6-O-methylnorlichexanthone	Xanthonnes
31	4,5-Di-O-methylhiassic acid	Depsides
31	4-O-Methylnorlobaridon	Depsidones
31	Boninic acid	Depsides
31	Methyl 2-O-methyleriodermate	Depsides
31	Methyl 4-O-demethylbarbatate	Depsides
31	Skyrin	Anthraquinones
31	<i>p</i> -Scrobiculin	Depsides
32	2'-O-Methylhyperphyllinic acid	Depsides
32	3'-Methylevernic acid	Depsides
32	3,5-Dichloro-2'-O-methylanziaic acid	Depsides
32	3-Chlorodivaricatic acid	Depsides
32	4-O-Methylcryptochlorophaeic acid	Depsides
32	5-Chloro-6-O-methylnorlichexanthone	Xanthonnes
32	Emodin	Anthraquinones
32	Methyl 5-chloronorobtusatate	Depsides
32	Obtusatic acid	Depsides
32	Secalonic acid B	Anthraquinones

TABLE I (continued)

<i>I</i>	Examined substance	Substance class
33	2"-O-Methyltenuiorin	Depsides
33	2-O-Methyltenuiorin	Depsides
33	4-O-Demethylsphaerophorin	Depsides
33	4-O-Methylolivivetic acid	Depsides
33	5-Chlorovirensic acid	Depsidones
33	Divaricatic acid	Depsides
33	Secalonic acid C	Anthraquinones
34	3,5-Dichloro-4-O-demethylplanaic acid	Depsides
34	4'-O-Methylnorcryptochlorophaeic acid	Depsides
34	4-Chloro-6-O-methylnorlichexanthone	Xanthonnes
34	4-O-Methylgyrophoric acid	Depsides
34	7-Chloro-1,6-di-O-methylemodin	Anthraquinones
34	Imbricatic acid	Depsides
34	Nephroarctin	Depsides
34	Planaic acid	Depsides
34	Rhizocarpic acid	Pulvinic acid derivatives
34	Secalonic acid A	Anthraquinones
34	Superpicrolichenic acid	Depsones
35	2-O-Methylstenosporic acid	Depsides
35	7-Chloro-1-O-methylemodin	Anthraquinones
35	Anziaic acid	Depsides
35	Arthothelin	Xanthonnes
35	Didymic acid	Dibenzofuranes
35	Eriodermin	Depsidones
35	Homosekikaic acid	Depsides
35	Hyperconfluentic acid	Depsides
35	Isovicanicin	Depsidones
35	Stenosporonic acid	Depsidones
35	Vinetorin	Xanthonnes
36	2'-O-Methylimbricatic acid	Depsides
36	2'-O-Methylstenosporic acid	Depsides
36	2,5-Dichloro-6-O-methylnorlichexanthone	Xanthonnes
36	Demethylchodatol	Xanthonnes
36	Epanorin	Pulvinic acid derivatives
36	Isoarthothelin	Xanthonnes
36	Leoidin	Depsidones
36	Usnic acid	Usnic acids
37	1'-Chlornephroarctin	Depsides
37	2'-O-Methyltenuiorin	Depsides
37	2,4,7-Trichloronorlichexanthone	Xanthonnes
37	3-Dechlorodiploicin	Depsidones
37	4,5-Dichloro-6-O-methylnorlichexanthone	Xanthonnes
37	Asemone	Xanthonnes
37	Barbatic acid	Depsides
37	Congrayanic acid	Diphenyl ether
37	Grayanic acid	Depsidones
37	Methyl 4-O-methyleriodermate	Depsidones
37	Pannarin	Depsidones
37	Vicanicin	Depsidones
38	4,5-Dichloro-3-O-methylnorlichexanthone	Xanthonnes
38	7-Chloroemodin	Anthraquinones
38	Atranorin	Depsides

(Continued on p. 424)

TABLE I (continued)

<i>I</i>	Examined substance	Substance class
38	Hyperhomosekikaic acid	Depsides
39	2'-O-Methylperlatolic acid	Depsides
39	3-Chlorostenosporic acid	Depsides
39	Caloploicin	Depsidones
39	Evernine	Depsides
39	Methyl eriodermate	Depsides
39	Tenuiorin	Depsides
40	7-Chloro-6-O-methylnorlichexanthone	Xanthones
40	Melacarpic acid	Dibenzofuranes
40	Methyl 5-chloro-4-O-demethylbarbatate	Depsides
40	Stenosporic acid	Depsides
41	4-O-Demethylgrayanic acid	Depsidones
41	Colensoic acid	Depsidones
41	Isousnic acid	Usnic acids
41	Superconfluentic acid	Depsides
41	Thiophanic acid	Xanthones
42	2-O-Methylperlatolic acid	Depsides
42	4-O-Methylsuperolivetic acid	Depsides
42	Chloroatranorin	Depsides
43	8-O-Methylthiomelin	Xanthones
43	Argopsin	Depsidones
43	Diploicin	Depsidones
43	Pulvinic dilactone	Pulvinic acid derivatives
44	2'-O-Methylisohyperlatolic acid	Depsides
44	Pseudocyphellarin A	Depsides
44	Thiophanic acid	Xanthones
44	Valsarin	Anthraquinones
45	3-Chloroperlatolic acid	Depsides
45	Thuringione	Xanthones
46	2,7-Dichloro-6-O-methylnorlichexanthone	Xanthones
46	4-Dechlorothiomelin	Xanthones
46	5,7-Dichloro-3-O-methylnorlichexanthone	Xanthones
46	Lichexanthone	Xanthones
46	Norsolorinic acid	Anthraquinones
46	Sphaerophorin	Depsides
47	2,5,7-Trichloro-3-O-methylnorlichexanthone	Xanthones
47	2-Chlorolichexanthone	Xanthones
47	Calycin	Pulvinic acid derivatives
47	Methyl barbatate	Depsides
47	Perlatolic acid	Depsides
48	1,8-Dihydroxy-3,6-dimethoxy-9-H-xanthen-9-one	Xanthones
48	2'-O-Methylsuperlatolic acid	Depsides
48	2,7-Dichloro-3-O-methylnorlichexanthone	Xanthones
48	5-Chlorolichexanthone	Xanthones
48	6-O-Methylarthothelin	Xanthones
49	6-O-Methylasemone	Xanthones
49	Chodatin	Xanthones
50	2,5-Dichlorolichexanthone	Xanthones
50	4-Chlorolichexanthone	Xanthones
50	Fragilin	Anthraquinones
50	Parietin	Anthraquinones
51	3-O-Methylasemone	Xanthones
51	6-O-Methylthiophanic acid	Xanthones

TABLE I (continued)

<i>I</i>	Examined substance	Substance class
52	7-Chlorolichexanthone	Xanthonnes
53	2,7-Dichlorolichexanthone	Xanthonnes
53	3-O-Methylthiophanic acid	Xanthonnes
53	Thiomelin	Xanthonnes
54	2,5,7-Trichlorolichexanthone	Xanthonnes
54	Hyperlatolic acid	Depsides
55	2,4-Dichlorolichexanthone	Xanthonnes
55	4,5-Dichlorolichexanthone	Xanthonnes
55	5,7-Dichlorolichexanthone	Xanthonnes
55	Isohyperlatolic acid	Depsides
56	1,3,6-Tri-O-methylarthothelin	Xanthonnes
56	6-O-Methylthiophanic acid	Xanthonnes
57	6-O-Methylaverythrin	Anthraquinones
59	4,4'-Disolorinic acid	Anthraquinones
59	Superlatolic acid	Depsides
62	2,4,5-Trichlorolichexanthone	Xanthonnes
75	Solorinic acid	Anthraquinones
84	Hierridin	Monocyclic phenol derivatives

RESULTS AND DISCUSSION

The aromatic lichen substances can be identified by comparison of the internal *I* values. The *I* values of 331 compounds are listed in Table I. These data have also been included in a computerized database with the TLC R_F values and further information, such as mass spectrum data, substance class, etc. [24].

The substance classes can be distinguished by their UV spectra and to some extent by their *I* value. Most monocyclic phenol derivatives elute very rapidly and have *I* values between -3 and $+5$, whereas the depsidones with highly variable hydrophobicities have *I* values which range between -1 and $+43$. The chromones also elute quite rapidly (with *I* values between 5 and 22). Whereas depsides with short alkyl side-chains elute rapidly, those with longer alkyl side-chains elute more slowly. In the extreme case of superlatolic acid ($I = 59$) with two C_7 side-chains, only the standard solorinic acid and 2,4,5-trichlorolichexanthone elute more slowly. Norlichexanthonnes and lichexanthonnes can be readily separated by gradient HPLC. The norlichexanthonnes have *I* values between 15 and 44 depending on the degree of chlorination, while the more hy-

drophobic lichexanthonnes have *I* values between 46 and 52. Similarly, the depsonnes have *I* values between 15 and 34 (depending on the length of the side-chains), while the usnic acids have *I* values between 25 and 36.

Given the large number of minor lichen substances still to be characterized and identified, it should be emphasized that compounds should not be identified solely on the basis of their *I* value using this HPLC method. Often substances that elute at the same time belong to different substance classes and can readily be distinguished by their UV spectra, though even then independent confirmation of their identity should be sought. Complementary analytical methods include standardized TLC [2–6], two-dimensional TLC [7], lichen mass spectrometry [25] or comparative chromatography with authentic lichen compounds. The resolution attainable by our HPLC method is illustrated in Fig. 1, which shows the chromatogram of a mixture of 30 lichen compounds and the two standards, and Fig. 2, which shows the chromatogram of an extract from *Lecanora leprosa*. The potency of this system can readily be appreciated when one considers that in practice relatively few peaks are encountered in the HPLC analyses of crude

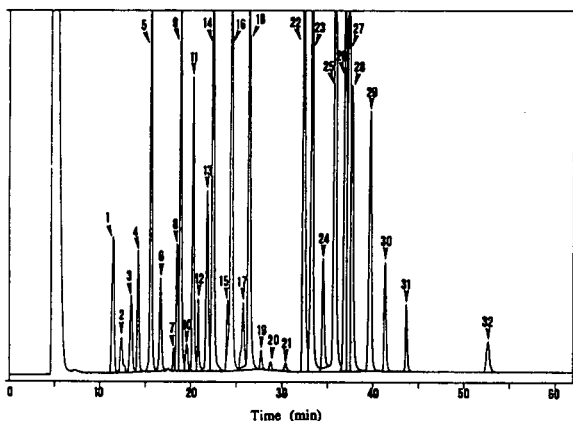


Fig. 1. HPLC of a mixture of 30 lichen substances. Peaks: 1 = orsellinic acid; 2 = benzoic acid, internal standard; 3 = constictic acid; 4 = variolaric acid; 5 = salazinic acid; 6 = stictic acid; 7 = diploschistesic acid; 8 = chiodectonic acid; 9 = norstictic acid; 10 = hypostictic acid; 11 = lecanoric acid; 12 = subpicrolichenic acid; 13 = fumarprotocetraric acid; 14 = thamnolic acid; 15 = gangaleoidin; 16 = picrolichenic acid; 17 = gyrophoric acid; 18 = placodiolic acid; 19 = confluentic acid; 20 = pseudocyphellarin B; 21 = divaricatic acid; 22 = usnic acid; 23 = atranorin; 24 = stenosporic acid; 25 = chloroatranorin; 26 = pseudocyphellarin A; 27 = lichexanthone; 28 = 2-chlorolichexanthone; 29 = 2,5-dichlorolichexanthone; 30 = isohyperlatolic acid; 31 = superlatolic acid; 32 = solorinic acid, internal standard.

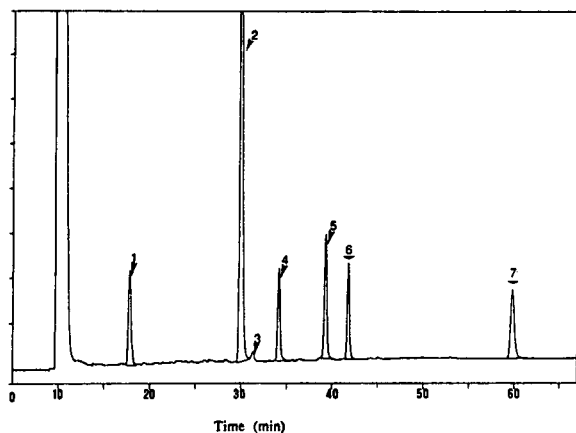


Fig. 2. HPLC of *Lecanora leprosa* (BRI-491270). Peaks: 1 = benzoic acid, internal standard; 2 = gangaleoidin; 3 = norgangaleoidin; 4 = chlorolecideoidin; 5 = atranorin; 6 = chloroatranorin; 7 = solorinic acid, internal standard.

lichen extracts. However, a few lichens are exceptional. In *Haematomma pachycarpum*, for example, twelve substances were detected [26], but this assemblage of secondary products was reported to be the most complex known in any one lichen species.

ACKNOWLEDGEMENTS

We wish to thank Dr. Alan W. Archer (Sydney), Dr. Chicita F. Culberson (Duke) and Professor A.G. Gonzales (Tenerife) for sending us authentic samples of lichen substances or lichen specimens for our examination. The technical assistance of M. Neugebauer is gratefully acknowledged.

REFERENCES

- 1 D.L. Hawksworth, in D.H. Brown, D.L. Hawksworth and R.H. Bailey (Editors), *Lichenology: Progress and Problems*, Academic Press, London, 1976, p. 139.
- 2 C.F. Culberson, *J. Chromatogr.*, 72 (1972) 113.
- 3 C.F. Culberson and K. Ammann, *Herzogia*, 5 (1979) 1.
- 4 C.F. Culberson, W.L. Culberson and A. Johnson, *Bryologist*, 84 (1981) 16.
- 5 C.F. Culberson and A. Johnson, *J. Chromatogr.*, 238 (1982) 483.
- 6 C.F. Culberson and H. Kristinsson, *J. Chromatogr.*, 46 (1970) 85.
- 7 C.F. Culberson and A. Johnson, *J. Chromatogr.*, 128 (1976) 253.
- 8 C.F. Culberson, *Bryologist*, 75 (1972) 54.
- 9 R. Nourish and R.W.A. Olivier, in D.H. Brown, D.L. Hawksworth and R.H. Bailey (Editors), *Lichenology: Progress and Problems*, Academic Press, London, 1976, p. 185.
- 10 C.F. Culberson and W.L. Culberson, *Exp. Mycol.*, 2 (1978) 245.
- 11 H.T. Lumbsch and J.A. Elix, *Pl. Syst. Evol.*, 150 (1985) 275.
- 12 G.B. Feige, B. Viethen, M. Geyer and G. Follmann, *J. Hattori Bot. Lab.*, 60 (1986) 143.
- 13 G. Follmann and M. Geyer, *Z. Naturforsch. C: Biosci.*, 41 (1986) 1117.
- 14 G. Follmann, M. Schulz and S. Huneck, *Crypt. Bot.*, 2/3 (1991) 298.
- 15 M. Geyer, *Dissertation*, University of Essen, Essen, 1985.
- 16 M. Geyer, T. Feuerer and G.B. Feige, *Pl. Syst. Evol.*, 145 (1985) 41.
- 17 K. Huovinen, R. Hiltunen and M. von Schantz, *Acta Pharm. Fenn.*, 94 (1985) 99.
- 18 D. Strack, G.B. Feige and R. Kroll, *Z. Naturforsch. C: Biosci.*, 34 (1979) 695.

- 19 H.T. Lumbsch, H. Kashiwadani and H. Streimann, *Pl. Syst. Evol.*, 185 (1993) 285.
- 20 H.T. Lumbsch, *Bryologist*, 95 (1992) 430.
- 21 H.T. Lumbsch and G.B. Feige, *Mycotaxon*, 45 (1992) 473.
- 22 H.T. Lumbsch, G.B. Feige and K.E. Schmitz, *Bibl. Lichenol.*, (1993) in press.
- 23 G.B. Feige, H.T. Lumbsch and B. Mies, *Crypt. Bot.*, 3 (1993) 101.
- 24 E. Mietzsch, H.T. Lumbsch and J.A. Elix, *Wintabolites (Mactabolites for Windows) Users Manual*, University of Essen, August 1992.
- 25 J. Santesson, *Ark. Kemi*, 30 (1969) 363.
- 26 C.F. Culberson, W.L. Culberson, S. Gowan and A. Johnson, *Am. J. Bot.*, 74 (1987) 403.

Short Communication

High-performance liquid chromatographic method for the monitoring of the synthesis of the precursor for tetramisole

Jitendra S. Wagh, Asmita A. Mokashi and Arunabha Datta*

Alchemie Research Centre, P.O. Box 155, Thane-Belapur Road, Thane, 400 601 Maharashtra (India)

(First received December 1st, 1992; revised manuscript received April 27th, 1993)

ABSTRACT

The synthesis of the monochloro precursor $C_6H_5CH_2(OH)CH_2NHCH_2CH_2Cl$ is the crucial step in the synthesis of the important anthelmintic drug tetramisole. HPLC methods using mobile phases consisting of methanol, water and acetonitrile in various combinations together with ammonium chloride as an inorganic modifier and Nova-Pak C_{18} and μ Porasil columns were developed for the monitoring and quantification of each step of the synthesis of the precursor. The methods provide important clues for increasing the yield of the product.

INTRODUCTION

Tetramisole hydrochloride is a potent anthelmintic drug [1,2] with antidepressant activity. Several methods based on polarography [3], spectrophotometry [4] and HPLC [5] have been reported for the determination of this drug. In this work, however, our aim was to develop HPLC methods for monitoring and optimizing the yields of the various steps in the synthesis of tetramisole hydrochloride by a commercial route. In this synthetic route (Fig. 1), the formation of the monochloro precursor **III** is the crucial step, as the subsequent steps of condensation with thiourea followed by ring closure to give tetramisole proceed in a facile manner. We

describe here efficient HPLC methods for monitoring and quantifying the yields of each step of the three-stage synthesis of the monochloro precursor **III**.

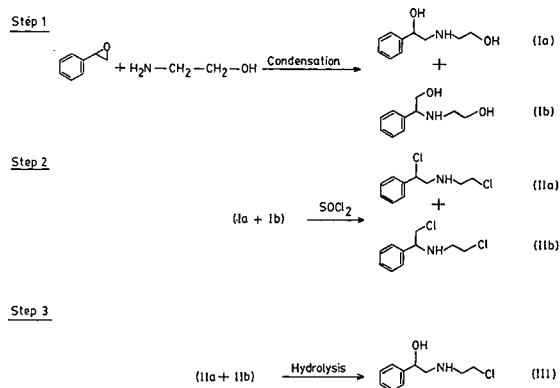


Fig. 1. Reaction scheme for the three-step synthesis of the monochloro precursor **III**.

* Corresponding author.

EXPERIMENTAL

Instrumentation

The HPLC system used has been described earlier [6] and consisted of a Model 590 alternating pump, a Nova-Pak C₁₈ column (4 μm, 150 mm × 3.9 mm I.D.), a μPorasil column (10 μm, 300 mm × 3.9 mm I.D.), a Model R 403 refractive index detector (all from Waters, Milford, MA, USA), a Rheodyne injector with a 10-μl loop and a Hewlett-Packard Model 3394 A integrator.

Reagents and solvents

Styrene oxide, ethanolamine and thionyl chloride were obtained from Fluka (Buchs, Switzerland) and ammonium chloride, methanol and acetonitrile from BDH (Poole, UK). Authentic samples of **Ia**, **Ib**, **IIa**, **IIb** and **III** were synthesized and characterized in our laboratory.

Chromatographic analyses

The following chromatographic conditions were used for monitoring the different steps of the synthesis route:

Step 1: the mobile phase was methanol–water (65:35, v/v) containing 0.8 M NH₄Cl and with the pH adjusted to 8 with ammonia solution. The flow-rate was 1.0 ml/min and the column was μPorasil.

Steps 2 and 3: the mobile phase was methanol–water (17:83, v/v) containing 0.8 M NH₄Cl and with the pH adjusted to 3 with phosphoric acid. A Nova-Pak C₁₈ column was used and the flow-rate was 0.8 ml/min.

The calibration and determination of the diol isomers **Ia** and **Ib** were done on a Nova-Pak C₁₈ column using a mobile phase of acetonitrile–water (5:95, v/v) containing 0.4 M NH₄Cl at pH 8 with a flow-rate of 1.0 ml/min. The calibration and determination of the monochloro compound **III** were done using the conditions employed in step 2. A refractive index detector was used for all the chromatographic analyses.

RESULTS AND DISCUSSION

The chromatogram for step 1 of the synthesis route is shown in Fig. 2. The condensation of

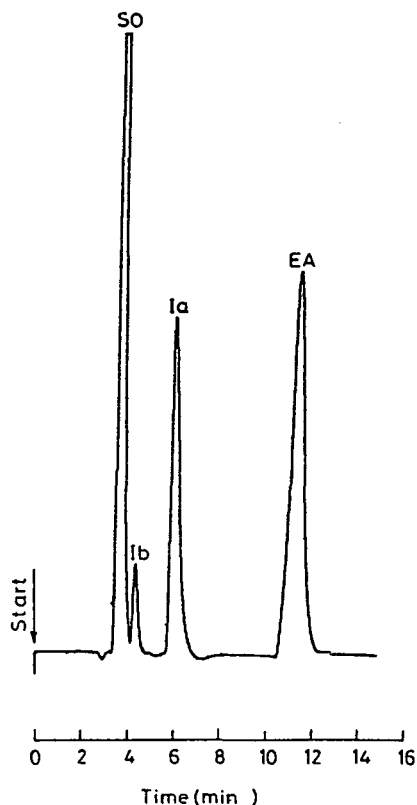


Fig. 2. Typical chromatogram for the reaction mixture in the synthesis of the diol isomers **Ia** and **Ib** from styrene oxide (SO) and ethanolamine (EA).

styrene oxide with ethanolamine gives rise to two isomeric diols (**Ia** and **Ib**) and the separation of these two isomers from each other and from the starting materials is clearly evident. Of the two isomers formed, **Ia** is the desired product. Consequently, the chromatographic analysis of this step was carried out not only for monitoring the completion of the reaction (through the disappearance of the peaks due to styrene oxide and ethanolamine) but also for minimizing the amount of the undesired isomer (**Ib**). The linearity of response for both the diol isomers **Ia** and **Ib** (Fig. 3) over the concentration range chosen is evident from Table I. The inter-assay precision of the method was established by triplicate analyses of synthetic mixtures of different compositions and the maximum error was found to be 1% (Table II). The results of the analysis of actual reaction mixtures for the synthesis of the diol isomers are shown in Table

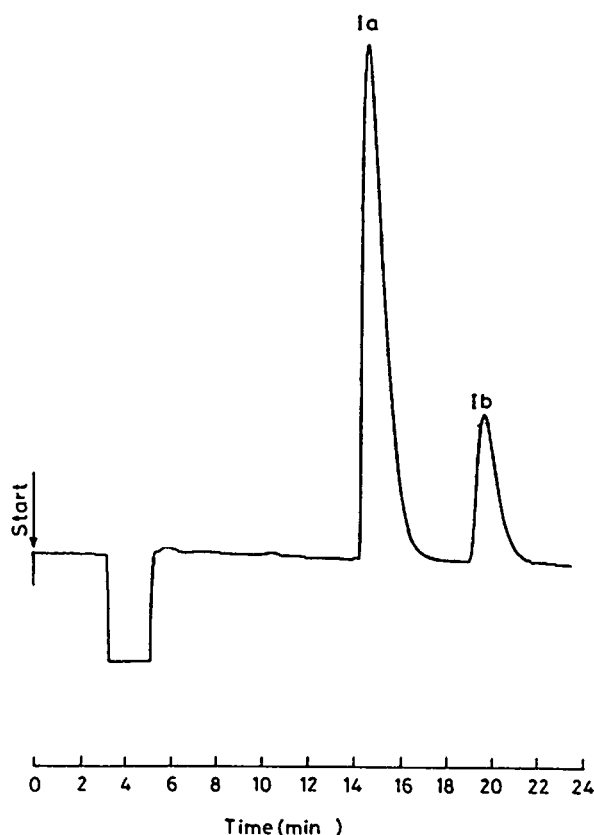


Fig. 3. Chromatogram of a synthetic mixture of diols **Ia** (15.51 μg) and **Ib** (3.51 μg) for calibration and quantification.

III and it was found that the purity of the diols synthesized in step 1 was lower than expected and varied with the reaction conditions. This was probably because of the formation of side-products such as the tertiary amine or the dimer of styrene oxide, which were not detected under the chromatographic conditions employed. However, it was possible to modify the reaction conditions of step 1 so as to improve the assay of the product from 73.5% to 88.3% in the case of three different samples shown in Table III.

The conversion of the diol isomers to the corresponding dichloro derivatives (step 2) was also monitored chromatographically (Fig. 4) and it was found that there was total conversion of the diols to the dichloro compounds. It was also observed from the area percentages that the ratio of the two dichloro isomers (**IIa** and **IIb**) was similar to that of the two corresponding diols (**Ia** and **Ib**). These observations were in good agreement with the nearly quantitative isolated yields of **IIa** and **IIb**. As this reaction step was quantitative and the amounts of the dichloro isomers isolated were in good agreement with the amounts determined from the area percentages of the respective peaks in the chromatogram, no further quantification of this step was done.

Chromatograms for step 3, the conversion of the dichloro isomers to the monochloro deriva-

TABLE I

LINEARITY OF RESPONSE FOR THE ISOMERIC DIOLS **Ia** AND **Ib** FOR CALIBRATION BY THE EXTERNAL STANDARD METHOD

Sample No.	Ia ^a			Ib ^b		
	Amount (μg)	Area ($\times 10^7$)	Area/amount	Amount (μg)	Area ($\times 10^7$)	Area/amount
1	14.47	23.57	1.63	1.40	2.18	1.56
2	15.51	25.05	1.62	2.11	3.25	1.56
3	16.54	26.64	1.61	2.81	4.36	1.55
4	17.57	28.50	1.62	3.51	5.45	1.55
5	18.62	29.39	1.59	4.21	6.54	1.55
6	20.68	32.83	1.59	14.04	2.15	1.53

^a Regression equation: $y = 0.1149 + 1.595C_{Ia}$. Linearity range: 14–21 μg .

^b Regression equation: $y = 0.05525 + 1.526C_{Ib}$. Linearity range: 1–15 μg .

TABLE II
RESULTS OF THE ANALYSIS OF SYNTHETIC MIXTURES OF DIOLS

Average of triplicate determination.

Ia			Ib		
Taken (mg)	Found (mg)	Error (%)	Taken (mg)	Found (mg)	Error (%)
17.10	16.98	0.70	2.38	2.40	0.83
15.00	14.85	1.00	2.50	2.48	0.80
18.00	17.87	0.70	4.50	4.45	1.00

tive **III**, are shown in Fig. 5. It is interesting that the two dichloro isomers give rise to only one monochloro compound on hydrolysis. In fact, when the progress of this hydrolytic reaction was monitored it was evident (Fig. 5B–E) that initially only one of the dichloro isomers, **Ia**, was selectively being converted into **III**. However, when the reaction conditions were changed, the peak due to the other dichloro isomer (**Ib**) gradually disappeared with a corresponding increase in the intensity of the peak due to **III** but no additional peak was observed (Fig. 5F). It was apparent, therefore, that both the dichloro isomers on hydrolysis gave only one product **III**. In order to confirm this observation, the chromatographic conditions were modified to increase substantially the capacity factor of **III** and it was found still to give rise to only a single symmetric peak. The present HPLC results therefore provided a clue for increasing the yield of **III** by demonstrating the necessity for modifying the reaction conditions for converting **Ib**

also into the desired product. In addition, the results also provide direct evidence for the mechanistically interesting conversion of both the dichloro isomers into a single monochloro compound.

The linearity of response for **III** over the concentration range chosen is shown in Table IV, and this was utilized for determining the assay of the final product of the three-step synthesis.

In conclusion, therefore, HPLC methods have been developed for each stage of the three-step synthesis of the monochloro precursor **III** and the methods have been used very effectively for the determination of the yield and purity of the product at each stage. Further, the analyses have provided useful clues for improving the yield of the product **III**.

Another aspect of this work is the use of NH_4Cl as a modifier in the mobile phase for a more efficient separation of the individual components in each step of the synthesis route. In particular, the separation of the two diol isomers

TABLE III
RESULTS OF THE ANALYSIS OF THE REACTION MIXTURE FOR THE SYNTHESIS OF THE DIOLS

Sample No.	Ia (mg)	Ib (mg)	Total (Ia + Ib) determined by HPLC (mg)	Total reaction product (mg)	Assay (%)
1	11.70	2.95	14.66	19.95	73.45
2	15.60	3.82	19.43	25.62	75.83
3	17.42	3.78	21.20	24.02	88.27

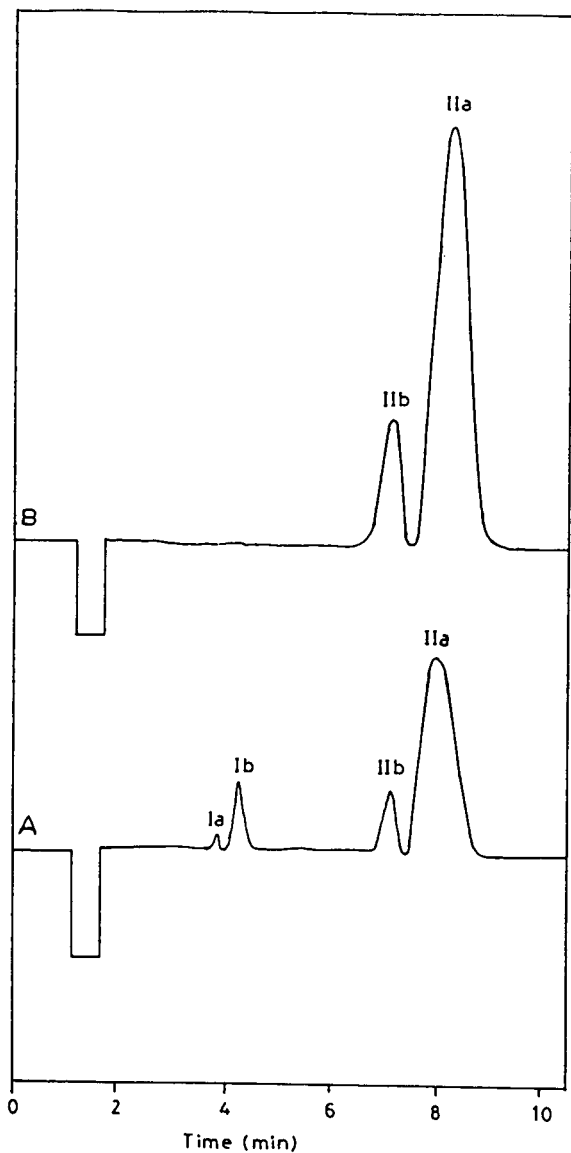


Fig. 4. Chromatograms for monitoring the conversion of the diol isomers **Ia** and **Ib** into the corresponding dichloro derivatives **IIa** and **IIb**: (A) on partial conversion, **IIa** = 19.11 μg , **IIb** = 2.46 μg and (B) on complete conversion, **IIa** = 63.12 μg , **IIb** = 15.41 μg .

Ia and **Ib** could be achieved only with the use of NH_4Cl in the mobile phase and the separation was not possible even with the addition to the mobile phase of conventional PIC reagents such as heptanesulphonic acid, which are known [7–9] to be effective in the separation of amines. We are currently engaged in a comprehensive study

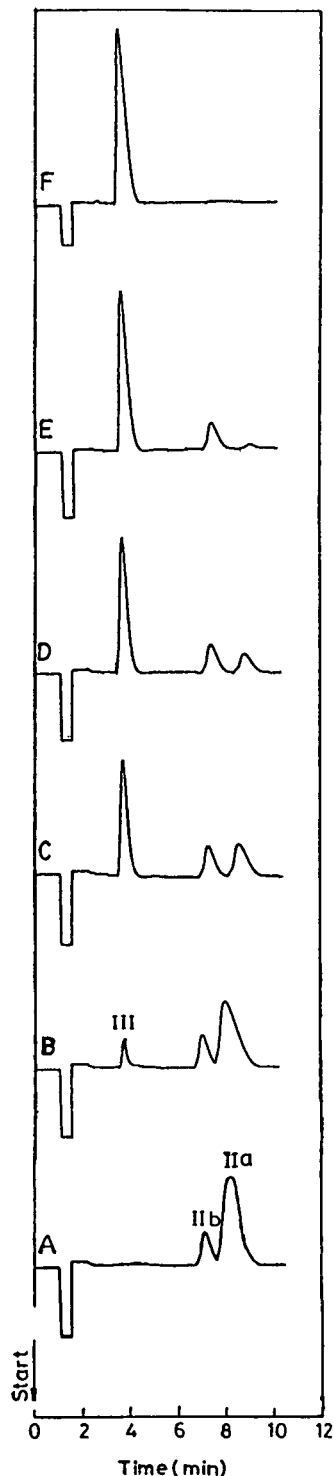


Fig. 5. Chromatograms for monitoring the gradual conversion of the dichloro isomers **IIa** and **IIb** into the monochloro precursor **III**: (A) at zero conversion, **IIa** = 106.8 μg , **IIb** = 26.2 μg ; (B)–(E) gradual selective conversion of only **IIa**; (F) total conversion to **III** (120.3 μg).

TABLE IV

LINEARITY OF RESPONSE FOR THE MONOCHLORO
PRECURSOR III FOR CALIBRATION BY THE EXTER-
NAL STANDARD METHOD

Regression equation: $y = (7.805 \times 10^5) + 2.005 \cdot 10^5 C_{III}$.
Linearity range 40–400 μg .

Sample No.	Amount (μg)	Area ($\times 10^7$)	Area/amount ($\times 10^5$)
1	40.1	0.85	2.12
2'	80.2	1.71	2.13
3	120.3	2.50	2.08
4	160.4	3.34	2.08
5	200.5	4.12	2.05
6	240.6	4.96	2.06
7	280.7	5.75	2.05
8	320.8	6.59	2.05
9	360.9	7.31	2.03
10	401.0	7.96	1.98

(the results of which will be published elsewhere) on the use of NH_4Cl as a mobile phase modifier in several different chromatographic separations and a comparison of its performance with other modifiers such as PIC reagents and other inorganic salts. This study, apart from its primary aim of developing suitable HPLC methods for monitoring the difficult steps in the synthesis of a commercially important compound and providing important clues for improving the yield of the product, is also a good example of the use of NH_4Cl as an efficient mobile phase modifier.

ACKNOWLEDGEMENTS

The authors are grateful to ICI India for financial support, to Dr. B.N. Roy for his encouragement of this work and to Dr. A. Kumar, R.A. Rane, R.V. Salunkhe and A.M. Nijasure for providing authentic analytes and samples.

REFERENCES

- 1 D.C.I. Thienpont, O.F.J. Vanparijs, A.H.M. Raeymaekers, J. Vandenberg, P.J.A. Detnoeh, F.T.N. Allewijn, R.P.H. Marsboom, C.J.E. Niernergeers, K.H.L. Schellekens and P.A.J. Janssen, *Nature*, 209 (1966) 1084.
- 2 A.H.M. Raeymaekers, F.T.N. Allewijn, J. Vandenberg, P.J.A. Demeon, T.T.T. Van Offenwert and P.A.J. Janssen, *J. Med. Chem.* 9 (1966) 545.
- 3 A. Holbrook and B. Scales, *Anal. Biochem.*, 18 (1967) 46.
- 4 R.T. Sane, D.S. Sapre and V.A. Nayak, *Talanta*, 32 (1985) 148.
- 5 D. Mourot, B. Deleptine, J. Boisseau and G. Gayout, *J. Pharm. Sci.*, 68 (1979) 796.
- 6 J.S. Wagh, A.A. Mokashi and A. Datta, *J. Chromatogr.*, 587 (1991) 280.
- 7 K.G. Wahlund and A. Sokolowski, *J. Chromatogr.*, 151 (1978) 299.
- 8 H. Zou, Y. Zhang and P. Lu, *J. Chromatogr.*, 545 (1991) 59.
- 9 I.M. Johansson, K.G. Wahlund and G. Schill, *J. Chromatogr.*, 149 (1978) 281.

Short Communication

Analysis of plant extracts by multiple development thin-layer chromatography

W. Markowski* and G. Matysik

Department of Inorganic and Analytical Chemistry, Medical Academy, Staszica 6, 20081 Lublin (Poland)

(First received February 8th, 1993; revised manuscript received May 12th, 1993)

ABSTRACT

The simplest version of multiple gradient development, two-stage development, is discussed. A computer program for calculation of final R_f values in this gradient mode for known retention *vs.* eluent composition relationships for different plant extracts was used. Comparison of predicted and experimental R_f values showed satisfactory agreement.

INTRODUCTION

The analysis of complex samples is a frequent problem in the development of chromatographic methods: the number of components in many samples, *e.g.*, plant extracts, is unknown and may be as high as several hundred. HPTLC is often coupled with other chromatographic techniques as a preliminary step before the main analysis can be done. The properties of the adsorbents used in HPTLC are well known and, combined with broad range of eluents, give good prospects for the analysis of complex samples.

For a mixture with a wide polarity range, it is unlikely that a gradient of mobile phase concentration will provide a complete separation of all sample components. A different kind of gradient

can be performed with the use of a sandwich chamber. One variation of this process, called incremental multiple development, can be applied [1]. Decreasing solvent strength gradients are very effective for simpler mixtures where a lower separation capacity can be employed adequately for the separation. A unique feature of incremental multiple development HPTLC is the spot reconcentration mechanism.

In multiple development, the zone widths are approximately constant after the first three or four developments [2]. Some simple guidelines for optimizing multiple development chromatography have been proposed [3]. No systematic investigations connected with an adequate mathematical model were reported until recently. In a previous paper [4], a simple model for two-stage development was proposed, later extended to multi-stage development [5]. The models [4,5] have been combined with computer

* Corresponding author.

programs that enable one to investigate the influence of various parameters on the final R_F value and, in consequence, the choice of the optimum conditions. In this work the method was verified for several plant extracts employed in therapy.

EXPERIMENTAL

A horizontal DS-type sandwich chamber [6] (Chromdes, Lublin, Poland) adapted to stepwise gradient elution was used. Precoated 50×100 mm glass plates for HPTLC (silica gel Si 60; Merck, Darmstadt, Germany) were applied. In isocratic development, an eluent of given composition was introduced into the reservoir. The samples were spotted on a dry layer of adsorbent as narrow strips. The solvent flow was observed and stopped after reaching the end line (distance *ca.* 80 mm). The components of the sample were detected by irradiation with a UV lamp. Calculations were performed on an IBM 486 computer with programs presented earlier [4].

Solutions of investigated mixtures (0.01%) were prepared by drying aliquots of the preparations, extracting with ethyl acetate, filtering, evaporating the extract and dissolving the residue in the eluent. The following mixtures were investigated: Cholesol (Herbapol, Wrocław, Poland), containing Extr. Cortex Frangulae, Herba Equiseti Fructus Rosae, Anthodium Chamomil-

lae, Fr. Coriandri, Fr. Juniperi, Herba Polygoni avic, Infl. Helichrysi, Herba Hyperici and Intr. Taraxaci; and Seboren (Herbapol), containing Extr. fl. ex Fr. Pastinacae, Rx. Bardanae, Rx. Urticae, Rhiz. Calami and Adiuvars.

In the two-stage mode, the plates were developed for part of the total distance with pure modifier as eluent or with a two-component mobile phase. The plates were dried in air at room temperature for 30 min and developed the full distance with an eluent of lower modifier concentration.

RESULTS AND DISCUSSION

In a series of isocratic developments the parameters of the retention *versus* eluent composition equation were determined by the least-squares method, assuming linear $\log k'$ vs. $\log c_{\text{mod}}$ relationships, which follows from the Snyder–Soczewiński competitive adsorption model [7,8]:

$$\log k_{(i,j)} = \log k_{0(j)} - m_{(j)} \log c_{(i)} \quad (1)$$

The parameters (capacity factor $k_{0(j)}$, slope $m_{(j)}$) for the investigated mixture are summarized in Tables I–IV. The data (*i.e.*, slopes and capacity factors) were introduced into the computer program. In the next step, various sets of the gradient program parameters were introduced.

TABLE I

COMPARISON OF PREDICTED ($R_{F(\text{calc.})}$) AND EXPERIMENTAL ($R_{F(\text{exp.})}$) R_F VALUES OF GLYCOSIDES

Two-stage development. System: Silica gel–ethyl acetate + methanol. Development program: $c_{(1)}^{\text{MeOH}} = 0.75$, $c_{(2)}^{\text{MeOH}} = 0.15$, $z_{(1)} = 0.15$, $z_{(2)} = 1.0$. k_0 , m and r are parameters of linear $\log k$ vs. $\log c_{\text{MeOH}}$ plots.

No.	Solute	k_0	m	r	$R_{F(\text{calc.})}$	$R_{F(\text{exp.})}$	Error, ΔR_F^a
1	Lanatoside C	0.025	2.23	0.9605	0.46	0.43	0.03
2	Digitoxin	0.077	0.90	0.9945	0.82	0.80	0.02
3	Digitalin	0.073	2.27	0.9779	0.27	0.30	0.03
4	Desacetyllanatoside C	0.047	2.44	0.9918	0.29	0.33	0.04
5	Strophantin G	0.082	2.31	0.9915	0.24	0.27	0.03
6	Acetyldigitoxin	0.304	2.21	0.9899	0.14	0.20	0.06
7	Convalatoxin	0.061	1.65	0.9899	0.50	0.50	0.00
8	Digoxin	0.023	1.53	0.9954	0.75	0.73	0.02

^a $\Delta R_F = R_{F(\text{exp.})} - R_{F(\text{calc.})}$.

TABLE II

COMPARISON OF PREDICTED ($R_{F(\text{calc.})}$) AND EXPERIMENTAL ($R_{F(\text{exp.})}$) R_F VALUES OF COMPONENTS OF SEBOREN EXTRACT

Two-stage development. System: silica gel-heptane + diisopropyl ether. Development program: $c_{(1)\text{mod}} = 1.0$, $c_{(2)\text{mod}} = 0.30$, $z_{(1)} = 0.33$, $z_{(2)} = 1.0$. k_0 and m are parameters of linear $\log k$ vs. $\log c_{\text{mod}}$ plots.

No.	k_0	m	$R_{F(\text{calc.})}$	$R_{F(\text{exp.})}$	Error, ΔR_F^a
1	0.13	0.84	0.73	0.81	0.08
2	0.33	0.63	0.57	0.68	0.11
3	0.31	1.24	0.53	0.55	0.02
4	0.68	1.12	0.48	0.41	0.07
5	0.93	1.03	0.43	0.36	0.07
6	0.80	2.73	0.40	0.20	0.20
7	2.32	1.34	0.32	0.16	0.16
8	3.39	1.65	0.30	0.10	0.20
9	9.06	3.59	0.25	0.03	0.22
10	10.36	2.79	0.01	0.03	0.02
11	0.01	0.72	0.73	0.87	0.02

$$^a \Delta R_F = R_{F(\text{exp.})} - R_{F(\text{calc.})}$$

The variables of the gradient programs were the development distance in the first step, $z_{(1)}$, smaller than 1, and the concentration of modifier in the first, $c_{(1)}$, and second steps, $c_{(2)}$. The development distance in the second step, $z_{(2)}$,

was always equal to 1.0. The final R_F values were calculated by computer from the equation derived previously [4]:

$$R_F(j) = z_{(1)}R_{F(1,j)} + [1 - z_{(1)}R_{F(1,j)}]R_{F(2,j)} \quad (2)$$

TABLE III

COMPARISON OF PREDICTED ($R_{F(\text{calc.})}$) AND EXPERIMENTAL ($R_{F(\text{exp.})}$) R_F VALUES OF COMPONENTS OF SEBOREN EXTRACT

Two-stage development. System: silica gel-chloroform + ethyl acetate. Development program: $c_{(1)\text{mod}} = 1.0$, $c_{(2)\text{mod}} = 0.05$, $z_{(1)} = 0.33$, $z_{(2)} = 1.0$. k_0 and m are parameters of linear $\log k$ vs. $\log c_{\text{mod}}$ plots.

No.	k_0	m	$R_{F(\text{calc.})}$	$R_{F(\text{exp.})}$	Error, ΔR_F^a
1	0.002	1.80	0.80	0.79	0.01
2	0.012	1.24	0.78	0.75	0.03
3	0.027	1.05	0.74	0.70	0.04
4	0.107	0.62	0.71	0.66	0.05
5	0.170	0.58	0.64	0.62	0.02
6	0.240	0.52	0.61	0.59	0.02
7	0.190	0.78	0.52	0.51	0.01
8	0.300	0.72	0.46	0.41	0.05
9	0.560	0.69	0.36	0.32	0.04
10	0.650	0.73	0.32	0.25	0.07
11	0.030	2.91	0.32	0.20	0.12
12	0.202	2.04	0.28	0.16	0.12

$$^a \Delta R_F = R_{F(\text{exp.})} - R_{F(\text{calc.})}$$

TABLE IV

COMPARISON OF PREDICTED ($R_{F(\text{calc.})}$) AND EXPERIMENTAL ($R_{F(\text{exp.})}$) R_F VALUES OF COMPONENTS OF CHOLESOL EXTRACTTwo-stage development. System: silica gel–heptane + diisopropyl ether. Development program: $c_{(1)\text{mod}} = 1.0$, $c_{(2)\text{mod}} = 0.30$, $z_{(1)} = 0.33$, $z_{(2)} = 1.0$. k_0 and m are parameters of linear log k vs. log c_{mod} plots.

No.	k_0	m	$R_{F(\text{calc.})}$	$R_{F(\text{exp.})}$	Error, ΔR_F^a
1	0.015	2.20	0.88	0.82	0.06
2	0.084	1.59	0.75	0.72	0.03
3	0.149	1.86	0.59	0.60	0.01
4	0.411	1.60	0.44	0.48	0.04
5	0.902	1.18	0.35	0.36	0.01
6	1.318	2.46	0.18	0.24	0.06
7	2.773	1.89	0.12	0.16	0.04
8	3.503	3.71	0.08	0.08	0.00
9	0.560	0.69	0.06	0.04	0.02

$$^a \Delta R_F = R_{F(\text{exp.})} - R_{F(\text{calc.})}$$

The experimental and calculated R_F values for the components investigated are compared in Tables I–IV together with the gradient programmes used. The error, calculated as $\Delta R_F = R_{F(\text{exp.})} - R_{F(\text{calc.})}$, did not exceed 0.1 R_F units in 82.5% of the results. Only a few errors were in the range 0.1–0.2 and only one exceeded 0.2 R_F units, so that the agreement is satisfactory.

In the series of experiments an artificial mixture of glycosides available in this laboratory was used for the comparison of computer-calculated and experimentally determined R_F values (Table I). The mean error was only 0.03 R_F units. This is satisfactory considering the visual determination of the position of the spots under the UV lamp. Similar results were obtained for Cholesol extracts (Table IV) with eluents composed of heptane and diisopropyl ether (modifier); the mean error was 0.035 R_F units. The results for Seboren extracts with eluents composed of chloroform and ethyl acetate (modifier) were also satisfactory too; the mean error was 0.05 R_F units (Table III).

The results obtained for Seboren with diisopropyl ether as modifier were less satisfactory (Table II). The mean error was 0.11 R_F units. One reason was presumably the high capacity factor for some of the components. Another cause is that the Snyder–Soczewiński equation is more useful for narrow ranges of modifier concentrations: during the development program the

modifier concentration was changed from the pure modifier to a concentration equal to 0.1 volume fraction.

CONCLUSIONS

The two-stage incremental gradient development mode of TLC resulted in good separations of mixtures of practical significance. The agreement between the predicted (on the basis of the Snyder–Soczewiński equation and eqn. 2 in this paper) and experimental R_F values was good to fair. The PTFE horizontal sandwich chambers of the DS type permit the use of incremental gradient development in a simple manner.

SYMBOLS

- $c_{(i)}$ concentration of modifier in the i th step (volume fraction);
- $c_{(\text{mod})}$ concentration of modifier (volume fraction);
- $z_{(i)}$ development distance in the i th step;
- $R_{F(j)}$ final R_F value of solute j in gradient development;
- $k_{0(j)}$ capacity factor of solute j for unit concentration of modifier (pure modifier) for normal-phase systems;
- $m_{(j)}$ slope of log k' vs. log c plot for solute j ;
- $R_{F(i,j)}$ R_F value for solute j corresponding to i th concentration of modifier;

$k_{(i,j)}$ capacity factor of solute j for the i th step;
 r correlation coefficient.

ACKNOWLEDGEMENT

The authors thank Professor Dr. E. Soczewiński for valuable discussions and help with the preparation of the manuscript.

REFERENCES

1 C.F. Poole, S.K. Poole, W.P.N. Fernando, T.A. Dean, H.D. Ahmed and J.A. Berndt, *J. Planar Chromatogr.*, 2 (1989) 336.

2 C.F. Poole and H.T. Belay, *J. Planar Chromatogr.*, 4 (1991) 345.
3 V. de la Vigne and D. Jänchen, *J. Planar Chromatogr.*, 4 (1990) 6.
4 W. Markowski and E. Soczewiński, *J. Chromatogr.*, 623 (1992) 139.
5 W. Markowski, *J. Chromatogr.*, 635 (1993) 283.
6 T.H. Dzido and E. Soczewiński, *J. Chromatogr.*, 516 (1990) 461.
7 L.R. Snyder, *Principles of Adsorption Chromatography*, Marcel Dekker, New York, 1968.
8 E. Soczewiński, *Anal. Chem.*, 41 (1969) 179.

Discussion

Discussion on “Alternatives to methanol–water elution of solid-phase extraction columns for the fractionation of high log K_{ow} organic compounds in aqueous environmental samples” by Durhan *et al.*, *J. Chromatogr.*, 629 (1993) 67–74

Sim-Lin Lau and Michael K. Stenstrom*

Department of Civil and Environmental Engineering, 4173 Engineering I, University of California, Los Angeles, CA 90024-1600 (USA)

(First received May 10th, 1993; revised manuscript received June 16th, 1993)

With reference to the recently published article by Durhan *et al.* [1], similar problems in eluting non-polar polyaromatic hydrocarbons (PAHs) from C_{18} solid-phase extraction (SPE) columns were also observed in our laboratory. Our results confirm and expand Durhan *et al.*'s with additional PAHs and different elution solvent mixtures.

The C_{18} SPE method developed by the US Environmental Protection Agency (EPA) [2] was used to fractionate the non-polar PAHs from storm drain waters for short-term chronic toxicity tests. Our recovery study of the C_{18} SPE method used standard water solutions which contained eight commonly detected PAHs in storm drain waters (naphthalene, 2-methylnaphthalene, acenaphthene, fluorene, anthracene, pyrene, chrysene and benzo[a]pyrene). Low recoveries of PAHs from the C_{18} column

were initially observed. The originally proposed methanol–water solvent system did not elute highly non-polar PAHs (as indicated by their high log K_{ow} values), such as chrysene and benzo[a]pyrene. We, like Durhan *et al.*, suspected that methanol–water mixtures and methanol were too polar to elute strongly sorbed PAHs from the C_{18} column. Therefore, a modified solvent system was developed so that compounds such as chrysene and benzo[a]pyrene could be fractionated for the toxicity tests.

The tolerance of the marine organisms (echinoderm fertilization test, red abalone embryo development test, and giant kelp germination/germ tube growth test, see ref. 3) in our toxicity tests limited the choice of organic solvents. Preliminary tolerance tests showed that methanol–water, methanol and methanol–methylene chloride were acceptable elution mixtures, although it was very desirable to limit the quantity of methylene chloride. Therefore, our effort was concentrated on the development of a modified

* Corresponding author.

elution system which used both methanol–water and methanol–methylene chloride mixtures.

The final elution mixture maximized recovery and separation of PAHs, although further improvements in recovery and separation are desirable. Our SPE procedures were essentially the same as those of the EPA and Durhan *et al.*, except the elution solvent volume. Our initial results showed that the overall recovery of PAHs used in the recovery study was not significantly different in using either elution solvent volumes of 2×1.5 ml or 2×1.0 ml. Therefore, 2×1.0 ml volumes of elution solvent were used in our recovery study as higher concentration of PAHs in the fractions could be obtained (a concentration factor of $500\times$ as compared to $333\times$ based on a sample volume of 1 l). Our modified elution scheme consists of six fractions: 80, 90, 100% (v/v) methanol in water and 10, 20, 50% (v/v) of methylene chloride in methanol. Unlike Durhan *et al.*, our first elution solvent is methanol–water (80:20, v/v); initial results showed that fractions with less than 80% methanol in water could not elute the most polar PAHs, such as naphthalene and 2-methylnaphthalene.

Fig. 1 is a typical elution profile of the 8 PAHs using the modified elution solvent system. Table I shows the average percent recovery and standard deviation of each PAH recovery over 8

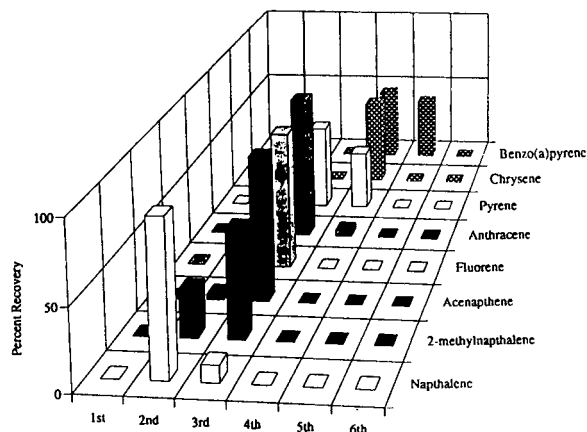


Fig. 1. An example of C_{18} SPE modified elution scheme using the modified solvent mixtures. 1st: methanol–water (80:20); 2nd: methanol–water (90:10); 3rd: 100% methanol; 4th: methylene chloride–methanol (10:90); 5th: methylene chloride–methanol (20:80); 6th: methylene chloride–methanol (50:50).

extractions. The extraction procedures of these extractions were identical except for the concentration of PAHs. For each extraction, the concentration of all PAHs except benzo[*a*]pyrene were equal; the range of concentrations of each PAH was varied from 10 to 40 $\mu\text{g/l}$ over the series of 8 extractions. The concentration of benzo[*a*]pyrene ranged from 20 to 80 $\mu\text{g/l}$. Repeatability of the extraction procedures, as

TABLE I

AVERAGE RECOVERY AND STANDARD DEVIATION OF EACH PAH FROM 8 DIFFERENT EXTRACTIONS USING THE MODIFIED ELUTION SCHEME

1st: methanol–water (80:20); 2nd: methanol–water; 3rd (90:10); 3rd: 100% methanol; 4th: methylene chloride–methanol (10:90); 5th: methylene chloride–methanol (20:80); 6th: methylene chloride–methanol (50:50).

Compound	Log K_{ow}	Average recovery (%) \pm standard deviation					
		1st	2nd	3rd	4th	5th	6th
Naphthalene	3.54	0	86 ± 11	3 ± 4	0	0	0
2-methylnaphthalene	–	0	37 ± 10	43 ± 21	0	0	0
Acenaphthene	–	0	7 ± 6	76.6 ± 14	0	0	0
Fluorene	4.12	0	9 ± 9	82 ± 6	0	0	0
Anthracene	4.45	0	0.5 ± 1	84 ± 12	0.5 ± 1	0	0
Pyrene	4.88	0	0	62 ± 9	22 ± 9	0	0
Chrysene	5.61	0	0	15 ± 17	53 ± 11	3 ± 7	2 ± 5
Benzo[<i>a</i>]pyrene	6.04	0	0	0	57 ± 14	23 ± 13	0

measured by the standard deviation of the recovery, was generally within 5% for fluorene as the most repeatable, and 21% for 2-methylnaphthalene as the least repeatable.

From Table I it is observed that the methanol-water (80:20) fraction (1st fraction) eluted no PAHs. Most of the naphthalene was recovered in the 90% methanol fraction (2nd fraction). Anthracene, fluorene and acenaphthene were eluted almost entirely in the 100% methanol fraction. 2-Methylnaphthalene, pyrene, chrysene and benzo[*a*]pyrene were not well separated. Table I also shows that elution with methylene chloride (4th and 5th fractions) is required to recover those PAHs with high log K_{ow} value. Most were recovered with a maximum of 20% methylene chloride.

These results show that higher recoveries were obtained with modified elution solvents; however, several compounds were eluted in the same

fraction. We worked with more varied solvent volume ratios but results were not significantly improved. Several other solvents (isopropanol, hexane and carbon tetrachloride) were also investigated but with limited success. Poor recoveries or high toxicity were observed. These results strengthen the conclusions by Durhan *et al.* and emphasize the need for further research and development.

REFERENCES

- 1 E. Durhan, M. Lukasewycz and S. Baker, *J. Chromatogr.*, 629 (1993) 67-74.
- 2 D.I. Mount and L. Anderson-Carnahan, *Method for Aquatic Toxicity Identification Evaluation Phase II: Toxicity Characterization Procedures*, EPA/600/3-88-035, US Environmental Protection Agency, Duluth, MN, 1989.
- 3 *Water Quality Control Plan, Ocean Waters of California, California Ocean Plan*, State Water Resources Control Board, Sacramento, CA, 1990.

Book Review

Detectors for capillary chromatography, edited by H.H. Hill and D.G. McMinn, Wiley, New York, Chichester, Brisbane, Toronto, Singapore, 1992, XVII + 444 pp., price £ 75, ISBN 0-471-50645-1.

This book constitutes Volume 121 of the series *Chemical Analysis*. A greater part of the book (12 chapters, about 340 pages) is concentrated on detectors in gas chromatography: flame ionization, helium ionization, far-UV ionization (photoionization) and absorbance, electron-capture, electrolytic conductivity, nitrogen-phosphorus, surface ionization, atomic plasma emission, fourier transform infrared, ion mobility, mass spectrometric and sulphur-selective detectors. In each chapter a historical background, a response mechanism, detector designs, effect of experimental conditions on the response, special comments on the detectors used with capillary columns and applications are described. Two chapters deal with the detectors used in supercritical fluid chromatography (38 pages) and in microcolumn liquid chromatography (30 pages).

The book describes and discusses all types of detectors used in gas chromatography without consideration of their occurrence in commercial instruments (some rather non-commercial detectors are included, *e.g.*, surface ionization and ion mobility types). In this respect, the omission of the thermal conductivity detector, some constructional types of which can be also used for capillary columns, namely the Hewlett-Packard detector, is notable.

A better balance of the contents of individual chapters would have been desirable. Some types of detection are analysed in considerable detail (*e.g.*, the electrolytic conductivity detector), whereas some others deserved more detailed analysis (*e.g.*, the flame ionization detector). The chapter on sulphur-selective detectors interferes

with the structure of the book. It includes flame photometric, chemiluminescence, electrolytic conductivity, electron-capture and atomic emission spectrometric detectors. With the exception of the first two detectors mentioned, the chapter coincides with other chapters on corresponding detectors. However, as the flame photometric and chemiluminescent detectors are presented only in the chapter on sulphur-selective detectors, their application to other types of compounds is not discussed. Application of the flame photometric detector to phosphorus compounds is fairly common.

It would have been useful if the Editors had unified the general terminology: detector limit, minimum detectable amount, detectivity, etc. The first general chapter defines the detection limit as a response that is three times the detector noise, whereas twice the detector noise is mostly used in the other chapters.

The authors of the chapters are experts in their field, hence the reader is provided with information on each detector directly from researchers studying that particular type of detector. The analysis of individual types of detectors is profound and will give the reader a very good orientation with regard to the various problems. The text is well arranged and easily comprehensible. It provides information on all the detectors used in chromatography (with the exception of the thermal conductivity detector). The book can be recommended to all the specialists concerned with chromatographic analysis.

Brno (Czech Republic)

Milan Dressler

Author Index

- Abraham, M.H., Andonian-Haftvan, J., Hamerton, I., Poole, C.F. and Kollie, T.O.
Hydrogen bonding. XXVIII. Comparison of the solvation theories of Abraham and Poole, using a new acidic gas-liquid chromatography stationary phase 646(1993)351
- Adamson, N., Riley, P.F. and Reynolds, E.C.
The analysis of multiple phosphoserine-containing casein peptides using capillary zone electrophoresis 646(1993)391
- Aguilar, M.I., Mougos, S., Boublik, J., Rivier, J. and Hearn, M.T.W.
High-performance liquid chromatography of amino acids, peptides and proteins. CXXVIII. Effect of D-amino acid substitutions on the reversed-phase high-performance liquid chromatography retention behaviour of neuropeptide Y[18-36] analogues 646(1993)53
- Aguilar, M., see Wirth, H.-J. 646(1993)129
- Alebić-Kolbah, T. and Wainer, I.W.
Enzyme-based high-performance liquid chromatography stationary phases as metabolic reactors. Immobilization of non-solubilized rat liver microsomes on an immobilized artificial membrane high-performance liquid chromatography support 646(1993)289
- Alewood, P.F., Bailey, A.J., Brinkworth, R.I., Fairlie, D. and Jones, A.
Characterisation of TNF- α -related peptides by high-performance liquid chromatography-mass spectrometry and high-performance liquid chromatography-tandem mass spectrometry 646(1993)185
- Alewood, P.F., see Grieve, P.A. 646(1993)175
- Altria, K.D.
Quantitative aspects of the application of capillary electrophoresis to the analysis of pharmaceuticals and drug related impurities (Review) 646(1993)245
- Andonian-Haftvan, J., see Abraham, M.H. 646(1993)351
- Bächmann, K., see Groh, T. 646(1993)405
- Bailey, A.J., see Alewood, P.F. 646(1993)185
- Barron, D., see Lübke, M. 646(1993)307
- Beeby, A., see Bishop, S.M. 646(1993)345
- Beeson, M.D., see Camacho-Torralba, P.L. 646(1993)259
- Benedek, K.
Kinetics of recombinant human brain-derived neurotrophic factor unfolding under reversed-phase liquid chromatography conditions 646(1993)91
- Berek, D., see Mislavíková, D. 646(1993)411
- Bishop, S.M., Khoo, B.J., MacRobert, A.J., Simpson, M.S.C., Phillips, D. and Beeby, A.
Characterisation of the photochemotherapeutic agent disulphonated aluminium phthalocyanine and its high-performance liquid chromatographic separated components 646(1993)345
- Bladier, D., see Caron, M. 646(1993)327
- Bombín, M., see García, M.A. 646(1993)297
- Boublik, J., see Aguilar, M.I. 646(1993)53
- Braaksma, M.A., see Welling-Wester, S. 646(1993)37
- Brinkworth, R.I., see Alewood, P.F. 646(1993)185
- Brownrigg, C.M., see Brumley, W.C. 646(1993)377
- Brumley, W.C. and Brownrigg, C.M.
Electrophoretic behavior of aromatic-containing organic acids and the determination of selected compounds in water and soil by capillary electrophoresis 646(1993)377
- Burgess, A.W., see Fabri, L. 646(1993)213
- Burgess, A.W., see Nice, E. 646(1993)159
- Cais, M., see Shimoni, M. 646(1993)99
- Camacho-Torralba, P.L., Beeson, M.D., Vigh, Gy. and Thompson, D.H.
High-performance chiral displacement chromatographic separations in the normal-phase mode. Separation of the enantiomers of 1,2-O-dihexadecyl-*rac*-glycerol-3-O-(3,5-dinitrophenyl)carbamate using the Pirkle-type naphthylalanine silica stationary phase 646(1993)259
- Cann, J.R., see Munro, P.D. 646(1993)3
- Caron, M., Joubert-Caron, R., Cartier, J.R., Chadli, A. and Bladier, D.
Study of lectin-ganglioside interactions by high-performance liquid affinity chromatography 646(1993)327
- Carruthers, R.A., see Davies, M.J. 646(1993)317
- Cartier, J.R., see Caron, M. 646(1993)327
- Castello, G., D'Amato, G. and Vezzani, S.
Evaluation of the polarity of packed and capillary columns by different classification methods 646(1993)361
- Chadli, A., see Caron, M. 646(1993)327
- Chai, W., see Davies, M.J. 646(1993)317
- D'Amato, G., see Castello, G. 646(1993)361
- Datta, A., see Wagh, J.S. 646(1993)428
- Davies, M.J., Smith, K.D., Carruthers, R.A., Chai, W., Lawson, A.M. and Hounsell, E.F.
Use of a porous graphitised carbon column for the high-performance liquid chromatography of oligosaccharides, alditols and glycopeptides with subsequent mass spectrometry analysis 646(1993)317
- De Broe, M.E., see Van Hoof, V.O. 646(1993)235
- Do, D.D., see Hu, S. 646(1993)31
- Douma, B.R.K., see Welling-Wester, S. 646(1993)37
- Dressler, M.
Detectors for capillary chromatography (by H.H. Hill and D.G. McMinn) (Book Review) 646(1993)442
- Ebdon, L., see Pretorius, W.G. 646(1993)369
- Elix, J.A., see Feige, G.B. 646(1993)417
- Engstrom, A., see Nice, E. 646(1993)159
- Eriksson, K.-O., see Wirth, H.-J. 646(1993)129
- Fabri, L., Maruta, H., Muramatsu, H., Muramatsu, T., Simpson, R.J., Burgess, A.W. and Nice, E.C.
Structural characterisation of native and recombinant forms of the neurotrophic cytokine MK 646(1993)213
- Fabri, L., see Nice, E. 646(1993)159
- Fadeev, A.Yu., see Mingalyov, P.G. 646(1993)267
- Fairlie, D., see Alewood, P.F. 646(1993)185
- Feige, G.B., Lumbsch, H.T., Huneck, S. and Elix, J.A.
Identification of lichen substances by a standardized high-performance liquid chromatographic method 646(1993)417

- Feijlbrief, M., see Welling-Wester, S. 646(1993)37
- García, M.A., Vera, S., Bombín, M. and Marina, M.L.
Optimization of the separation selectivity of a group of benzene and naphthalene derivatives in micellar high-performance liquid chromatography using a C₁₈ column and alcohols as modifiers in the mobile phase 646(1993)297
- Goldshleger, R., see Tal, D.M. 646(1993)153
- Gorman, J.J. and Shiell, B.J.
Isolation of carboxyl-termini and blocked amino-termini of viral proteins by high-performance cation-exchange chromatography 646(1993)193
- Grieve, P.A., Jones, A. and Alewood, P.F.
Analytical methods for differentiating minor sequence variations in related peptides 646(1993)175
- Groh, T. and Bächmann, K.
Investigation of vanadate as a pH sensitive analyte anion using capillary zone electrophoresis 646(1993)405
- Hail, M., see Mock, K. 646(1993)169
- Hamerton, I., see Abraham, M.H. 646(1993)351
- Hancock, D.K. and Reeder, D.J.
Analysis and configuration assignments of the amino acids in a pyoverdine-type siderophore by reversed-phase high-performance liquid chromatography 646(1993)335
- Hearn, M.T.W.
Foreword 646(1993)1
- Hearn, M.T.W., see Aguilar, M.I. 646(1993)53
- Hearn, M.T.W., see Mao, Q.M. 646(1993)67
- Hearn, M.T.W., see Mao, Q.M. 646(1993)81
- Hearn, M.T.W., see Wirth, H.-J. 646(1993)129
- Hearn, M.T.W., see Wirth, H.-J. 646(1993)143
- Hearn, M.T.W., see Zachariou, M. 646(1993)107
- Hellman, U., see Nice, E. 646(1993)159
- Hidaka, Y., see Zhang, R. 646(1993)45
- Hjertén, S., Mohammad, J. and Nakazato, K.
Improvement in flow properties and pH stability of compressed, continuous polymer beds for high-performance liquid chromatography 646(1993)121
- Hodges, R.S., see Sereda, T.J. 646(1993)17
- Holt, P., see Wirth, H.-J. 646(1993)129
- Hounsell, E.F., see Davies, M.J. 646(1993)317
- Huneck, S., see Feige, G.B. 646(1993)417
- Hu, S. and Do, D.D.
Histidine-ligand chromatography of proteins. Multiple modes of binding mechanism 646(1993)31
- Jardine, I., see Mock, K. 646(1993)169
- Johnson, K., see Mock, K. 646(1993)169
- Jones, A., see Alewood, P.F. 646(1993)185
- Jones, A., see Grieve, P.A. 646(1993)175
- Jones, A.T., Keen, J.N. and Roberts, N.B.
Human pepsin 3b peptide map sequence analysis, genotype and hydrophobic nature 646(1993)207
- Joubert-Caron, R., see Caron, M. 646(1993)327
- Karlish, S.J.D., see Tal, D.M. 646(1993)153
- Keen, J.N., see Jones, A.T. 646(1993)207
- Khoo, B.J., see Bishop, S.M. 646(1993)345
- Kiyohara, C., Saitoh, K. and Suzuki, N.
Micellar electrokinetic capillary chromatography of haematoporphyrin, protoporphyrin and their copper and zinc complexes 646(1993)397
- Koedijk, D.G.A.M., see Welling-Wester, S. 646(1993)37
- Kollie, T.O., see Abraham, M.H. 646(1993)351
- Lau, S.-L. and Stenstrom, M.K.
Discussion on "Alternatives to methanol-water elution of solid-phase extraction columns for the fractionation of high log K_{ow} organic compounds in aqueous environmental samples" by Durhan *et al.*, *J. Chromatogr.*, 629 (1993) 67-74 646(1993)439
- Lawson, A.M., see Davies, M.J. 646(1993)317
- Layton, J., see Nice, E. 646(1993)159
- Lepoutre, L.G., see Van Hoof, V.O. 646(1993)235
- Le Quééré, J.-L., see Lübke, M. 646(1993)307
- Lisichkin, G.V., see Mingalyov, P.G. 646(1993)267
- Liu, G., see Zhang, R. 646(1993)45
- Lübke, M., Le Quééré, J.-L. and Barron, D.
Retention behaviour of volatile compounds in normal-phase high-performance liquid chromatography on a diol column 646(1993)307
- Lumbsch, H.T., see Feige, G.B. 646(1993)417
- Lunina, E.V., see Mingalyov, P.G. 646(1993)267
- MacRobert, A.J., see Bishop, S.M. 646(1993)345
- Mant, C.T., see Sereda, T.J. 646(1993)17
- Mao, Q.M., Stockmann, R., Prince, I.G. and Hearn, M.T.W.
High-performance liquid chromatography of amino acid, peptides and proteins. CXXVI. Modelling of protein adsorption with non-porous and porous particles in a finite bath 646(1993)67
- Mao, Q.M., Prince, I.G. and Hearn, M.T.W.
High-performance liquid chromatography of amino acids, peptides and proteins. CXXXII. Optimisation of operating parameters for protein purification with chromatographic columns 646(1993)81
- Marina, M.L., see García, M.A. 646(1993)297
- Markowski, W. and Matysik, G.
Analysis of plant extracts by multiple development thin-layer chromatography 646(1993)434
- Maruta, H., see Fabri, L. 646(1993)213
- Matysik, G., see Markowski, W. 646(1993)434
- Mingalyov, P.G., Fadeev, A.Yu., Staroverov, S.M., Lisichkin, G.V. and Lunina, E.V.
Nitroxide radicals in studies of the fine bonded layer structure of modified silicas 646(1993)267
- Mislovičová, D., Petro, M. and Berek, D.
Behaviour of polyhydroxyethyl methacrylate sorbent with dextran-filled macropores in dye-affinity chromatography of proteins 646(1993)411
- Mock, K., Hail, M., Mylchreest, I., Zhou, J., Johnson, K. and Jardine, I.
Rapid high-sensitivity peptide mapping by liquid chromatography-mass spectrometry 646(1993)169
- Mohammad, J., see Hjertén, S. 646(1993)121
- Mokashi, A.A., see Wagh, J.S. 646(1993)428
- Mougos, S., see Aguilar, M.I. 646(1993)53
- Munro, P.D., Winzor, D.J. and Cann, J.R.
Experimental and theoretical studies of rate constant evaluation by affinity chromatography. Determination of rate constants for the interaction of saccharides with concanavalin A 646(1993)3
- Muramatsu, H., see Fabri, L. 646(1993)213
- Muramatsu, T., see Fabri, L. 646(1993)213
- Mylchreest, I., see Mock, K. 646(1993)169

- Nakazato, K., see Hjertén, S. 646(1993)121
- Nice, E.C., see Fabri, L. 646(1993)213
- Nice, E., Layton, J., Fabri, L., Hellman, U., Engstrom, A., Persson, B. and Burgess, A.W.
Mapping of the antibody- and receptor-binding domains of granulocyte colony-stimulating factor using an optical biosensor. Comparison with enzyme-linked immunosorbent assay competition studies 646(1993)159
- Oesch, F., see Schaumann, C. 646(1993)227
- Persson, B., see Nice, E. 646(1993)159
- Petro, M., see Mislovičová, D. 646(1993)411
- Phillips, D., see Bishop, S.M. 646(1993)345
- Poole, C.F., see Abraham, M.H. 646(1993)351
- Pretorius, W.G., Ebdon, L. and Rowland, S.J.
Development of a high-temperature gas chromatography-inductively coupled plasma mass spectrometry interface for the determination of metalloporphyrins 646(1993)369
- Prince, I.G., see Mao, Q.M. 646(1993)67
- Prince, I.G., see Mao, Q.M. 646(1993)81
- Quinn, A.M., see Sereda, T.J. 646(1993)17
- Reeder, D.J., see Hancock, D.K. 646(1993)335
- Reuveni, R., see Shimoni, M. 646(1993)99
- Reynolds, E.C., see Adamson, N. 646(1993)391
- Riley, P.F., see Adamson, N. 646(1993)391
- Rivier, J., see Aguilar, M.I. 646(1993)53
- Roberts, N.B., see Jones, A.T. 646(1993)207
- Rowland, S.J., see Pretorius, W.G. 646(1993)369
- Saitoh, K., see Kiyohara, C. 646(1993)397
- Schaumann, C., Oesch, F., Unger, K.K. and Wieser, R.J.
Analytical technique for studying the structure of glycoprotein N-glycans 646(1993)227
- Sereda, T.J., Mant, C.T., Quinn, A.M. and Hodges, R.S.
Effect of the α -amino group on peptide retention behaviour in reversed-phase chromatography.
Determination of the pK_a values of the α -amino group of 19 different N-terminal amino acid residues 646(1993)17
- Shiell, B.J., see Gorman, J.J. 646(1993)193
- Shimoni, M., Reuveni, R. and Cais, M.
Non-dialysis method of rapid and facile sample preparation for the desalting and purification of enzymes and other proteins from plant extracts 646(1993)99
- Shimonishi, Y., see Zhang, R. 646(1993)45
- Simpson, M.S.C., see Bishop, S.M. 646(1993)345
- Simpson, R.J., see Fabri, L. 646(1993)213
- Smith, K.D., see Davies, M.J. 646(1993)317
- Staroverov, S.M., see Mingalyov, P.G. 646(1993)267
- Stenstrom, M.K., see Lau, S.-L. 646(1993)439
- Stockmann, R., see Mao, Q.M. 646(1993)67
- Suzuki, N., see Kiyohara, C. 646(1993)397
- Svec, F., see Tennikova, T.B. 646(1993)279
- Tal, D.M., Goldshleger, R. and Karlish, S.J.D.
Separation of membrane-embedded tryptic peptides of Na,K-ATPase by size-exclusion chromatography 646(1993)153
- Tennikova, T.B. and Svec, F.
High-performance membrane chromatography: highly efficient separation method for proteins in ion-exchange, hydrophobic interaction and reversed-phase modes 646(1993)279
- Thompson, D.H., see Camacho-Torralba, P.L. 646(1993)259
- Traverso, I., see Zachariou, M. 646(1993)107
- Unger, K.K., see Schaumann, C. 646(1993)227
- Van Hoof, V.O., Van Mullem, M., De Broe, M.E. and Lepoutre, L.G.
Comparison of two commercially available systems for the electrophoretic separation of alkaline phosphatase isoenzymes 646(1993)235
- Van Mullem, M., see Van Hoof, V.O. 646(1993)235
- Vera, S., see García, M.A. 646(1993)297
- Vezzani, S., see Castello, G. 646(1993)361
- Vigh, Gy., see Camacho-Torralba, P.L. 646(1993)259
- Wagh, J.S., Mokashi, A.A. and Datta, A.
High-performance liquid chromatographic method for the monitoring of the synthesis of the precursor for tetramisole 646(1993)428
- Wainer, I.W., see Alebić-Kolbah, T. 646(1993)289
- Welling, G.W., see Welling-Wester, S. 646(1993)37
- Welling-Wester, S., Feijlbrief, M., Koedijk, D.G.A.M., Braaksmá, M.A., Douma, B.R.K. and Welling, G.W.
Effect of different amounts of the non-ionic detergents $C_{10}E_5$ and $C_{12}E_5$ present in eluents for ion-exchange high-performance liquid chromatography of integral membrane proteins of Sendai virus 646(1993)37
- Wieser, R.J., see Schaumann, C. 646(1993)227
- Winzor, D.J., see Munro, P.D. 646(1993)3
- Wirth, H.-J., Eriksson, K.-O., Holt, P., Aguilar, M. and Hearn, M.T.W.
High-performance liquid chromatography of amino acids, peptides and proteins. CXXIX. Ceramic-based particles as chemically stable chromatographic supports 646(1993)129
- Wirth, H.-J. and Hearn, M.T.W.
High-performance liquid chromatography of amino acids, peptides and proteins. CXXX. Modified porous zirconia as sorbents in affinity chromatography 646(1993)143
- Zachariou, M., Traverso, I. and Hearn, M.T.W.
High-performance liquid chromatography of amino acids peptides and proteins. CXXXI. O-Phosphoserine as a new chelating ligand for use with hard Lewis metal ions in the immobilized-metal affinity chromatography of proteins 646(1993)107
- Zhang, R., Zhang, Z., Liu, G., Hidaka, Y. and Shimonishi, Y.
High-performance liquid chromatographic determination of neutral and amino monosaccharides by ultraviolet and fluorescence detection of sugar 9-fluorenylmethoxycarbonyl hydrazones and 9-fluorenylmethoxycarbonyl amino sugars at picomole and sub-picomole levels 646(1993)45
- Zhang, Z., see Zhang, R. 646(1993)45
- Zhou, J., see Mock, K. 646(1993)169

Journal of Chromatography

NEWS SECTION

AWARD

MARCEL GOLAY AWARD 1993 TO DR. K. GROB

Traditionally during the opening session of the International Symposia on Capillary Chromatography the Golay medal, sponsored by Perkin Elmer Corporation, is presented to a leading scientist in the field. The Golay Award Committee decided to pre-

sent the 1993 medal to Dr. Konrad Grob, Kantonales Labor, Zürich, Switzerland. He was elected because of his pioneering work in relation to capillary gas chromatography. The medal was presented by Dr. Giovanni D'Este, managing director of Perkin Elmer Italy.

Konrad Grob was born in 1949 near Zürich, Switzerland. He had the intention to become a forest engineer, but at the last minute changed his mind and studied natural sciences with an emphasis on chemistry. He graduated in 1976 at the University of Zü-



rich. In the period of 1971 - 1974 he was teaching elementary chemistry. Teaching since then has always played an important role in his scientific career.

Already in 1972 he became acquainted with capillary GC as he performed his first injection under the guidance of his famous parents. In the following years his attention shifted more and more to capillary GC. He combined positions in his parents lab in Dübendorf and the Kantonales Labor in Zürich. After 1976, his work in the Kantonales Labor gradually increased to almost a fulltime position, he is now the leader of the GC-department of that institution. In 1978 he obtained his Ph.D in plant physiology on a study on compartmentation of some biochemicals in horse radish cells. The essence of his thesis, in his own words: Why does horse radish only become hot when cells are injured? Konrad Grob is married and the proud father of four sons ranging in age from 12 to 17.

Dr. Grob contributed a large share of original pioneering work in capillary gas chromatography and closely related areas. This is reflected in almost 200 publications and three monographs dealing with classical split and splitless injection; on column injection and coupling LC-GC. His original contributions have a large impact in a number of important areas of capillary gas chromatography. More specifically:

- Column preparation and evaluation
- Sample introduction (split-splitless, large volume sample introduction, PTV, on-column)
- On-line LC-GC
- Application, many in food chemistry.

Thanks to Dr. Grob the chromatographic nomenclature is enriched with many new terms, to mention a few: retention gap, band broadening in space, concurrent solvent evaporation.

Dr. Grob is a strong advocate of further research in capillary GC, which according to his point of view will degenerate without continuous support by basic research.

Announcements are included free of charge. Information on planned events should be sent well in advance (6 months) to:
Journal of Chromatography, News Section, P.O. Box 330,
1000 AH Amsterdam, Netherlands, or by Fax: (+ 31 20)
5862304.

ANNOUNCEMENTS

FREDERICK CONFERENCE ON CAPILLARY ELECTROPHORESIS, FREDERICK, MD, USA, OCTOBER 19-20, 1993

The focus of this meeting is the scientific exchange and dissemination of the technical aspects of capillary electrophoresis (CE). Discussions of established methodologies are invited as well as creative and innovative new approaches and techniques. Participation at this conference is encouraged by continuing to offer registration at no cost.

The format will include oral and poster presentations by individual conference participants, and optional enrollment in a definitive CE course. Invited speakers will provide expert overviews of the basic aspects and applications of CE and MECC including, but not limited to, instrument and column design, detection, optimization and factors that influence mobility, selectivity, resolution, and the application of CE to the separation of small ions as well as large biomolecules.

Exhibitions of the most recent CE instrumentation and equipment will be on site throughout the duration of the conference.

The proceedings will be published by the *Journal of Chromatography*.

A one-day definitive course on capillary electrophoresis will be offered to interested participants on Monday, October 18, 1993.

For further details, please contact: Margaret L. Fanning, PRI, NCI-FCRDC, P.O. Box B, Frederick, MD 21702-1201, USA. Tel.: (+ 1 301) 846-1089; Fax: (+ 1 301) 846-5866.

WCFA 94, WINTER CONFERENCE ON FLOW INJECTION ANALYSIS, SAN DIEGO, CA, USA, JANUARY 5-7, 1994

The conference will focus on industrial FIA and SIA techniques solving real world problems. New hardware and state-of-the-art software driven applications will be presented by leaders in the field.

The following areas will be highlighted:

- sequential injection analysis,
- process chemistry,
- industrial applications,
- biotechnology,
- instrument design,
- automation,
- new methods,
- atomic spectroscopy,
- electrochemistry.

Several short courses will be given in addition to the symposium. There will be an exhibition of leading FIA equipment and related systems.

The deadline for registration is October 15, 1993.

For further details contact: WCFIA 94, Gary D. Christian, Department of Chemistry, BG-10, University of Washington, Seattle, WA 98195, USA. Tel.: (+1 206) 543-5340; Fax: (+1 206) 685-3479; E-mail: christia@chem.washington.edu.

HPCE '94, 6th INTERNATIONAL SYMPOSIUM ON HIGH-PERFORMANCE CAPILLARY ELECTROPHORESIS, SAN DIEGO, CA, USA, JANUARY 31-FEBRUARY 3, 1994

The four-day meeting will include invited and contributed lectures, and posters will again play a major role in the scientific program. Ample time will be set aside to view the posters and to speak with their authors. Lecture and poster topics will include:

- zone electrophoresis;
- isoelectric focusing;
- micellar separations;
- CE/mass spectrometry;
- control of electroosmosis;
- gel columns;
- isotachopheresis;
- detector design;
- chiral separations;
- column coatings;
- analytical and micropreparative applications: pharmaceuticals, peptides and proteins, carbohydrates, oligonucleotides, sub-cellular structures and whole cells, and small molecules and ions.

You are invited to submit an abstract describing original research in the area of capillary electrophoresis. Papers presented at the Symposium will be

reviewed for publication in a special volume of the *Journal of Chromatography*. Complete manuscripts will be due at the Symposium (February 1) and are to be published in July or August, 1994.

Students and academic post-doctoral fellows presenting papers at HPCE'94 are eligible for travel grants to help cover the cost of attending the symposium. Students should send a letter of application and a supporting letter from their research advisor to the Symposium Manager by October 1, 1993.

For further details, contact: Shirley E. Schlessinger, Symposium Manager HPCE'94, Suite 1015, 400 East Randolph Dr., Chicago, IL 60601, USA. Tel.: (+1 312) 527-2011.

HTC 3 – 3rd INTERNATIONAL SYMPOSIUM ON HYPHENATED TECHNIQUES IN CHROMATOGRAPHY, ANTWERP, BELGIUM, FEBRUARY 22-25, 1994

The purpose of this symposium will again be to highlight and treat in-depth recent developments and progress in the field of hyphenations. It will cover all fundamental aspects, instrumental developments and applications of the various hyphenated chromatographic techniques such as GC-GC, GC-MS, PTV-GC-MS, GC-MS-MS, GC-FTIR, GC-AED, on-line air traps-GC, purge-and-trap-GC, extractors-GC (or LC), LC-MS, LC-NMR, LC-LC, LC-GC-MS, LC-LC-GC, LC-FIA-DAD, LC-SFC, SFC-LC, SFC-MS, SFC-FTIR, SFE-GC, SFE-LC, CZE-MS, and ITP-MS.

During HTC 3, emphasis will also be placed on the design of hyphenated, on-line and at-line, "chromatographic analyzers".

Oral presentations in plenary and parallel sessions as well as poster presentations will be included in the scientific program.

Papers presented at the symposium will be reviewed for publication in a special volume of the *Journal of Chromatography*.

A major portion of the symposium will be devoted to discussion sessions. Workshop type seminars will be organized in which scientists of the instrument manufacturers will present and discuss latest developments in instrumentation. A technical exhibition (instruments, books and accessories) will be or-

ganized during the meeting.

In connection with HTC 3, a number of short courses and hands-on workshops will be organized.

The official language of the symposium will be English.

For further information contact: Dr. R. Smits, c/o BASF Antwerpen N.V., Central Laboratory, Scheldelaan, B-2040 Antwerp, Belgium. Tel.: (+32-3) 561-2831; Fax: (+32-3) 561-3250.

HPLC'94, 18th INTERNATIONAL SYMPOSIUM ON COLUMN LIQUID CHROMATOGRAPHY, MINNEAPOLIS, MN, USA, MAY 8-13, 1994

The program will attempt to maintain parallel sessions on fundamental and theoretical aspects of chromatography; applications and automation of chromatography and ancillary techniques; and focus on topics such as specific detector technology.

Areas of particular focus for HPLC'94 will include:

- preparative chromatography;
- new advances/characterization in packing materials;
- advances in robotics, automation, and sample preparation;
- advances in separations of biomolecules;
- new detection technologies;
- physicochemical measurements using chromatography; and
- mobile phase modifiers for capillary zone electrophoresis.

All presentations will be displayed as posters to ensure interactions between speakers and attendees. In addition to traditional plenary, symposia, and discussion sessions, HPLC'94 will offer workshops prior to the official opening of the meeting. Topics under development include HPLC methods development, chiral separations, capillary zone electrophoresis, preparative chromatography, and HPLC-CZE-MS.

The deadline for submission of Abstracts is October 1, 1993.

Papers accepted for lectures or posters at the symposium will be peer-reviewed and published in a special issue of *Journal of Chromatography*. Manuscripts must be delivered to the editor at the symposium.

sium.

All registrants will receive a copy of this issue as part of their registration fee.

Please direct any inquiries about HPLC'94 to the Symposium/Exhibit Manager: Mrs. Janet Cunningham, HPLC'94, c/o Barr Enterprises, P.O. Box 279, Walkersville, MD 21793, USA. Tel.: (+1 301) 898-3772; Fax: (+1 301) 898-5596

3rd SYMPOSIUM ON MOLECULAR CHIRALITY, KYOTO, JAPAN, MAY 24-27, 1994

Attention will be directed to recent developments in molecular chirality. All fundamental aspects and new applications, including the following will be dealt with:

- generation of molecular chirality;
- chiral discrimination and chiral separation;
- crystal, surface and interfacial chirality;
- functions of chiral compounds in chemistry;
- dynamic aspects of chiral compounds in bio-systems;
- drug metabolism, pharmaco-kinetics and toxicokinetics;
- industrial applications of molecular chirality.

Invited plenary and keynote lectures will be presented by internationally recognized scientists. Contributed Papers will be presented as oral communications and posters.

A Book of Abstracts of all scientific contributions will be distributed to each participant at the meeting. Submitted papers including chromatographic separation will be considered for publication in the proceedings, a special issue of the *Journal of Chromatography*, after refereeing.

Travel expenses will be partly provided for participants who submit their papers to the proceedings, on request.

The Symposium languages will be English and Japanese.

For further details contact: Prof. Terumichi Nakagawa, Symposium on Molecular Chirality (SMC), Faculty of Pharmaceutical Sciences, Kyoto University, Yoshida-Shimoadachi-cho, Sakyo-ku, 606 Japan. Fax: (+81 48) 471-0310 (Professor Hara).

6th INTERNATIONAL CONFERENCE ON FLOW ANALYSIS, TOLEDO, SPAIN, JUNE 8-11, 1994

The Conference will basically be concerned with the following flow analysis topics: general aspects, FI-chemometrics, detection systems, separation techniques (on-line sample treatment), sensors and continuous flow techniques, applications (environmental, food, clinical, industrial analysis), and process control (biotechnology). Two special sessions devoted to "Flow Analysis Nomenclature" and Foundation of an International Society for Flow Analysis" will be arranged.

The scientific program will consist of invited lectures and oral and poster presentations. There will also be an exhibition of commercially available instrumentation for flow analysis.

The deadline for submission of abstracts is March 1, 1994.

As with the earlier conferences the papers will be published in a special issue of *Analytica Chimica Acta*.

For further information contact: M. Valcarcel/M.D. Luque de Castro (Flow Analysis VI). Departamento de Química Analítica, Facultad de Ciencias, E-14004 Córdoba, Spain. Tel.: (+34-57) 218616; Fax: (+34-57) 218606.

20th INTERNATIONAL SYMPOSIUM ON CHROMATOGRAPHY, BOURNEMOUTH, UK, JUNE 19-24, 1994

The Symposium program will focus on topical issues in separation science, which will be presented in plenary sessions and in thematic groups of poster presentations.

The Symposium will concentrate on the following themes and their applications in contemporary separation science:

- planar, capillary gas, supercritical and liquid chromatography;
- chiral separations;
- capillary electrophoresis;
- hyphenated techniques;
- chemometrics in separation science;
- computer-aided methods in the design and vali-

daion of separation systems;

- on-line sample preparation systems for chromatography and preparative techniques.

Poster presentations will form the central core of the Symposium with allocation of prime time in the programme. Scientists involved in any aspect of separation science, theoretical or applied are cordially invited to contribute papers, describing original scientific work in the field. The deadline for Abstracts is 30 September, 1993. The proceedings will be published as a special symposium volume of the *Journal of Chromatography*.

Registration and submission of abstracts should be sent to: 20th ISC Symposium Secretariat, The Chromatographic Society, Suite 4, Clarendon Chambers, 32 Clarendon Street, Nottingham NG1 5JD, UK., Tel.: (+44 602) 500596; Fax: (+44 602) 500614.

5th INTERNATIONAL SYMPOSIUM ON PHARMACEUTICAL AND BIOMEDICAL ANALYSIS, STOCKHOLM, SWEDEN, SEPTEMBER 21-23, 1994

The objective of this symposium is to provide a forum for presentations and discussions on all analytical techniques of importance in the pharmaceutical and biomedical fields. The general theme of this symposium will be "analytical techniques and methods used in the development of drugs and in therapy". Emphasis will be put on new instrumental and methodological developments and applications related to the analysis of drugs, their impurities and metabolites, as well as on endogenous compounds of importance in drug therapy.

The oral session will be organized as a single stream of lectures comprising of invited speakers and submitted lectures. An essential part of the program will be the poster sessions, which will include poster discussion sessions, where authors will be able to present a short lecture on their poster.

A series of Short Courses on topical analytical techniques will be arranged in close connection with the symposium.

A range of new analytical instrumentation, materials, chemicals and literature related to pharmaceutical and biomedical analysis will be exhibited during the symposium.

For further details contact: Swedish Academy of Pharmaceutical Sciences, 5th International Symposium on Pharmaceutical and Biomedical Analysis, PO Box 1136, S-11 81 Stockholm, Sweden. Tel.: (+ 46-8) 245-085; Fax: (46-8) 205-511.

5th INTERNATIONAL SYMPOSIUM ON CHIRAL DISCRIMINATION, STOCKHOLM, SWEDEN, SEPTEMBER 26-28, 1994

This symposium is essentially interdisciplinary in character, comprising aspects of chiral discrimination from many scientific disciplines such as chemistry, biochemistry, pharmacology, biology, pharmacy, medicine and analytical chemistry. The aim of the symposium is to highlight the principal features of chiral discrimination of importance in biology, medicine, pharmacy and environmental research. The program will focus on novel aspects of chiral synthesis, new techniques for chiral separations, recent perceptions regarding stereochemistry and biological activity, as well as on any other item of importance for chiral discrimination. International regulatory issues for the development and control of optically active drugs and other biologically active compounds will also be considered.

The oral session will comprise of lectures by invited speakers and submitted lectures on topics of current interest for chiral discrimination. Most papers will be presented as posters, and these sessions will form the central core of the symposium.

New instrumentation, materials, chemicals and literature related to all aspects of chiral discrimination will be on display during the symposium. All inter-

ested exhibitors are invited to contact the organizers for further information.

For further details contact: Swedish Academy of Pharmaceutical Sciences, 5th International Symposium on Chiral Discrimination, PO Box 1136, S-11 81 Stockholm, Sweden. Tel.: (+ 46-8) 245-085; Fax: (+ 46-8) 205-511.

PROGRAM ANNOUNCEMENT

RESEARCH ON HAIR TESTING FOR DRUG ABUSE, PROGRAM ANNOUNCEMENT NO. PA-92-18, NOVEMBER 1, 1991-NOVEMBER 1, 1994.

Department of Health and Human Services, Public Health Service, National Institutes of Health, National Institute on Drug Abuse, Research Grants Program.

The National Institute on Drug Abuse (NIDA) has an interest in research on the utility of hair as a specimen for the detection of drug abuse. The goals of this program are to encourage systematic research on the use of hair testing to detect drugs of abuse in an accurate and reliable manner, and to develop the necessary procedures and safeguards. Specific areas of interest are: pharmacological studies; analytical studies; and cost/benefit ratio analyses. Further information may be obtained from Rao S. Rapaka, Ph.D., or M. Beth Grigson Babecki, M.A., Division of Basic Research, National Institute on Drug Abuse, 5600 Fishers Lane, Rm. 10A-31, Rockville, MD 20857, USA. Tel.: (+ 1 301) 443-6975.

Atmospheric Oxidation and Antioxidants

edited by G. Scott

Oxidation by molecular oxygen is one of the most practically important of all chemical processes. It is the basis of energy production in animals and, at the same time, a major cause of irreversible deterioration and ultimate death. Man uses oxygen positively in the production of energy by combustion, and many important industrial processes in the petrochemical industry are based on the controlled oxidation of hydrocarbons. At the same time, oxidation is the main cause of deterioration of foodstuffs and of many industrial polymers.

It is clearly of great practical importance that the mechanisms of oxidation and its prevention should be understood in order to utilise the reactions of oxygen more effectively but, equally important, to control the adverse effects of oxygen on man-made products and in biological systems. The three volumes of this work are directed towards these objectives. Although complementary to one another, the three volumes form a single whole and it is hoped that, by frequent cross-reference, the reader will be enabled to utilise ideas and experience from other disciplines to enlighten his own.

Volume I

Volume I reviews current understanding of autoxidation, largely on the basis of the reactions of oxygen with characterised chemicals. From this flows the modern mechanism of antioxidant actions and their application in stabilisation technology.

Contents: 1. Autoxidation and Antioxidants: Historical Perspective (*G. Scott*). 2. Autoxidation (*S. Al-Malaika*). 3. Initiators, Prooxidants and Sensitisers (*G. Scott*). 4. Antioxidants: Chain-Breaking Mechanisms (*G. Scott*). 5. Antioxidants - Preventive Mechanisms (*S. Al-Malaika*). Subject Index.

© 1993 xii + 234 pages

Price: US \$ 182.75 / Dfl. 320.00

ISBN 0-444-89615-5

Volume II

This volume examines the oxidation chemistry of carbon-based materials in more detail with emphasis on the technological phenomena that result from the attack of oxygen and the practical procedures developed to prevent them.

Contents: 1. Lubricating Oil Oxidation and Stabilisation (*T. Colclough*). 2. Deterioration of Edible Oils and Foodstuffs (*S.P. Kochhar*). 3. Oxidation and Stabilisation of Polymers during Processing (*G. Scott*). 4. The Physical Chemistry of Polymer Oxidation and Stabilisation (*N.C. Billingham*). 5. Macromolecular and Polymer-Bound Antioxidants (*G. Scott*). 6. Metal Catalysed Oxidation and its Inhibition (*Z. Osawa*). 7. Ozone Degradation and Antiozonants (*R.P. Lattimer, R.W. Layer, C.K. Rhee*). 8. Photodegradation and Photostabilisation (*G. Scott*). 9. Synergism and Antagonism (*G. Scott*). 10. Fire Retardant Polymeric Materials

(*C. Camino*). 11. Degradation and Stabilisation of Polymers Subjected to High Energy Radiation (*D.J. Carlsson*). Subject Index.

© 1993 xiv + 542 pages

Price: US \$ 254.25 / Dfl. 445.00

ISBN 0-444-89616-3

Volume III

Volume III addresses our present understanding of how oxidation is involved both positively and negatively in life processes. This is a more recent and rapidly developing aspect of oxidation chemistry and many of the concepts still have to be proved by rigorous scientific investigation. Nevertheless, the mechanistic principles developed as a result of studies *in vitro* over the years now provide the basis for understanding the complex oxidation chemistry of life processes and its control by biological antioxidants.

Contents: 1. Lipid Peroxidation and its Inhibition (*E. Niki*). 2. Electron Spin Resonance and Spin Trapping (*P.J. Thornalley*). 3. Transition Metal Ions and Antioxidant Proteins in Extracellular Fluids (*J.M. Gutteridge, B. Halliwell*). 4. Sensitization and Protection of Oxidative Damage Caused by High Energy Radiation (*P. Wardman*). 5. Interactions of Melanin with Oxygen

(and Related Species) (*T. Sarna, H.M. Swartz*). 6. Oxidation of Tetrahydrofolates and Tetrahydrobiopterin by Molecular Oxygen (*J.A. Blair, G. Farrar*). 7. Prostaglandin Synthesis and Co-oxidation: Prostaglandin H Synthase-Linked Radical Reactions (*G.A. Reed*). 9. Mechanisms of Antioxidant Action in Living Organisms (*D.G. Pobedimskij, E.B. Burlakova*). 10. Antioxidant Role of Vitamin E (*H.H. Draper*). 11. Medical Aspects and Techniques for Peroxidases and Catalases (*D. Metodiewa, H.B. Dunford*). 12. Antioxidants and Oncogenesis: Roles in Cancer Causation and Prevention (*T.W. Kensler, N.E. Davidson, K.Z. Guyton*). Subject Index.

© 1993 xiv + 376 pages

Price: US \$ 220.00 / Dfl. 385.00

ISBN 0-444-89617-1

Volumes I, II and III

Set price: US \$ 557.00 / Dfl. 975.00

Set ISBN 0-444-89618-X

ORDER INFORMATION

For USA and Canada
ELSEVIER SCIENCE
PUBLISHERS
Judy Weislogel, P.O. Box 945
Madison Square Station,
New York, NY 10160-0757
Fax: (212) 633 3880

In all other countries
ELSEVIER SCIENCE
PUBLISHERS
P.O. Box 211, 1000 AE Amsterdam
The Netherlands
Fax: (+31-20) 5803 705

US\$ prices are valid only for the USA & Canada and are subject to exchange rate fluctuations; in all other countries the Dutch guilder price (Dfl.) is definitive. Customers in the European Community should add the appropriate VAT rate applicable in their country to the price(s). Books are sent postfree if prepaid.



ELSEVIER
SCIENCE PUBLISHERS

Sampling of Heterogeneous and Dynamic Material Systems

Theories of Heterogeneity, Sampling and Homogenizing

by P.M. Gy, Sampling Consultant, Cannes, France

Data Handling in Science and Technology Volume 10

Although sampling errors inevitably lead to analytical errors, the importance of sampling is often overlooked. The main purpose of this book is to enable the reader to identify every possible source of sampling error in order to derive practical rules to (a) completely suppress avoidable errors, and (b) minimise and estimate the effect of unavoidable errors. In short, the degree of representativeness of the sample can be known by applying these rules.

The scope covers the derivation of theories of probabilistic sampling and of bed-blending from a complete theory of heterogeneity which is based on an original, very thorough, qualitative and quantitative analysis of the concepts of homogeneity and heterogeneity. All sampling errors result from the existence of one form or another of heterogeneity. Sampling theory is derived from the theory of heterogeneity by application of a probabilistic operator to a material whose heterogeneity has been characterized either by a simple scalar (a variance: zero-dimensional batches)

or by a function (a variogram: one-dimensional batches). A theory of bed-blending (one-dimensional homogenizing) is then easily derived from the sampling theory.

The book should be of interest to all analysts and to those dealing with quality, process control and monitoring, either for technical or for commercial purposes, and mineral processing.

Although this book is primarily aimed at graduates, large portions of it are suitable for teaching sampling theory to undergraduates as it contains many practical examples provided by the author's 30-year experience as an international consultant. The book also contains useful source material for short courses in Industry.

Contents:

Foreword. First Part: General Introduction. Second Part: Heterogeneity. Third Part: General Analysis of the Concept of Sampling. Fourth Part: Achievement of Sampling Correctness. Fifth Part: One-Dimensional Sampling Model. Sixth Part: Zero-Dimensional Sampling Model. Seventh Part: Sampling by Splitting. Ninth Part: Sampling for Commercial Purposes: Specific Problems. Tenth Part: Homogenizing. Useful References. Index.

1992 xxx + 654 pages
Price: Dfl. 425.00 / US\$ 243.00
ISBN 0-444-89601-5

ORDER INFORMATION

For USA and Canada
ELSEVIER SCIENCE PUBLISHERS

Judy Weislogel
P.O. Box 945
Madison Square Station,
New York, NY 10160-0757
Tel: (212) 989 5800
Fax: (212) 633 3880

In all other countries
ELSEVIER SCIENCE PUBLISHERS

P.O. Box 211
1000 AE Amsterdam
The Netherlands
Tel: (+31-20) 5803 753
Fax: (+31-20) 5803 705

US\$ prices are valid only for the USA & Canada and are subject to exchange fluctuations; in all other countries the Dutch guilder price (Dfl.) is definitive. Books are sent postfree if prepaid.



ELSEVIER
SCIENCE PUBLISHERS

PUBLICATION SCHEDULE FOR THE 1993 SUBSCRIPTION

Journal of Chromatography and Journal of Chromatography, Biomedical Applications

MONTH	1992	J-A	M	J	J	A	S	O	N	D	1994
Journal of Chromatography	Vols. 623-627	Vols. 628-636	637/1 637/2 638/1 638/2	639/1 639/2 640/1 + 2	641/1 641/2 642/1 + 2 643/1 + 2 644/1	644/2 645/1 645/2 646/1	646/2 647/1 647/2	648/1 648/2			
Cumulative Indexes, Vols. 601-650											651/1 + 2
Bibliography Section		649/1		649/2			650/1			650/2	
Biomedical Applications		Vols. 612, 613 and 614/1	614/2 615/1	615/2 616/1	616/2 617/1	617/2 618/1 + 2	619/1 619/2	620/1 620/2	621/1 621/2	622/1 622/2	

INFORMATION FOR AUTHORS

(Detailed *Instructions to Authors* were published in Vol. 609, pp. 437-443. A free reprint can be obtained by application to the publisher, Elsevier Science Publishers B.V., P.O. Box 330, 1000 AH Amsterdam, Netherlands.)

Types of Contributions. The following types of papers are published in the *Journal of Chromatography* and the section on *Biomedical Applications*: Regular research papers (Full-length papers), Review articles, Short Communications and Discussions. Short Communications are usually descriptions of short investigations, or they can report minor technical improvements of previously published procedures; they reflect the same quality of research as Full-length papers, but should preferably not exceed five printed pages. Discussions (one or two pages) should explain, amplify, correct or otherwise comment substantively upon an article recently published in the journal. For Review articles, see inside front cover under Submission of Papers.

Submission. Every paper must be accompanied by a letter from the senior author, stating that he/she is submitting the paper for publication in the *Journal of Chromatography*.

Manuscripts. Manuscripts should be typed in **double spacing** on consecutively numbered pages of uniform size. The manuscript should be preceded by a sheet of manuscript paper carrying the title of the paper and the name and full postal address of the person to whom the proofs are to be sent. As a rule, papers should be divided into sections, headed by a caption (e.g., Abstract, Introduction, Experimental, Results, Discussion, etc.) All illustrations, photographs, tables, etc., should be on separate sheets.

Abstract. All articles should have an abstract of 50-100 words which clearly and briefly indicates what is new, different and significant. No references should be given.

Introduction. Every paper must have a concise introduction mentioning what has been done before on the topic described, and stating clearly what is new in the paper now submitted.

Illustrations. The figures should be submitted in a form suitable for reproduction, drawn in Indian ink on drawing or tracing paper. Each illustration should have a legend, all the legends being typed (with double spacing) together on a *separate sheet*. If structures are given in the text, the original drawings should be supplied. Coloured illustrations are reproduced at the author's expense, the cost being determined by the number of pages and by the number of colours needed. The written permission of the author and publisher must be obtained for the use of any figure already published. Its source must be indicated in the legend.

References. References should be numbered in the order in which they are cited in the text, and listed in numerical sequence on a separate sheet at the end of the article. Please check a recent issue for the layout of the reference list. Abbreviations for the titles of journals should follow the system used by *Chemical Abstracts*. Articles not yet published should be given as "in press" (journal should be specified), "submitted for publication" (journal should be specified), "in preparation" or "personal communication".

Dispatch. Before sending the manuscript to the Editor please check that the envelope contains four copies of the paper complete with references, legends and figures. One of the sets of figures must be the originals suitable for direct reproduction. Please also ensure that permission to publish has been obtained from your institute.

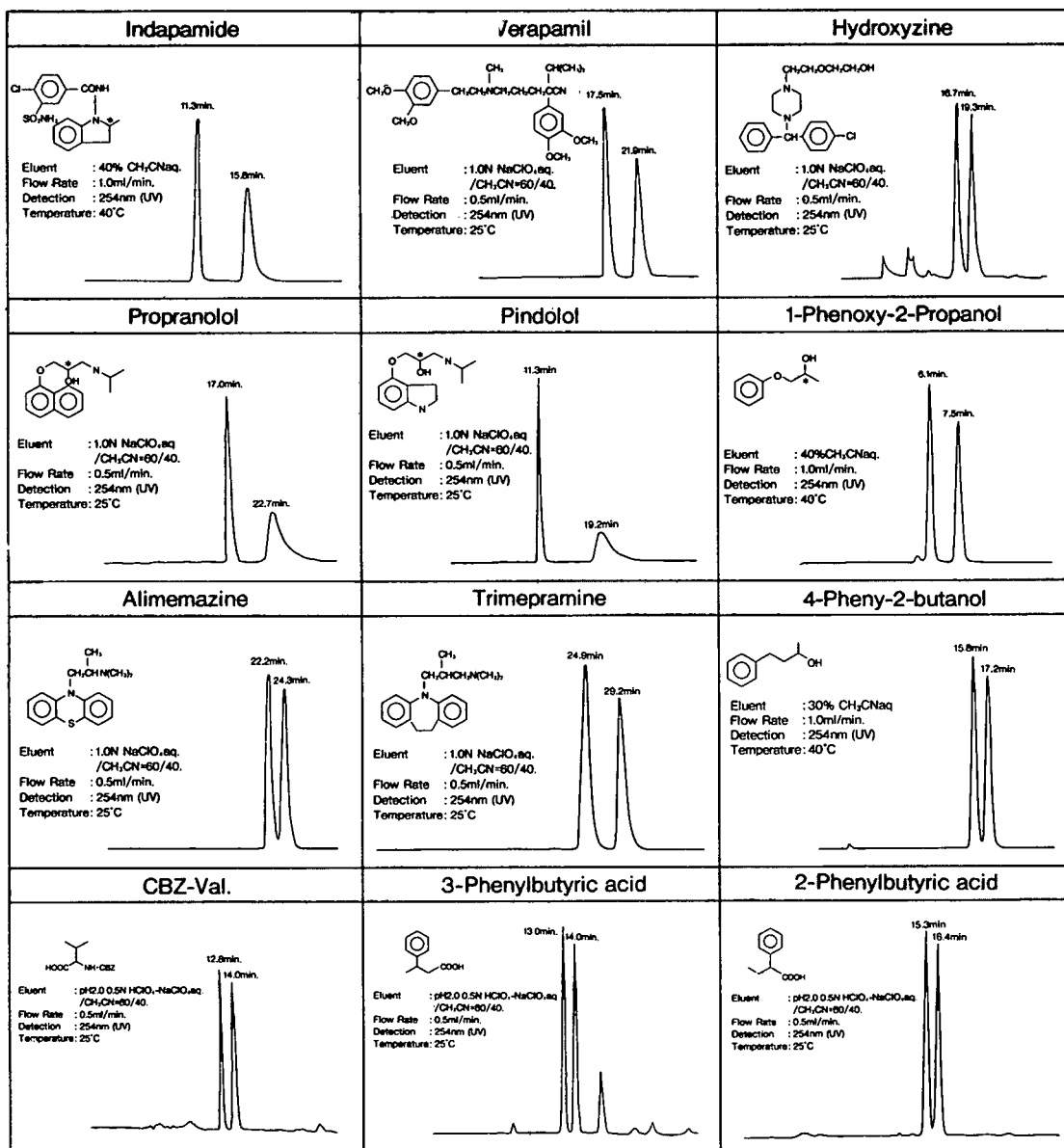
Proofs. One set of proofs will be sent to the author to be carefully checked for printer's errors. Corrections must be restricted to instances in which the proof is at variance with the manuscript. "Extra corrections" will be inserted at the author's expense.

Reprints. Fifty reprints will be supplied free of charge. Additional reprints can be ordered by the authors. An order form containing price quotations will be sent to the authors together with the proofs of their article.

Advertisements. The Editors of the journal accept no responsibility for the contents of the advertisements. Advertisement rates are available on request. Advertising orders and enquiries can be sent to the Advertising Manager, Elsevier Science Publishers B.V., Advertising Department, P.O. Box 211, 1000 AE Amsterdam, Netherlands; courier shipments to: Van de Sande Bakhuyzenstraat 4, 1061 AG Amsterdam, Netherlands; Tel. (+31-20) 515 3220/515 3222, Telefax (+31-20) 6833 041, Telex 16479 els vi nl. UK: T.G. Scott & Son Ltd., Tim Blake, Portland House, 21 Narborough Road, Cosby, Leics. LE9 5TA, UK; Tel. (+44-533) 753 333, Telefax (+44-533) 750 522. USA and Canada: Weston Media Associates, Daniel S. Lipner, P.O. Box 1110, Greens Farms, CT 06436-1110, USA; Tel. (+1-203) 261 2500, Telefax (+1-203) 261 0101.

Reversed Phase CHIRAL HPLC Column

NEW CHIRALCEL® OD-R



For more information about CHIRALCEL OD-R column, please give us a call.



DAICEL CHEMICAL INDUSTRIES, LTD.

CHIRAL CHEMICALS DIVISION 8-1, Kasumigaseki 3-chome, Chiyoda-ku, Tokyo 100, JAPAN
Phone: +81-3-3507-3151 Facsimile: +81-3-3507-3193

AMERICA

CHIRAL TECHNOLOGIES, INC.
730 SPRINGDALE DRIVE
DRAWER I EXTON, PA 19341
Phone: 215-594-2100
Facsimile: 215-594-2325

EUROPE

DAICEL (EUROPA) GmbH
Ost Street 22
4000 Düsseldorf 1, Germany
Phone: +49-211-369848
Facsimile: +49-211-364429

ASIA/OCEANIA

DAICEL CHEMICAL (ASIA) PTE. LTD.
65 Chulia Street #40-07
OCBC Centre, Singapore 0104.
Phone: +65-5332511
Facsimile: +65-5326454

3 0 0 0 2525